QUALITY CHANGES, DUST GENERATION, AND COMMINGLING DURING GRAIN ELEVATOR HANDLING

by

JOSEPHINE MINA BOAC

B.Sc., University of the Philippines Los Baños, 1996
M.Sc., University of the Philippines Los Baños, 1999

AN ABSTRACT OF A DISSERTATION

submitted in partial fulfillment of the requirements for the degree

DOCTOR OF PHILOSOPHY

Department of Biological and Agricultural Engineering
College of Engineering

KANSAS STATE UNIVERSITY
Manhattan, Kansas

2010

Abstract

The United States grain handling infrastructure is facing major challenges to meet worldwide customer demands for wholesome, quality, and safe grains and oilseeds for food and feed. Several challenges are maintaining grain quality during handling; reducing dust emissions for safety and health issues; growing shift from commodity-based to specialty (trait-specific) markets; proliferation of genetically modified crops for food, feed, fuel, pharmaceutical, and industrial uses; and threats from biological and chemical attacks. This study was conducted to characterize the quality of grain and feed during bucket elevator handling to meet customer demand for high quality and safe products. Specific objectives were to (1) determine the effect of repeated handling on the quality of feed pellets and corn; (2) characterize the dust generated during corn and wheat handling; (3) develop and evaluate particle models for simulating the flow of grain during elevator handling; and (4) accurately simulate grain commingling in elevator boots with discrete element method (DEM).

Experiments were conducted at the research elevator of the USDA-ARS Center for Grain and Animal Health Research (CGAHR) to determine the effect of repeated handling on the quality of corn-based feed pellets and corn. Repeated handling did not significantly influence the durability indices of feed pellets and corn. The feed pellets, however, had significantly greater breakage (3.83% per transfer) than the corn (0.382% per transfer). The mass of particulate matter < 125 μm was less for feed pellets than for corn. These corn-based feed pellets can be an alternative to corn in view of their handling characteristics.

Another series of experiments was conducted in the same elevator to characterize the dust generated during corn and wheat handling. Dust samples were collected from the lower and upper ducts upstream of the cyclones in the elevator. Handling corn produced more than twice as much total dust than handling wheat (185 g/t vs. 64.6 g/t). Analysis of dust samples with a laser diffraction analyzer showed that the corn samples produced smaller dust particles, and a greater proportion of small particles, than the wheat samples.

Published data on material and interaction properties of selected grains and oilseeds that are relevant to DEM modeling were reviewed. Using these material and interaction properties and soybeans as the test material, the DEM fundamentals were validated by modeling the flow of

soybean during handling with a commercial software package (EDEM). Soybean kernels were simulated with single- and multi-sphere particle shapes. A single-sphere particle model best simulated soybean kernels in the bulk property tests. The best particle model had a particle coefficient of restitution of 0.6; particle static friction of 0.45 for soybean-soybean contact (0.30 for soybean-steel interaction); particle rolling friction of 0.05; normal particle size distribution with standard deviation factor of 0.4; and particle shear modulus of 1.04 MPa.

The single-sphere particle model for soybeans was implemented in EDEM to simulate grain commingling in a pilot-scale bucket elevator boot using 3D and quasi-2D models. Pilot-scale boot experiments of soybean commingling were performed to validate these models. Commingling was initially simulated with a full 3D model. Of the four quasi-2D boot models with reduced control volumes (4d, 5d, 6d, and 7d; i.e., control volume widths from 4 to 7 times the mean particle diameter) considered, the quasi-2D (6d) model predictions best matched those of the initial 3D model. Introduction of realistic vibration motion during the onset of clear soybeans improved the prediction capability of the quasi-2D (6d) model.

The physics of the model was refined by accounting for the initial surge of particles and reducing the gap between the bucket cups and the boot wall. Inclusion of the particle surge flow and reduced gap gave the best predictions of commingling of all the tested models. This study showed that grain commingling in a bucket elevator boot system can be simulated in 3D and quasi-2D DEM models and gave results that generally agreed with experimental data. The quasi-2D (6d) models reduced simulation run time by 29% compared to the 3D model. Results of this study will be used to accurately predict impurity levels and improve grain handling, which can help farmers and grain handlers reduce costs during transport and export of grains and make the U.S. grain more competitive in the world market.

QUALITY CHANGES, DUST GENERATION, AND COMMINGLING DURING GRAIN ELEVATOR HANDLING

by

JOSEPHINE MINA BOAC

B.Sc., University of the Philippines Los Baños, 1996
M.Sc., University of the Philippines Los Baños, 1999

A DISSERTATION

submitted in partial fulfillment of the requirements for the degree

DOCTOR OF PHILOSOPHY

Department of Biological and Agricultural Engineering
College of Engineering

KANSAS STATE UNIVERSITY
Manhattan, Kansas

2010

Approved by:

Co-Major Professor
Ronaldo G. Maghirang, Ph.D.

Approved by:

Co-Major Professor
Mark E. Casada, Ph.D., P.E.

Copyright

Abstract

The United States grain handling infrastructure is facing major challenges to meet worldwide customer demands for wholesome, quality, and safe grains and oilseeds for food and feed. Several challenges are maintaining grain quality during handling; reducing dust emissions for safety and health issues; growing shift from commodity-based to specialty (trait-specific) markets; proliferation of genetically modified crops for food, feed, fuel, pharmaceutical, and industrial uses; and threats from biological and chemical attacks. This study was conducted to characterize the quality of grain and feed during bucket elevator handling to meet customer demand for high quality and safe products. Specific objectives were to (1) determine the effect of repeated handling on the quality of feed pellets and corn; (2) characterize the dust generated during corn and wheat handling; (3) develop and evaluate particle models for simulating the flow of grain during elevator handling; and (4) accurately simulate grain commingling in elevator boots with discrete element method (DEM).

Experiments were conducted at the research elevator of the USDA-ARS Center for Grain and Animal Health Research (CGAHR) to determine the effect of repeated handling on the quality of corn-based feed pellets and corn. Repeated handling did not significantly influence the durability indices of feed pellets and corn. The feed pellets, however, had significantly greater breakage (3.83% per transfer) than the corn (0.382% per transfer). The mass of particulate matter < 125 μm was less for feed pellets than for corn. These corn-based feed pellets can be an alternative to corn in view of their handling characteristics.

Another series of experiments was conducted in the same elevator to characterize the dust generated during corn and wheat handling. Dust samples were collected from the lower and upper ducts upstream of the cyclones in the elevator. Handling corn produced more than twice as much total dust than handling wheat (185 g/t vs. 64.6 g/t). Analysis of dust samples with a laser diffraction analyzer showed that the corn samples produced smaller dust particles, and a greater proportion of small particles, than the wheat samples.

Published data on material and interaction properties of selected grains and oilseeds that are relevant to DEM modeling were reviewed. Using these material and interaction properties and soybeans as the test material, the DEM fundamentals were validated by modeling the flow of

soybean during handling with a commercial software package (EDEM). Soybean kernels were simulated with single- and multi-sphere particle shapes. A single-sphere particle model best simulated soybean kernels in the bulk property tests. The best particle model had a particle coefficient of restitution of 0.6; particle static friction of 0.45 for soybean-soybean contact (0.30 for soybean-steel interaction); particle rolling friction of 0.05; normal particle size distribution with standard deviation factor of 0.4; and particle shear modulus of 1.04 MPa.

The single-sphere particle model for soybeans was implemented in EDEM to simulate grain commingling in a pilot-scale bucket elevator boot using 3D and quasi-2D models. Pilot-scale boot experiments of soybean commingling were performed to validate these models. Commingling was initially simulated with a full 3D model. Of the four quasi-2D boot models with reduced control volumes (4d, 5d, 6d, and 7d; i.e., control volume widths from 4 to 7 times the mean particle diameter) considered, the quasi-2D (6d) model predictions best matched those of the initial 3D model. Introduction of realistic vibration motion during the onset of clear soybeans improved the prediction capability of the quasi-2D (6d) model.

The physics of the model was refined by accounting for the initial surge of particles and reducing the gap between the bucket cups and the boot wall. Inclusion of the particle surge flow and reduced gap gave the best predictions of commingling of all the tested models. This study showed that grain commingling in a bucket elevator boot system can be simulated in 3D and quasi-2D DEM models and gave results that generally agreed with experimental data. The quasi-2D (6d) models reduced simulation run time by 29% compared to the 3D model. Results of this study will be used to accurately predict impurity levels and improve grain handling, which can help farmers and grain handlers reduce costs during transport and export of grains and make the U.S. grain more competitive in the world market.

Table of Contents

List of Figures

List of Tables

List of Symbols

C_i	Instantaneous commingling, dimensionless
C_a	Average commingling, dimensionless
D_{avg}	Average screen particle diameter, cm
d	Particle or seed diameter, mm
d_a	Equivalent aerodynamic diameter of particles, μm
d_e	Equivalent particle or seed diameter, mm
d_p	Equivalent sphere diameter of dust particles from laser diffraction, μm
DI	Durability index, dimensionless
E_{n}	Particle Young's modulus or modulus of elasticity, MPa (n = *i*, *j*, for particles *i* and *j*)
E^*	Equivalent Young's modulus of particles in contact, MPa
e	Coefficient of restitution, dimensionless
F	Force of friction, N
F_n	Normal force, N
$F_{n_{ij}}$	Normal force acting on particles *i* and *j* at contact points, N
F_t	Tangential force, N
$F_{t_{ij}}$	Tangential force acting on particles *i* and *j* at contact points, N
f_c	Bucket cup rate, cup·s^{-1}
G_{n}	Particle shear modulus, MPa (n = *i*, *j*, for particles *i* and *j*)
G^*	Equivalent shear modulus of particles in contact, MPa
g	Acceleration due to gravity, 9.8 m·s^{-2}
GMD	Geometric mean diameter, mm
GSD	Geometric standard deviation, dimensionless
GSD_w	Geometric standard deviation of the particle diameter by mass, mm
H_i	Initial height of drop of grain, m
H_r	Height of rebound of grain, m
h	Particle thickness, mm
h_b	Height of soybean, mm
I_i	Moment of inertia of particle *i*, kg·m^2

K_n	Normal stiffness coefficient, $N \cdot m^{-1}$
K_t	Tangential stiffness coefficient, $N \cdot m^{-1}$
KE_i	Total kinetic energy before collisions, J
KE_r	Total kinetic energy after collisions, J
l	Particle length, mm
l_b	Length of soybean, mm
M	Added percentage moisture content, dimensionless
M_i	Mixing index, dimensionless
m_n	Mass of one seed or particle, kg (n = *i*, *j*, for particles *i* and *j*)
m_c	Mass of clear soybeans, kg
m_d	Mass of dust collected on the filter, g
m_r	Mass of red soybeans, kg
m^*	Equivalent mass of particles in contact, kg
m_{cf}	Bucket cup filling or mass of grain in a bucket cup, $g \cdot cup^{-1}$
m_p	Total mass of particles filling the test weight kettle, kg
$\dot{m}_0$	Mass flow rate of particles in simulation with original control volume, $kg \cdot s^{-1}$
$\dot{m}_n$	Mass flow rate of particles in simulation with reduced control volume, $kg \cdot s^{-1}$ (n = 4, 5, 6, 7)
$\dot{m}_d$	Mass flow rate of dust, $g \cdot s^{-1}$
$\dot{m}_e$	Mass flow rate equivalent of dust generated during handling, $g \cdot t^{-1}$
$\dot{m}_g$	Mass flow rate of grain, $t \cdot s^{-1}$
$\dot{m}_s$	Mass flow rate of soybeans, $t \cdot h^{-1}$
N	Number of particles in simulation, dimensionless
N	Number of samples from dividing the entire batch of the mixture, dimensionless
N_b	Boot pulley speed, rpm
n_s	Number of spot samples, dimensionless
n_f	Specific surface of the solid relative to a sphere, dimensionless
n_p	Number of particles in each sample, dimensionless
$\dot{n}_0$	Particle rate in simulation with original control volume, $particle \cdot s^{-1}$
$\dot{n}_n$	Particle rate in simulation with reduced control volume, $particle \cdot s^{-1}$ (n = 4, 5, 6, 7)

P	Conditional probability of the random variable
p	Overall proportion of particles of a given component in the whole mixture
PM-2.5	Particulate matter with equivalent aerodynamic diameter of 2.5 μm or less
PM-4.0	Particulate matter with equivalent aerodynamic diameter of 4.0 μm or less
PM-10	Particulate matter with equivalent aerodynamic diameter of 10 μm or less
Q_c	Volumetric flow rate of air through the collection duct, $m^3 \cdot s^{-1}$
Q_s	Sampling volumetric flow rate (through the sampling probe), $m^3 \cdot s^{-1}$
R^*	Equivalent radius of particles in contact, m
R_0	Distance of the contact point from the center of the mass, m
R_n	Radius of sphere or particle, mm (n = *i*, *j*, for particles *i* and *j*)
$\overline{R}$	Average particle radius, m
r_b	Radius of the boot pulley (and the belt thickness), m
r_e	Equivalent particle or seed radius, mm
S	Specific gravity of the granular material, dimensionless
s	Tangential decomposition of the unit vector, dimensionless
s_c	Bucket cup spacing, $m \cdot cup^{-1}$
s_s	Sample standard deviation from spot samples
t	Time, s
t_c	Critical time step, s
t_i	Sampling time interval, s
t_R	Rayleigh time step, s
t_S	Simulation time step, s
t_θ	Time when particles began to move during angle of repose test, s
V	Particle or seed volume, mm^3
V_k	Volume of the test weight kettle, m^3
v_n	Translational velocity of the particle, $m \cdot s^{-1}$ (n = *i*, *j*, for particles *i* and *j*)
v_b	Boot belt speed, $m \cdot s^{-1}$
v_{rel}^t	Relative tangential velocity of colliding particles, $m \cdot s^{-1}$
w	Particle width, mm
w_b	Width of soybeans, mm

w_{bc}	Width of bucket cup, mm
w_{Q2D}	Width of quasi-2D model, mm
W	Force normal to the surface of contact, N
X	Random variable in the conditional probability
x_i	Concentration in the ith sample
$\overline{x}$	Average sample concentrations of a key component in a mixture

Greek Letters

δ_n	Normal overlap, m
δ_t	Tangential overlap, m
$\dot{\delta}_n$	Normal component of relative velocity, $m \cdot s^{-1}$
$\dot{\delta}_t$	Tangential component of relative velocity, $m \cdot s^{-1}$
ε	Roughness of the sliding surface, cm
ζ_n	Reduction factor, dimensionless (n = 4, 5, 6, 7)
η_n	Normal damping coefficient, $N \cdot s \cdot m^{-1}$
η_t	Tangential damping coefficient, $N \cdot s \cdot m^{-1}$
θ	Angle of friction or repose, deg
μ	Coefficient of angle of friction or repose, dimensionless
μ_k	Coefficient of kinetic friction, dimensionless
μ_s	Coefficient of static friction, dimensionless
$\mu_{s(so\text{-}so)}$	Coefficient of static friction for soybean-soybean contact, dimensionless
$\mu_{s(so\text{-}st)}$	Coefficient of static friction for soybean-steel contact, dimensionless
μ_r	Coefficient of rolling friction, dimensionless
ν_n	Particle Poisson's ratio, dimensionless (n = *i*, *j*, for particles *i* and *j*)
ρ_b	Bulk density of a grain sample, $kg \cdot m^{-3}$
ρ_p	Seed or particle density, $kg \cdot m^{-3}$
ρ_0	Unit density, 1.0 $g \cdot cm^{-3}$
σ	Standard deviation of sample concentrations of a key component in a mixture

σ_r	Standard deviation of sample concentrations for completely random mixture
σ_o	Standard deviation of sample concentrations for a totally segregated mixture
τ_i	Rolling friction torque, N·m
τ_{ij}	Torque acting on particle i and j at contact point, N·m
ω_b	Angular velocity of the tilting box, deg·s^{-1}
ω_n	Rotational or angular velocity of the particle, rad·s^{-1} ($n = i, j$)
ω_0	Unit angular velocity vector of the object at the contact point, dimensionless

Acknowledgements

I'd like to thank the following people, without whom this dissertation would not have come to fruition.

- To Dr. Mark E. Casada and Dr. Ronaldo G. Maghirang, my co-major professors, for their guidance, patience, encouragements, and valuable inputs in the dissertation;
- To Dr. L. T. Fan and Dr. Joseph P. Harner, III, both members of my graduate committee; and to Dr. Kristan L. Corwin, my outside committee chair, for their insights and advice to improve the dissertation;
- To U. S. Department of Agriculture (CRIS No. 5430-43440-005-00D) and Kansas Agricultural Experiment Station, for research funding;
- To Dr. Keith Behnke, Prof. Fred Fairchild, and Dr. Rommel Sulabo from Kansas State University (KSU); Drs. Jeff Wilson, Jasper Tallada, Daniel Brabec, Tom Pearson, Paul Armstrong, Floyd Dowell, Larry Wagner, Fred Fox, Larry Hagen, John Tatarko, and Ed Skidmore from USDA-ARS Center for Grain and Animal Health Research (CGAHR) (formerly Grain Marketing and Production Research Center); Drs. Oleh Baran, David Curry, Mark Cook, Sam Wai Wong, and Stephen Cole from DEM Solutions, Inc.; Dr. Otis Walton from Grainflow Dynamics, Inc. and Lawrence Livermore National Laboratory; Dr. Ray Bucklin from University of Florida; and Drs. Paul Sundell and Mathew Shane from USDA Economic Research Service, for their technical advice and support;
- To Dennis Tilley, Rhett Kaufman, Jay St. Clair, Abby Mertens, and Taylor McFall from USDA-ARS-CGAHR; Haidee Gonzales, Li Guo, Darrell Oard, Matthew Dickson, Edna Razote, Dr. Susana Pjesky, Henry Bonifacio, and Howell Gonzales from KSU, for their assistance in preparing and conducting the experiments and simulations;
- To Dr. Bill Schapaugh, Vernon Schaffer, Shaun Winnie, and Dustin Miller, for soybean samples; to Jane Fox, Tim Henderson, Dr. Amelia Asperin, and Mary Rankin, for editing parts of my manuscript; to Dr. Yoonsung Jung, Scott Kreider, Christian Mina, and Girly Ramirez, for their statistical advice; and to Marty Courtois, Edna Razote, Henry Bonifacio, and Betsy Edwards, for their help in the ETDR;
- To my mentors, Mr. Timothy Henderson, Mr. Matheen Sait, Dr. Rick Bajema, Dr. Kimberly Douglas-Mankin, Mrs. Judy Davis, Mrs. Mila Snider, Mrs. Sheryl Casada, Mrs. Elizabeth Maghirang, Mrs. Michelle Edie, and Mrs. Jane Fox, for their advice, encouragements, and support;

- To Mrs. Maxine Jevons and all my colleagues at USDA-ARS CGAHR; and to Mrs. Barb Moore and all faculty members, staff, and graduate students at the Department of Biological and Agricultural Engineering at KSU, for their help, advice and support;
- To all friends, colleagues, members of the Philippine Student Association (PhilSA), and the entire Filipino community in Manhattan and beyond, for their encouragements, advice, insights and lessons shared;
- To my mom Chit; my dad John; my sister Monette and her family, Jovy, Belle, and Bea; my brother Ian; my grandaunt Leonida; and my best friend Janny, for their encouragements and prayers;
- To my husband Jose Joy and my daughter Jean Renee, for all their sacrifices, encouragements, prayers, and unconditional love; and
- To my Lord and King Jesus Christ, who was, who is, and is to come, for the steadfast love, forgiveness, mercy, and grace; for always being with me even when I don't seem to feel it, for all the precious promises kept, and for the constant meeting of all our needs. Thank you very much.

Dedication

For my wonderful husband and daughter,

Jose Joy and Jean Renee

***Joy**, thank you for your sacrifice of being separated with me for one year, three months, and twenty-seven days so I can start my graduate program. **Jean**, thank you for your sacrifice of not having your mom around for two years, five months, and fifteen days, and for encouraging me with your smiles and sweet stories. You are both precious. I thank God you are in my life.*

CHAPTER 1 - INTRODUCTION

1.1 Background

The United States (U.S.) agricultural infrastructure is one of the most efficient and productive systems in the world. It allows Americans to spend less than 11% of their disposable income on food, which is considerably less than the global average of 20 to 30% (Cupp et al., 2004). It also allows the U.S. to play a major role in the global agricultural market. The agricultural sector alone accounts for 13% of the current Gross Domestic Product (GDP) (Cupp et al., 2004; Allan and Leitner, 2006). In 2008, the agriculture sector generated $115 billion in exports (USDA ERS, 2009).

The U.S. grain handling infrastructure, however, is facing a major challenge to meet worldwide customer demands for wholesome, quality, and safe grains and oilseeds for food and feed. Maintaining grain quality and reducing dust emissions for safety and health issues are familiar concerns during handling, especially in grain elevators. Grain quality traits can be described in terms of physical, sanitary, and intrinsic quality characteristics (Maier, 1995). Physical quality traits include moisture content, test weight, kernel size, total damaged kernels, heat damage, broken kernels, stress cracking, and breakage susceptibility. Sanitary characteristics include fungi and mycotoxins count, insects and insect fragments, rodent excrements, foreign material, toxic seeds, pesticide residue, odor, and dust. Intrinsic grain quality characteristics include milling yield, oil content, protein content, hardness, density, starch content, feed value, viability, and storability. Transporting grain and feed from the farm to the end user through the grain handling systems can affect their quality, particularly their physical quality. Dust generated during transport and handling also poses safety and health hazards.

Challenges continue to increase with the growing shift from commodity-based to specialty (trait-specific) markets; proliferation of genetically modified (GM) crops for food, feed, fuel, pharmaceutical, and industrial uses; and threats from biological and chemical attacks. Specialty markets target specific needs of end users. For corn, value-adding traits leading to differentiated product marketing are waxy, nutritionally dense, and high oil. For each trait there can be multiple components such as increased protein levels, altered level of amino acids, and high oil content (Boland et al., 1999). High protein content is preferred by livestock feeders,

while high oil and starch contents are desired by corn wet millers. Processors, on the other hand, want high protein, low linolenic acid, and high stearic acid contents in soybeans (Hurburgh, 1997).

In 2008, the global area planted to GM or biotech crops has increased to 125 million hectares and amounted to $7.5 billion (James, 2008). Fifty percent of this crop area is located in the U.S. The GM crops planted are not only for food, feed, and fuel, but also include those for pharmaceutical and industrial purposes (Maier, 2002).

Intentional threats to grain purity through introduction of contaminants are also a major concern in grain handling. Grain elevator and storage facilities are among post-harvest sites that are critical nodes for assessment because of vulnerability to terrorist attack with biological (US FDA, 2006) or chemical weapons.

1.2 Effect of Handling on Quality and Dust Generation of Grain and Feed

Repeated handling of grain and feed products in an elevator affects their physical quality, including breakage. Martin and Stephens (1977) repeatedly transferred corn alternately between two bins in the USDA-ARS, Center for Grain and Animal Health Research (CGAHR), formerly Grain Marketing and Production Research Center (GMPRC) research elevator at Manhattan, Kansas. Percentage of breakage of corn kernels increased linearly during the repeated-handling tests. Converse and Eckhoff (1989) observed increases in broken corn and fine materials during repeated handling of corn, depending on drying temperatures. Baker et al. (1986) found that breakage susceptibility of shelled corn increased significantly during handling in pneumatic conveying systems. Foster and Holman (1973) noted that free-fall height, impact surface, and corn moisture content and temperature were involved in corn breakage during commercial handling. Aarseth (2004) studied the susceptibility of feed pellets for livestock to attrition during pneumatic conveying.

Corn-based feed pellets can be an alternative to shelled corn. Pelleting of feed is important for improved efficiency in animal feeding and for convenience in feed handling. Research has shown that animals fed with good quality pellets have better growth performance and feed conversion than those fed with mash, reground pellets, or pellets with more fines (Jensen et al., 1962; Jensen and Becker, 1965; Kertz et al., 1981; Brewer et al., 1989; Zatari et

al., 1990). Repeated handling data for feed pellets in an elevator will be valuable for feed handlers in evaluating and improving their feed handling and transportation procedures.

Moreover, handling of grain generates dust, which can be a safety and health hazard as well as an air pollutant. Grain dust is composed of approximately 70% organic matter, which may include particles of grain kernels, spores of smuts and molds, insect debris (fragments), pollens, and field dust (US EPA, 2003). Due to high organic content and a substantial suspendible fraction, concentrations of grain dust above the minimum explosive concentration (MEC) pose an explosion hazard (US EPA, 2003). Published MEC values ranged from 45 to 150 $g \cdot m^{-3}$ (Jacobsen et al., 1961; Palmer, 1973; Noyes, 1998).

In addition to being a safety hazard to grain elevator workers, grain dust is also a health hazard (NIOSH, 1983). Prolonged exposure to grain dust can cause respiratory symptoms in grain-handling workers and in some cases affect workers' performance and sense of well-being. The American Conference of Governmental Industrial Hygienists (ACGIH, 1997) has defined three particulate mass fractions in relation to potential health effects: (1) inhalable fraction (particulate matter (PM) with a median cut point aerodynamic diameter of 100 μm that enters the airways region), (2) thoracic fraction (PM with a median cut point aerodynamic diameter of 10 μm that deposits in the tracheobronchial regions), and (3) respirable fraction (PM with a median cut point aerodynamic diameter of 4 μm that enters in the gas-exchange regions), herein referred to as PM-4. The U.S. EPA (2007), on the other hand, regulates PM-2.5 or fine PM (i.e., PM with equivalent aerodynamic diameter of 2.5 μm or less) and PM-10 (i.e., PM with equivalent aerodynamic diameter of 10 μm or less).

Several studies have determined the amount of dust emitted from external and process emission sources in grain elevators and measured particle size distributions (PSD) for dust collected from grain elevators. Martin and Lai (1978) reported values of 0.080%, 0.037%, and 0.028% for dust < 125 μm generated per transfer for corn, sorghum, and wheat, respectively, with a similar handling system. Converse and Eckhoff (1989) found that the total dust emission per transfer varied from 0.084% to 0.21% of the total mass with the greater emission associated with corn dried at higher temperatures. Parnell et al. (1986) reported mass median diameters (geometric standard deviation) of grain dust < 100 μm for corn and wheat of 13.2 μm (1.80) and 13.4 μm (2.08), respectively. Martin and Lai (1978) cited average mass median diameters of residual dust (that sticks to grain) of 13 and 14 μm for wheat and sorghum, respectively.

However, data on the PSD of dust generated during grain handling in a bucket-elevator system and the fraction that might be health hazards are limited (Wallace, 2000). Published studies either did not consider the PSD (Martin and Sauer, 1976) or were limited to dust <100 μm, the most explosive fraction (Parnell et al., 1986). Thus, limited data exist on the complete range of particle sizes generated during bucket elevator handling even though this system is the primary grain and feed handling system used in the U.S.

1.3 Impact of Undesirable Grain Commingling During Commercial Handling

Aside from improving the physical quality of grain and feed and reducing dust emissions during elevator handling, maintaining safety and purity of the grain is also important. Identity preservation programs are aimed at maintaining the genetic and physical purity of the grain. Segregation of grain with specific traits has been increasing in the grain industry in recent years and is anticipated to continue growing. Introduction of genetically modified (also called transgenic or biotech) crops into the U.S. grain handling system has shown that the infrastructure is often unable to preserve the identity of specialty grains that enter the system to the desired level of purity (Ingles et al., 2006). For example, the Aventis' Starlink™ incident (Bucchini and Goldman, 2002) resulted in a massive, tedious, and expensive sampling and buyback program to gradually remove this corn from the grain system. Another example is the case of Monsanto's GT200-containing canola seed, which contained a protein not approved for any end use that found its way into the grain production system (Kilman and Carroll, 2002).

Grain commingling, an unintentional introduction of a different grain type during typical handling operations, directly reduces the level of purity maintained in grain that enters an elevator facility. There are three approaches for addressing commingling during grain handling. The traditional approach is to largely ignore commingling. This approach, however, is not useful for identity-preserved (IP) grain handling or for segregation of specialty grains. The second approach involves attempting to eliminate all possibility of grain commingling by containerizing the IP grain or handling it only in dedicated facilities. Effective, but expensive, programs have been developed using the second approach. Animal feed, soybeans, corn, wheat, barley, sorghum, oats, and pulses are examples of products being exported in IP containers to other countries (Vachal and Reichert, 2003; Reichert and Vachal, 2003). The customers' preferences for specific variety (e.g., non-biotech or organic grain) and quality attributes (e.g., high protein)

have increased the demand for IP containerization (Prentice, 1998). A third approach is to segregate or handle the IP grain in non-dedicated facilities. Due to limited scientific data on grain commingling in normal handling operations, it is not currently possible to predict the level of purity that could be achieved with the third, less expensive approach.

In addition to unintentional and natural threats to grain purity, intentional introduction of contaminants is also possible. The Strategic Partnership Program Agroterrorism (SPPA) Initiative, a joint effort of various federal agencies to help secure the nation's food supply, listed corn farms, grain elevator and storage facilities, grain export facilities, rice mills, and soybean farms as five of the 14 pre- and post-harvest sites that are critical nodes for assessment because of vulnerability to terrorist attack with biological weapons (US FDA, 2006). As with unintentional commingling, current lack of data on commingling during grain handling makes it difficult to predict the levels of intentionally introduced contaminants that would propagate through the grain handling system. Because full-scale tests of contaminant mixing in the grain handling system are unrealistic, the inability to make useful predictions seriously hampers any efforts to conduct a scientific study of the fate of contaminants introduced into the system. Obtaining sufficient field data would require numerous resource-intensive experiments in grain elevators. A validated mechanistic model for predicting grain commingling in various types of elevator equipment will be valuable for extending the knowledge of grain commingling beyond the few current experimental studies.

Continuum models, kinetic theory-based models, and discrete element models (DEM) (Wightman et al., 1998) have potential to simulate grain commingling in elevators. Due to the need to track individual particles, DEM is a proven way to simulate discrete objects like grain kernels and to predict the movement and commingling of grains in bucket-elevator equipment.

DEM is an explicit numerical scheme in which particle interaction is monitored contact by contact, and the particle motion is modeled particle by particle. First introduced by Cundall (1971) and Cundall and Strack (1979) to model soil and rock mechanics, this method has been successfully applied to modeling of similar processes such as particle mixing in a rotating cylinder (Wightman et al., 1998); three-dimensional, horizontal- and vertical-type screw conveyors (Shimizu and Cundall, 2001); and filling and discharge of a plane rectangular silo (Masson and Martinez, 2000).

In DEM modeling, particle interaction is treated as a dynamic process, which assumes that equilibrium states develop whenever internal forces in the system balance (Theuerkauf et al., 2007). Contact forces and displacement of a stressed particle assembly are found by tracking the motion of individual particles. Motion results from disturbances that propagate through the assembly. Mechanical behavior of the system is described by motion of each particle and force and moment acting at each contact.

Newton's law of motion gives the relationship between particle motion and the forces acting on each particle, and particles are assumed to interact only at contact points. Thus, their motion is independent of the other particles. The soft-sphere approach commonly used in DEM models allows the particles to overlap each other, giving realistic contact areas. Overlaps, however, are assumed to be small in relation to particle size. Force-displacement laws at the contacts can be represented by a Hertz-Mindlin no-slip contact model (Mindlin, 1949; Mindlin and Deresiewicz, 1953; Tsuji et al., 1992; Di Renzo and Di Maio, 2004, 2005). Normal and tangential forces, velocities, and related parameters are described by appropriate equations from the mechanics of particles (Tsuji et al., 1992; DEM Solutions, 2009; Remy et al., 2009).

With demand for high-quality grain and feed, research to ensure safety and purity of the grain and minimize dust emissions during elevator handling is vital. Repeated handling data on quality and durability of corn-based alternative feed pellets compared with data for shelled corn is valuable to improve feed handling and transportation procedures. A dust study to fill the gap where no complete PSD is available for wheat and corn dusts and provide more specific data, particularly on small particle sizes, is needed. A validated mechanistic model to accurately predict grain commingling in grain elevators is important for extending the knowledge of grain commingling beyond the few current experimental studies.

1.4 Research Objectives

The overall objective of this research was to characterize the quality of grain and feed during handling in a bucket elevator in terms of durability, purity, and safety to improve transportation and handling practices for grain and feed handlers. Specific objectives were to

(1) determine the effects of repeated handling on the quality of feed pellets and shelled corn;

(2) characterize the dust generated during corn and wheat handling;

(3) develop and evaluate particle models for simulating the flow of grain during elevator handling; and

(4) accurately simulate grain commingling in bucket elevator boot systems with discrete element method (DEM).

Findings from this research are useful to feed and grain handlers and grain elevator operators for evaluating and improving their handling, transportation, and sanitation procedures in order to reduce their safety and health hazards and air pollution problems. In addition, results of this research will be used for grain commingling simulation of major crops to accurately predict impurity levels in the grain handling system, which can help farmers and grain handlers reduce costs during transport and export of grains and make the U.S. grain more competitive in the world market.

1.5 Organization of the Dissertation

This dissertation has seven chapters and an Appendix section. Chapter 1 presents the significance and objectives of the research. Chapter 2 is an overview of existing literature related to the research topic and is divided into two major topics regarding (1) handling quality related to damage, breakage, and dust generated during elevator handling of grain and feed; and (2) handling quality related to purity and commingling, and its simulation modeling. The first section discusses literature as it relates to Chapters 3 and 4 of this research. The second section is about previous studies related to Chapters 5 and 6 of this dissertation. Chapter 3 summarizes results of the study on the effect of repeated handling on the quality of corn-based feed pellets and shelled corn. Chapter 4 characterizes size distribution, size fraction, and dust generated during handling of shelled corn and wheat. Chapter 5 discusses physical properties relevant to modeling different grains and oilseeds, and presents an appropriate particle model for soybeans in DEM. Chapter 6 presents three-dimensional and quasi-two-dimensional DEM models of grain commingling in a pilot-scale bucket elevator boot system. Chapter 7 provides a summary of conclusions and recommendations for additional research. The Appendices contain supporting data and figures of experiments.

1.6 References

Aarseth, K. A. 2004. Attrition of feed pellets during pneumatic conveying: the influence of velocity and bend radius. *Biosystems Engineering* 89(2): 197-213.

ACGIH. 1997. *1997 Threshold Limit Values and Biological Exposure Indices.* Cincinnati, Ohio: American Conference of Governmental Industrial Hygienists.

Allan, S. M., and P. Leitner. 2006. Attacking agriculture with radiological materials — a possibility? *World Affairs* 168(3): 99-112.

Baker, K. D., R. L. Stroshine, K. J. Magee, G. H. Foster, and R. B. Jacko. 1986. Grain damage and dust generation in a pressure pneumatic conveying system. *Transactions of the ASAE* 29(2): 840-847.

Boland, M., M. Domine, K. Dhuyvetter, and T. Herrman. 1999. Economic issues with value-enhanced corn (MF 2430). Manhattan, Kansas: Kansas State University Agricultural Experiment Station and Cooperative Extension Service.

Brewer, C. E., P. R. Ferket, and T. S. Winowiski. 1989. The effect of pellet integrity and lignosulfonate on performance of growing tom. *Poultry Science* 68(Suppl.1): 18.

Bucchini, L., and L. R. Goldman. 2002. Starlink corn: a risk analysis. *Environmental Health Perspectives* 110(1): 5-12.

Converse, H. H., and S. R. Eckhoff. 1989. Corn dust emissions with repeated elevator transfers after selected drying treatment. *Transactions of the ASAE* 32(6): 2103-2107.

Cundall, P. A. 1971. A computer model for simulating progressive large-scale movements in blocky rock systems. In *Proceedings of the Symposium of the International Society of Rock Mechanics*, Vol. 1, Paper No. II-8: 132-150. Nancy, France: International Society of Rock Mechanics.

Cundall, P. A., and O. D. L Strack. 1979. A discrete numerical model for granular assemblies. *Geotechnique* 29(1): 47-65.

Cupp, O. S., D. E. Walker, and J. Hillison. 2004. Agroterrorism in the U.S.: key security challenges for the 21st century. *Biosecurity and Bioterrorism: Biodefense Strategy, Practice, and Science* 2(2): 97-105.

DEM Solutions. 2009. *EDEM 2.1.2 User Guide*. Lebanon, N.H.: DEM Solutions (USA), Inc. 138p.

Di Renzo, A., and F. P. Di Maio. 2004. Comparison of contact-force models for the simulation of collisions in DEM-based granular flow codes. *Chemical Engineering Science* 59(3): 525-541.

Di Renzo, A., and F. P. Di Maio. 2005. An improved integral non-linear model for the contact of particles in distinct element simulations. *Chemical Engineering Science* 60(5): 1303-1312.

Foster, G. H., and L. E. Holman. 1973. Grain breakage caused by commercial handling method. USDA Res. Serv. Mrktg. Res. Rpt. No. 968. Washington, D.C.: U.S. Department of Agriculture-Agricultural Research Service.

Hurburgh, C. R. 1997. Initiation of end-user specific grain marketing at Iowa elevators. MATRIC Working Paper 97 - MWP 2. Ames, Iowa: Midwest Agribusiness Trade Research and Information Center.

Ingles, M. E. A., M. E. Casada, R. G. Maghirang, T. J. Herrman, and J. P. Harner, III. 2006. Effects of grain-receiving system on commingling in a country elevator. *Applied Engineering in Agriculture* 22(5): 713-721.

Jacobsen, M., J. Nagy, A. R. Cooper, and F. J. Ball. 1961. Explosibility of agricultural dusts. U.S Bureau of Mines - Report of Investigations No. 5753. Washington, D.C.: U.S. Department of Interior Bureau of Mines.

James, C. 2008. Global status of commercialized biotech/GM crops: 2008. ISAAA Briefs No. 39-2008. Available at: http://www.isaaa.org/resources/ publications/briefs/39/executivesummary/default.html. Accessed 22 May 2009.

Jensen, A. H., and D. E. Becker. 1965. Effect of pelleting diets and dietary components on the performance of young pigs. *Journal of Animal Science* 24(2): 392-397.

Jensen, L. S., L. H. Merrill, C. V. Reddy, and J. McGinnis. 1962. Observation on eating patterns and rate of food passage of birds fed pelleted and unpelleted diets. *Poultry Science* 41(5): 1414-1419.

Kertz, A. F., B. K. Darcy, and L. R. Prewitt. 1981. Eating rate of lactating cows fed four physical forms of the same grain ration. *Journal of Dairy Science* 64(12): 2388-2391.

Kilman, S., and J. Carroll. 2002. Monsanto says crops may contain genetically modified canola seed. *The Wall Street Journal*. Available at: http://www.connectotel.com/ gmfood/monsanto.html. Accessed 15 May 2008.

Maier, D. E. 1995. Quality grain needs TLC (GQ-23). Indianapolis, Ind.: Purdue University Cooperative Extension Service. Available at: http://cobweb.ecn.purdue.edu/~grainlab /exten-pubs.htm. Accessed 14 May 2008.

Maier, D. E. 2002. Concerns over pharmaceutical traits in grains and oilseeds (GQ-47). Indianapolis, Ind.: Purdue University Cooperative Extension Service. Available at: http://cobweb.ecn.purdue.edu/ ~grainlab/exten-pubs.htm. Accessed 14 May 2008.

Martin, C. R., and F. S. Lai. 1978. Measurement of grain dustiness. *Cereal Chemistry* 55(5): 779-792.

Martin, C. R., and D. B. Sauer. 1976. Physical and biological characteristics of grain dust. *Transactions of the ASAE* 19(4): 720-723.

Martin, C. R., and L. E. Stephens. 1977. Broken corn and dust generated during repeated handling. *Transactions of the ASAE* 20(1): 168-170.

Masson, S., and J. Martinez. 2000. Effect of particle mechanical properties on silo flow and stresses from distinct element simulations. *Powder Technology* 109(1-3): 164-178.

Mindlin, R. 1949. Compliance of elastic bodies in contact. *Journal of Applied Mechanics* 16: 259-268.

Mindlin, R. D., and H. Deresiewicz. 1953. Elastic spheres in contact under varying oblique forces. *Transactions of ASME, Series E. Journal of Applied Mechanics* 20: 327-344.

NIOSH. 1983. Occupational Safety in Grain Elevators and Feed Mills. Washington, D.C.: National Institute for Occupational Safety and Health. Available at: www.cdc.gov/ niosh/pubs/criteria _date_asc_nopubnumbers.html. Accessed 30 January 2008.

Noyes, R. T. 1998. Preventing grain dust explosions. Current Report-1737. Stillwater, Okla.: Oklahoma Cooperative Extension Service. Available at: www.osuextra.okstate.edu/pdfs/CR-1737web.pdf. Accessed 01 April 2008.

Palmer, K. N. 1973. *Dust Explosions and Fires.* London, England: Chapman and Hall.

Parnell, Jr. C. B., D. D. Jones, R. D. Rutherford, and K. J. Goforth. 1986. Physical properties of five grain dust types. *Environmental Health Perspectives* 66: 183-188.

Prentice, B. E. 1998. Re-engineering grain logistics: bulk handling versus containerization. *Proceedings of the 40th Annual Transportation Research Forum Meeting* 1: 339-352.

Reichert, H., and K. Vachal. 2003. Identity preserved grain - logistical overview. *Paper presented at the Symposium on Product Differentiation and Market Segmentation in Grains and Oilseeds: Implication for Industry in Transition.* Washington, D.C.: U.S. Department of Agriculture Economic Research Service and The Farm Foundation.

Remy, B., J. G. Khinast, and B. J. Glasser. 2009. Discrete element simulation of free-flowing grains in a four-bladed mixer. *AIChE Journal* 55(8): 2035-2048.

Shimizu, Y., and P. A. Cundall. 2001. Three-dimensional DEM simulations of bulk handling by screw conveyors. *Journal of Engineering Mechanics* 127(9): 864-872.

Theuerkauf, J., S. Dhodapkar, and K. Jacob. 2007. Modeling granular flow using discrete element method – from theory to practice. *Chemical Engineering* 114(4): 39-46.

Tsuji, Y., T. Tanaka, and T. Ishida. 1992. Lagrangian numerical simulation of plug flow of cohesionless particles in a horizontal pipe. *Powder Technology* 71(3): 239-250.

USDA ERS. 2009. Value of U.S. trade by fiscal year. Foreign Agricultural Trade of the United States (FATUS). Washington, D.C.: U.S. Department of Agriculture Economic Research Service. Available at: http://www.ers.usda.gov/Data/FATUS/#fiscal. Accessed 21 May 2009.

US EPA. 2003. Grain elevator and processes. In *Chapter 9: Food and Agricultural Industries. Emission Factors/ AP-42*. 5th ed. Vol. I. Research Triangle Park, N.C.: U.S. Environmental Protection Agency. Available at: www.epa.gov/ ttn/chief/ap42/ch09/index.html. Accessed 29 May 2008.

US EPA. 2007. Particulate Matter (PM) Standards. Research Triangle Park, N.C.: U.S. Environmental Protection Agency. Available at: www.epa.gov/pm/ standards.html. Accessed 31 March 2008.

US FDA. 2006. Strategic partnership program agroterrorism (SPPA) initiative. First-Year Status Report. September 2005 - June 2006. Silver Spring, Md.: U.S. Food and Drug Administration. Available at: http://www.cfsan.fda.gov/~dms/agroter5.html. Accessed 15 May 2007.

Vachal, K., and H. Reichert. 2003. U.S. containerized grain and oilseed exports industry survey. *Research Report for Transportation and Marketing Programs, Agricultural Marketing Service, U.S. Department of Agriculture.*

Wallace, D. 2000. Grain handling and processing. In *Air Pollution Engineering Manual*, 463-473. W. T. Davis, ed. New York: John Wiley & Sons.

Wightman, C., M. Moakher, F. J. Muzzio, and O. R. Walton. 1998. Simulation of flow and mixing of particles in a rotating and rocking cylinder. *Journal of American Institute of Chemical Engineers* 44(6): 1266-1276.

Zatari, I. M., P. R. Ferket, and S. E. Scheideler. 1990. Effect of pellet integrity, calcium lignosulfonate, and dietary energy on performance of summer-raised broiler chickens. *Poultry Science* 69(Suppl. 1): 198.

CHAPTER 2 - REVIEW OF LITERATURE

2.1 Effect of Handling on Quality and Dust Generation in Grain and Feed

2.1.1 Handling of Grain

Repeated handling in an elevator affects quality of grains. Previous studies have been conducted on the durability of corn during handling. Baker et al. (1986) found that breakage susceptibility of shelled corn increased significantly during handling in pneumatic conveying systems with approximately 100-mm-diameter pipe. Tests involved total lengths of 31 to 60 m, with two to four 90-degree elbows with a 1.22-m radius of curvature.

Foster and Holman (1973) studied physical damage (breakage) to corn, wheat, soybeans, and dry edible peas by commercial handling methods. Commercial handling methods included in their study were dropping products by free fall (simulating bin filling), dropping products through a spout (simulating railcar filling), grain throwing (simulating the loading of barges and ship holds), and handling products in a bucket elevator. Variables involved in corn breakage caused by commercial handling were free-fall height, impact surface, and corn moisture content, and temperature. Corn dropped from a height of 12 m onto corn in the commercial handling study caused 4.3% breakage with 12.6% moisture content at -3.8°C, and 0.25% breakage with 15.2% moisture content at -5.0°C. Breakage of corn handled decreased at higher grain temperatures.

Data on repeated handling of shelled corn in the USDA-ARS-CGAHR research elevator at Manhattan, Kansas, have been reported. Martin and Stephens (1977) repeatedly transferred corn alternately between two bins. Percentage of breakage of corn kernels increased linearly during the repeated handling tests. They observed breakage within the range reported by Foster and Holman (1973). The corn had an average free fall of 16 m in the two bins. It had a moisture content of about 13% and a temperature of 11°C. A constant increase in breakage during 20 repeated transfers was also observed similar to the observations of Foster and Holman (1973).

Converse and Eckhoff (1989) observed linear increases in broken corn and fine materials during repeated handling of six lots of corn that had been subjected to different drying treatments. Rates of increase were generally higher for corn dried at higher temperatures.

Fiscus et al. (1971) found that corn had the highest breakage during various handling techniques compared with wheat and soybeans because of the structurally weak kernel of corn that fragmentized into random particle sizes during the breakage process. Wheat, on the other hand, had the lowest breakage and generated dust and small kernel particles mainly by abrasion.

2.1.2 Handling of Feed

Studies on feed pellets showed the effect of handling on the quality of the pellets. Aarseth (2004) studied the susceptibility of feed pellets for livestock to attrition during pneumatic conveying. He investigated the effects of air velocity, bend radius, and number of repeated impacts for three commercially available feeds in a 100-mm-diameter pipeline. The three commercial feeds were produced by Felleskjøpet (Kambo, Norway). Feeds 'Formel Favør 30' (FF30) and 'Formel Elite' (FE) had pellet diameters of 6 mm and were formulated for ruminants, whereas, 'Kombi Norm' (KN) had a smaller pellet diameter (3 mm) that was formulated for pigs. The author found that particle attrition differed between feeds, but product damage increased exponentially with conveying air velocity. Shorter radius bends caused more product damage than bends of longer radius for all conveying air velocities.

Aarseth (2004) used Weibull analysis to assess the quality of the three commercial pellets mentioned earlier. This analysis incorporates fracture mechanics with statistics in order to describe the strength of brittle materials. Brittle materials show high scatter in strength due to variations in crack or flaw sizes, called Griffith cracks. Weibull analysis considers a relationship between the scatter in fracture strength and the size distribution of Griffith cracks. Aarseth and Prestløkken (2003) also demonstrated that Weibull analysis can be applied to feed pellets for ruminants and swine.

2.1.3 Importance of Feed Pelleting

Pelleting of animal feed is important for improved efficiency in animal feeding and for convenience in feed handling. Research has shown that animals fed with good quality pellets have better growth performance and feed conversion than those fed with mash, reground pellets, or pellets with more fines (Jensen et al., 1962; Jensen and Becker, 1965; Kertz et al., 1981; Brewer et al., 1989; Zatari et al., 1990).

Zatari et al. (1990) indicated that broilers fed 75% whole pellets and 25% broken pellets had better feed efficiency and higher body weight than those fed 25% whole and 75% broken.

Amornthewaphat et al. (1999) found a linear decrease in efficiency of growth of finishing pigs as the percentage of broken pellets was increased from 0% (7% greater gain/feed ratio than meal control) to 50% (2% greater gain/feed ratio than meal control).

Dozier (2001) reported that minimum acceptable Pellet Durability Index (PDI) values differed for different meat birds: 96% for ducks, 90% for turkeys, and 80% for broilers. Hanrahan (1984) reported no difference in finishing pig performance between pigs restrictedly fed pellets with PDI of 69% or 62%.

Behnke (1994) indicated that the observed improvements in animal performance have been attributed to decreased feed wastage, reduced selective feeding, decreased ingredient segregation, less time and energy expended for eating, destruction of pathogens, thermal modification of starch and protein, and improved palatability. A significant part of the improvement is related to the quality of the pellet. Good quality pellets are needed to withstand repeated handling processes and reduce the formation of fines by mechanical action during transport.

The quality of the pellets may be described by their durability and resistance to attrition and/or breakage during handling. Gustafson (1959) classified the forces acting on the pellets as impact, compression, and shear. Impact forces shatter the pellet surface and any natural cleavage planes in the pellet. Compression forces crush the pellet and also cause failure along cleavage planes. Shear forces cause abrasion of the edges and surface of the pellet.

2.1.4 Pellet Durability Measurement

Several laboratory methods have been developed to measure the durability of pellets. The tumbling box, which is popular in North America (Winowiski, 1998) and is the basis for ASAE Standard S269.4 (*ASAE Standards*, 2003), uses 500 g of prescreened pellets placed in a box that revolves for 10 min at 50 rpm (Young, 1962).

The Holmen durability tester is the most common method in Europe because it simulates the pneumatic conveyors in European feed mills (Winowiski, 1998). In this method, a sample size of 100 g of pellets is transported through tubes with high-velocity air for 30 to 120 s, simulating the handling process. Pellets are subjected to impact and shear forces. Fracture occurs when pellets strike the right-angle corners of the tester.

The Lignotester uses a sample of 100 g of pellets and blows them around a perforated chamber for 30 s (Winowiski, 1998). Pellets come out at the end of the cycle because the fines are removed as they are generated.

The DURAL tester, which was developed for hard alfalfa pellets, subjects 100 g of pellets to impact and shear forces for 30 s at 1600 rpm (Larsen et al., 1996; Sokhansanj and Crerar, 1999; Adapa et al., 2004). In all of the abovementioned methods, PDI was calculated as the percentage of the mass of remaining whole pellets after the PDI test over the total mass of whole pellets before the test.

2.1.5 Grain Dust: Health and Safety Hazard and Air Pollutant

Handling of grain generates dust, which can be a safety and health hazard as well as an air pollutant. Grain dust is composed of approximately 70% organic matter, which may include particles of grain kernels, spores of smuts and molds, insect debris (fragments), pollens, and field dust (US EPA, 2003).

Concentrations of grain dust above the minimum explosive concentration (MEC) pose an explosion hazard (US EPA, 2003) due to the high organic content and a substantial suspendible fraction. Published MEC values ranged from 45 to 150 $g \cdot m^{-3}$ (Jacobsen et al., 1961; Palmer, 1973; Noyes, 1998).

Moreover, grain dust is not only a safety hazard but also a health hazard (NIOSH, 1983). Prolonged exposure to grain dust can cause respiratory symptoms in grain-handling workers and in some cases affect workers' performance and sense of well-being. The American Conference of Governmental Industrial Hygienists (ACGIH, 1997) has defined three particulate mass fractions in relation to potential health effects: (1) inhalable fraction (PM with a median cut point aerodynamic diameter of 100 μm that enters the airways region), (2) thoracic fraction (PM with a median cut point aerodynamic diameter of 10 μm that deposits in the tracheobronchial regions), and (3) respirable fraction (PM with a median cut point aerodynamic diameter of 4 μm that enters in the gas-exchange regions), herein referred to as PM-4.

The US EPA (2007), on the other hand, regulates PM-2.5 or fine PM (i.e., PM with equivalent aerodynamic diameter of 2.5 μm or less) and PM-10 (i.e., PM with equivalent aerodynamic diameter of 10 μm or less). PM-2.5 has been linked to serious health problems ranging from increased symptoms to premature death in people with lung and heart disease (US

EPA, 2007). PM-2.5, PM-4, and PM-10 are more dangerous in terms of grain dust explosions because MEC generally decreases with decreasing particle sizes and increasing surface area (Garrett et al., 1982).

2.1.6 Grain Dust in Elevators

Under the 1990 Clean Air Act, state environmental agencies are required to regulate emission of airborne dust from the grain elevator industry (US EPA, 1990). The US EPA AP-42 document cited recent research on dust emission from grain handling operations indicating the mean PM-10 value was approximately 25% of total PM or total dust and the fraction of PM-2.5 averaged about 17% of PM-10 (US EPA, 2003). Mean PM-10 values for country and export elevators were 20% and 26%, respectively, of total dust (Midwest Research Institute, 1998). Elevators primarily handling wheat had mean PM-10 of about 30% of total dust, whereas those primarily handling corn and soybeans had an average PM-10 of slightly less than 20% of total dust.

Several studies have been conducted to determine the amount of dust generated from external and process emission sources in grain elevators. Kenkel and Noyes (1995) found the amount of airborne dust generated from grain receiving of wheat from a straight truck was 19.5 $g \cdot t^{-1}$, receiving from a hopper-bottom truck was 9.5 $g \cdot t^{-1}$, and loading out or grain shipping was 4.0 $g \cdot t^{-1}$. Shaw et al. (1998) measured a mean dust emission rate of 8.5 $g \cdot t^{-1}$ during corn receiving operations at three feed mills in cattle feedyards. Emission tests conducted by Midwest Research Institute (1998) during grain receiving and shipping operations in both country and terminal elevators yielded mean dust emission rates of 90 $g \cdot t^{-1}$ (29.5 $g \cdot t^{-1}$ of PM-10) for straight truck receiving, 17.5 $g \cdot t^{-1}$ (3.9 $g \cdot t^{-1}$, PM-10) for hopper truck receiving, 43 $g \cdot t^{-1}$ (14.5 $g \cdot t^{-1}$, PM-10) for truck shipping, and 13.5 $g \cdot t^{-1}$ (1.1 $g \cdot t^{-1}$, PM-10) for railcar shipping. Billate et al. (2004) measured dust emission rates during grain receiving operations from simulated hopper-bottom trucks. They found that emission rates of total suspended particulate (TSP) (8.3 - 52.1 $g \cdot t^{-1}$ of corn received) and those of PM-10 (0.6 - 6.1 $g \cdot t^{-1}$) decreased with increasing grain flow rate and decreasing drop height. Dust generated from process emission sources in the grain elevator were reported to be 37.5 $g \cdot t^{-1}$ for grain cleaning using cyclones, 110 $g \cdot t^{-1}$ for column grain drying, 30.5 $g \cdot t^{-1}$ for headhouse and internal handling operations, and 12.5 $g \cdot t^{-1}$ for storage bin vents (US EPA, 2003).

2.1.7 Particle Size Distribution of Grain Dust

Particle size distributions (PSD) for dust collected from grain elevators have been reported in several studies. Martin and Sauer (1976) found that particles <125 μm accounted for an average of 80% of the mass of total corn dust collected at the cyclone tail, and with an average of 43.5% for total wheat dust. Dust particles <8 μm averaged 7.5% for corn dust and 3.5% for wheat dust.

Likewise, Martin and Stephens (1977) reported the amount of dust <125 μm was 70% of the mass of the dust. They observed an initial increase in the amount of corn dust <125 μm emitted in the first eight transfers, while the amount of dust <125 μm became constant during subsequent transfers.

Martin and Lai (1978) cited mean mass median diameters of residual dust (that sticks to grain) of 13 and 14 μm for wheat and sorghum, respectively. In the same study, mean percentages of residual dust with a diameter ≤10 μm were about 34%, 33%, and 45% for sorghum, corn, and wheat, respectively. They reported the percentage of dust <125 μm was 85%, 78%, and 60% of the total dust collected for corn, wheat, and sorghum, respectively.

Martin (1981) studied the particle size distribution of grain dusts from both cyclone separators and baghouses. The fraction of the dust particles less than 10 μm represented about 20% of dust from the baghouse and about 9% of dust from a cyclone.

Lai et al. (1984) reported the weight percentages of grain dust particles with diameters less than 105 μm (sieve aperture) were > 84%, 100% and >70% for corn, wheat, and grain sorghum, respectively. The weight percentages of dust particles with a geometric mean diameter of 114 μm (sieve aperture = 105 μm lower) were 34%, 32%, and 72% for corn, wheat, and grain sorghum, respectively.

Baker et al. (1986) reported similar size distribution of dust collected during pneumatic conveying of shelled corn with that collected from grain handling by a bucket-elevator system (Martin and Lai, 1978; Martin, 1981). The percentage of mass of dust <100 μm was around 80%; <10 μm, around 10%; <4 μm, around 2%; and <2.5 μm, around 0.6%.

Parnell et al. (1986) measured the weight percentage of grain dust <100 μm collected by baghouses of terminal elevators and obtained 54.1%, 34.3%, 34.3%, 44.2%, and 50.6% for corn, wheat, sorghum, rice, and soybeans, respectively. They reported the mass mean diameter

(geometric standard deviation) of corn, wheat, sorghum, rice, and soybean dusts < 100 μm to be 13.2 (1.80), 13.4 (2.08), 14.0 (2.16), 10.7 (2.24), and 13.6 μm (1.87 μm), respectively.

Converse and Eckhoff (1989) found that total dust emission per transfer, during repeated handling of six lots of corn that had been subjected to different drying treatments, varied from 0.084% to 0.21% of the total mass, with greater emissions associated with corn dried at higher temperatures.

Piacitelli and Jones (1992) studied the size distribution of sorghum dust collected by impactors during on-farm handling (harvesting, on-farm storage, delivery truck). Their results indicated that about 2% of the particles had ≤ 3.5 μm aerodynamic diameter; 10% were ≤ 10 μm, 24% were ≤ 15 μm, 48% were ≤ 21 μm, and 52% were > 21 μm.

2.1.8 Summary

Repeated handling in grain elevator affects the quality of grain and feed. Previous studies investigated the effect of commercial (i.e., bins, railcars, barges, ships, and bucket elevators), pneumatic, and repeated elevator handling on the quality of shelled corn, wheat, soybeans, and dry edible peas. Other studies dealt with the effect of pneumatic conveying on the quality of feed pellets. The effect of repeated handling in an elevator, however, on the quality of feed pellets has not been investigated. Corn-based feed pellets incorporated with other feed ingredients to improve nutritive value can be an alternative to shelled corn. Repeated handling data for feed pellets compared with data for shelled corn in an elevator will be valuable for feed handlers in evaluating and improving their feed handling and transportation procedures.

Likewise, data on the particle size distribution (PSD) of dust generated during grain handling in a bucket-elevator system and the fraction that might be health hazards are limited (Wallace, 2000). Published studies either did not consider the PSD (Martin and Sauer, 1976) or were limited to dust < 100μm, the most explosive fraction (Parnell et al., 1986). Thus, limited data exist on the complete range of particle sizes generated during bucket elevator handling, even though this system is the primary grain and feed handling system used in the U.S. A study is needed that fills the gap where no complete PSD is available for wheat and corn and that provides more detailed data than previous studies, particularly on small particle sizes, PM-2.5 and PM-4.

2.2 Impact of Undesirable Grain Commingling During Commercial Handling

2.2.1 Trends in Biotech Crops

In 2008, the global value of approved genetically modified (GM) or biotech crops has reached $7.5 billion, with an accumulated historical milestone value of $50 billion from the period 1996 to 2008 (James, 2008). GM crops are planted by 13.3 million farmers globally in 25 countries, 90% of which are small and resource-poor farmers in developing countries. The top eight countries each growing more than 1 million hectares were USA, Argentina, Brazil, India, Canada, China, Paraguay, and South Africa (Table 2.1). Among GM crops planted worldwide were soybeans, corn, cotton, canola, squash, papaya, alfalfa, sugar beets, tomatoes, poplars, petunias, sweet peppers, and carnations. Advantages cited from using GM crops were more affordable food, feed, and fiber; less pesticide usage (Falck-Zepeda et al., 2000; Marra et al., 2002; James, 2004); reduced production cost; increased yield; reduced dockage (i.e., for Roundup Ready wheat); and increased profitability (Fernandez-Cornejo and McBride, 2000; Price et al., 2003; Wilson et al., 2003).

Table 2.1 Global area planted with genetically modified crops.[a]

Country	Planted Area (million ha)	Global Percentage
United States	62.5	50.0
Argentina	21.0	16.8
Brazil	15.8	12.7
India	7.6	6.1
Canada	7.6	6.1
China	3.8	3.0
Paraguay	2.7	2.2
South Africa	1.8	1.4
Other countries	2.1	1.7
TOTAL	**124.9**	**100.0**

[a] James, 2008

Uncertainty about genetically modified foods and products, however, has led customers worldwide to demand grains that are purer, safer, more wholesome, and either containing no GM grain or strictly controlled levels of GM grain. The 2000 incident on the accidental mixing of an unapproved variety of GM corn in human food, specifically Aventis' Starlink™ corn, and the massive recall of food containing its traces (Taylor and Tick, 2001), added to the customers'

demand for safer identity-preserved (IP) grains and grain products. Another example is the case of Monsanto's GT200-containing canola seed, which contained a protein not approved for any end use that found its way into the grain production system (Kilman and Carroll, 2002). Consequently, countries around the world introduced rules for labeling the presence of GM ingredients.

2.2.2 Legal Issues and Customers' Preferences

Different countries have specified threshold or tolerance levels for accidental GM material in their labeling schemes (Table 2.2). European Commission (EC) Regulation 49/2000 set the minimum GM threshold of 1% for adventitious contamination of non-GM material for labeling requirements (Food Standards Agency, 2001). If the GM material is less than 1%, however, there is no need to label it. If it is more than 1%, there is a need to prove that the material is of non-GM origin that has been contaminated by GM material. Since then, the EU adopted Regulation (EC) No. 1829/2003 on "genetically modified food and feed," and Regulation (EC) No. 1830/2003 on "the traceability and labeling of genetically modified organisms," which were more stringent than the former resolution. These regulations include a 0.9% threshold for the "adventitious" or accidental and technically unavoidable presence of authorized GM event in a non-GM food or feed, above of which should be labeled; and a 0.5% threshold for GM material unavoidably present and not yet authorized by the EU but declared safe (Joy, 2003; Wilson et al., 2003; USDA FAS, 2008).

In addition, the Bioterrorism Act in the U.S. and the General Law of 2005 in the European Union have required producers and processors to have a traceability program. These laws commanded producers, processors, distributors and all involved in the supply chain to create reliable systems to track and trace ingredients and products (Pehanich, 2005). Moreover, the declining domestic demand on soybean meal and the increasing demand on soybean oil for use in bio-diesel production (Good, 2006) would eventually require identity preservation and segregation of specialty grains. Furthermore, international institutions such as the Codex Alimentarius, the Biosafety Protocol, and the World Trade Organization are directly involved in discussions over labeling of GM food (Gruere and Rao, 2007), which may eventually need identity preservation or segregation.

Table 2.2 Threshold or tolerance levels used by selected countries for labeling requirements.[a]

Country	Labeling Scheme	Threshold Level
European Union	Mandatory and national voluntary guidelines	0.9%
Brazil	Mandatory	1%
China	Mandatory	None (0%)
Australia-New Zealand	Mandatory and voluntary	1%
Japan	Mandatory and voluntary	5% [b]
Indonesia	Mandatory	5% [b]
Russia	Mandatory	0.9%
Ukraine	Mandatory	0.9%
Saudi Arabia	Mandatory	1%
South Korea	Mandatory and voluntary	3% [c]
Taiwan	Mandatory and voluntary	5%
Thailand	Mandatory	5% [b]
Chile	Mandatory	1.0%
Norway	Mandatory	2.0%
Argentina	Voluntary	Not specified
South Africa	Voluntary	Not specified
Philippines	Voluntary	5.0%
Canada	Voluntary	5.0%
United States	Voluntary	None available

[a] Phillips and McNeill, 2000; Sheldon, 2002; Carter and Gruere, 2003; Wilson et al., 2003; Cevallos, 2006; Gruere and Rao, 2007; USDA FAS, 2009.
[b] On three main ingredients in each product.
[c] On top five major ingredients in each product.

2.2.3 Identity Preservation, Segregation, Labeling, and Traceability

The introduction of GM crops into the U.S. grain handling system and the demand for specialty grains have shown that the infrastructure is largely unable to preserve the identity of these grains to the desired level of purity. Identity preservation and segregation would be vital in the grain handling systems. The EU Committee (2001) issued a position paper that clarified the concepts of labeling, traceability, and identity preservation. Labeling is about fulfilling the needs of the end customers and imposes one set of ethical values and associated costs on all consumers. It is encouraged to be done voluntarily, but is mandatory in certain countries. Traceability is the ability to track down the identity, history, and source of a raw material, ingredient, or foodstuff. This depends on record keeping and is an important food safety concept for all food supplies. Identity preservation is when farmers have an advance contract to grow and to preserve the identity of the crop for a specific customer or market, and when an added value is placed on the commodity.

Identity preservation is the process of segregating crops that involve separate storage and handling, and documentation of separation (Wilcke, 1999). It is also defined as a traceable chain of custody that starts with the farmer's choice of seed and ends through the shipping and handling system (Dye, 2000). It includes a coordinated transportation and identification system to transfer product and information that make a product more valuable (Sonka et al., 2000). It is also referred to as a closed-loop channel that facilitates the production and delivery of an assured quality by allowing traceability of a commodity from the germplasm or breeding stock to the processed product on a retail shelf (Buckwell et al., 1998; Lin et al., 2000). It is a system of production, handling, and marketing practices that segregates and maintains the integrity and purity of the agricultural commodity in order to enhance the value of the final product (Sundstrom et al., 2002). Figure 2.1 shows an example of an identity preservation process and factors that need to be considered at each step of the process.

According to USDA ERS (2001), identity preservation is a more stringent and expensive process of differentiating commodities that require strict separation be maintained at all times. It usually involves containerized shipping and testing for GM and non-GM status just prior to containerization. It is often used for marketing commodities like food-grade corn and soybeans. This handling process might be required in order to meet the threshold level of 0.9% as per EU

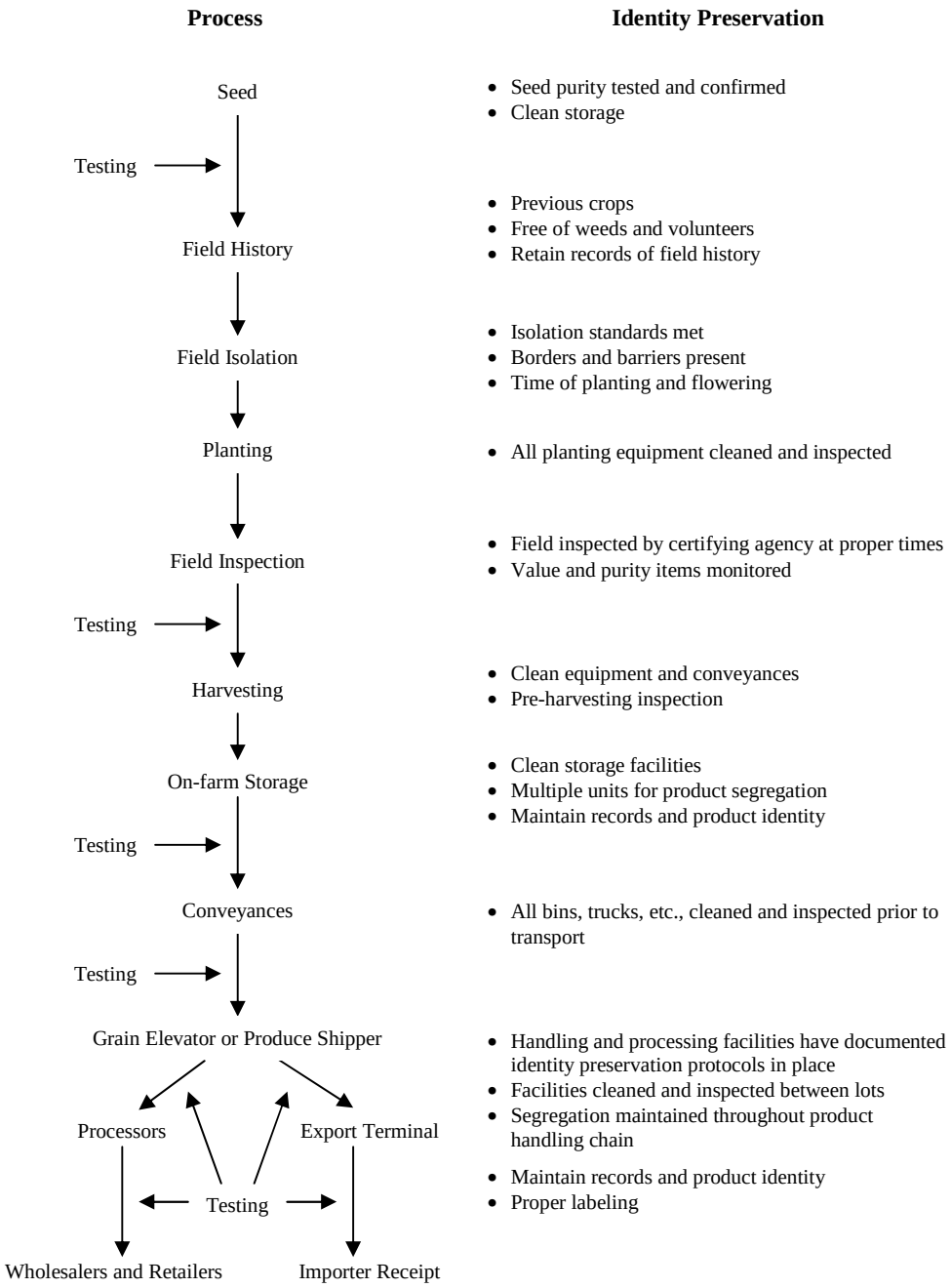

Figure 2.1 Identity preservation process and factors to consider at each step, including testing and auditing points (Sundstrom et al., 2002).

labeling regulations. On the other hand, segregation refers to a process that keep crops separate to avoid commingling during harvesting, loading and unloading, storing, and transporting. It requires cleaning of equipment, such as combines and augers, and transportation and storage facilities. It is a handling process that has been placed for some time for specialty grains (e.g., high-oil corn). However, containerization is generally not involved, thus testing for presence of GM content is more critical (USDA ERS, 2001). This process is usually for meeting a biotech-content threshold level of about 5%, as in the case of Japan's 2000 labeling regulations. These two methods are the ones referred to as the second approach to grain commingling in Chapter 1, which attempts to eliminate all possibility of grain commingling by containerizing the identity-preserved grain or handling it only in dedicated facilities.

2.2.4 Economics of Identity Preservation and Segregation

Several studies have dealt with the cost of identity preservation and segregation of various grains. Wilson et al. (2003) summarized previous studies on the costs of these processes, which ranged from 1.0 to 72 cents per bushel ($¢ \cdot bu^{-1}$) (Table 2.3).

The EU Committee (2001) reported potential consequences of legislation on the traceability and labeling of genetically modified organisms (GMOs). The EU is dependent on imported raw material from countries adopting GMOs. According to the EU Committee, GM labeling could increase retail food prices by up to 10%.

2.2.5 Prevention and Detection of GM Crop Contamination and Other Threats

Several practices to protect GM and non-GM crops from contaminating each other are summarized by Wilcke (1999) and Nielsen (2000). Practical management strategies are as follows:

- Develop the proper attitude of separating GM crops from non-GM crops.
- Know what the buyer wants and deliver according to specifications.
- Make sure that seeds are pure, or at least know what the seed company's purity standards are.
- Develop a plan for segregating the crop. To some extent, it is possible to manipulate planting date and crop maturity to minimize for pollen drift or cross-pollination between adjacent fields of GM and non-GM crops.
- Consider growing and storing non-GM crops in separate locations. If this cannot be done, plant buffer rows so as to separate the GM crops from non-GM.

- Keep detailed records.
- Plan to harvest the non-GM crops before the GM crops to minimize the risk of commingling.
- Clean equipment between crops.
- Keep an eye on custom operations and make sure they understand the concept of identity preservation.
- Keep samples until the final buyer is satisfied with the crop.

Table 2.3 Previous studies on costs of identity preservation and segregation. [a]

Researcher	Methodology/ scope of analysis	Estimated cost of segregation/identity preservation
Askin (1988)	Econometric model of costs for primary elevators	Increase of 2 grades handled increased costs <0.5¢·bu^{-1}
Jirik (1994)	Survey of elevator managers and processors	11-15¢·bu^{-1}
Hurburgh et al. (1994)	Cost-accounting model for high-oil soybeans	3.7¢·bu^{-1}
McPhee and Bourget (1995)	Econometric model of costs for terminal elevators	Increasing grades handled increased operating costs 2.6%
Herrman et al. (1999)	Stochastic simulation model	1.9-6.5¢·bu^{-1}
Maltsbarger and Kalaitzandonakes (2000)	Simulation model for high-oil corn	1.6-3.7¢·bu^{-1}
Nelson et al. (1999)	Survey of grain handlers	6¢·bu^{-1} (corn) 18¢·bu^{-1} (soybeans)
Bullock et al. (2000)	Cost accounting	30-40¢·bu^{-1} (soybeans)
Dahl and Wilson (2002)	Survey	25-50¢·bu^{-1}
Wilson and Dahl (2001)	Survey of elevator managers for wheat	15¢·bu^{-1}
USDA ERS (Lin et al., 2000)	Cost-accounting adjustments to survey results for specialty grain handlers	22¢·bu^{-1} (corn) 54¢·bu^{-1} (soybeans)
Smyth and Phillips (2001)	Analysis of GM identity preservation system for canola in Canada, 1995-96	21-27¢·bu^{-1}
Gosnell (2001)	Added transportation and segregation costs for dedicated GM elevators	15-42¢·bu^{-1} (high throughput) 23-28¢·bu^{-1} (wooden elevators)
Sparks Company (2000)		38-45¢·bu^{-1} (non-GM canola) 63-72¢·bu^{-1} (non-GM soybeans)

[a] Wilson et al., 2003

USDA ERS (2001) enumerated several methods for detecting the presence of biotech content in grains and oilseeds and their processed products. These include: 1) pre-emergence treatment and germination test that determine the presence of the Roundup Ready gene in soybean seeds; 2) the polymerase chain reaction (PCR) that detects specific foreign genetic material inserted into the plant's DNA; 3) the protein-based, enzyme-linked immunosorbent assay (ELISA) that analyzes a specific antibody reaction marking the presence of the new protein produced in biotech crops; and 4) the near-infrared (NIR) spectroscopy that detects the presence of input-trait biotech material through its pattern of absorption or reflection of NIRS light.

In addition to preventing GM crop contamination, the Strategic Partnership Program Agroterrorism (SPPA) Initiative, a joint effort of various federal agencies to help secure the nation's food supply, also worked to prevent intentional threats to the grain and food handling system (US FDA, 2006). This initiative listed corn farms, grain elevator and storage facilities, grain export facilities, rice mills, and soybean farms as five of the 14 pre- and post-harvest sites that are critical nodes for assessment because of vulnerability to terrorist attack with biological weapons.

2.2.6 Grain Handling

Grain handling is the process of transporting grain from the field after harvest, to on-farm storage, and then to country elevators, before the grain is transferred to terminal elevators for export, or to mill elevators for domestic processing. Grains are usually moved from field to country elevators by means of trucks and box cars, and to export elevators by means of barges and rail cars.

Herrman et al. (2002) reported that a typical country elevator consists of a main receiving station elevator structure and an annex storage structure, large steel storage bins, or both annex storage and steel bins. A platform scale for weighing trucks containing grains is usually located at the receiving area. During truck arrival, the grains are weighed and sampled for quality determination. The main elevator has a driveway that may run through grates under which is one or more receiving pits, where grain is dumped. The bottom of the receiving pit is connected to a conveyor and a spouting leading to the boot of the bucket elevator or elevator leg. The grain is elevated by the bucket elevator and conveyed through the distributor to the storage bins. The grain that is not directly conveyed to the storage bin can be spouted to the upper garner of the

scale for weighing, or the grain scalper for cleaning. Grain samples may also be collected from the elevated grain flow using a diverter-type sampler. After passing from the sampler or scale, grain may be cleaned in an aspirated cleaner before it is distributed and spouted to storage bins. Figure 2.2 illustrates different flow paths that the grain can follow in the elevator.

Bouland (1964) analyzed for the best capacity of truck-receiving facilities of country elevators. He reported that 20% of the total grain received at country elevators usually arrived in only one day out of the average 10-day harvest season. He also observed that although the elevator was open for 16 hours a day, more than 10% of the day's receipt arrived in one hour, typically late in the afternoon. The time to dump a truck ranged from 1 to 6 min. At high arrival rates, say 80% of the daily potential service capacities, trucks' waiting time can be as long as 1 hour and 20 min. From the distribution curves and using the Monte Carlo approach, the waiting times prior to weighing were determined and the truck movement was simulated.

Baker et al. (1997) characterized the potential of country elevators to segregate wheat during harvest rush based upon an analysis of grain-receiving systems of 20 country elevators in north central, central, and south central crop reporting districts of Kansas. They reported that approximately 2 min were necessary to sample and evaluate wheat quality parameters including moisture content, dockage, and test weight. Most country elevators had two receiving pits per bucket elevator, which greatly enhanced the ability to segregate wheat. Less than 45% of the grain-receiving systems were operated at or above 70% of their capacity. The percentage of operating hours during harvest versus the percent of burden showed a skewed distribution with 10% burden as the most frequent. A normal distribution centered on 40% burden was observed between the percentages of bushels received during harvest versus percent burden. Observations led to the conclusions that there is an opportunity to improve the operating efficiency of receiving systems at country elevators and that it is possible to segregate.

Herrman et al. (2001) made a follow-up study of 50 Kansas grain elevators to assess the capability of country elevators to segregate wheat. They found that approximately 8% of Kansas country elevators have one leg and one pit, which prohibits segregation. On the other hand, 74% of Kansas elevators possessed two or more bucket elevators, which is suitable for segregating wheat during the harvest rush. Larger grain elevators received fewer small trucks (29%) than small grain elevators (66%). Receiving wheat from the same field in larger trucks enhances segregation.

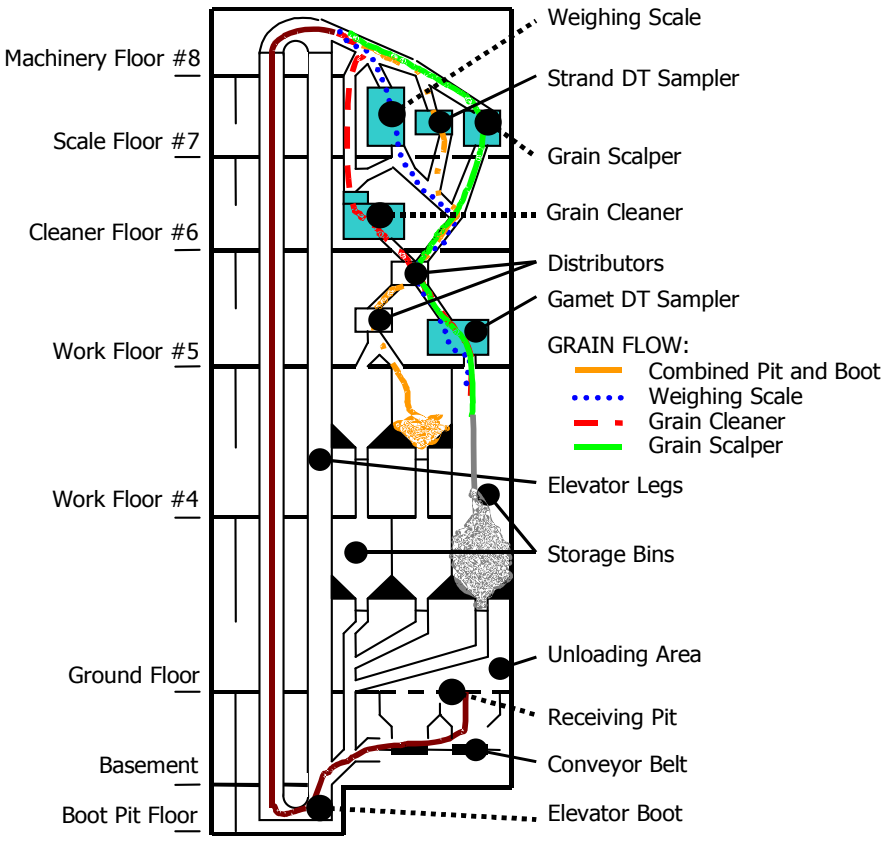

Figure 2.2 Grain flow paths in different elevator equipment (Ingles et al., 2003).

The time study data showed that at large elevators, 28 s less time was spent in sampling and evaluating wheat samples for moisture, dockage, and test weight than at small elevators. The time study data also revealed that operators spent 2.5 min sampling and evaluating grain quality. Incorporation of the most rapid detection equipment that requires less than 1.5 min to evaluate samples would appear feasible (Herrman et al., 2001). The authors concluded that the equipment-receiving capacity of most country grain elevators did not appear to hinder segregation activities.

Herrman et al. (2002) developed a simulation model using SIMAN and ARENA (Systems Modeling Corp., Sewickley, Pa.) software packages. They simulated the segregation operations for typical elevator configurations based on statistical analysis of the operations of existing elevators. Three different country elevator configurations (i.e., small, medium, and large), representing approximately 75% of the traffic flow configurations of Kansas grain elevators, were input into the model. These configurations were created to assess the impact on queue length and time in the system of segregating wheat into two different quality-category (65% of the wheat in one category and 35% of the wheat in a second category) strategies compared with a no-segregation strategy. An infrastructure study of the grain receiving systems and the scale-ticket-summary reports were the basis of the three configurations. Variables in the model configurations included sampling location, number of drives and receiving pits, number and capacity of bucket elevators, truck sizes, and storage capacity. Time study data revealed that locating the sampling station ahead of, rather than at, the scale had greater benefit on the total time the trucks spend in the facility when segregation was performed. An elevator configuration with two legs (bucket elevators) and two drives was superior to a single-drive system. The number of trucks arriving per hour affected delay time, independent of the percent utilization of the grain-receiving system.

Berruto and Maier (2001) worked under the assumption that no two elevators have identical receiving capacities. Unlike Herrman et al. (2002), who tackled the segregation problem of incoming grains using statistical averages of numerous existing elevators, Berruto and Maier (2001) addressed segregation issues for individual elevator configurations. They developed a simulation model using EXTEND (ImagineThat, Inc., San Jose, Cal.) that can track the waiting and service times of each truck that enters a country elevator (Berruto and Maier, 2000). The model investigated two queuing methods: the segregated BATCH versus the FIFO

(first-in, first-out) queue service method in receiving multiple grain streams in a single-unloading-pit country elevator. Results revealed that the BATCH queue service method reduced average waiting times per customer by up to 27%, compared with the traditional FIFO queue strategy when the daily grain received in the elevator was near maximum receiving capacity. The traditional FIFO service had shorter average waiting times per customer when the receiving rates fell below 72% (Berruto and Maier, 2001).

The EXTEND simulation model was also applied to investigate the option of enlarging the receiving pit holding capacity and dimensions to increase the throughput of the unloading operation for a country elevator (Berruto and Maier, 2002). Enlarging the pit size in order for the two hoppers of a trailer to unload simultaneously without moving the semi-truck back and forth reduced the average unloading time by 1.1 min·truck^{-1}. This also reduced the average service time for each customer by about 2.8, 7.0, and 18.8 min·truck^{-1} for the average, busy, and peak days, respectively. During peak days, enlargement of the two existing receiving pits resulted in service times of about 32 min·load^{-1} for the proposed configuration versus 59 min·load^{-1} for the present configuration. Enlarging the receiving pit was also envisioned to reduce the truck cycle time per load for farmers, which would increase their daily crop-harvesting capacities without having to add additional transportation equipment (Berruto and Maier, 2002).

Berruto et al. (2003) developed a network simulation model by means of EXTEND to evaluate transportation efficiency of delivery trucks from fields to elevators. The transportation capacity in the model was based on a Class VII combine harvesting 1,036 ha (2,560 acres). When three, 30-m^3 (850-bu) grain carts were available, maximum predicted field efficiency was 92% compared with 82% with only two, 30-m^3 (850-bu) grain carts. Another comparison was made for use of 31 trucks versus 22 trucks to serve 11 combines. Total delivery time of 225 load·d^{-1} decreased by 25% (948 vs. 1189 min) when 40% more trucks were deployed. Average service time at the elevator for each truck was 12.7 min (31 trucks) versus 11.8 min (22 trucks).

The EXTEND network model also simulated the effect of improved logistic and management strategies of the unloading operation on the performance of a commercial inland terminal elevator (Berruto and Maier, 2004). In this case, the terminal elevator was considered as part of the harvest-transport grain supply chain of the network model. The indicator of elevator performance chosen was average service time expressed as the difference between the time the truck enters and leaves the facility, including all unit operation times and waiting times incurred

while delivering the truckload. The effects of four logistics and management strategies, which included 1) baseline, 2) enlargement of one pit, 3) enlargement of two pits, and 4) traffic pattern change, on unloading operations were explored. Enlargement of two pits appeared to be the best strategy compared with the baseline, since it allowed the elevator to collect up to 16.7% more grain per day and reduced service times by about 34.7 $min \cdot truck^{-1}$. Traffic pattern change was the strategy less sensitive to cleaning operations and provided, in most cases, the same performance as enlargement of one pit, but with more flexibility and less capital expenditure for elevator using IP.

Rosentrater and Bern (2002) developed the Grain Elevator Simulation System (GRELSS) to model operations of a typical terminal grain elevator. The model was programmed in an electronic spreadsheet for easy operation by the end user. There were 17 separate tables comprising the electronic spreadsheets. Each table carried out one of three tasks: (1) define operational and logistical inputs, (2) conduct model calculations, or (3) display simulation outputs. A simple simulation was done using a single-commodity scenario. The timeline was one calendar year and the scenario was based on a constant grain-receiving rate of 176 $m^3 \cdot h^{-1}$ (5000 $bu \cdot h^{-1}$) throughout the year. The harvest season, during which receiving was at maximum levels, was incorporated into the simulation. Based on a 9-h work day at the elevator, no grains were received between 5pm and 8am. When the facility reached full capacity, the grain was loaded onto a train to empty the facility and to receive more grain again. During the course of the year, a train was required approximately every 10 days; however, during peak harvest season; a train was required every three days.

2.2.7 Grain Commingling

2.2.7.1 Commingling Studies in Grain Combines

Greenlees and Shouse (2000) estimated grain contamination from a combine using two cleaning methods: farmyard cleanout and field cleanout. Farmyard cleanout includes removing the grain by gravity, hand cleaning, and vacuum cleaning; field cleanout excludes vacuum cleaning. Yellow corn (as the offending color) and dark red ornamental corn (as the trace color) were used. Results showed that nearly 27 kg of yellow corn residue was removed from a John Deere 4420 combine after the farmyard cleanout. The effect of farmyard cleaning was not different from that of field cleaning due to the small amount of red corn harvested during the

experiment. Data suggested that contamination levels were near 2% or less after one minute of unloading and near 0.2% or less after 1500-1800 kg of grain had been unloaded from the combine.

Hanna et al. (2006) studied the amount of grain residuals and time requirements for combine cleaning. They found the greatest amounts of corn and soybean materials (8 to 34 kg) were in the grain tank and rock trap. Total grain residual in the combine ranged from 38 to 84 kg, 61% of which were whole grain. Time spent to clean the combine ranged from about two to seven hours, in which the head, grain tank, threshing rotor/cylinder, and cleaning shoe required the most cleaning time. Immediately after cleaning, approximately 0.5 to 1.1 kg of previous residual grains and foreign materials were found in the first 7 to 23 kg of subsequent crop harvested. After cleanouts, commingled grain levels dropped below 0.5% after 9 kg had been harvested, but did not always uniformly decrease below this level. Over 6 kg of wheat were found during the first cleanout of a combine after 20 ha of oats had been harvested; this was without physical cleanout prior to oat harvest.

Hirai et al. (2006) developed a system for delivering tracing caplets into the grain on a combine as part of a grain traceability system. Tracing caplets were added into the wheat grain stream close to the unloading auger to attain uniform distribution. The number of caplets in the samples was reasonably consistent at unloading times of 20 and 30 s when the grain unloading rate was stable. The caplet concentration increased as grain flow subsided at the beginning and end of each unloading event.

2.2.7.2 Commingling Studies in Grain Elevators

Hurburgh (1999) enumerated the following sources of adventitious commingling at the elevator/handling function: (1) handling, 10-100 bu can remain depending on the size of components; (2) shipping, 10-50 bu often remain in railcars and barges; and (3) accidental mixing, one 80-bu truck in error can contaminate 80,000 bu if the limit is 1%. Other commingling points were: (1) planting system cleanout, 500 seeds in planter box can have 1%; (2) cross pollination, mostly for corn and should have at least 1000-ft isolation distance; (3) combine cleanout, 3-5 bu can remain; (4) wagons and farm handling systems; (5) storage bins; (6) export elevator handling; (7) ship hold; and (8) cleanup operations.

Ingles et al. (2003) studied the effects of handling equipment on commingling and residual grain in an elevator by first handling white corn in various elevator equipment followed

by yellow corn without any special cleanout. Commingling was calculated as the percentage of white corn mixed in with yellow corn. They found that commingling was greater than 1% during the first 38 s and declined to less than 0.5% after the first metric ton of grain transfer in all tested equipment. The grain cleaner had the highest cumulative commingling value of 0.24%. Mean cumulative commingling values for weighing scale, combined pit and boot, and grain scalper were, respectively, 0.22%, 0.18%, and 0.01%. The largest amount of residual grain was from the elevator boot (120 kg, 1.4% of the total load) followed by the receiving pit (20 kg). Amounts of residual grain from the grain cleaner, weighing scale, and grain scalper were negligible (< 1 kg) by comparison.

Ingles et al. (2006) also conducted three types of tests on (1) combined leg and gravity pit, (2) combined leg and pit with drag conveyor, and (3) bucket elevator to determine the effect of facility configuration on commingling. Tests involved handling soybeans through one of three receiving pits followed by corn without any special cleanout. Commingling was calculated as the percentage of soybean kernels mixed in with the corn samples. It was found that commingling was greater than 1% only during the first 75 to 135 s (1 to 2 t of grain received), except for the gravity-type dump pit configuration. Commingling in the gravity-type configuration remained more than 1% for the duration of the test (840 s or 7.3 t of grain). The mean cumulative commingling percentages were measured to be 1.31% for the combined leg and gravity-type pit effect, 0.3% for the combined leg and pit with drag conveyor effect, and 0.23% for the bucket elevator alone. The ARENA simulation model predicted a total commingling of at least 0.28%, of which 0.27% was generated at the bucket elevator, for a 10-t load handled in a facility equipped with bucket elevator and receiving pit with a drag conveyor. The model also predicted that handling different grain types at a 50:50-load ratio generated the most commingling compared with other load combinations.

2.2.8 Grain Mixing

Mixing or commingling of grains in a grain elevator is an example of solids mixing or more specifically, bulk-solids mixing. Solids mixing is the operation by which two or more solid particulates are dispersed by random or chaotic movement among themselves in a container, i.e., mixer (Fan et al., 1970; Fan et al., 1979; Too et al., 1980). Uhl and Gray (1986) generally defined mixing as any operation that tends to reduce non-uniformities or gradients in

compositions, properties, or temperatures of a material in bulk. Mixing results in the exchange of positions of the material in various parts of the mixer. It can be carried out simultaneously with other processes, or operations or can be a stand-alone operation in different processes and technologies. Solids mixing is an essential operation in plastic processing, pharmaceutical preparation, ore smelting, fertilizer production, food and feed manufacture, chemical synthesis, and other processes (Lacey, 1954; Fan et al., 1970; Too et al., 1980; Fan et al., 1990; Fan, 2001).

2.2.8.1 Classification of Mixtures

Mixtures are generally classified in two categories: (1) free-flowing mixtures, and (2) cohesive or interactive mixtures. Free-flowing mixtures generally permit individual particles freedom to move independently. In contrast, cohesive mixtures are endowed with inter-particulate bonding mechanisms that prevent particles from moving independently; instead, they move only with other particles in an associated cluster (Fan et al., 1990). The dichotomy between these two classes of mixtures, however, is not distinct but "fuzzy" (Fan et al., 1970; Geldhart et al., 1984; Harnby et al., 1985).

2.2.8.2 Characteristics of Mixtures

Described herein are major properties of a mixture of particulate materials that characterize it: uniformity and homogeneity, degree of mixedness, and mixing indices.

2.2.8.2.1 Uniformity and Homogeneity

Fan et al. (1970) defined a homogeneous mixture to be a particulate system in which concentrations of all constituents are uniform throughout the whole mixture. Ideally, spatial distribution of constitutive particles in a mixture of two components, i.e., a binary mixture, can be characterized such that all particles of a component are regularly or evenly distributed among the particles of the other component in any part or direction of the mixture. The homogeneity of a solids mixture or the distribution of its composition is usually quantified by a mixing index (Fan et al., 1979; Fan et al., 1990).

A mixture with regularly arranged components, i.e., an ordered mixture, however, can be formed even if sizes and numbers of the component particles are different. An ideally ordered mixture is one in which individual particles of a given component are evenly dispersed, filling up the intervening spaces, in the matrix of the other component. The number of particles of the

former is equal or less than that of the latter. Moreover, the distance between the particles of the former is identical in all directions (Lacey, 1943; Fan, 2001). Particles of either component in this mixture must be arranged according to a regular spatial pattern. Not all regular spatial patterns can form an ideally ordered mixture: a striated arrangement represents a regular pattern but cannot always be regarded as ideally mixed.

For an ideally ordered mixture, the degree of homogeneity must be highest when measured in terms of any mixing index (Fan et al., 1990; Fan, 2001). The standard deviation or variance of the sample concentrations must be zero or nearly zero in such a mixture (Lacey, 1943; Fan, 2001). Nevertheless, in practice, it is almost impossible to create a perfectly or ideally ordered mixture of freely moving particles by ordinary mixing processes. Any disturbance can cause a relative displacement of the particles, thereby rendering the mixture non-homogenous. An almost ideally ordered and stable mixture can be generated by resorting to one or more unique methods such as agglomeration, coating, and micro-encapsulation (Hersey, 1974, 1976; Fan et al., 1990; Fan, 2001).

Unlike an ideally ordered mixture, a completely random mixture is one in which arrangement of particles of one component is totally randomly dispersed among the particles of the other component(s) (Fan et al., 1970; Akao et al., 1976; Too et al., 1979; Fan, 2001). The probability of finding a particle of any given component in the completely random mixture is identical in every location and is equal to the global, volumetric ratio of this component. The concentration of any component can be measured in terms of either weight or volume fraction in evaluating the randomness of a solids mixture (Kaye, 1989, 1997). The particles compete for space and are distributed along spatial coordinates in the bulk of the mixture; thus, it is more significant to measure the volume fraction than the weight fraction.

The geometry of particles, e.g., differences in size, and possible surface interactions, e.g. adhesion and electric static attraction, are two obstacles to the total randomization of particles (Fan et al., 1970; Fan et al., 1990; Fan, 2001). Smaller particles can be concentrated in the interstices of the larger ones, which can cause segregation and prevent the particles from being completely randomly distributed. Profound surface interactions among particles of different components can lead to the formation of partially ordered arrangements, which can also hinder complete random mixing. In addition, density or weight differences can lead to segregation.

2.2.8.2.2 Degree of Mixedness

Weidenbaum and Bonilla (1955) defined the degree of mixedness or mixing as the ratio of a theoretically calculated standard deviation for a completely random mixture to the experimentally determined standard deviation among spot samples of an incomplete mixture. An incomplete mixture is defined as any mixture that is at an intermediate state between the totally segregated and completely random states (Akao et al., 1976; Shindo et al., 1978; Fan et al., 1990; Fan, 2001). It can be the consequence of mixing initially separated components or spontaneously segregating a completely random mixture. The degree of mixedness measured by various mixing indices characterizes the actual state between the two extremes.

A partially segregated mixture is defined as a mixture yet to be fully homogenized; it can be a mixture homogenized once but then experienced subsequent segregation (Shindo et al., 1978; Too et al., 1979; Fan, 2001). The scale of segregation and the intensity of segregation serve to measure the actual state between totally segregated and completely random states.

As described previously, in a completely random state, the arrangement of individual particles of one component is totally randomly dispersed among the particles of the other components. In contrast, components in a totally segregated mixture are clearly separated from each other in different and distinct regions in a batch of particles, the usual situation prior to mixing. To form a mixture, e.g., a stratified one, a given component is fed into the mixer in the form of layers separated by other components. The relative positions, sizes, and numbers of these layers and the distances between them affect the attainable rate of mixing. The configuration of the layers can be described by the scale of segregation.

The degree of homogeneity of a mixture expressing the extent of approach to perfectness has often been predicted by the uniformity of sample concentrations. This is illustrated by the standard deviation of the concentrations of a key component in a mixture in the following equation (Fan, 2001).

$$\sigma = \sqrt{\frac{\sum_{i=1}^{N} (x_i - \bar{x})^2}{N}} \qquad (2.1)$$

where σ is the standard deviation of the sample concentrations; x_i, the concentration in the ith sample; $\bar{x}$, the average of x_i's; and N, the number of samples yielded by dividing the entire batch of the mixture. In a perfectly homogeneous fluid mixture, σ is zero; in a totally segregated mixture, the value of σ is maximal (Fan et al., 1970; Too et al., 1979; Fan, 2001).

The maximum achievable degree of mixedness corresponds to a completely random arrangement of different particles in conventional mixing. Based on the assumption that the particle size of an individual component is identical, Lacey (1943, 1954) demonstrated that the minimal possible standard deviation of sample concentrations for a binary mixture can be expressed as (Fan, 2001):

$$\sigma_r = \sqrt{\frac{p(1-p)}{n_p}} = \sqrt{\frac{\bar{x}(1-\bar{x})}{n_p}} \qquad (2.2)$$

where p is the overall proportion of the particles of a given component in the whole mixture, which is equal to the average concentration, $\bar{x}$, and n_p is the number of particles in each sample. In principle, the values of the σ even less than σ_r can be achieved by forming an ideally ordered mixture, which can be accomplished by regularly arranging the particles. In practice, this can only be implemented by means of unique processes, e.g., surface adhesion or agglomeration, as mentioned earlier. The ideally ordered arrangement, however, is unstable when the particles can move relative to each other without appreciable hindrance.

Logically, the value of σ for an incomplete mixture is greater than σ_r. The closer the mixture to the totally segregated state, the greater the value of the σ. The standard deviation of the totally segregated mixture, denoted by σ_o, is maximal, which depends on the average concentration of the key component of interest as given by the following equation (Fan, 2001).

$$\sigma_o = \sqrt{\bar{x}(1-\bar{x})} \qquad (2.3)$$

In mixing, the σ value of an incomplete mixture must be in the range between the two extremes; one of the extremes is the standard deviation of the completely random mixture given by equation 2.2, and the other is that of the totally segregated mixture given by equation 2.3 (Akao et al., 1976; Fan, 2001). It is not always the case, however, for an ordered mixture. This is due to the fact that the lower bound, as defined by the standard deviation of the completely random mixture, can be exceeded by the standard deviation of the ideally ordered mixture. Thus, measuring the quality of the incomplete mixture in mixing is crucial in controlling and optimizing the process. It is frequently impossible, however, to determine the standard deviation from the entire sample. This implies that uncertainties exist in estimating the standard deviation due to the finiteness of the number spot samples, n_s. The sample standard deviation, s_s, is defined as follows (Fan, 2001):

$$s_s = \sqrt{\frac{\sum_{i=1}^{n-1}\left(x_i - \bar{x}\right)^2}{n_s - 1}} \qquad (2.4)$$

Compared with a fluid mixture, the quality of a solids mixture is difficult to determine because of the discrete nature of any particulate system, and the finiteness of particles and sample sizes. Sample concentrations and their standard deviations can be affected by the error caused by the tendency of any component's particle or particle cluster to straddle the boundaries of the sample containing it. It follows that the measured standard deviation depends on the average concentration of the given key component's particles and on the relative size of the sample. For a completely random mixture whose component particles are identical in size and density, such uncertainty is minimized and can be determined mathematically; this uncertainty is magnified for other mixtures. To account for the effects of the sample number and size, the general rule is to take a sufficient number of samples from well-distributed points in representative regions of the mixture. Each sample must also contain a sufficient number of particles; such a number can be determined from practical points of view (Fan et al., 1970; Fan, 2001).

2.2.8.2.3 Mixing Indices

Fan et al. (1970) and Poux et al. (1991) reviewed more than 30 different mixing indices in solids mixing, whereas Boss (1987) collected nearly 40 mixing indices. They determined the interrelations among these mixing indices, which are based on the notion of sample variance or standard deviation.

Fan and Wang (1975) and Boss (1987) compared some mixing indices and derived conversion formulae among them. Table 2.4 lists some of the frequently adopted mixing indices in terms of statistical analysis of sample concentrations. Some of the mixing indices are affected by the sample size. A value of unity or zero for the completely random and totally segregated mixtures, respectively, can be achieved only when there is a sufficiently large sample size. For multi-component mixtures, it is imperative that their quality be evaluated and controlled because the components may behave differently at specific periods of mixing. This implies that at a given stage, one of the components may be well homogenized, while other components may still be partially segregated. The mixture as a whole, therefore, does not meet the necessary homogeneity

specification. Too et al. (1978) summarized the majority of mixing indices defined for multi-component mixtures based on the concentration variance.

Table 2.4 Important mixing indices based on the variance or standard deviation of sample concentrations. [a]

No.	Equation	Value in the totally segregated state $\sigma = \sigma_o$	Value in the ideally ordered mixture $\sigma = 0$	Value in the completely random mixture $\sigma = \sigma_r$
1	$M_1 = \frac{\sigma^2}{\sigma_o^{\,2}}$	1	0	$\frac{1}{n}$
2	$M_2 = \frac{\sigma}{\sigma_o}$	1	0	$\frac{1}{\sqrt{n}}$
3	$M_3 = 1 - \frac{\sigma^2}{\sigma_o^{\,2}}$	0	1	$1 - \frac{1}{n}$
4	$M_4 = 1 - \frac{\sigma}{\sigma_o}$	0	1	$1 - \frac{1}{\sqrt{n}}$
5	$M_5 = \frac{\sigma_o^{\,2} - \sigma^2}{\sigma_o^{\,2} - \sigma_r^{\,2}}$	0	$\frac{n}{n-1}$	1
6	$M_6 = \frac{\sigma_o - \sigma}{\sigma_o - \sigma_r}$	0	$\frac{\sqrt{n}}{\sqrt{n}-1}$	1
7	$M_7 = \frac{\log\sigma_o - \log\sigma}{\log\sigma_o - \log\sigma_r}$	0	∞	1
8	$M_8 = \frac{\sigma^2}{\bar{x}^2}$	$\frac{1-\bar{x}}{\bar{x}}$	0	$\frac{1-\bar{x}}{\bar{x} \cdot n}$
9	$M_9 = \frac{\sigma}{\bar{x}}$	$\sqrt{\frac{1-\bar{x}}{\bar{x}}}$	0	$\sqrt{\frac{1-\bar{x}}{\bar{x} \cdot n}}$

[a] Fan and Wang, 1975; Boss, 1987; Fan, 2001

2.2.8.3 Mechanisms of Solids Mixing

The fact that the particulate materials in solids mixtures are small but finite in size, i.e., discrete renders mixing to be complex. Conventionally, it has been postulated that the three mechanisms mainly involved in solids mixing are (1) convective mixing, involving the transfer

of groups or clusters of adjacent particles from one location in the mass to another; (2) diffusive mixing, portraying the distribution of particles over a freshly developed surface; and (3) shear mixing, portraying the establishment of slipping planes within the mass of particles (Lacey, 1954; Fan et al., 1970; Wang and Fan, 1974; Weinekotter and Gericke, 2000). All three mechanisms always occur simultaneously in varying degrees in the mixing process, depending on the mixer in use.

Another mechanism of solids mixing is chaos. Chaotic mixing contributes substantially to the mixing of particles and powders (Ottino et al., 1988; Ottino, 1989, 1990; Fan, 2001). It exhibits highly complex patterns of mixing. Nevertheless, chaos is a deterministic phenomenon; chaotic mixing results in convective and shear mixing, which are irregularly interwoven and interacting.

Mixing of solids mixtures is frequently accompanied by demixing or segregation. It does not occur when the mixing components have identical physical properties and geometrical characteristics but differ only in chemical composition. Williams (1986) indicated that among the physical properties and geometrical characteristics, the particle size influences segregation most.

Four mechanisms of segregation have been mentioned by Weinekotter and Gericke (2000). These are elaborated in what follows.

One of the mechanisms is induced through the agglomeration of one component in a binary or two-ingredient mixture. Agglomeration occurs when strong inter-particle forces exist between particles in close contact with each other. Particles of one component adhere to each other as a consequence of one or more factors, including (i) the presence of a small quantity of liquid forming liquid bridges in the solid particles; (ii) electrostatic forces causing cohesion of particles; and (iii) Van der Waals forces operating upon finer grains (<30μm) and binding them together. Adhesion of the particles of one component would give rise to their agglomeration, which, in turn, would cause them to segregate from the particles of the other component.

Another mechanism of segregation is floating due to vibration. When a solids mixture undergoes vibration, coarser or larger particles climb up or float over the smaller ones. Smaller particles flow into the resultant vacant space, which prevents larger particles from reclaiming their original position. Thus, larger particles collect at the surface, thereby causing segregation (Fan et al., 1970; Staniforth, 1982; Fan et al., 1990; Weinekotter and Gericke, 2000).

Percolation of a particulate component among the interstices of the remaining component(s) is another mechanism of segregation; it is by far the most important segregating effect (Staniforth, 1982; Fan et al., 1990; Weinekotter and Gericke, 2000). If size of the voids is sufficiently large or enlarged by mechanical vibration or aeration, smaller particles drop or trickle down through the voids or gaps between the larger ones. Segregation tends to magnify when density of the smaller particles increases over the large particles. This trend is also affected by differences in shape and surface characteristics (Roseman and Donald, 1962; Campbell and Bauer, 1966; Fan et al., 1970; Fan, 2001).

Trajectory segregation is another mechanism that is activated when two particles of different sizes and densities are blown horizontally into a confined space, e.g., silo, at a given speed. Differences in size and density affect the velocities of the particles, thus causing their separation (Weinekotter and Gericke, 2000).

2.2.8.4 Simulation Models of Solids Mixing

Monte Carlo techniques are numerical methods involving sampling from statistical distributions, either theoretical or empirical, to approximate the real physical phenomena without reference to the actual physical systems (Fan et al., 1970). A random walk is the simplest subclass of the Markov processes, which constitute a class of stochastic processes. In a random walk, the random variable is the position of a particle moving on a straight line in such a manner that the particle either remains where it is or moves one step to the left or to the right at each step (Parzen, 1962). The Markov processes can be defined mathematically as shown (Parzen, 1962):

$$P\left[X(t_n) \le x_n \middle| X(t_1) = x_1, \ldots, X(t_{n-1}) = x_{n-1}\right] = P\left[X(t_n) \le x_n \middle| X(t_{n-1}) = x_{n-1}\right] \qquad (2.5)$$

where *P* with a bar separating random variables is the conditional probability and random variables (*X*) on the right of the bar are those that have given values of *x*. This expression implies that given the "present" of the process, the "future" is independent of its "past" (Parzen, 1962). The conditional probability is often termed a transition probability in a Markov process. It describes the transition from the state $X(t_{n-1})$ to the state $X(t_n)$.

2.2.9 Discrete Element Method

Grains are considered finite and discrete materials. Williams et al. (1985) described a method of solving problems involving discrete elements like grains, called the discrete element method (DEM). DEM belongs to a family of numerical modeling techniques designed to solve

problems in engineering and applied science that display gross discontinuous behavior (Hustrulid and Mustoe, 1996; Hustrulid, 1998; Dewicki, 2003). Problems exhibiting discontinuous behavior cannot be simulated with conventional continuum-based computer modeling such as finite-element or finite-difference methods. Examples of engineering problems dominated by discontinuum behavior include stability of underground mine openings; stability of rock slopes; micro-mechanical behavior of particular media; mineral processing; and flow of bulk solids in hoppers, feeders, chutes, screens, crushers, ball mills, mixers, and all types of conveyor systems (Dewicki, 2003).

The DEM can analyze multiple, interacting, deformable, discontinuous, or fractured bodies undergoing rotations and large displacements. The basic assumption is that every discrete element has distinct boundaries which physically separate it from every other element in the analysis. Basic equations of elasticity are written under an inertial frame, and then transferred to a non-inertial frame, which is translating and rotating. This is performed so that to an observer in the non-inertial frame, i.e., the new frame, the object exhibits no mean translation or rotation. The deformation can then be decoupled from the mean motion and is written as the sum of the bodies' normal modes, which in turn gives a newly derived set of decoupled modal equations. These equations are applied on an element-by-element basis. The elements communicate through boundary forces. The decoupled equations may be solved by an explicit central difference scheme. The final solution is obtained by means of modal superposition (Williams et al., 1985).

Cundall and Strack (1979) also defined DEM as a numerical model capable of describing the mechanical behavior of assemblies of discs and spheres. It is based on an explicitly numerical scheme in which the particle interaction is monitored contact by contact and the particle motion is modeled particle by particle. In DEM modeling, particle interaction is treated as a dynamic process, which assumes that equilibrium states develop whenever internal forces in the system balance (Theuerkauf et al., 2007). Contact forces and displacements of a stressed particle assembly are found by tracking the motion of individual particles. Motion results from disturbances that propagate through the assembly. The mechanical behavior of the system is described by the motion of each particle and the force and moment acting at each contact.

2.2.9.1 Theoretical Basis of DEM

In DEM, contact forces and displacements of the particle assembly are computed by tracking the motion of each individual particle using explicit numerical scheme with very small time step discussed in detail3 by Cundall and Strack (1979). The process uses Newton's Law of Motion that gives the relationship between the particle motion and forces acting on each particle. Translational and rotational motions of particle *i* are defined as (Remy et al., 2009):

$$m_i \frac{dv_i}{dt} = \sum_j \left(F_{n_{ij}} + F_{t_{ij}}\right) + m_i g \qquad (2.6)$$

$$I_i \frac{d\omega_i}{dt} = \sum_j \left(R_i \times F_{t_{ij}}\right) + \tau_{ij} \qquad (2.7)$$

where m_i, R_i, v_i, ω_i, and I_i are the mass, radius, linear velocity, angular velocity, and moment of inertia of particle *i*; $F_{n_{ij}}$, $F_{t_{ij}}$, and τ_{ij} are, respectively, normal force, tangential force, and torque acting on particles *i* and *j* at contact points; *g* is the acceleration due to gravity; and *t* is the time.

Particles interact only at contact points with their motion independent of other particles. Forces on the particles at contact points include contact force and viscous contact damping force (Zhou et al., 2001). These forces have normal and tangential components. The soft-sphere approach commonly used in DEM models allows particles to overlap each other, giving realistic contact areas. Overlaps of particles are allowed but are small in comparison to particle size.

Force-displacement laws at the contacts can be represented by different contact models. The simplest contact model is the linear contact law, in which the spring stiffness is assumed to be constant (e.g., linear-spring dashpot model for spherical particles at contact) (Mishra, 2003). Another model, which is an improvement over the linear law, employs the Hertz theory to obtain the force deformation relation for the contact (e.g., nonlinear-spring dashpot model). Unlike the linear contact model, the Hertzian contact law considers that normal stiffness varies with the amount of overlap. This approach has been extended to cases in which colliding bodies tend to deform (constrained plastic deformation). Numerical models of interaction at the contact involve the force-deformation equation which is augmented with a damping term to reflect dissipation in the contact area.

Specific for this study, force-displacement laws at the contacts are represented by the Hertz-Mindlin no-slip contact model (Mindlin, 1949; Mindlin and Deresiewicz, 1953; Tsuji et

al., 1992; Di Renzo and Di Maio, 2004, 2005). This non-linear model features both the accuracy and simplicity derived from combining Hertz theory in the normal direction and Mindlin no-slip model in the tangential direction (Tsuji et al., 1992; Remy et al., 2009).

The normal force, F_n, is given as follows (Tsuji et al., 1992; Remy et al., 2009):

$$F_n = -K_n \delta_n^{3/2} - \eta_n \dot{\delta}_n \delta_n^{1/4} \tag{2.8}$$

where K_n is the normal stiffness coefficient; δ_n is the normal overlap or displacement; $\dot{\delta}_n$ is the normal velocity; and η_n is the normal damping coefficient. Normal stiffness and normal damping coefficients are given, respectively, by (Tsuji et al., 1992; DEM Solutions, 2009; Remy et al., 2009):

$$K_n = \frac{4}{3} E^* \sqrt{R^*} \tag{2.9}$$

$$\eta_n = \frac{\ln e}{\sqrt{\ln^2 e + \pi^2}} \sqrt{m^* K_n} \tag{2.10}$$

where E^* is the equivalent Young's modulus, R^* is the equivalent radius, m^* is the equivalent mass, and e as the coefficient of restitution. Equivalent properties (R^*, m^*, and E^*) during collision of particles with different materials such as particles i and j are defined as (Di Renzo and Di Maio, 2004; DEM Solutions, 2009):

$$R^* = \left(\frac{1}{R_i} + \frac{1}{R_j} \right)^{-1} \tag{2.11}$$

$$E^* = \left(\frac{1-\nu_i^2}{E_i} + \frac{1-\nu_j^2}{E_j} \right)^{-1} \tag{2.12}$$

$$m^* = \left(\frac{1}{m_i} + \frac{1}{m_j} \right)^{-1} \tag{2.13}$$

where ν is the Poisson's ratio (Di Renzo and Di Maio, 2004; DEM Solutions, 2009). Similarly, for a collision of a sphere i with a wall j, the same relations apply for Young's modulus E^*, whereas $R^* = R_i$ and $m^* = m_i$.

The tangential force, F_t, is governed by the following equation (Tsuji et al., 1992; Remy et al., 2009):

$$F_t = -K_t \delta_t - \eta_t \dot{\delta}_t \delta_n^{1/4} \tag{2.14}$$

where K_t is the tangential stiffness coefficient; δ_t is the tangential overlap; $\dot{\delta}_t$ is the tangential velocity; and η_t is the tangential damping coefficient. Tangential stiffness and tangential damping coefficients, are defined, respectively, as follows (Tsuji et al., 1992; DEM Solutions, 2009; Remy et al., 2009):

$$K_t = 8G^* \sqrt{R^* \delta_n} \tag{2.15}$$

$$\eta_t = \frac{\ln e}{\sqrt{\ln^2 e + \pi^2}} \sqrt{m^* K_t} \tag{2.16}$$

where G^* is the equivalent shear modulus defined by (Li et al, 2005):

$$G^* = \left(\frac{2-\nu_i}{G_i} + \frac{2-\nu_j}{G_j} \right)^{-1} \tag{2.17}$$

G_i and G_j are shear moduli of particles *i* and *j*, respectively. The tangential overlap is calculated by (Remy et al, 2009):

$$\delta_t = \int v_{rel}^t dt \tag{2.18}$$

where v_{rel}^t is the relative tangential velocity of colliding particles and is defined by (Remy et al., 2009):

$$v_{rel}^t = \left(v_i - v_j\right) \cdot s + \omega_i R_i + \omega_j R_j \tag{2.19}$$

where *s* is the tangential decomposition of the unit vector connecting the center of the particle.

Additionally there is a tangential force limited by Coulomb friction $\mu_s F_n$, where μ_s is the coefficient of static friction. When necessary, rolling friction can be accounted for by applying a torque to contacting surfaces. The rolling friction torque, τ_i, is given by (DEM Solutions, 2009; Remy et al., 2009):

$$\tau_i = -\mu_r F_n R_0 \omega_0 \tag{2.20}$$

where μ_r is the coefficient of rolling friction, R_0 is the distance of the contact point from the center of the mass, and ω_0 is the unit angular velocity vector of the object at the contact point (Tsuji et al., 1992; Di Renzo and Di Maio, 2004; Li et al., 2005; DEM Solutions, 2009; Remy et al., 2009).

For dynamic processes, important factors to consider are the propagation of elastic waves across the particles, the time for load transfer from one particle to adjacent contacting particles, and the need not to transmit energy across a system that is faster than nature (Li et al., 2005). In

the non-linear contact model (e.g., Hertzian), the critical time increment or critical time step cannot be calculated beforehand, unlike with the linear contact model in which the critical time step is related to the ratio of contact stiffness to particle density. Miller and Pursey (1955), however, showed that Rayleigh waves or surface waves account for 67% of the radiated energy, whereas dilational or pressure waves and distortional or shear waves, respectively, are 7% and 26% of the radiated energy. Thus, it is assumed that all of the energy is transferred by the Rayleigh waves since the difference between the speeds of the Rayleigh wave and the distortional wave is small and the energy transferred by the dilational wave is negligible (Li et al., 2005). Moreover, the average time of arrival of the Rayleigh wave at any contact is the same irrespective of the location of the contact point. For simplicity, the critical time step is based on the average particle size and a fraction of this is used in the simulations (Li et al., 2005; DEM Solutions, 2009). The critical time step is given by the following equation (Li et al., 2005; DEM Solutions, 2009):

$$t_c = \frac{\pi \overline{R}}{\beta} \sqrt{\frac{\rho_p}{G}} \tag{2.21}$$

where $\overline{R}$ is the average particle radius, ρ_p is the particle density, G is the particle shear modulus, and β can be approximated by (Li et al., 2005):

$$\beta = 0.8766 + 0.163\nu \tag{2.22}$$

2.2.9.2 History and Applications of DEM

The DEM was first introduced by Cundall (1971) when he employed a computer model for simulating progressive large-scale movements in blocky rock systems. In the model, realistic friction laws and simple stiffness parameters governed interaction between the blocks. The computer program allowed individual study of the effects of joint geometry, joint parameters, loading conditions, and excavation procedures. Its application was more fitted in rock situations in which general stresses were small (i.e., in near-surface excavations in heavily jointed rock) compared to when they were large (i.e., deep underground mines).

From then on, the DEM has been widely implemented to solve different engineering problems such as simulation of soil deformation and resistance at bar penetration (Tanaka et al., 2000), full-scale vehicle-soil interaction (Horner et al., 2001), green sand molding (Maeda et al., 2003), ore breakage in a semi-autogenous mill (Morrison and Cleary, 2004), large-scale

industries (Cleary, 2004), effect of lifter heights (Djordjevic, 2003) and vertical and horizontal shaft impact crushers (Djordjevic et al., 2003) on power consumption, and organic fertilizer land application (Landry et al., 2006a, b). A complete description of the DEM can be found in Williams et al. (1985), Cundall (1988), Hart et al. (1988), and Cundall and Hart (1989).

DEM applications that may be related to mixing or commingling of grains in bucket elevators were as follows. Hustrulid and Mustoe (1996) applied DEM to simulate bulk solids movement through transfer point in large industrial conveyor system in mining operations. The information obtained included the velocity distribution of the bulk solids and the stresses within them, and the impact forces acting on the transfer structure and the conveyor belts from the bulk solids flow. Hustrulid (1998) successfully simulated the position, velocity, and applied forces for every particle and boundary at increments of 10^{-5} seconds. Dewicki (2003) also modeled transfer points in conveyor systems using DEM and simulated the performance of a belt conveyor to improve its design.

Shimizu and Cundall (2001) examined the performance of horizontal- and vertical-type screw conveyors to transport spherical materials (instead of sand) by means of three-dimensional (3D) DEM. Simulation results were in good agreement with empirical equations and previous work on both screw conveyors.

Masson and Martinez (2000) performed a set of DEM simulations of the filling and the discharge of grains represented as circular particles (mean diameter = 10 mm, and particle density = 1190 $kg \cdot m^{-3}$) in a plane rectangular silo. Computed wall pressures at the end of filling were compared with analytical and finite-element results, and the influence of friction and stiffness on contacts was analyzed. Results showed these parameters play a major role in flow kinematics and in the stress field during filling and discharge processes.

Cleary (1998) simulated the filling of draglines buckets in open-cut coal mining by means of DEM. The DEM assisted in differentiating between the flow patterns for two competing bucket designs, evaluating the effect of rigging and variations in material properties, calculating fill times, estimating wear and its distribution, and determining regions of high compaction. The design of the buckets in the simulation model could be compared in terms of filling pattern and drag coefficient. Stability and motion of the buckets were found to be dependent upon the density and size distribution of the particles. It was concluded that such a discrete element model could become a tool to optimize bucket design.

Wightman et al. (1998) applied DEM to characterize particle mixing in a rotating cylinder. They compared rotational motion augmented with rocking to purely rotational motion via linear density profiles, velocity fields, and axial concentration profiles. The rocking motion dramatically enhanced mixing in laboratory studies and the simulation results agreed well with experimental results and observations.

Gyenis et al. (1999) investigated gravity flow of particles through a vertical tube containing a static mixer element through DEM, also called discrete particle simulation (DPS). In applying DPS, the authors were able to reproduce and explain theoretically the main characteristics of the flow regimes that they usually observed experimentally. They also obtained vast information that is hardly measurable by experiments. Some important features of the gas-solids two-phase flows were revealed regarding the re-dispersing effect of the static mixer elements, their potential to improve axial mixing, or the efficiency of other transport processes during pneumatic conveying.

Raji and Favier (2004a, b) used DEM to model the deformation of agricultural and food particulate materials under bulk compressive loading. They concluded that DEM was a useful tool in the study of the behavior of deformable soft particulates and the provision of data necessary in the design of appropriate machinery for agricultural processes.

Ketterhagen et al. (2008) investigated the causes and extent of segregation of granular materials during discharge from a hopper using DEM. They modeled a quasi-3D, wedge-shaped hopper using two parallel periodic boundary conditions. They found key factors affecting segregation during hopper discharge were particle diameter ratio, mass fraction, ratio of hopper outlet to mean particle diameter, sliding friction coefficient, and hopper wall angle and its roughness. The method used to fill the hopper also plays a significant role in determining segregation upon discharge.

Some of the most recent developments in DEM included representations of various particle shapes and configurations: (1) ellipse-based particles (Ting et al., 1993; Vu-Quoc et al., 2000; Ng, 2001); (2) axi-symmetrical and non-spherical particles (Favier et al., 1999, 2001); (3) arbitrary-shaped models and fully kinematic boundaries (Kremmer and Favier, 2000, 2001a, b); (4) noncircular-shaped granular media (Mustoe and Miyata, 2001); and (5) non-uniform-sized circular or spherical particles bonded together (Potyondy and Cundall, 2004).

2.2.10 Grain Material and Interaction Properties Relevant for DEM Modeling

Different DEM models have used varying parameters for simulation modeling. The most widely used parameters can be divided into two categories: material properties and interaction properties (Mohsenin, 1986; Vu-Quoc et al., 2000; Raji and Favier, 2004a, b). Material properties may be defined as intrinsic characteristics of the particle (i.e., grain kernels) being modeled. Material properties critical as inputs in DEM modeling are shape, size distribution, density, Poisson's ratio, and shear modulus. Interaction properties are characteristics exhibited by the particle in relation to its contact with boundaries, surfaces, and other (or same) particles. Interaction properties, vital in DEM modeling, are coefficients of restitution, and static and rolling friction (LoCurto et al., 1997; Chung et al., 2004).

2.2.10.1 Particle Shape and Particle Size

Shape and size are inseparable physical properties in a grain kernel. In defining shape, some dimensional parameters of the grain must be measured. Mohsenin (1986) and Nelson (2002) reported measuring three orthogonally oriented dimensions of 50 kernels randomly selected from a grain lot to determine kernel shape and size. Volume was taken as one of the parameters defining kernel shape, and the three mutually perpendicular axes were taken as a measure of kernel size.

2.2.10.2 Particle Density

Particle density (ρ_p) of the grain is determined by measuring the volume occupied by the kernels in a known sample weight randomly taken from each grain lot. Nelson (2002) measured the volume of an approximately 20- to 25-g sample with a Beckman model 930 air-comparison pycnometer. Kernel density was calculated by dividing the weighed mass by the measured volume. The number of kernels in the sample weighed for pycnometer measurements was manually counted to determine mean kernel weight and volume.

2.2.10.3 Particle Poisson's Ratio and Particle Shear Modulus

Poisson's ratio (ν) is the absolute value of the ratio of transverse strain (perpendicular to the axis) to the corresponding axial strain (parallel to the longitudinal axis) resulting from uniformly distributed axial stress below the proportional limit of the material (Mohsenin, 1986). Based on Hooke's law and together with Poisson's ratio, shear modulus or modulus of rigidity

(G) for an elastic, homogenous, and isotropic material is the ratio of the stress component tangential to the plane on which the forces acts (i.e., shear stress) over its strain. Shear modulus defined in terms of Poisson's ratio and Young's modulus or modulus of elasticity (E) is given by (Mohsenin, 1986):

$$G = \frac{E}{2 + 2\nu} \tag{2.23}$$

Several values of Poisson's ratio and elastic or Young's modulus for different grains and oilseeds were cited in the literature (Misra and Young, 1981; Mohsenin, 1986; Bilanski et al., 1994; Vu-Quoc et al., 2000; Chung et al., 2004; Raji and Favier, 2004a, b; Molenda and Horabik, 2005; Chung and Ooi, 2008). ASAE Standards S368.4 (2006b) enumerated values of Poisson's ratio and apparent modulus of elasticity for soybeans, corn, and wheat. The equations for apparent modulus of elasticity are based on Hertz equations for contact stresses used in solid mechanics, which assume that deformations are small and the material being compressed is elastic. They are, however, useful for making comparisons of the deformation behavior of viscoelastic materials, like grains, when the deformations and loading rates are similar for all samples tested.

For soybeans (Misra and Young, 1981) and wheat (Arnold and Roberts, 1969), apparent moduli of elasticity were calculated based on the parallel-plate contact method. For corn (Shelef and Mohsenin, 1969), the elastic modulus was obtained with a method using a spherical indenter on a curved surface.

2.2.10.4 Particle Coefficient of Restitution

Different methods have been used to determine the coefficient of restitution, e (Sharma and Bilanski, 1971; Smith and Liu, 1992; Yang and Schrock, 1994; LoCurto et al., 1997). Smith and Liu (1992) obtained e in three ways leading to the same value, as the (1) ratio of the normal component of impulse during compression and during restitution, (2) ratio of the normal component of approach (or impact) and separation (or rebound) velocities (Sharma and Bilanski, 1971; Yang and Schrock, 1994), and (3) ratio of work of normal components of reaction forces at the contact point during the compression phase and the work for the restitution phase (LoCurto et al., 1997).

LoCurto et al. (1997) described e as the square root of the total kinetic energy before (KE_i) and after (KE_r) collisions that did not involve tangential frictional losses. They measured

the *e* of soybeans impacting aluminum, glass, and acrylic at drop heights of 151, 292, and 511 mm and at moisture contents of 10.7% and 15.5%, dry basis (db). The *e* value decreased with increased moisture content and drop height, and contact with aluminum gave the highest value. Drop and rebound heights were measured only from those soybeans that fell with minimal rotation and whose rebound trajectories were almost vertical (90 ± 1.6% to the plate). This was different from the results of Yang and Schrock (1994), which involved cases of grain kernels with and without rotation. Assuming no loss of energy except during contact, the *e* value was computed as the ratio of the square root of the initial height of drop (H_i) and the height of rebound (H_r) (LoCurto et al., 1997; Zhang and Vu-Quoc, 2002):

$$e \equiv \left(\frac{KE_r}{KE_i} \right)^{\frac{1}{2}} \equiv \left(\frac{H_r}{H_i} \right)^{\frac{1}{2}} \tag{2.24}$$

2.2.10.5 Particle Coefficient of Static Friction

The coefficient of friction (μ) is the ratio of the force of friction (F) to the force normal to the surface of contact (W) (Mohsenin, 1986):

$$\mu = \frac{F}{W} \tag{2.25}$$

Frictional forces acting between surfaces at rest with respect to each other and those existing between the surfaces in relative motion are, respectively, called forces of static and kinetic friction. Static and kinetic coefficients of friction can be denoted by μ_s and μ_k, respectively (Mohsenin, 1986).

Several coefficients of static friction of grain-on-grain (Stahl, 1950; Mohsenin, 1986; Raji and Favier, 2004a, b) and grain-on-surfaces such as sheet metal, stainless steel, acrylic, aluminum, and glass (Brubaker and Pos, 1965; Mohsenin, 1986; Gupta and Das, 1997; Chung et al., 2004; Calisir et al., 2005; Molenda and Horabik, 2005; Chung and Ooi, 2008) were published in the literature. Static friction of soybean-steel contact is 67% of that of soybean on itself (Stahl, 1950).

2.2.10.6 Particle Coefficient of Rolling Friction

The coefficient of rolling friction (μ_r) is defined as the ratio of the force of friction to the force normal to the surface of contact that prevents a particle from rolling. Rolling friction or resistance can be a couple (or pure moment) that may be transferred between the grains via the

contacts, and this couple resists particle rotations (Jiang et al., 2005) without affecting translation. It may exist even at contacts between cylindrical grains (Bardet and Huang, 1993). The concept of taking into account rolling resistance at particle contacts is an alternative approach in DEM modeling to establish contact laws related to particle rotation (Jiang et al., 2005), instead of using non-spherical particles to inhibit particle rolling and produce a realistic rolling behavior (Rothenburg and Bathurst, 1992; Sawada and Pradhan, 1994; Ting et al., 1995; Ullidtz, 1997; Thomas and Bray, 1999; Ng, 2001; Mirghasemi et al., 2002; Mustoe and Miyata, 2001). In Jiang et al.'s (2005) micro-mechanical model, only the normal basic element, composed of a spring and dashpot in parallel with a divider series, contributes to rolling resistance at grain contact. Rolling resistance directly affects only the angular motion and not the translational motion of grains.

Zhou et al. (2002) investigated the effect of rolling friction on the angle of repose of coarse glass beads. They included coefficients of rolling friction with a base value of 0.05 (range: 0 - 0.1) on particle-to-particle contact and twice that value for particle-wall contact in their simulations. The authors found that increasing both rolling frictions increased the angle of repose. This is due to a large resistance force to the rotational motion of spheres providing an effective mechanism to consume the kinetic energy, stop the rotational motion, and lead to the formation of a "sand pile" with high potential energy (Zhou et al., 1999).

2.2.10.7 Bulk Density

Bulk density (ρ_b) is the ratio of the mass to a given volume of a grain sample including the interstitial voids between the particles (Hoseney and Faubion, 1992; Gupta and Das, 1997). In the U.S., bulk density or test weight per bushel is the weight (in lb) per Winchester bushel (2,150.42 in.^{3}) as determined using an approved device (USDA GIPSA, 2004). The USDA GIPSA (2004) method involves allowing a sufficient amount of grain from a hopper, suspended two inches above, to overflow the test weight kettle, leveling the kettle by three full-length, zigzag motions with a stroker, and weighing the grain from the kettle with an appropriate scale.

Bulk densities of most of the grain and seed lots from Nelson (2002) were tested for standard test weight using a Fairbanks Morse grain tester weight-per-bushel apparatus equipped with a one-quart measure. In Poland, Molenda and Horabik (2005) determined bulk density based on measurement of the mass of a granular material poured freely into a cylindrical container of constant volume, typically 0.25 or 1.0 L. In India, Gupta and Das (1997) measured

bulk density of sunflower seeds and kernels by filling a 500-mL container with grain from a height of 15 cm, striking the top level, and then weighing the contents. Several experimental ρ_b values for grains and oilseeds were found in the literature (Henderson and Perry, 1976; Mohsenin, 1986; Hoseney and Faubion, 1992; Shroyer et al., 1996; Gupta and Das, 1997; LoCurto et al., 1997; Nelson, 2002; Molenda and Horabik, 2005; *ASAE Standards*, 2006a).

2.2.10.8 Bulk Angle of Repose

Angle of repose (θ) is defined as the angle with the horizontal at which the granular material will stand when piled (Mohsenin, 1986; Hoseney and Faubion, 1992). The angle of repose of grains is determined by numerous factors which include frictional forces generated by the grain flowing against itself, distribution of weight throughout the grain mass, and moisture content of the grain (Hoseney and Faubion, 1992). At least two angles of repose are commonly defined, namely the static angle of repose and the dynamic angle of repose. The dynamic angle of repose is generally smaller than the static angle of repose by at least 3 - 10º (Fowler and Wyatt, 1960).

It is generally believed that the angle of repose and the angle of internal friction are approximately the same (Mohsenin, 1986; Walton, 1994). Fowler and Chodziesner (1959) derived an empirical equation for the coefficient of angle of friction using the tilting-box method. Fowler and Wyatt (1960) used a similar form to define the coefficient of the angle of repose. Fowler and Chodziesner's (1959) equation is of the form:

$$\mu = \tan\theta = a\, n_f^2 + b\sqrt{\frac{\varepsilon}{D_{avg}}} - c\,S + d \qquad (2.26)$$

where μ is the coefficient of angle of friction, θ is the angle of friction, n_f is the specific surface of the solid relative to a sphere, ε is roughness of the sliding surface, D_{avg} is the average screen particle diameter, S is specific gravity of the granular material, and a, b, c, and d are constants.

The term $\sqrt{\frac{\varepsilon}{D_{avg}}}$ is replaced by $\frac{M}{D_{avg}}$ by Fowler and Wyatt (1960) to define the coefficient of the angle of repose, with M as the added percentage moisture content. Fowler and Chodziesner (1959) noted that when the term, $\frac{\varepsilon}{D_{avg}}$, also called "relative roughness factor," is equal to unity (i.e., materials are sliding over themselves), the angle of repose is equal to the

angle of friction and is independent of the diameter of the granular material. The same holds true when $\frac{\varepsilon}{D_{avg}}$ is zero (i.e., smooth surface). Stewart (1968), however, showed that for at least one seed (i.e., grain sorghum), the angle of repose and internal friction are different.

There are several methods for measuring the angle of repose. The method to measure static angle includes (1) the fixed funnel and the free-standing cone, (2) the fixed-diameter cone and the funnel, and (3) the tilting box (Train, 1958). Fraczek et al. (2007) also referred to the first two methods, respectively, as "emptying," in which the material pours through the outlet in the container bottom (or fixed funnel) to form a free-standing cone, and "piling," in which the material flows onto a circular plate with a fixed diameter from an established height through a funnel and mounds up into a cone prism. The tilting-box or inclined-plane method has been used for rough rice (Kramer, 1944) and cereal grains (Burmistrova et al., 1963). In this method, the grain sample is placed inside a special box (i.e., wooden box with top side open) and placed on the upper part of an inclined plane, which has a base connected to a lifting mechanism. It is then tilted or lifted to a point at which the sample begins to move. The angle of the inclined surface when the sample begins to move is measured as the angle of repose of the particular sample.

For dynamic angle, the methods include (1) the revolving cylinder (Train, 1958) and (2) that of Brown and Richards (1959). In the revolving-cylinder method, a sealed hollow cylinder with one end transparent is half-filled with granular material and is made to revolve horizontally. The free surface of the granular material forms a diametrical plane. The angle of repose is the maximum angle that this plane makes with the horizontal on rotation of the container before the sample begins to cascade. Brown and Richards' (1959) method consists of a platform of fixed diameter immersed in a container of granular materials. The materials are allowed to escape from the box, leaving a free-standing cone of material on the platform. Fraczek et al. (2007) also named this method "submerging." Fowler and Wyatt (1960) employed this method to measure the effect of moisture content on the angle of repose of rape seed, wheat, sand, basalt chips, polythene chips, and canary seed.

Fraczek et al. (2007) also cited a fourth method in addition to "emptying," "piling," and "submerging." The method is called "pouring," where the grain is poured into a cylinder that is then slowly lifted up to allow the grain to mound up on the base and form a characteristic cone. The angle of repose is calculated based on cone height and diameter of the repose base measured

at four points on the cone's perimeter. The "pouring" method is another way of determining the angle of repose that minimizes inertial effects existing when the material is dropped from a height, gains sufficient kinetic energy and inertia near the mound peak, and then flattens considerably after the fill stream is stopped (Walton and Braun, 1993).

The four abovementioned methods are based on the assumption that the mounted granular slope acquires a cone shape, but results of experimental measurements often contradicted this assumption (Fraczek et al., 2007). In only a few cases did the authors witness the forming of a cone shape. Usually, depending on the properties of the granular materials, the following deviations from the cone shape were observed: truncation of the top, and convexity and concavity of slope. The authors recommended using digital-image analysis for a more precise measurement of angle of repose. Deviations from the cone shape increased with increasing moisture content of the material as was also noted by other authors (Horabik and Lukaszuk, 2000). However, the more spherical-like the materials, the more regular the cone that forms.

Zhou et al. (2002) found that the angle of repose of mono-sized coarse glass spheres is significantly affected by sliding and rolling frictions, particle size, and container thickness, but not density, Poisson's ratio, damping coefficient, or Young's modulus. The authors observed that the angle of repose increases with increasing rolling or sliding friction coefficients, and with decreasing particle size or container thickness. However, container thickness larger than a critical value (about a 20-particle diameter) gives a constant angle of repose corresponding to a situation without any wall effects. This was shown by simulation results with periodic boundaries applied to opposite walls of the container. Periodic boundary conditions enable any particle leaving the domain in that direction to instantly re-enter on the opposite side (DEM Solutions, 2009), simulating infinite length in that direction and, thereby eliminating wall friction. In addition, the effect of particle size was mainly the result of its effect on rolling friction and not on sliding friction.

Published angles of repose of grains and oilseeds for filling or piling and for emptying or funneling were found in the literature (Mohsenin, 1986; Gupta and Das, 1997; Molenda and Horabik, 2005; Boyles et al., 2006).

2.2.11 Summary

Customers around the globe demand for high quality and safe grains and their by-products. Challenges have increased with growth of the trait-specific market, proliferation of GM crops, and threats from biological and chemical attacks. Several researchers have recommended ways to identity preserve, segregate, label, and trace the grain to maintain its purity and determine its origin. Studies have also dealt with the economics of identity preserved handling and segregation, and specific measures to assess and prevent threats from genetically modified crop contamination and from biological and chemical weapons. Grain handling studies have examined the potential to segregate grains in different elevator sizes, the logistics and management strategies of grain receiving and loading operations, and grain commingling in various farm and elevator equipment.

However, studies on grain commingling (i.e., introduction of contaminants) in bucket elevators, even though it is identified as a critical node vulnerable to terrorist attack, are limited to two types of grain elevators (Ingles et al., 2003; 2006). Problems arise since full-scale tests of viable contaminant mixing in the actual grain handling system are unrealistic; and obtaining sufficient field data requires numerous resource-intensive experiments in grain elevators. Thus, a validated mechanistic model for predicting grain commingling in various types of elevator equipment is valuable for extending the knowledge of grain commingling beyond the few current experimental studies. The discrete element method with its capability to track individual particles is a proven way to simulate discrete objects like grain kernels, and to predict the movement and commingling of grains in bucket-elevator equipment.

2.3 References

Aarseth, K. A. 2004. Attrition of feed pellets during pneumatic conveying: the influence of velocity and bend radius. *Biosystems Engineering* 89(2): 197-213.

Aarseth, K. A., and E. Prestløkken. 2003. Mechanical properties of feed pellets: Weibull analysis. *Biosystems Engineering* 84(3): 349-361.

ACGIH. 1997. *1997 Threshold Limit Values and Biological Exposure Indices*. Cincinnati, Ohio: American Conference of Governmental Industrial Hygienists.

Adapa, P. K., L. G. Tabil, G. J. Schoenau, and S. Sokhansanj. 2004. Pelleting characteristics of fractionated, sun-cured, and dehydrated alfalfa grinds. *Applied Engineering in Agriculture* 20(6): 813-820.

Akao, Y., H. Kunisawa, L. T. Fan, F. S. Lai, and R. H. Wang. 1976. Degree of mixedness and contact number: a study on the mixture of particulate solids and the structure of solids mixtures. *Powder Technology* 15: 267-277.

Amornthewaphat, N., J. D. Hancock, K. C. Behnke, R. H. Hines, G. A. Kennedy, H. Cao, J. S. Park, C. S. Maloney, D. W. Dean, J. M. Derouchey, and D. J. Lee. 1999. Effects of feeder design and pellet quality on growth performance, nutrient digestibility, carcass characteristics, and water usage in finishing pigs. *Journal of Animal Science* 77(Suppl.1): 55.

Arnold, P. C., and A. W. Roberts. 1969. Fundamental aspects of load-deformation behavior of wheat grains. *Transactions of the ASAE* 12(1): 104-108.

ASAE Standards. 2003. S269.4: Cubes, pellets, and crumbles — definitions and methods for determining density, durability, and moisture content. St. Joseph, Mich.: ASAE.

ASAE Standards. 2006a. D241.4. Density, specific gravity, and mass-moisture relationships of grain for storage. St. Joseph, Mich.: ASAE.

ASAE Standards. 2006b. S368.4. Compression test of food materials of convex shape. St. Joseph, Mich.: ASAE.

Askin, T. 1998. The cost of grade segregating to primary elevators. Winnipeg, Canada: Canadian Grain Commission.

Baker, S., T. Herrman, and F. Fairchild. 1997. Capability of Kansas grain elevators to segregate wheat during harvest. Report of Progress 781. Manhattan, Kansas: Kansas State University Agricultural Experiment Station and Cooperative Extension Service.

Baker, K. D., R. L. Stroshine, K. J. Magee, G. H. Foster, and R. B. Jacko. 1986. Grain damage and dust generation in a pressure pneumatic conveying system. *Transactions of the ASAE* 29(2): 840-847.

Bardet, J. P., and Q. Huang. 1993. Rotational stiffness of cylindrical particle contacts. In *Powders and Grains 93*, 39-43. C. Thornton, ed. Rotterdam: Balkema.

Behnke, K. C. 1994. Processing factors influencing pellet quality. AFMA Matrix. South Africa: Animal Feed Manufacturers Association. Available at: http://www.afma.co.za. Accessed 26 April 2005.

Berruto, R., and D. E. Maier. 2000. Using modeling techniques to test the feasibility of GMO grain segregation and traceability at commercial elevators. In *Proceedings of the IFAC Conference: Modeling and Control in Agriculture, Horticulture, and Post-harvest Processing*, 339-344. 12-14 July 2000. Wageningen, The Netherlands.

Berruto, R., and D. E. Maier. 2001. Analyzing the receiving operation of different types of grain in a commercial elevator with a single pit. *Transactions of the ASAE* 44(3): 631-638.

Berruto, R., and D. E. Maier. 2002. Improvement of the grain elevator receiving operation by means of object-oriented simulation. ASAE Paper No. 026011. St. Joseph, Mich: ASAE.

Berruto, R., and D. E. Maier. 2004. Simulation of logistics effects during IP handling of quality grains. In *2004 International Quality Grains Conference Proceedings.* July 19-22. Indianapolis, Ind.: International Quality Grains Council.

Berruto, R., D. Ess, D. E. Maier, and F. Dooley. 2003. Network simulation of crops harvesting and delivery from farm field to commercial elevator. ASAE Publication No. 701P1103e. Electronic: Proc. Int. Conf. Crop Harvesting and Processing, 9 -11 February, Louisville, Ky. G.R. Quick, ed. St. Joseph, Mich.: ASAE.

Bilanski, W. K., B. Szot, I. Kushwaha, and A. Stepneiwski. 1994. Comparison of strength features of rape pods and seeds for varieties cultivated in various countries. *International Agrophysics* 8(4): 177-184.

Billate, R. D., R. G. Maghirang, and M. E. Casada. 2004. Measurement of particulate matter emissions from corn-receiving operations with simulated hopper-bottom trucks. *Transactions of the ASAE* 47(2): 521-529.

Boss, J. 1987. *Mieszanie materialow ziarnistych* (Polish). Warszawa-Wroclaw: Panstwowe Wydawn. Nauk. pp. 62-65.

Bouland, H. D. 1964. Selecting the best capacity of truck-receiving facilities for country grain elevators. USDA Marketing Research Report No. 671. Washington, D.C.: U.S. Department of Agriculture-Agricultural Research Service.

Boyles, M., T. Peeper, and M. Stamm. 2006. Great plains canola production handbook (MF-2734). Manhattan, Kansas: Kansas State University Cooperative Extension Service.

Brewer, C. E., P. R. Ferket, and T. S. Winowiski. 1989. The effect of pellet integrity and lignosulfonate on performance of growing tom. *Poultry Science* 68(Suppl.1): 18.

Brown, R. L., and J. C. Richards. 1959. Exploratory study of the flow of granules through apertures. *Chemical Engineering Research and Design (Transactions of the Institution of Chemical Engineers)* 37a: 108-119.

Brubaker, J. E., and J. Pos. 1965. Determining static coefficient of friction of grains on structural surfaces. *Transactions of the ASAE* 8(1): 53-55.

Buckwell, A., G. Brookes, and D. Bradley. 1998. *Economics of Identity Preservation for Genetically Modified Crops*. Wye, England: CEAS Consultants.

Bullock, D. S., M. Desquilbet, and E. I. Nitsi. 2000. The economics of non-GMO segregation and identity preservation. Urbana, Ill.: University of Illinois Department of Agricultural and Consumer Economics.

Burmistrova, M. F., I. K. Komol'kova, N. V. Klemm, M. T. Panina, I. M. Polunochev, A. I. P'yankov, A. F. Sokolov, N. G. Tetyanko, V. M. Chaus, and E. G. Eglit. 1963. *Physicomechanical Properties of Agricultural Crops.* Translated from Russian and published for the National Science Foundation. Jerusalem: Israel Program for Scientific Translations, Ltd.

Calisir, S., T. Marakoglu, H. Ogut, and O. Ozturk. 2005. Physical properties of rapeseed (Brassica napus oleifera L.). *Journal of Food Engineering* 69(1):61-66.

Campbell, H., and W. C. Bauer. 1966. Cause and care of demixing in solid-solid mixers. *Chemical Engineering* 73: 179-184.

Carter, C. A., and G. P. Gruere. 2003. International approaches to the labeling of genetically modified foods. *Choices* 18(2): 1-4. Available at: www.choicesmagazine.org. Accessed on 17 December 2009.

Cevallos, D. 2006. Wanted: labels for genetically engineered products. *Inter Press Service News Agency (IPS).* February 22. Available at: http://ipsnews.net/news.asp?idnews=32244. Accessed on 17 December 2009.

Chung, Y. C., J. Y. Ooi, and J. F. Favier. 2004. Measurement of mechanical properties of agricultural grains for DE models. In *17th ASCE Engineering Mechanics Conference.* Newark, Del.: American Society of Civil Engineers.

Chung, Y. C., and J. Y. Ooi. 2008. Influence of discrete element model parameters on bulk behavior of a granular solid under confined compression. *Particulate Science and Technology* 26(1): 83-96.

Cleary, P. W. 1998. The filling of dragline buckets. *Mathematical Engineering in Industry* 7(1): 1-24.

Cleary, P. W. 2004. Large-scale industrial DEM modelling. *Engineering Computations* 21(2-4): 169-204.

Converse, H. H., and S. R. Eckhoff. 1989. Corn dust emissions with repeated elevator transfers after selected drying treatment. *Transactions of the ASAE* 32(6): 2103-2107.

Cundall, P. A. 1971. A computer model for simulating progressive large-scale movements in blocky rock systems. In *Proceedings of the Symposium of the International Society of Rock Mechanics,* Vol. 1, Paper No. II-8: 132-150. Nancy, France: International Society of Rock Mechanics.

Cundall, P. A. 1988. Formulation of a three-dimensional distinct element method, part I: a scheme to detect and represent contacts in a system composed of many polyhedral blocks. *International Journal of Rock Mechanics and Mining Sciences and Geomechanics Abstracts* 25(3): 107-116.

Cundall, P. A., and R. D. Hart. 1989. Numerical modeling of discontinua. In *Proceedings of the 1st U.S. Conference on Discrete Element Methods*. G.G.W. Mustoe, M. Henriksen, and H.P. Huttelmaier, eds. Golden, Colo.: CSM Press.

Cundall, P. A., and O. D. L. Strack. 1979. A discrete numerical model for granular assemblies. *Geotechnique* 29(1): 47-65.

Dahl, B. L., and W. W. Wilson. 2002. The logistical costs of marketing identity preserved wheat (Report No. 495). Fargo, N.D.: North Dakota State University Department of Agribusiness and Applied Economics.

DEM Solutions. 2009. *EDEM 2.1.2 User Guide*. Lebanon, N.H.: DEM Solutions (USA), Inc. 138p.

Dewicki, G. 2003. Bulk material handling and processing – numerical techniques and simulation of granular material. *Bulk Solids Handling: International Journal of Storing and Handling Bulk Materials* 23(2): 110-113.

Di Renzo, A., and F. P. Di Maio. 2004. Comparison of contact-force models for the simulation of collisions in DEM-based granular flow codes. *Chemical Engineering Science* 59(3): 525-541.

Di Renzo, A., and F. P. Di Maio. 2005. An improved integral non-linear model for the contact of particles in distinct element simulations. *Chemical Engineering Science* 60(5): 1303-1312.

Djordjevic, N. 2003. Discrete element modeling of the influence of lifters on power draw of tumbling mills. *Minerals Engineering* 16(4): 331-336.

Djordjevic, N., F. N. Shi, and R. D. Morrison. 2003. Applying discrete element modeling to vertical and horizontal shaft impact crushers. *Minerals Engineering* 16(10): 983-991.

Dozier, W. A. 2001. Cost-effective pellet quality for meat birds. *Feed Management* 52(2): 21-24.

Dye, D. 2000. Building the identity preservation system of the future (speech presented at the 2000 Institute of Food Technologists). June. Available at: http://www.cargill.com/today/speeches. Accessed on 01 June 2006.

EU Committee. 2001. Position paper on proposed commission regulations on genetically modified food and feed, and the traceability and labeling of GMOs and labeling of derived food and feed products. Available at: www.eucommittee.be. Accessed on 01 June 2006.

Falck-Zepeda, J. B., G. Traxler, and R. G. Nelson. 2000. Rent creation and distribution from biotechnology innovations: the case of Bt Cotton and herbicide-tolerant soybeans in 1997. *Agribusiness* 16(1): 21-32.

Fan, L. T. 2001. Bulk-solids mixing: overview. In *Handbook of Conveying and Handling of Particulate Solids*, 647-658. A. Levy and H. Kalman, eds. Amsterdam, The Netherlands: Elsevier Science.

Fan, L. T., and R. H. Wang. 1975. On mixing indices. *Powder Technology* 11(1): 27-32.

Fan, L. T., S. J. Chen, and C. A. Watson. 1970. Solids mixing. *Annual Review of Industrial and Engineering Chemistry* 62: 53-69.

Fan, L. T., Y. M. Chen, and F. S. Lai. 1990. Recent developments in solids mixing. *Powder Technology* 61(3): 255-287.

Fan, L. T., J. R. Too, R. M. Rubison, and F. S. Lai. 1979. Studies on multicomponent solids mixing and mixtures, part III: mixing indices. *Powder Technology* 24(1): 73-89.

Favier, J. F., M. H. Abbaspour-Fard, and M. Kremmer. 2001. Modeling of nonspherical particles using multisphere discrete elements. *Journal of Engineering Mechanics* 127(10): 971-977.

Favier, J. F., M. H. Abbaspour-Fard, M. Kremmer, and A. O. Raji. 1999. Shape representation of axi-symmetrical, non-spherical particles in discrete element simulation using multi-element model particles. *Engineering Computations* 16(4): 467-480.

Fernandez-Cornejo, J., and W. McBride. 2000. Genetically engineered crops for pest management in U.S. agriculture. Agricultural Economics Report No. 786: 1-28. Washington, D.C.: U.S. Dept. of Agriculture Economic Research Service.

Fiscus, D. E., G. H. Foster, and H. H. Kaufman. 1971. Physical damage of grain caused by various handling techniques. *Transactions of the ASAE* 14(3): 480-485, 491.

Food Standards Agency. 2001. Your food — farm to fork: labeling of GM foods. Available at: www.foodstandards.gov.uk. Accessed on 20 February 2002.

Foster, G. H., and L. E. Holman. 1973. Grain breakage caused by commercial handling method. USDA Res. Serv. Mrktg. Res. Rpt. No. 968. Washington, D.C.: U.S. Department of Agriculture-Agricultural Research Service.

Fowler, R. T., and W. B. Chodziesner. 1959. The influence of variables upon the angle of friction of granular materials. *Chemical Engineering Science* 10: 157-162.

Fowler, R. T., and F. A. Wyatt. 1960. The effect of moisture content on the angle of repose of granular solids. *Australian Journal for Chemical Engineers* 1: 5-8.

Fraczek, J., A. Zlobecki, and J. Zemanek. 2007. Assessment of angle of repose of granular plant material using computer-image analysis. *Journal of Food Engineering* 83(1): 17-22.

Garrett, D. W., F. S. Lai, and L. T. Fan. 1982. Minimum explosible concentration as affected by particle size and composition. ASAE Paper No. 823580. St. Joseph, Mich.: ASAE.

Geldhart, D., N. Harnby, and A. C. Wong. 1984. Fluidization of cohesive powders. *Powder Technology* 37: 25-37.

Good, D. 2006. Soybean meal consumption drops. *Weekly Outlook: Soybeans*. Available at: http://www.aces.uiuc.edu/news/stories/news3662.html. Accessed on 01 June 2006.

Gosnell, D. 2001. Non-GM wheat segregation strategies: comparing the costs. Unpublished MS thesis. Saskatoon, Canada: University of Saskatchewan.

Greenlees, W. J., and S. C. Shouse. 2000. Estimating grain contamination from a combine. ASAE Paper No. MC00103. St. Joseph, Mich.: ASAE.

Gruere, G. P., and S. R. Rao. 2007. A review of international labeling policies of genetically modified food to evaluate India's proposed rule. *AgBioForum* 10(1): 51-64.

Gupta, R. K., and S. K. Das. 1997. Physical properties of sunflower seeds. *Journal of Agricultural Engineering Research* 66(1): 1-8.

Gustafson, M. L. 1959. The durability test — a key to handling wafers and pellets. ASAE Paper No. 59621. St. Joseph, Mich.: ASAE.

Gyenis, J., Zs. Ulbert, J. Szepvolgyi, and Y. Tsuji. 1999. Discrete particle simulation of flow regimes in bulk-solids mixing and conveying. *Powder Technology* 104(3): 248-257.

Hanna, H. M., D. H. Jarboe, and G. R. Quick. 2006. Grain residuals and time requirements for combine cleaning. ASAE Paper No. 066082. St. Joseph, Mich.: ASAE.

Hanrahan, T. J. 1984. Effect of pellet size and pellet quality on pig performance. Animal *Feed Science and Technology* 10(4): 277.

Harnby, N., M. F. Edwards, and A. W. Nienow. 1985. *Mixing in the Process Industries*. London: Butterworths.

Hart, R., P. A. Cundall, and J. Lemos. 1988. Formulation of a three-dimensional, distinct element method, part II: mechanical calculations for motion and interaction of a system composed of many polyhedral blocks. *International Journal of Rock Mechanics and Mining Sciences and Geomechanics Abstracts* 25(3): 117-125.

Henderson, S. M., and R. L. Perry. 1976. *Agricultural Process Engineering*. 3rd. ed. Westport, Conn.: The AVI Publishing Company. 430p.

Herrman, T. J., S. Baker, and F. J. Fairchild. 2001. Characterization of receiving systems and operating performance of Kansas grain elevators during wheat harvest. *Applied Engineering in Agriculture* 17(1): 77-82.

Herrman, T. J., M. Boland, and A. Heishman. 1999. Economic feasibility of wheat segregation at country elevators. 1999. In *The 2nd Annual National Wheat Industry Research Forum Proceedings*. Vol. 1, 13-16. February 4-5. Nashville, Tennessee.

Herrman, T. J., M. Boland, K. Agrawal, and S. Baker. 2002. Use of a simulation model to evaluate wheat segregation strategies for country elevators. *Applied Engineering in Agriculture* 18(1): 105-112.

Hersey, J. A. 1974. Powder mixing by frictional pressure: specific example of the use of ordered mixing. *Journal of Pharmaceutical Sciences* 63(12): 1960.

Hersey, J. A. 1976. Powder mixing: theory and practice in pharmacy. *Powder Technology* 15: 149-153.

Hirai, Y., M. D. Schrock, D. L. Oard, and T. J. Herrman. 2006. Delivery system of tracing caplets for wheat-grain traceability. *Applied Engineering in Agriculture* 22(5): 747-750.

Horabik, J., and J. Lukaszuk. 2000. Measurement of internal friction angle of wheat grain using triaxial compression test. *Acta Agrophysica* 37: 39-49 (in Polish).

Horner, D. A., J. F. Peters, and A. Carillo. 2001. Large-scale discrete element modeling of vehicle-soil interaction. *Journal of Engineering Mechanics* 127(10): 1027-1032.

Hoseney, R. C., and J. M. Faubion. 1992. Chapter 1: Physical properties of cereal grains. In *Storage of Cereal Grains and Their Products*. 4th. ed. D. B. Sauer, ed. St. Paul, Minn.: American Association of Cereal Chemists, Inc.

Hurburgh, C. R., Jr. 1999. The GMO controversy and grain handling for 2000. Paper presented at the Iowa State University Integrated Crop Management Conference. Available at: http://www.exnet.iastate.edu/Pages/grain/gmo/ 99gmoy2k.pdf. Accessed on 21 June 2006.

Hurburgh, C. R., Jr., J. L. Neal, M. L. McVea, and P. Baumel. 1994. The capability of elevators to segregate grain by intrinsic quality. ASAE Paper No. 946050. St. Joseph, Mich.: ASAE.

Hustrulid, A. I. 1998. Transfer station analysis. Paper presented at the 1998 SME Annual Meeting, Orlando, Fla., February 1998. Available at: http://www.chutemaven.com. Accessed on: August 10, 2006.

Hustrulid, A. I., and G. G. W. Mustoe. 1996. Engineering analysis of transfer points using discrete element analysis. Paper presented at the 1996 SME Annual Meeting, Phoenix, Ariz., February 1996. Available at: http://www.chutemaven.com. Accessed 10 August 2006.

Ingles, M. E. A., M. E. Casada, and R. G. Maghirang. 2003. Handling effects on commingling and residual grain in an elevator. *Transactions of the ASAE* 46(6): 1625-1631.

Ingles, M. E. A., M. E. Casada, R. G. Maghirang, T. J. Herrman and J. P. Harner, III. 2006. Effects of grain-receiving system on commingling in a country elevator. *Applied Engineering in Agriculture* 22(5): 713-721.

Jacobsen, M., J. Nagy, A. R. Cooper, and F. J. Ball. 1961. Explosibility of agricultural dusts. U.S Bureau of Mines - Report of Investigations No. 5753. Washington, D.C.: U.S. Department of Interior Bureau of Mines.

James, C. 2004. Global status of commercialized biotech/GM crops: 2004. ISAAA Briefs No. 32-2004. Available at: http://www.isaaa.org. Accessed on 15 January 2005.

James, C. 2008. Global status of commercialized biotech/GM crops: 2008. ISAAA Briefs No. 39-2008. Available at: http://www.isaaa.org/resources/publications/briefs/39/executivesummary/default.html. Accessed 22 May 2009.

Jensen, A. H., and D. E. Becker. 1965. Effect of pelleting diets and dietary components on the performance of young pigs. *Journal of Animal Science* 24(2): 392-397.

Jensen, L. S., L. H. Merrill, C. V. Reddy, and J. McGinnis. 1962. Observation on eating patterns and rate of food passage of birds fed pelleted and unpelleted diets. *Poultry Science* 41(5): 1414-1419.

Jiang, M. J., H. S. Yu, and D. Harris. 2005. A novel discrete model for granular material incorporating rolling resistance. *Computers and Geotechnics* 32(5): 340-357.

Jirik, P. J. 1994. Identity preserved grain marketing. Unpublished MS thesis. Winnona, Minn.: Saint Mary's College.

Joy, D. 2003. Regulatory issues: E.U. issues new GMO regulations. Available at: http://www.foodprocessing.com/articles/2003/197.html. Accessed on 27 June 2006.

Kaye, B. H. 1989. *A Random Walk Through Fractal Dimensions*. Weinheim, Germany: VCH Publishers.

Kaye, B. H. 1997. *Powder Mixing*. London: Chapman and Hall.

Kenkel, P., and R. Noyes. 1995. Summary of OSU grain elevator dust-emission study and proposed grain elevator emission factors. Report to the Oklahoma Air Quality Council. Stillwater, Okla: Oklahoma State University.

Kertz, A. F., B. K. Darcy, and L. R. Prewitt. 1981. Eating rate of lactating cows fed four physical forms of the same grain ration. *Journal of Dairy Science* 64(12): 2388-2391.

Ketterhagen, W. R., J. S. Curtis, C. R. Wassgren, and B. C. Hancock. 2008. Modeling granular segregation in flow from quasi-three-dimensional, wedge-shaped hoppers. *Powder Technology* 179(3): 126-143.

Kilman, S., and J. Carroll. 2002. Monsanto says crops may contain genetically modified canola seed. *The Wall Street Journal*. Available at: http://www.connectotel. com/gmfood/ monsanto.html. Accessed 15 May 2008.

Kramer, H. A. 1944. Factors influencing the design of bulk storage bins for rough rice. *Agricultural Engineering* 25: 463-466.

Kremmer, M., and J. F. Favier. 2000. Calculating rotational motion in discrete element modeling of arbitrary-shaped model objects. *Engineering Computations* 17(6):703-714.

Kremmer, M., and J. F. Favier. 2001a. A method of representing boundaries in discrete element modeling, part I: geometry and contact detection. *International Journal for Numerical Methods in Engineering* 51(12): 1407-1421.

Kremmer, M., and J. F. Favier. 2001b. A method of representing boundaries in discrete element modeling, part II: kinematics. *International Journal for Numerical Methods in Engineering* 51(12): 1423-1436.

Lacey, P. M. C. 1943. The mixing of solid particles. *Transactions of the Institute of Chemical Engineers* 21: 53-59.

Lacey, P. M. C. 1954. Developments in the theory of particles mixing. *Journal of Applied Chemistry* 4: 257-268.

Lai, F. S., D. W. Garrett, and L. T. Fan. 1984. Study of mechanisms of grain dust explosion as affected by particle size and composition, part 2: characterization of particle size and composition of grain dust. *Powder Technology* 39(2): 263-278.

Landry, H., C. Lague, and M. Roberge. 2006a. Discrete element modeling of machine-manure interactions. *Computers and Electronics in Agriculture* 52(1-2): 90-106.

Landry, H., F. Thirion, C. Lague, and M. Roberge. 2006b. Numerical modeling of the flow of organic fertilizers in land application equipment. *Computers and Electronics in Agriculture* 51(1-2): 35-53.

Larsen, T. B., S. Sokhansanj, R. T. Patil, and W. J. Crerar. 1996. Breakage susceptibility studies on alfalfa and animal feed pellets. *Canadian Agricultural Engineering* 38(1): 21-24.

Li, Y., Y. Xu, and C. Thornton. 2005. A comparison of discrete element simulations and experiments for 'sandpiles' composed of spherical particles. *Powder Technology* 160(3): 219-228.

Lin, W. W., W. Chambers, and J. Harwood. 2000. Biotechnology: U.S. grain handlers look ahead. *Agricultural Outlook,* April. Washington, D.C.: U. S. Department of Agriculture.

LoCurto, G. J., X. Zhang, V. Zarikov, R. A. Bucklin, L. Vu-Quoc, D. M. Hanes, and O. R. Walton. 1997. Soybean impacts: experiments and dynamic simulations. *Transactions of the ASAE* 40(3): 789-794.

Maeda, Y., Y. Maruoka, H. Makino, and H. Nomura. 2003. Squeeze modeling simulation using discrete element method considering green sand properties. *Journal of Materials Processing Technology* 135(2-3): 172-178.

Maltsbarger, R., and N. Kalaitzandonakes. 2000. Studies reveal hidden costs in IP supply chain. *Feedstuffs* 72(36): 1, 31.

Marra, M. C., P. G. Pardey, and J. M. Alston. 2002. The payoffs to agricultural biotechnology – an assessment of the evidence. Washington, D.C.: Environment and Production Technology Division (EBTD), International Food Policy Research Institute, 87: 1-57.

Martin, C. R. 1981. Characterization of grain dust properties. *Transactions of the ASAE* 24(3): 738-742.

Martin, C. R., and F. S. Lai. 1978. Measurement of grain dustiness. *Cereal Chemistry* 55(5): 779-792.

Martin, C. R., and D. B. Sauer. 1976. Physical and biological characteristics of grain dust. *Transactions of the ASAE* 19(4): 720-723.

Martin, C. R., and L. E. Stephens. 1977. Broken corn and dust generated during repeated handling. *Transactions of the ASAE* 20(1): 168-170.

Masson, S., and J. Martinez. 2000. Effect of particle mechanical properties on silo flow and stresses from distinct element simulations. *Powder Technology* 109(1-3): 164-178.

McPhee, T. L., and A. Bourget. 1995. Cost of grain and grade segregation at terminal elevators in Canada. Winnipeg, Canada: Canadian Grain Commission.

Midwest Research Institute. 1998. Emission-factor documentation for AP-42. Section 9.9.1 Grain Elevators and Grain Processing Plants: Final Report to US EPA Contract 68-D2-0159. Research Triangle Park, N.C.: U.S. Environmental Protection Agency.

Miller, G. F., and H. Pursey. 1955. On the partition of energy between elastic waves in a semi-infinite solid. *Proceedings of the Royal Society of London Series A: Mathematical and Physical Sciences* 233(1192): 55-69.

Mindlin, R. 1949. Compliance of elastic bodies in contact. *Journal of Applied Mechanics* 16: 259-268.

Mindlin, R. D., and H. Deresiewicz. 1953. Elastic spheres in contact under varying oblique forces. *Transactions of ASME, Series E. Journal of Applied Mechanics* 20: 327-344.

Mirghasemi, A. A., L. Rothenburg, and E. L. Matyas. 2002. Influence of particle shape on engineering properties of assemblies of two-dimensional polygon-shaped particles. *Geotechnique* 52(3): 209-217.

Mishra, B. K. 2003. A review of computer simulation of tumbling mills by the discrete element method: part I – contact mechanics. *International Journal of Mineral Processing* 71(1-4): 73-93.

Misra, R. N., and J. H. Young. 1981. A model for predicting the effect of moisture content on the modulus of elasticity of soybeans. *Transactions of the ASAE* 24(5): 1338-1341, 1347.

Mohsenin, N. N. 1986. *Physical Properties of Plant and Animal Materials*. 2nd ed. New York: Gordon and Breach Science Publishers.

Molenda, M., and J. Horabik. 2005. Characterization of mechanical properties of particulate solids for storage and handling. Part 1. In *Mechanical Properties of Granular Agro-Materials and Food Powders for Industrial Practice*. J. Horabik and J. Laskowski. eds. Lublin: Institute of Agrophysics Polish Academy of Sciences.

Morrison, R. D., and P. W. Cleary. 2004. Using DEM to model ore breakage within a pilot-scale SAG mill. *Minerals Engineering* 17(11-12): 1117-1124.

Mustoe, G. G. W., and M. Miyata. 2001. Material flow analyses of noncircular-shaped granular media using discrete element method. *Journal of Engineering Mechanics* 127(10): 1017-1026.

Nelson, S. O. 2002. Dimensional and density data for seeds of cereal grain and other crops. *Transactions of the ASAE* 45(1): 165-170.

Nelson, G. C., T. Josling, D. Bullock, L. Unnevehr, M. Rosegrant, and L. Hill. 1999. The economics and politics of genetically modified organisms in agriculture: implications for WTO 2000 (Bulletin 809). Urbana, Ill.: University of Illinois Office of Research Consumer and Environmental Science Department.

Ng, T. T. 2001. Fabric evolution of ellipsoidal arrays with different particle shapes. *Journal of Engineering Mechanics* 127(10): 994-999.

Nielsen, R. L. 2000. Minimizing pollen drift and commingling of GMO and non-GMO corn grain. The Chat ‘n Chew Café. West Lafayette, Ind.: Department of Agronomy, Purdue University. Available at: www.kingcorn.org/news/articles.00 /GMO_Issues-000307.html. Accessed on: 03 January 2005.

NIOSH. 1983. Occupational Safety in Grain Elevators and Feed Mills. Washington, D.C.: National Institute for Occupational Safety and Health. Available at: www.cdc.gov/ niosh/pubs/criteria _date_asc_nopubnumbers.html. Accessed 30 January 2008.

Noyes, R. T. 1998. Preventing grain dust explosions. Current Report-1737. Stillwater, Okla.: Oklahoma Cooperative Extension Service. Available at: www.osuextra.okstate.edu/pdfs/CR-1737web.pdf. Accessed 01 April 2008.

Ottino, J. M. 1989. The mixing of fluids. *Scientific American* 258(1): 56-67.

Ottino, J. M. 1990. *The Kinematics of Mixing: Stretching Chaos and Transport.* Cambridge: Cambridge University Press.

Ottino, J. M., C. W. Leong, H. Rising, and P. D. Swanson. 1988. Morphological structures produced by mixing in chaotic flows. *Nature* 333(6172): 419-425.

Palmer, K. N. 1973. *Dust Explosions and Fires*. London, England: Chapman and Hall.

Parnell, Jr. C. B., D. D. Jones, R. D. Rutherford, and K. J. Goforth. 1986. Physical properties of five grain dust types. *Environmental Health Perspectives* 66: 183-188.

Parzen, E. 1962. *Stochastic Processes*. San Francisco, Cal.: Holden Day, Inc.

Pehanich, M. 2005. Race to traceability. Itasca, Ill.: Food Processing. Available at: http://www.foodprocessing.com/articles/2005/368.html. Accessed on 31 May 2006.

Phillips, P. W. B., and H. McNeill. 2000. A survey of national labeling policies for GM foods. *AgBioforum* 3(4): 219-224. Available at: www.agbioforum.org/v3n4/v3n4a07-phillipsmcneill.htm. Accessed on 27 June 2006.

Piacitelli, C. A., and W. G. Jones. 1992. Health Hazard Evaluation (HHE) Report No. 92-0122-2570. Available at: www.cdc.gov/niosh/hhe/reports/pdfs/1992-0122-2570.pdf. Accessed 31 March 2008.

Potyondy, D. O., and P. A. Cundall. 2004. A bonded-particle model for rock. *International Journal of Rock Mechanics and Mining Sciences* 41(8): 1329-1364.

Poux, M. P., P. Fayolle, J. Bertrand, D. Bridoux, and J. Bousquet. 1991. Powder mixing: some practical rules applied to agitated systems. *Powder Technology* 68(3): 213-234.

Price, G. K., W. Lin, J. B. Falck-Zepeda, and J. Fernandez-Cornejo. 2003. Size distribution of market benefits from adopting biotech crops. Technical Bulletin No. 1906: 1-40. Washington, D.C.: U.S. Department of Agriculture Economic Research Service.

Raji, A. O., and J. F. Favier. 2004a. Model for the deformation in agricultural and food particulate materials under bulk compressive loading using discrete element method, part I: theory, model development and validation. *Journal of Food Engineering* 64(3): 359-371.

Raji, A. O., and J. F. Favier. 2004b. Model for the deformation in agricultural and food particulate materials under bulk compressive loading using discrete element method, part II: compression of oilseeds. *Journal of Food Engineering* 64(3): 373-380.

Remy, B., J. G. Khinast, and B. J. Glasser. 2009. Discrete element simulation of free-flowing grains in a four-bladed mixer. *AIChE Journal* 55(8): 2035-2048.

Roseman, B., and M. B. Donald. 1962. Mixing and demixing of solid particles, part II: effect of varying the operating conditions of a horizontal drum mixer. *British Chemical Engineering.* 7: 823-827.

Rosentrater, K. A., and C. J. Bern. 2002. Framework for computer simulation model of terminal elevators. ASAE Paper No. MC02104. St. Joseph, Mich.: ASAE.

Rothenburg, L., and R. J. Bathurst. 1992. Micromechanical features of granular assemblies with planar elliptical particles. *Geotechnique* 42(1): 79-95.

Sawada, S., and T. B. S. Pradham. 1994. Analysis of anisotropy and particle shape by distinct element method. In *Computer Methods and Advancements in Geomechanics*, Vol. 1, 665-670. Siriwardane, H. and M. M. Zaman, eds. Rotterdam, The Netherlands: Balkema.

Sharma, R. K., and W. K. Bilanski. 1971. Coefficient of restitution of grains. *Transactions of the ASAE* 14(2): 216-218.

Shaw, B. W., P. P. Buharivala, C. B. Parnell Jr., and M. A. Demny. 1998. Emission factors for grain-receiving and feed-loading operations at feed mills. *Transactions of the ASAE* 41(3): 757-765.

Sheldon, I. A. 2002. Regulation of biotechnology: will we ever “freely” trade GMOs? *European Review of Agricultural Economics* 29(1): 155-176.

Shelef, L., and N. N. Mohsenin. 1969. Effect of moisture content on mechanical properties of shelled corn. *Cereal Chemistry* 46(3): 242-253.

Shimizu, Y., and P. A. Cundall. 2001. Three-dimensional DEM simulations of bulk handling by screw conveyors. *Journal of Engineering Mechanics* 127(9): 864-872.

Shindo, H., T. Yoshizawa, Y. Akao, L. T. Fan, and F. S. Lai. 1978. Estimation of mixing index and contact number by spot sampling of a mixture in an incompletely mixed state. *Powder Technology* 21(1): 105-111.

Shroyer, J. P., P. D. Ohlenbusch, S. Duncan, C. Thompson, D. L. Fjell, G.L. Kilgore, R. Brown, and S. Staggenborg. 1996. Kansas crop planting guide (L-818). Manhattan, Kansas: Kansas State University Cooperative Extension Service.

Smith, C. E., and P. Liu. 1992. Coefficient of restitution. *Journal of Applied Mechanics* 59(4): 963-969.

Smyth, S., and P. W. B. Phillips. 2001. Identity-preserving production and marketing systems in the global agri-food market: implications for Canada. Saskatoon, Canada: University of Saskatchewan.

Sokhansanj, S., and W. J. Crerar. 1999. Development of a durability tester for pelleted and cubed animal feed. SAE 1999-01-2830. *Agriculture Machinery, Tires, Tracks, and Traction* SP-1474: 83-87.

Sonka, S. R., C. Schroeder, and C. Cunningham. 2000. Transportation, handling, and logistical implications of bioengineered grains and oilseeds: a prospective analysis. In *Agricultural Transportation Challenges of the 21st Century*. USDA Agricultural Marketing Service, Washington, D.C. and National Soybean Research Laboratory, Urbana-Champaign, Ill., November.

Sparks Company. 2000. The IP future: Identity preservation in North American agriculture. Memphis, Tenn.: Sparks Company.

Stahl, B. M. 1950. Grain bin requirements. USDA Circular 835. Washington, D.C.: U.S. Department of Agriculture.

Staniforth, J. N. 1982. Determination and handling of total mixes in pharmaceutical systems *Powder Technology* 33(2): 147-159.

Stewart, B. R. 1968. Effect of moisture content and specific weight on internal-friction properties of sorghum grain. *Transactions of the ASAE* 11(2): 260-266.

Sundstrom, F. J., J. Williams, A.Van Deynze, and K. J. Bradford. 2002. Identity preservation of agricultural commodities. Agricultural Biotechnology in California Series Publication No. 8077. Available at: anrcatalog.ucdavis.edu/pdf/8077.pdf. Accessed on 01 June 2006.

Tanaka, H., M. Momozu, A. Oida, and M. Yamazaki. 2000. Simulation of soil deformation and resistance at bar penetration by the distinct element method. *Journal of Terramechanics* 37(1): 41-56.

Taylor, M. R., and J. S. Tick. 2001. StarLink case: issues for the future. Pew Initiative on Food and Biotechnology. October. Available at: http://pewagbiotech.org/ resources/issuebriefs/starlink/starlink.pdf. Accessed on 30 October 2004.

Theuerkauf, J., S. Dhodapkar, and K. Jacob. 2007. Modeling granular flow using discrete element method – from theory to practice. *Chemical Engineering* 114(4): 39-46.

Thomas, P. A., and J. D. Bray. 1999. Capturing nonspherical shape of granular media with disk clusters. *Journal of Geotechnical and Geoenvironmental Engineering* 125(3): 169-178.

Ting, J. M., M. Khwaja, L. R. Meachum, and J. D. Rowell. 1993. An ellipse-based, discrete element model for granular materials. *International Journal for Numerical and Analytical Methods in Geomechanics* 17(9): 603-623.

Ting, J. M., L. R. Meachum, and J. D. Rowell. 1995. Effect of particle shape on the strength and deformation mechanism of ellipse-shaped granular assemblages. *Engineering Computations* 12(2): 99-108.

Too, J. R., L. T. Fan, and F. S. Lai. 1978. Mixtures and mixing of multicomponent solid particles – a review. *Journal of Powder and Bulk Solids Technology* 2(4): 2-8.

Too, J. R., R. M. Rubison, L. T. Fan, and F. S. Lai. 1979. Studies on multicomponent solids mixing and mixtures. II. Estimation of mixing index and contact number by spot sampling of a multicomponent mixture in an incompletely mixed state. *Powder Technology* 23(1): 99-113.

Too, J. R., L. T. Fan, R. M. Rubison, and F. S. Lai. 1980. Applications of nonparametric statistics to multicomponent solids mixing. *Powder Technology* 26(2): 131-146.

Train, D. J. 1958. Some aspects of the property of angle of repose of powders. *Journal of Pharmacy and Pharmacology (Supplement)* 10: 127-135.

Tsuji, Y., T. Tanaka, and T. Ishida. 1992. Lagrangian numerical simulation of plug flow of cohesionless particles in a horizontal pipe. *Powder Technology* 71(3): 239-250.

Uhl, V. W., and J. B. Gray. 1986. *Mixing.* Vols. 1-3. Orlando, Fla.: Academic Press, Inc.

Ullidtz, P. 1997. Modelling of granular materials using the discrete element method. In *Proceedings of the 8th International Conference on Asphalt Pavements*, Vol. 1, 757-769. August 10-14. Seattle, Wash.: University of Washington.

USDA ERS. 2001. Economic issues in agriculture biotechnology. ERS Agricultural Information Bulletin No. AIB762. Washington, D.C.: U.S. Department of Agriculture Economic Research Service.

USDA FAS. 2008. EU-27 Biotechnology Annual Report. GAIN Report No. E48082. Washington, D.C.: U.S. Department of Agriculture Foreign Agricultural Service.

USDA FAS. 2009. Foreign Agricultural Service Attaché Reports for multiple countries. Available at: www.fas.usda.gov/scriptsw/attacherep/default.asp. Accessed 17 December 2009.

USDA GIPSA. 2004. *Grain Inspection Handbook, Book II, Grain Grading Procedures*. Washington, D.C.: USDA Grain Inspection, Packers, and Stockyards Administration, Federal Grain Inspection Service.

US EPA. 1990. The Clean Air Act. Research Triangle Park, N.C.: U.S. Environmental Protection Agency. Available at: www.epa.gov/air/caa. Accessed 29 May 2008.

US EPA. 2003. Grain Elevator and Processes. In *Chapter 9: Food and Agricultural Industries. Emission Factors/ AP-42*. 5th ed. Vol. I. Research Triangle Park, N.C.: U.S. Environmental Protection Agency. Available at: www.epa.gov/ ttn/chief/ap42/ch09/index.html. Accessed 29 May 2008.

US EPA. 2007. Particulate Matter (PM) Standards. Research Triangle Park, N.C.: U.S. Environmental Protection Agency. Available at: www.epa.gov/pm/ standards.html. Accessed 31 March 2008.

US FDA. 2006. Strategic Partnership Program Agroterrorism (SPPA) Initiative. First-Year Status Report. September 2005 - June 2006. Silver Spring, Md.: U.S. Food and Drug Administration. Available at: http://www.cfsan.fda.gov/~dms/agroter5.html. Accessed 15 May 2007.

Vu-Quoc, L., X. Zhang, and O. R. Walton. 2000. A 3-D, discrete-element method for dry granular flows of ellipsoidal particles. *Computer Methods in Applied Mechanics and Engineering* 187(3-4): 483-528.

Wallace, D. 2000. Grain handling and processing. In *Air Pollution Engineering Manual*, 463-473. W. T. Davis, ed. New York: John Wiley & Sons.

Walton, O. R. 1994. Effects of interparticle friction and particle shape on dynamic angles of repose via particle-dynamic simulation. Presented at the Workshop on Mechanics and Statistical Physics of Particulate Materials, June 8-10, La Jolla, Cal.

Walton, O. R., and R. L. Braun. 1993. Simulation of rotary-drum and repose tests for frictional spheres and rigid-sphere clusters. In *Proceedings of DOE/NSF Workshop on Flow of Particulates and Fluids*, Sept. 29-Oct. 1, Ithaca, N.Y.

Wang, R. H., and L. T. Fan. 1974. Methods of scaling-up tumbling mixers. *Chemical Engineering* 81(11): 88-94.

Weidenbaum, S. S., and C. F. Bonilla. 1955. A fundamental study of the mixing of particulate solids. *Journal of Chemical Engineering Progress* 51: 27-36.

Weinekotter, R., and H. Gericke. 2000. *Mixing of Solids*. Dordrecht, The Netherlands: Kluwer Academic Publishers.

Wightman, C., M. Moakher, F. J. Muzzio, and O. R. Walton. 1998. Simulation of flow and mixing of particles in a rotating and rocking cylinder. *AIChE Journal* 44(6): 1266-1276.

Wilcke. B. 1999. Segregating genetically modified crops. St. Paul, Minn.: University of Minnesota Extension Service. Available at: http://www.bae.umn.edu/extens/postharvest/gmoip.html. Accessed on 01 August 2006.

Williams, J. C. 1986. Mixing, theory and practice. In *Mixing.* Vol. 3. V.W. Uhl and J.B. Gray, eds. Orlando, Fla.: Academic Press.

Williams, J. R., G. Hocking, and G. G. W. Mustoe. 1985. The theoretical basis of the discrete element method. In *NUMETA '85 Numerical Methods in Engineering, Theory and Applications*. Rotterdam, The Netherlands: Balkema.

Wilson, W. W., and B. L. Dahl. 2001. Evaluation of changes in grade specifications for dockage in wheat (Report No. 458). Fargo, N.D.: North Dakota State University Department of Agribusiness and Applied Economics.

Wilson, W. W., E. L. Janzen, and B. L. Dahl. 2003. Issues in development and adoption of genetically modified (GM) wheats. *Agbioforum* 6(3): 1-12.

Winowiski, T. S. 1998. Examining a new concept in measuring pellet quality: which test is best? *Feed Management* 49(1): 23-26.

Yang, Y., and M. D. Schrock. 1994. Analysis of grain kernel rebound motion. *Transactions of the ASAE* 37(1): 27-31.

Young, L. R. 1962. Mechanical durability of feed pellets. Unpublished MS Thesis. Manhattan, Kansas: Kansas State University, Department of Grain Science and Industry.

Zatari, I. M., P. R. Ferket, and S. E. Scheideler. 1990. Effect of pellet integrity, calcium lignosulfonate, and dietary energy on performance of summer-raised broiler chickens. *Poultry Science* 69(Suppl. 1): 198.

Zhang, X., and L. Vu-Quoc. 2002. A method to extract the mechanical properties of particles in collision based on a new elasto-plastic, normal-force-displacement model. *Mechanics of Materials* 34(12): 779-794.

Zhou, Y. C., B. H. Xu, A. B. Yu, and P. Zulli. 2001. Numerical investigation of the angle of repose of monosized spheres. *Physical Review E: Statistical Physics, Plasmas, Fluids, and Related Interdisciplinary Topics* 64(2): 0213011-0213018.

Zhou, Y. C., B. H. Xu, A. B. Yu, and P. Zulli. 2002. An experimental and numerical study of the angle of repose of coarse spheres. *Powder Technology* 125(1): 45-54.

Zhou, Y. C., B. D. Wright, R. Y. Yang, B. H. Xu, and A. B. Yu. 1999. Rolling friction in the dynamic simulation of sandpile formation. *Physica A* 269(2-4): 536-553.

CHAPTER 3 - Feed Pellet and Corn Durability and Breakage During Repeated Elevator Handling[1]

3.1 Introduction

Pelleting of animal feed is important for improved efficiency in animal feeding and for convenience in feed handling. Research has shown that animals fed with good quality pellets have better growth performance and feed conversion than those fed with mash, reground pellets, or pellets with more fines (Jensen et al., 1962; Jensen and Becker, 1965; Kertz et al., 1981; Brewer et al., 1989; Zatari et al., 1990). Behnke (1994) indicated that improvements in animal performance have been attributed to decreased feed wastage, reduced selective feeding, decreased ingredient segregation, less time and energy expended for eating, destruction of pathogens, thermal modification of starch and protein, and improved palatability. A significant part of the improvement is related to the quality of the pellet. Good quality pellets are needed to withstand repeated handling processes and reduce the formation of fines by mechanical action during transport.

The quality of the pellets may be described by their durability and resistance to attrition and/or breakage during handling. Gustafson (1959) classified the forces acting on the pellets as impact, compression, and shear. Impact forces shatter the pellet surface and any natural cleavage planes in the pellet. Compression forces crush the pellet and also cause failure along cleavage planes. Shear forces cause abrasion of the edges and surface of the pellet.

Several laboratory methods have been developed to measure the durability of pellets. The tumbling box, which is popular in North America and is the basis for ASAE Standard S269.4 (*ASAE Standards*, 2003a), uses 500 g of prescreened pellets placed in a box that revolves for 10 min at 50 rpm (Young, 1962). The DURAL tester, which was developed for hard alfalfa pellets, subjects 100 g of pellets to impact and shear forces for 30 s at 1600 rpm (Larsen et al., 1996; Sokhansanj and Crerar, 1999; Adapa et al., 2004). The Lignotester uses a sample of 100 g of pellets and blows them around a perforated chamber for 30 s (Winowiski, 1998). In all of these

[1] Boac, J. M., M. E. Casada, and R. G. Maghirang. 2008. Feed pellet and corn durability and breakage during repeated elevator handling. *Applied Engineering in Agriculture* 24(5): 637-643.

methods, the Pellet Durability Index (PDI) was calculated as the percentage of the mass of surviving pellets over the total mass of pellets.

Aarseth (2004) studied the susceptibility of feed pellets for livestock to attrition during pneumatic conveying. He investigated the effects of air velocity, bend radius, and number of repeated impacts for three commercially available feeds in a 100-mm-diameter pipeline. The three commercial feeds were produced by Felleskjøpet (Kambo, Norway). Feeds 'Formel Favør 30' (FF30) and 'Formel Elite' (FE) had pellet diameters of 6 mm and were formulated for ruminants, whereas, 'Kombi Norm' (KN) had a smaller pellet diameter (3 mm) that was formulated for pigs. He used Weibull analysis to assess pellet quality. This analysis incorporates fracture mechanics with statistics in order to describe the strength of brittle materials. Brittle materials show high scatter in strength due to variation in crack or flaw sizes, called Griffith cracks. Weibull analysis considers a relationship between the scatter in fracture strength and the size distribution of Griffith cracks. Aarseth and Prestløkken (2003) demonstrated that this method can be applied to feed pellets for ruminants and swine. Aarseth (2004) used the same method to analyze the three commercial pellets mentioned earlier.

Repeated handling in an elevator affects pellet breakage and quality. Repeated handling data for feed pellets in an elevator will be valuable for feed handlers in evaluating and improving their feed handling and transportation procedures. Corn-based feed pellet incorporated with other feed ingredients to improve its nutritive value can be an alternative to shelled corn.

Previous studies have been conducted on the durability of corn during handling. Baker et al. (1986) found that breakage susceptibility of shelled corn increased significantly during handling in pneumatic conveying systems with approximately 100-mm-diameter pipe. Tests involved using total lengths of 31 to 60 m, with two to four 90-degree elbows with a 1.22-m radius of curvature.

Foster and Holman (1973) studied physical damage (breakage) to corn, wheat, soybeans, and dry edible peas by commercial handling methods. Commercial handling methods included in their study were dropping products by free fall (simulating bin filling), dropping products through a spout (simulating railcar filling), grain-throwing (simulating the loading of barges and ship holds), and handling products in a bucket elevator. They enumerated the variables involved in corn breakage caused by commercial handling, namely: free fall height, impact surface, and corn moisture content and temperature. Corn that dropped from a height of 12 m onto corn in the

commercial handling study caused 4.3% breakage for corn with 12.6% moisture at -3.8°C, and 0.25% breakage for corn with 15.2% moisture at -5.0°C. It was also observed that breakage of corn handled decreased at higher grain temperatures.

Data on repeated handling of shelled corn in the USDA-ARS, Center for Grain and Animal Health Research (CGAHR), formerly Grain Marketing and Production Research Center (GMPRC) research elevator at Manhattan, Kansas have been reported. Martin and Stephens (1977) repeatedly transferred corn alternately between two bins. Percentage of breakage of corn kernels increased linearly during the repeated-handling tests. They observed breakage within the range reported by Foster and Holman (1973). The corn had a fall similar to the average 16-m free fall in bins 1 and 2. It had a moisture content of about 13% and a temperature of 11°C. A constant increase in breakage during 20 repeated transfers was also observed, in line with the observation of Foster and Holman (1973).

Martin and Lai (1978) reported values of 0.080%, 0.037%, and 0.028% for dust < 125 μm generated per transfer for corn, sorghum, and wheat, respectively, with a similar handling system. Converse and Eckhoff (1989) observed linear increases in broken corn and fine materials during repeated handling of six lots of corn that had been subjected to different drying treatments. The rates of increase were generally higher for corn dried at higher temperatures. Total dust emission per transfer varied from 0.084% to 0.21% of the total mass with the greater emission associated with corn dried at higher temperatures.

The objective of this study was to compare the effect of repeated handling in an elevator on the quality of feed pellets and shelled corn. The measures of quality included percentage of broken materials, PDI, and dust generated. The feed pellets in this study was compared to shelled corn due to the manufacturer's interest in making this pellet as a direct alternative to corn.

3.2 Materials and Methods

3.2.1 Test Facility and Materials

Tests were performed in the research grain elevator at the USDA-ARS, CGAHR (Manhattan, Kansas), which has a storage capacity of 1,400 t (55,000 bu). The elevator has one receiving pit and two bucket elevator legs, each with a maximum feed rate of 81.6 $t \cdot h^{-1}$ (3,000 $bu \cdot h^{-1}$). It is equipped with a pneumatic dust-control system, including cyclone separators (Figure 3.1). In this research, the system was operated so that the airflow rate through the upper cyclone

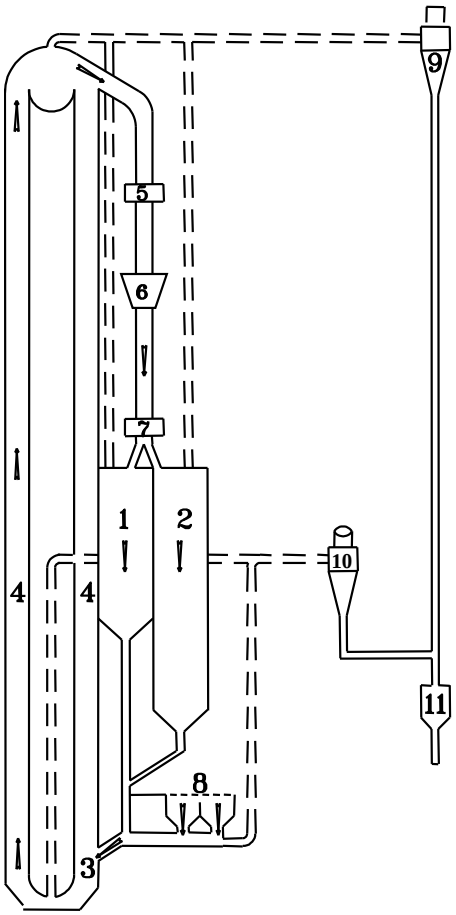

Figure 3.1 Schematic diagram of USDA-ARS-CGAHR research elevator, showing the flow of handled materials and location of equipment (not drawn to scale): 1-storage bin 1; 2-storage bin 2; 3-elevator boot; 4-elevator legs; 5-diverter-type (DT) sampler; 6-hopper; 7-distributor; 8-receiving area; 9-upper cyclone separator; 10-lower cyclone separators; and 11-dust bin.

separators was 5.0 $m^3 \cdot s^{-1}$ and that through the lower cyclone separators was 6.4 $m^3 \cdot s^{-1}$. These settings were the typical operating conditions for the elevator.

Tests were conducted with 22.6 t of feed pellets and 25.3 t of shelled corn. The mass of pellets and corn was determined by weighing the delivery truck containing the material before and after unloading in the elevator receiving area. During unloading, samples were taken every 2.5 min with a pelican sampler. These initial samples were labeled as Transfer 0. The materials were then moved from the receiving pit by belt conveyor and were bucket elevated and dropped into bin 1 for storage before testing (Figure 3.1).

The feed pellets were made of corn meal, with a moisture content of 13.2% wet basis (wb) after pelleting. The crude fat/oil, protein, and starch contents were 1.53%, 8.55%, and 65.6%, respectively. The pellets had an initial bulk density of 643 $kg \cdot m^{-3}$, nominal diameter of 6.40 mm, average pellet length of 10.5 mm (standard deviation (SD) = 1.2 mm), and initial moisture content of 10.5% wb [with mean moisture content of 10.3% (SD = 0.321%) wb for eight transfers]. The shelled corn was U.S. Grade No. 2, with the following initial properties: test weight, 752 $kg \cdot m^{-3}$; broken corn and foreign materials (BCFM), 3.13%; geometric mean diameter (GMD), 6.91 mm; and initial moisture content, 12.6% wb [with mean moisture content of 12.6% (SD = 0.302%) wb for eight transfers].

3.2.2 Test Procedure

3.2.2.1 Elevator Transfers and Sampling

Figure 3.1 shows a schematic diagram of the material flow during the test. The material was transferred alternately between storage bin 1 (with a volume of approximately 85 m^3 and a depth of 20 m) and bin 2 (with a volume of approximately 411 m^3 and depth of 26 m). From storage bin 1, the material descended by gravity through spouts and entered the boot on the descending side of the bucket elevator. The bucket elevator raised it 54.9 m, where it was discharged through a spout. It descended 3.0 m to pass through an automatic diverter-type (DT) sampler (Carter-Day Co., Minneapolis, Minn.). The material then descended 1.5 m to a hopper, and then another 3.0 m to the distributor, before it descended 4.6 m to enter storage bin 2 and then fell to the bottom of the bin. Transfer from bin 1 to bin 2 constituted one transfer and one-half of a cycle.

From storage bin 2, the material was spouted by gravity to the belt conveyor, descended 3.0 m to enter the boot, elevated 54.9 m before it descended and passed through the DT sampler, descended again to the hopper, and then to the distributor, and finally back to storage bin 1. This second transfer completed one cycle. A total of six transfers, or three cycles, at an average material flow rate of 62.2 $t \cdot h^{-1}$ (range: 52.7 to 68.6 $t \cdot h^{-1}$) for feed pellets and 56.6 $t \cdot h^{-1}$ (range: 51.4 to 65.1 $t \cdot h^{-1}$) for shelled corn, were done initially. In both cases the material was left in bin 1 for one week before it was again transferred to bin 2. It was left for one more week in bin 2 before the eighth and final transfer back to bin 1. This scenario was selected because it simulated the number and type of transfers in a typical handling process for the feed pellets.

Each transfer was designated serially from Transfer 1 to Transfer 8. Samples were taken every 2.5 min during each transfer with the DT sampler. An average of nine samples were taken during each transfer, with a mean sample mass of 642 g (SD = 51.9 g) for the feed pellets. An average of 10 samples were obtained from shelled corn per transfer, with a mean sample mass of 679 g (SD = 42.5 g).

Material samples during receiving (Transfer 0) and those from Transfers 1 to 8 were divided appropriately with a Boerner divider for particle sizing (100 g), durability measurement (500 g), and moisture-content determination (25 g for pellet; 15 g for corn). A 250-g portion of each shelled corn sample was also separated for BCFM determination. Samples were placed in sealed plastic bags and stored inside sealed plastic buckets at 4°C in a refrigerated room for subsequent analyses for particle size distribution, durability index, and moisture content.

3.2.2.2 Particle Sizing

The 100-g portions of each material sample were sieved in accordance with ASAE Standard S319.3 (*ASAE Standards,* 2003b) by using a Ro-Tap RX-29 sieve shaker (W.S. Tyler, Mentor, Ohio). The screen sizes were U.S. Standard sieve screen size openings: 8.00, 6.70, 6.30, 5.60, 3.35, 1.70, 1.00 mm, and pan (0.850 mm), which was adjusted from the screen sizes in ASAE Standard S319.3 to accommodate larger pellet sizes. Samples were initially sieved and shaken until they reached endpoint (*ASAE Standards*, 2003b). Endpoint was determined by comparing the mass on each sieve at 1-min intervals after an initial sieving time of 10 min. If the mass on the smallest sieve containing any of the pellets changed by 0.1% or less of the material mass during a 1-min period, then sieving was considered complete. In accordance with ASAE

Standard S269.4 (*ASAE Standards*, 2003a), feed pellet samples passing through the 5.60-mm-mesh sieves were considered broken pellets. Pellets that were retained on sieve sizes 8.00, 6.70, 6.30, and 5.60 mm were considered whole pellets. Shelled corn samples passing through the 4.76-mm round-hole sieve (12/64-in.) were considered broken corn and those that were retained on the 4.76-mm round hole sieve were considered whole corn (USDA GIPSA, 2004). Samples were weighed on a digital balance (O-Haus Adventurer Pro AV 4101, O-Haus Corp., Pine Brook, N.J.) with a resolution of 0.1 g.

From the particle size distribution data, the GMD of particles by mass, geometric standard deviation (GSD), and geometric standard deviation of the particle diameter by mass (GSDw) were calculated (*ASAE Standards*, 2003b).

3.2.2.3 Durability Measurement

The durability of the pellets was evaluated by using a durability tester in accordance with ASAE Standard S269.4 (*ASAE Standards*, 2003a). Samples from Transfers 0 (initial), 1 (first), 4 (middle), and 7 (second to last) were selected for the durability test. The durability tester consisted of four 130-mm wide tumbling boxes. The device was rotated about an axis perpendicular to, and centered in, the 300-mm sides. A 230-mm-long baffle was affixed symmetrical to a diagonal of one 300- × 300-mm side inside the box.

With four tumbling boxes, four samples were tested simultaneously. Four 500-g samples from each of Transfers 0, 1, 4, and 7 were selected as specified by ASAE Standard S269.4 (*ASAE Standards*, 2003a) for pellets with a nominal diameter of 6.40 mm. The samples (i.e., pellets greater than 5.60 mm) were tumbled for 10 min at 50 rpm. Immediately after tumbling the samples were removed and sieved with the 5.60-mm screen for approximately 30 s to remove the fines and broken pellets. The pellets that were retained on the sieve were weighed. A similar procedure was used for shelled corn from Transfers 0, 1, 4, and 7, using the standard 4.76-mm round-hole sieve to screen the whole kernels and determine broken kernels before and after tumbling. The durability index was computed by using the following equation:

$$Durability\ Index = \frac{mass\ of\ \ material\ retained\ on\ the\ sieve\ after\ tumbling}{mass\ of\ \ material\ before\ tumbling} \qquad (3.1)$$

Durability index (DI) was calculated for both pellets and shelled corn. For pellets the durability index is commonly known as PDI, a term retained in this article.

Moisture content of the feed pellet samples was determined by oven-drying at 60°C for 72 h according to ASAE Standard S358.2 (*ASAE Standards*, 2003c) as indicated in ASAE Standard S269.4 (*ASAE Standards*, 2003a). Moisture content of shelled corn was determined by oven-drying at 103°C for 72 h according to ASAE Standard S352.2 (*ASAE Standards*, 2003d).

3.2.2.4 Dust Sampling

Handling of the materials generated dust. The pneumatic dust control system collected the dust through the cyclone separators and into the dust bin (Figure 3.1). After each transfer, the dust collected in the dust bin was emptied into a plastic bag, weighed, labeled, and stored at 4°C in a refrigerated room for later analysis. Representative dust samples from the plastic bag were obtained in accordance with ASTM Standard E-300 (*ASTM Standards*, 2000). Nine samples from the plastic bag from each transfer were obtained by using a grain sampling probe. The samples were sieved with a U.S. Sieve No. 120 (125 μm). Particles collected by the cyclones that passed through the 125-μm sieve aperture (ca. 10 to 125 μm) (Martin and Sauer 1976; Martin and Stephens, 1977; Martin and Lai, 1978) were weighed.

3.2.2.5 Data Analyses

The experiment was designed with repeated handling (transfers) and materials as the class variables. The experimental units were the feed pellets and the corn. This design was devised to control the cost involved in conducting this large-scale experiment.

Comparisons of results between materials (feed pellets and shelled corn) and between transfers (Transfer 1 to 8) were done by using Analysis of Variance (ANOVA) in SAS (SAS Institute Inc., Cary, N.C.). The percentage of dust for the eight transfers in this study was compared with published data on corn (Martin and Stephens, 1977) by using the ANOVA procedure in SAS.

3.3 Results and Discussion

3.3.1 Particle Size Distribution

The initial GMD of the pellets was 5.62 mm (Table 3.1). The apparent GMD decreased as the number of transfers increased. From Transfers 0 to 4, GMD decreased by approximately 1.9 mm; from Transfers 4 to 8, the GMD remained relatively constant. For shelled corn, the initial GMD was 6.91 mm (Table 3.1). The apparent GMD for shelled corn did not differ among transfers, except with Transfer 0. The apparent GMD, GSD, and GSDw of the pellets were significantly different ($p < 0.01$) from that of shelled corn.

Table 3.1 Apparent geometric mean diameter (GMD), geometric standard deviation (GSD), apparent geometric standard deviation of the particle diameter by mass (GSD_w), and change in percent breakage of feed pellets and shelled corn during repeated handling.[a]

	Apparent GMD (mm)		GSD		Apparent GSDw (mm)		Change in % Breakage	
Transfer	Feed Pellet	Corn	Feed Pellet	Corn	Feed Pellet	Corn	Feed Pellet	Corn
0	5.62	6.91	1.69	1.28	3.09	1.74		
1	5.01	6.69	1.88	1.35	3.38	2.02	7.42	1.72
2	4.55	6.75	2.00	1.31	3.42	1.83	7.29	0.315
3	4.54	6.67	1.99	1.37	3.38	2.11	0.543	-0.066
4	3.71	6.70	2.19	1.32	3.22	1.90	12.9	-0.308
5	3.90	6.62	2.10	1.38	3.16	2.14	-0.992	0.401
6	3.87	6.68	2.12	1.34	3.19	1.97	-0.048	0.051
7	3.60	6.58	2.14	1.37	3.02	2.12	5.58	1.02
8	3.81	6.56	2.09	1.37	3.06	2.08	-2.02	-0.079
Mean (SD)	**4.29 (0.688)**	**6.69 (0.104)**	**2.02 (0.156)**	**1.34 (0.033)**	**3.21 (0.147)**	**1.99 (0.142)**	**3.83 (5.26)**	**0.382 (0.676)**

[a] Feed pellets and shelled corn differed significantly in GMD, GSD, GSD_w, and change in % breakage at the 5% level of significance. Negative values of change in % breakage are due to inherent variability in the materials.

3.3.2 Whole and Broken Materials

No pellets were retained on the 8.00-mm sieve. The mass percentage of whole pellets (≥ 5.60 mm) decreased with subsequent transfers, from 82.5% to 49.8% (Figure 3.2). This was due to pellet breakage occurring during transfers. As expected, the mass of broken pellets (< 5.60 mm) increased with subsequent transfers. The mass percentage of broken pellets increased from an initial value of 17.5% to 50.2%, equivalent to an average of 3.83% increase with each transfer (Table 3.1). The nonlinear increase in breakage differed from the linear increase observed by Foster and Holman (1973) and Martin and Stephens (1977) for shelled corn.

For the shelled corn in this study, the mass percentage of whole corn (≥ 4.76 mm) from Transfer 0 differed from all the other transfers. The mass percentage of whole corn decreased from 96.9% to 93.8% and the mass percentage of broken corn (<4.76 mm) increased from 3.13% to 6.18% for the eight transfers. The mass percentage of broken corn increased by an average value of 0.382%, which was significantly less ($p < 0.05$) than that of the pellets (Table 3.1). This difference indicated that this corn was relatively durable, which is typical for corn that did not undergo high temperature drying.

The least-squares best-fit line showed a second-order polynomial relationship between number of transfers and broken pellets or whole pellets, with a coefficient of determination, R^2 = 0.96 (Figure 3.2). This relationship was expected because the weaker pellets break easily and faster during the earlier transfers.

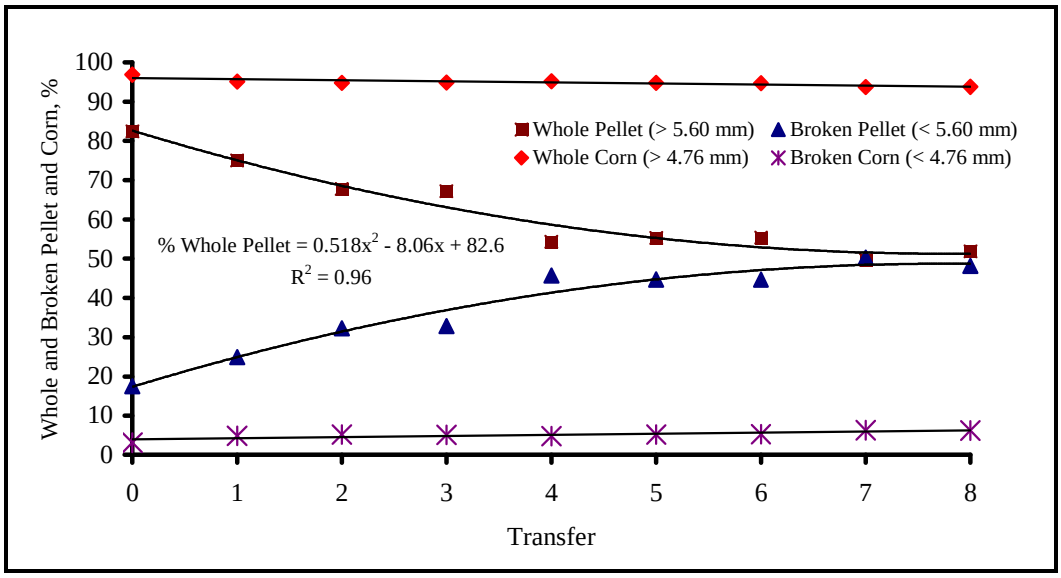

Figure 3.2 Whole and broken feed pellets and shelled corn (in percentage of total mass during repeated handling.

Zatari et al. (1990) indicated that broilers fed 75% whole pellets and 25% broken pellets, as compared with 25% whole and 75% broken, had better feed efficiency and higher body weight. For this study, a percentage of whole pellets of 75% or better was attained up to Transfer 1 only; the percentage of whole pellets decreased to approximately 50% as the final transfer was reached. Amornthewaphat et al. (1999) found a linear decrease in efficiency of growth of finishing pigs as broken pellets was increased from 0% (7% greater gain/feed than meal control) to 50% (2% greater gain/feed than meal control). In this study, 50% broken pellets occurred after Transfer 8.

3.3.3 Durability Index

The initial PDI value (Transfer 0) for the feed pellets was 92.8% (SD = 1.2%). For Transfers 1, 4, and 7, the mean PDI values were 92.0% (SD = 1.5%), 93.3% (SD = 0.2%), and 93.4% (SD = 2.0%), respectively. The PDI values increased only slightly and transfers were not significantly different ($p > 0.05$). Shelled corn had mean DI values of 99.8% for Transfers 0, 99.7% for Transfer 1, and 99.6% for both Transfers 4 and 7. The corn DI values for the transfers were not significantly different ($p > 0.05$) (Table 3.2). The PDI and corn DI, however, were significantly different from each other ($p < 0.05$).

Table 3.2 Durability indices of feed pellets and shelled corn during repeated handling.[a]

Transfer	Durability Index (%)	
	Feed Pellet	**Corn**
0	92.8 (1.22)	99.8 (0.059)
1	92.0 (1.51)	99.7 (0.080)
4	93.3 (0.200)	99.6 (0.079)
7	93.4 (1.97)	99.6 (0.064)
Mean (SD)	**92.9 (0.633)**	**99.7 (0.081)**

[a] Mean durability index of feed pellets was significantly different from that of shelled corn at the 5% level of significance.

Dozier (2001) reported that minimum PDI values differ for different meat birds: 96% for ducks, 90% for turkeys, and 80% for broilers. Hanrahan (1984) reported no difference in finishing pig performance between pigs restrictedly fed pellets with PDI of 69% or 62%. The feed pellets in this study have nominal size suitable for pigs. This pellet has a higher measured

PDI and, based on that PDI, can be expected to give similar or better performance in swine compared to the pellet reported by Hanrahan (1984).

Aarseth (2004), who compared three types of feed pellets: FF30, FE, and KN, indicated that the pellet with highest bulk density (BD) was also the least susceptible to attrition in the Holmen pellet tester. The BDs of the FE and FF30 tested for 120 s in the Holmen tester were 641 and 664 $kg \cdot m^{-3}$ and the PDIs were 92% and 96%, respectively. The KN pellet, which was tested for 30 s, had BD = 623 $kg \cdot m^{-3}$ and PDI = 94%. The feed pellets in this study had a BD of 643 $kg \cdot m^{-3}$ and initial PDI of 92.8%, which is comparable to FE in Aarseth's study. It should be noted, however, that the Holmen tester seemed to be harsher than the tumbling box method, and therefore would yield lower PDI values (Winowiski, 1998). The feed pellets in this study may have a lower PDI value if tested with the Holmen tester.

3.3.4 Dust

The mean pellet dust collected by the cyclones was 0.694 $kg \cdot t^{-1}$ of pellet mass. Shelled corn had mean collected dust of 0.614 $kg \cdot t^{-1}$ of corn mass, which was not significantly different from that of the feed pellets ($p > 0.05$) (Table 3.3).

The mean mass of dust <125 μm per unit mass of pellets (0.337 $kg \cdot t^{-1}$ of pellet mass) was significantly different ($p < 0.05$) from that of shelled corn (0.403 $kg \cdot t^{-1}$ of corn mass) (Table 3.3). Overall, the mass of dust <125 μm for the feed pellets was 50% of the total dust collected, which was significantly different from that of corn (66% of the total dust) in this study.

Compared with published values, the mean percentages of dust of both feed pellets (0.069% of pellet mass) and shelled corn (0.061% of corn mass) were significantly different from that of Martin and Stephens (1977) (0.082% of corn mass) for the eight transfers ($p < 0.05$). The percentages of dust of both materials in this study were also less than that from Martin and Lai (1978), which was 0.095% of the corn mass. The shelled corn from this study was relatively cleaner than that of Martin and Stephens (1977) and Martin and Lai (1978).

The amounts of dust <125 μm in Martin and Stephens' (1977) shelled corn (70% of the mass of the dust) and in Martin and Lai's (1978) shelled corn (85% of the mass of dust) were greater than that from the pellets (50%) and shelled corn (66%) from this study. The percentage of dust <125 μm of the pellet was significantly different ($p < 0.01$) from that of Martin and Stephens' (1977) shelled corn.

Table 3.3 Mean total collected dust and calculated amount of dust <125 µm of feed pellets and shelled corn during repeated handling.

Transfer	Total Collected Dust ($kg \cdot t^{-1}$ of materials handled)		Collected Dust < 125 µm (SD) ($kg \cdot t^{-1}$ of materials handled)	
	Feed Pellet	Corn	Feed Pellet	Corn
1	0.629	0.529	0.312 (0.022)	0.374 (0.024)
2	0.718	0.816	0.341 (0.004)	0.477 (0.017)
3	0.681	0.593	0.332 (0.003)	0.397 (0.023)
4	0.706	0.710	0.329 (0.006)	0.452 (0.014)
5	0.674	0.522	0.325 (0.002)	0.392 (0.012)
6	0.838	0.666	0.413 (0.017)	0.453 (0.028)
7	0.516	0.541	0.237 (0.003)	0.370 (0.021)
8	0.793	0.532	0.406 (0.013)	0.309 (0.020)
Mean[a] (SD)	**0.694 b (0.099)**	**0.614 b (0.108)**	**0.337 c (0.056)**	**0.403 d (0.055)**

[a] Means (within the same parameter) with the same letter were not significantly different at the 5% level of significance.

3.4 Summary

Pelleting of animal feeds is important for improved feeding efficiency and for convenience of handling. Pellet quality impacts the feeding benefits for the animals and pellet integrity during handling. To compare the effect of repeated handling on the quality of feed pellets and corn, a 22.6-t (1000-bu) lot of feed pellets made from corn meal and a 25.3-t (1000-bu) lot of shelled corn, were each transferred alternately between two storage bins in the USDA-ARS, Center for Grain and Animal Health Research (CGAHR) research elevator at Manhattan, Kansas, at an average flow rate of 59.4 $t \cdot h^{-1}$. Samples from a diverter-type sampler were analyzed for particle size distribution (by sieving) and durability (by the tumbling box method).

The apparent geometric mean diameter of pellet samples decreased with repeated transfers, whereas the mass of accumulated broken pellets increased with repeated transfers. The percentage of broken pellets (< 5.60 mm) increased from an initial value of 17.5% to 50.2% after eight transfers, an average percentage increase in breakage of 3.83%. The percentage of broken corn, which was significantly different from that of broken pellets ($p < 0.05$), increased from 3.13% to 6.18%; the average percentage increase was 0.382%. Repeated handling did not significantly affect the durability index of the feed pellets, which ranged from 92.0% to 93.4%, nor that of shelled corn, which ranged from 99.6% to 99.8%.

Analysis of dust removed by the cyclone separators showed that the average mass of dust removed per transfer was 0.069% of the mass of pellets, which was not significantly different from that of shelled corn (0.061%) but was significantly different from that reported by Martin and Stephens (1977) for a different lot of corn. Overall, 50% of pellet dust collected in the cyclones were <125 μm in diameter, which was a smaller percentage than that collected with shelled corn (66%). The mean mass of dust < 125 μm was significantly less for feed pellets (0.337 $kg \cdot t^{-1}$ of pellet mass) than for shelled corn (0.403 $kg \cdot t^{-1}$ of corn mass), indicating that these pellets produced less dust in the range of 10 to 125 μm during handling than did shelled corn.

3.5 References

Aarseth, K. A. 2004. Attrition of feed pellets during pneumatic conveying: the influence of velocity and bend radius. *Biosystems Engineering* 89(2): 197-213.

Aarseth, K. A., and E. Prestløkken. 2003. Mechanical properties of feed pellets: Weibull analysis. *Biosystems Engineering* 84(3): 349-361.

Adapa, P. K., L. G. Tabil, G. J. Schoenau, and S. Sokhansanj. 2004. Pelleting characteristics of fractionated, sun-cured, and dehydrated alfalfa grinds. *Applied Engineering in Agriculture* 20(6): 813-820.

Amornthewaphat, N., J. D. Hancock, K. C. Behnke, R. H. Hines, G. A. Kennedy, H. Cao, J. S. Park, C. S. Maloney, D. W. Dean, J. M. Derouchey, and D. J. Lee. 1999. Effects of feeder design and pellet quality on growth performance, nutrient digestibility, carcass characteristics, and water usage in finishing pigs. *Journal of Animal Science* 77(Suppl.1): 55.

ASAE Standards. 2003a. S269.4: Cubes, pellets, and crumbles — definitions and methods for determining density, durability, and moisture content. St. Joseph, Mich.: ASAE.

ASAE Standards. 2003b. S319.3: Methods of determining and expressing fineness of feed materials by sieving. St. Joseph, Mich.: ASAE.

ASAE Standards. 2003c. S358.2: Moisture measurement - Forages. St. Joseph, Mich.: ASAE.

ASAE Standards. 2003d. S352.2: Moisture measurement - Unground grain and seeds. St. Joseph, Mich.: ASAE.

ASTM Standards. 2000. E300-92: Standard practice for sampling industrial chemicals. West Conshohocken, Pa.: ASTM.

Baker, K. D., R. L. Stroshine, K. J. Magee, G. H. Foster, and R. B. Jacko. 1986. Grain damage and dust generation in a pressure pneumatic conveying system. *Transactions of the ASAE* 29(2): 840-847.

Behnke, K. C. 1994. Processing factors influencing pellet quality. AFMA Matrix. South Africa: Animal Feed Manufacturers Association. Available at: http://www.afma.co.za. Accessed 26 April 2005.

Brewer, C. E., P. R. Ferket, and T. S. Winowiski. 1989. The effect of pellet integrity and lignosulfonate on performance of growing tom. *Poultry Science* 68(Suppl.1): 18.

Converse, H. H., and S. R. Eckhoff. 1989. Corn dust emissions with repeated elevator transfers after selected drying treatment. *Transactions of the ASAE* 32(6): 2103-2107.

Dozier, W. A. 2001. Cost-effective pellet quality for meat birds. *Feed Management* 52(2): 21-24.

Foster, G. H., and L. E. Holman. 1973. Grain breakage caused by commercial handling method. USDA Res. Serv. Mrktg. Res. Rpt. No. 968. Washington, D.C.: U.S. Department of Agriculture-Agricultural Research Service.

Gustafson, M. L. 1959. The durability test — a key to handling wafers and pellets. ASAE Paper No. 59621. St. Joseph, Mich.: ASAE.

Hanrahan, T. J. 1984. Effect of pellet size and pellet quality on pig performance. *Animal Feed Science and Technology* 10(4): 277.

Jensen, A. H., and D. E. Becker. 1965. Effect of pelleting diets and dietary components on the performance of young pigs. *Journal of Animal Science* 24(2): 392-397.

Jensen, L. S., L. H. Merrill, C. V. Reddy, and J. McGinnis. 1962. Observation on eating patterns and rate of food passage of birds fed pelleted and unpelleted diets. *Poultry Science* 41(5): 1414-1419.

Kertz, A. F., B. K. Darcy, and L. R. Prewitt. 1981. Eating rate of lactating cows fed four physical forms of the same grain ration. *Journal of Dairy Science* 64(12): 2388-2391.

Larsen, T. B., S. Sokhansanj, R. T. Patil, and W. J. Crerar. 1996. Breakage susceptibility studies on alfalfa and animal feed pellets. *Canadian Agricultural Engineering* 38(1): 21-24.

Martin, C. R., and F. S. Lai. 1978. Measurement of grain dustiness. *Cereal Chemistry* 55(5): 779-792.

Martin, C. R., and D. B. Sauer. 1976. Physical and biological characteristics of grain dust. *Transactions of the ASAE* 19(4): 720-723.

Martin, C. R., and L. E. Stephens. 1977. Broken corn and dust generated during repeated handling. *Transactions of the ASAE* 20(1): 168-170.

Sokhansanj, S., and W. J. Crerar. 1999. Development of a durability tester for pelleted and cubed animal feed. SAE 1999-01-2830. *Agriculture Machinery, Tires, Tracks, and Traction* SP-1474: 83-87.

USDA GIPSA. 2004. Chapter 4: Corn. In *Grain Inspection Handbook, Book II, Grain Grading Procedures*. Washington, D.C.: USDA Grain Inspection, Packers, and Stockyards Administration, Federal Grain Inspection Service.

Winowiski, T. S. 1998. Examining a new concept in measuring pellet quality: which test is best? *Feed Management* 49(1): 23-26.

Young, L. R. 1962. Mechanical durability of feed pellets. Unpublished MS Thesis. Manhattan, Kansas: Kansas State University, Department of Grain Science and Industry.

Zatari, I. M., P. R. Ferket, and S. E. Scheideler. 1990. Effect of pellet integrity, calcium lignosulfonate, and dietary energy on performance of summer-raised broiler chickens. *Poultry Science* 69(Suppl. 1): 198.

CHAPTER 4 - Size Distribution and Rate of Dust Generated During Grain Elevator Handling[1]

4.1 Introduction

Dust emitted during grain handling is a safety and health hazard as well as an air pollutant. Grain dust is composed of approximately 70% organic matter, which may include particles of grain kernels, spores of smuts and molds, insect debris (fragments), pollens, and field dust (US EPA, 2003) that become airborne during grain handling (Aldis and Lai, 1979). Due to the high organic content and a substantial suspendible fraction, concentrations of grain dust above the minimum explosive concentration (MEC) pose an explosion hazard (US EPA, 2003). Published MEC values range from 45 to 150 $g \cdot m^{-3}$ (Jacobsen et al., 1961; Palmer, 1973; Noyes, 1998).

In addition to being a safety hazard to grain elevator workers, grain dust is also a health hazard (NIOSH, 1983). Prolonged exposure to grain dust can cause respiratory symptoms in grain-handling workers and in some cases affect workers' performance and sense of well-being (NIOSH, 1983). The American Conference of Governmental Industrial Hygienists (ACGIH, 1997) has defined three particulate mass fractions in relation to potential health effects: (1) inhalable fraction (particulate matter (PM) with a median cut point aerodynamic diameter of 100 μm that enters the airways region), (2) thoracic fraction (PM with a median cut point aerodynamic diameter of 10 μm that deposits in the tracheobronchial regions), and (3) respirable fraction (PM with a median cut point aerodynamic diameter of 4 μm that enters in the gas-exchange regions), herein referred to as PM-4. The US EPA (2007), on the other hand, regulates PM-2.5 or fine PM (i.e., PM with equivalent aerodynamic diameter of 2.5 μm or less) and PM-10 (i.e., PM with equivalent aerodynamic diameter of 10 μm or less). PM-2.5 has been linked to serious health problems ranging from increased symptoms to premature death in people with lung and heart disease. Fine particulates such as PM-2.5, PM-4, and PM-10 are more dangerous

[1] Boac, J. M., R. G. Maghirang, M. E. Casada, J. D. Wilson, and Y. S. Jung. 2009. Size distribution and rate of dust generated during grain elevator handling. *Applied Engineering in Agriculture* 25(4): 533-541.

in terms of grain dust explosions because MEC generally decreases with decreasing particle sizes and increasing surface area (Garrett et al., 1982).

Under the 1990 Clean Air Act, the state environmental agencies are required to regulate the grain elevator industry's emission of airborne dust (US EPA, 1990). The US EPA AP-42 document has listed emission factors for grain elevators (US EPA, 2003). The document cites recent research on dust emission from grain handling operations indicating the mean PM-10 value was approximately 25% of total PM or total dust, and the fraction of PM-2.5 averaged at about 17% of PM-10. Mean PM-10 values for country and export elevators were 20% and 26%, respectively, of total dust (Midwest Research Institute, 1998). The elevators primarily handling wheat had mean PM-10 of about 30% of total dust, whereas those primarily handling corn and soybean had an average PM-10 of slightly less than 20% of total dust.

Several studies have been conducted to determine the amount of dust emitted from external and process emission sources in grain elevators (Table 4.1) and measure the particle size distributions (PSD) for dust collected from the same system (Table 4.2). Parnell et al. (1986) reported mass median diameter (geometric standard deviation) of grain dust < 100 μm for corn and wheat of 13.2 and 13.4 μm (1.80 and 2.08), respectively. Martin and Lai (1978) cited mean mass median diameters of residual dust (that sticks to grain) of 13 and 14 μm for wheat and sorghum, respectively. In the same study, the mean percentages of residual dust with diameter ≤ 10 μm were about 34%, 33%, and 45% for sorghum, corn, and wheat, respectively.

Piacitelli and Jones (1992) studied the size distribution of sorghum dust collected by impactors during on-farm handling (harvesting, on-farm storage, delivery truck). Their results indicated that about 2% of the particles had ≤ 3.5 μm aerodynamic diameter; 10% were ≤ 10 μm, 24% were ≤ 15 μm, 48% were ≤ 21 μm, and 52% were > 21 μm.

However, data on the PSD of dust generated during grain handling in a bucket-elevator system and the fraction that might be health hazards are limited (Wallace, 2000). Martin and Sauer (1976) studied the dust fraction that was contaminated by mold spores and fungal metabolites, which can be health hazards to grain elevator workers; however, they did not consider PSD. The most comprehensive PSD study was conducted by Parnell et al. (1986), but their study was limited to dust < 100 μm, the most explosive fraction. Thus, limited data exists on the complete range of particle sizes generated during bucket elevator handling even though this system is the primary grain and feed handling system used in the United States. This study

fills the gap where no complete PSD is available for wheat and corn and provides more specific data than previous studies particularly on small particle sizes, PM-2.5 and PM-4.

The objective of this study was to characterize the PSD and dust generated (i.e., mass flow rate) in a bucket-elevator system collected upstream of the cyclone separator. The fractions of interest were particles with aerodynamic diameters ≤ 2.5 and ≤ 10 μm for regulatory purposes and ≤ 4 μm for health reasons. Specific objectives were to determine the effects of grain lots (part 1), repeated transfers (part 2), and grain types on PSD of the dust.

Table 4.1 Published particulate emission factors for grain handling.

Emission Source	Emission Factor ($g \cdot t^{-1}$ of grain)		
	Total PM	**PM-10**	**PM-2.5**
Grain Receiving (hopper and straight truck, railcar, barge, ships)	8.30 – 90.0 [a] [b] [c] [d] [e]	0.600 – 29.5 [b] [d] [e]	0.650 – 5.00 [d]
Grain Cleaning (internal vibrating - with cyclone)	37.5 [b] [d]	9.50 [d]	1.60 [d]
Headhouse and Internal Handling (legs, belts, distributor, scale, etc.)	30.5 [b] [d]	17.0 [b] [d]	2.90 [d]
Storage Vents	12.5 [b] [d]	3.15 [d]	0.550 [d]
Grain Drying (column and rack dryers)	110 – 1500 [b] [d]	27.5 – 375 [d]	4.70– 65.0 [d]
Grain Shipping (truck, railcar, barge, ships)	4.00 – 43.0 [a] [b] [d]	1.10 – 14.5 [b] [d]	0.185 – 2.45 [d]

[a] Kenkel and Noyes, 1995)
[b] Midwest Research Institute, 1998
[c] Shaw et al., 1998
[d] US EPA, 2003
[e] Billate et al., 2004

Table 4.2 Published size distribution of grain dust from grain elevators.

Grain Type	Percentage PM Dust of the Total Dust Collected (%)					
	< 125 μm	**< 100** μm	**< 10** μm	**< 8** μm	**< 4** μm	**< 2.5** μm
Corn	62.0 - 86.0 [a] [b] [c]	54.1 [d]	5.00 - 12.0 [e] [f]	5.00 - 12.0 [a]	0.600 - 3.00 [f]	0.200 - 1.00 [f]
Wheat	33.0 - 78.0 [a] [c]	34.3 [d]	-	3.00 - 4.00 [a]	-	-
Sorghum	60.0 [c]	34.3 [d]	-	-	-	-
Rice	-	44.2 [d]	-	-	-	-
Soybean	-	50.6 [d]	-	-	-	-
Cyclone dust	-	-	9.00 [g]	-	-	-
Baghouse dust	-	-	20.0 [g]	-	-	-

[a] Martin and Sauer, 1976 (from table 2)
[b] Martin and Stephens, 1977 (from table 1)
[c] Martin and Lai, 1978 (from table 3)
[d] Parnell et al., 1986 (from table 3, paper also gave PSD graphs of dust < 100 μm)
[e] Lai et al., 1984 (interpolated from PSD graph, figure 5)
[f] Baker et al., 1986 (interpolated from PSD graph, figure 2)
[g] Martin, 1981 (interpolated from PSD graph, figure 5)

4.2 Materials and Methods

4.2.1 Test Facility

Dust samples from handling of wheat and shelled corn were collected upstream of the cyclone separators in the research grain elevator at the USDA-ARS, Center for Grain and Animal Health Research (CGAHR) (Manhattan, Kans.). The grain elevator has a storage capacity of 1400 t (55,000 bu). It has one receiving pit and two bucket elevator legs, each with a maximum feed rate of 81.6 $t \cdot h^{-1}$ (3,000 $bu \cdot h^{-1}$). It is equipped with a pneumatic dust-control system, which includes a 2.74 m diameter low pressure upper cyclone separator and twin 2.24 m diameter low pressure lower cyclone separators (Figure 4.1). In this research, the system was operated so that the airflow rate through the upper cyclone separators—serving the upper spouting, distributors, and storage bin headspace—was 5.0 $m^3 \cdot s^{-1}$ and the rate through the lower cyclone separators—collecting dust from the ground level area, particularly the elevator boot—was 6.4 $m^3 \cdot s^{-1}$. These settings were the typical operating conditions for the elevator.

4.2.2 Test Materials and Grain Handling

4.2.2.1 Part 1: Wheat

The initial study determined the effect of grain lot on the PSD of the grain dust. The test material, Hard Red Winter wheat from a 2005 crop, was purchased from a local elevator on July 19-21, 2005, and stored under aeration in small metal bins for two years. The wheat was then unloaded in the CGAHR research elevator receiving area, moved from the receiving pit by belt conveyor, bucket elevated, and then dropped into the storage bin before testing (Figure 4.1). It was weighed on the inline weighing scale. There were four lots of wheat. Each of the four lots, with a mean mass of 28.3 t (1000 bu), was transferred each time at an average material flow rate of 52.2 $t \cdot h^{-1}$ (range: 44.3 to 56.9 $t \cdot h^{-1}$). Transfer 1 was a transfer from storage bin 2 (with a volume of approximately 411 m^3 and depth of 26 m) to storage bin 3 (with the same volume and depth as storage bin 2) (Figure 4.1) on August 27, 2007 with mean temperature (T) and mean relative humidity (RH) of 30.4 °C and 56.0 %, respectively, during transfer. Transfer 2 was performed from storage bin 3 to storage bin 2 on August 28, 2007 (T = 34.5 °C, RH = 36.4 %) and August 29, 2007 (T = 22.9 °C, RH = 84.2 %). The initial grain drop height for each transfer

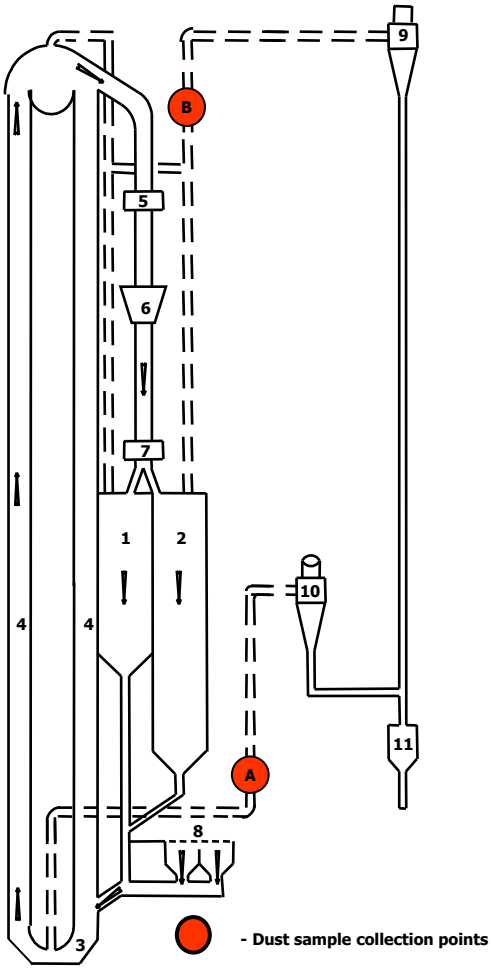

Figure 4.1 Schematic diagram of USDA-ARS-CGAHR research elevator showing flow of the handled grain and location of equipment (not drawn to scale): 1 - storage bin 1; 2 - storage bin 2; 3 - elevator boot; 4 - elevator legs; 5 - diverter-type sampler; 6 - hopper; 7 - distributor; 8 - receiving area; 9 - upper cyclone separator; 10 - lower cyclone separators; 11 - dust bin; A – lower duct sample collection point; and B – upper duct sample collection point.

was 26 m. During each of the two transfers for each of the four lots, dust was sampled upstream of the lower and upper collection ducts (Figure 4.1)

4.2.2.2 Part 2: Shelled Corn

The second part of the study was conducted to determine the effect of repeated transfers on the PSD of the dust particles. The test material was shelled yellow-dent corn from 2006 crop, air-dried, and also purchased from the same local elevator on April 4, 2007. The shelled corn was weighed while in the truck, unloaded, and bucket elevated into the storage bin before testing. Shelled corn, with a mean mass of 25.3 t (1000 bu), was transferred at an average material flow rate of 56.6 $t \cdot h^{-1}$ (range: 51.4 to 65.1 $t \cdot h^{-1}$). Transfer 1 was a transfer from storage bin 1 (with a volume of approximately 85 m^3 and a depth of 20 m) to storage bin 2. The shelled corn lot was transferred alternately between storage bin 1 and storage bin 2 six times (Transfers 1 to 6) on April 24, 2007 (T = 22.2 °C, RH = 76.8 %). It was left in storage bin 1 for a week before it was again transferred to storage bin 2 (Transfer 7) on May 1, 2007 (T = 19.7 °C, RH = 89.3 %). It was left for one more week in storage bin 2 before the final transfer (Transfer 8) on May 8, 2007 (T = 18.2 °C, RH = 73.5 %). The initial grain drop height to storage bin 1 was 20 m and to storage bin 2 was 26 m. During each of the eight transfers, dust samples were collected upstream of the lower and upper collection ducts (Figure 4.1).

4.2.3 Dust Sampling

Prior to dust sampling, velocity traverses were conducted inside the lower and upper collection ducts in accordance with US EPA Method 1 (US EPA, 2000) to establish the isokinetic collection velocity in the sampling duct. The mean measured velocities for the lower and upper collection ducts were 17.8 and 19.2 $m \cdot s^{-1}$, respectively. The cross-sectional areas of the lower and upper ducts were 0.36 and 0.26 m^2, respectively. Based on the mean velocities and cross-sectional areas, the volumetric flow rates of air through the lower and upper collection ducts were 6.4 and 5.0 $m^3 \cdot s^{-1}$, respectively.

Dust samples were then collected isokinetically upstream of the cyclones every 5 minutes during each grain transfer. A total of three samples per grain transfer were collected from each sampling point (Figure 4.1). Each dust sample was extracted on a 0.20- × 0.25-m glass fiber filter by using a high volume sampling train in accordance with ASTM D4536-96 and US EPA CTM-003 (US EPA, 1989; *ASTM Standards*, 2000). The high volume sampling train consisted of a 35-

mm diameter sampling probe, a 0.20- × 0.25-m filter holder, a differential pressure gauge, and a variable-speed vacuum motor. To achieve isokinetic sampling conditions, the sampling volumetric flow rates for the lower and upper ducts were set at 0.017 and 0.018 $m^3 \cdot s^{-1}$, respectively.

To minimize the effect of humidity on filter mass, the glass fiber filters were conditioned in a constant humidity chamber (25°C, 50% relative humidity) for at least 24 h prior to weighing both before and after sampling. All filters were weighed on an electronic scale (model PC 440, Mettler Instrument Corp., Hightstown, N.J.) with a sensitivity of 0.001 g. The change in mass before and after sampling represented the mass of dust collected on the filter (m_d).

From the measured data, the dust mass flow rate, $\dot{m}_d$ ($g \cdot s^{-1}$), was calculated using:

$$\dot{m}_d = \frac{m_d \, Q_c}{t \, Q_s} \tag{4.1}$$

where Q_c is the volumetric flow rate through the collection duct ($m^3 \cdot s^{-1}$), t is the sampling time (s), and Q_s is the sampling volumetric flow rate ($m^3 \cdot s^{-1}$).

The dust mass flow rate was converted to a mass flow rate equivalent, $\dot{m}_e$ ($g \cdot t^{-1}$) by the following equation:

$$\dot{m}_e = \frac{\dot{m}_d}{\dot{m}_g} \tag{4.2}$$

where $\dot{m}_g$ is the grain (i.e., wheat or shelled corn) mass flow rate ($t \cdot s^{-1}$).

4.2.4 Particle Sizing

The PSD of the collected dust was measured with a laser diffraction particle size analyzer (model LS 13 320, Beckman Coulter, Inc., Fullerton, Cal.). Laser diffraction particle sizing uses a light source that generates a monochromatic beam, which passes through several optical components that condition it to create an expanded, collimated beam (Beckman-Coulter, Inc., 2006). The beam illuminates the particles in the scattering volume usually in the sample module. The particles then scatter the light, creating unique angular scattering patterns, which are then Fourier transformed into a spatial intensity pattern detected by a multi-element photodetector array. The photocurrent from the detectors is then processed and digitized into an intensity flux pattern. Computer software that utilizes appropriate scattering theories, such as the Mie theory or Fraunhofer theory, then converts the set of flux values into PSD values. The analyzer could

measure a particle size range from 0.4 to 2000 μm. Laser diffraction reduces the analysis time to minutes per sample with results tabulated into number, surface area, and volume percentage (Pearson et al., 2007).

The measurement procedure was as follows. First, a quarter of each collection filter was cut and separated for laser diffraction particle sizing. The quarter filter was then washed with isopropyl alcohol to extract the dust on the filter. Isopropyl alcohol was used for the suspension solution to minimize clumping/aggregation of the dust particles. The suspension was placed into plastic centrifuge tubes and centrifuged for 5 min at 4000 rpm setting inside the Durafuge (model Precision Durafuge 300, Thermo-Fisher Scientific, Inc., Waltham, Mass.). The excess isopropyl alcohol was discarded, and the dust suspension was collected into one 50-mL plastic centrifuge tube. The dust suspension was agitated on a vortex mixer (model Sybron Thermolyne Maxi Mix, Thermolyne Corp., Dubuque, Iowa) just prior to analysis.

A subsample consisting of drops of the dust suspension was added into the wet module of the laser diffraction analyzer until the manufacturer-recommended obscuration value of between 8% and 12% was reached. Sonication of the subsample was done for 90 s just prior to analysis to minimize aggregation of the subsample. The instrument duplicated the 60-s analysis time for each subsample (Pearson et al., 2007). There were at least two subsamples analyzed for every sample.

Particle size distribution and statistics data on the dust samples were extracted from the instrument's computer software. The geometric mean diameter (GMD) and geometric standard deviation (GSD) of the equivalent sphere particles were determined from each of the data set.

The equivalent sphere diameter (d_p) of the dust particles from laser diffraction was converted into equivalent aerodynamic diameter (d_a) by:

$$d_a = d_p \sqrt{\frac{\rho_p}{\rho_0}} \tag{4.3}$$

where ρ_p is the particle density and ρ_0 is the unit density (i.e., 1.0 g·cm^{-3}). A multi-pycnometer (model MVP-1, Quantachrome Corp., Syosset, N.Y.) was used to measure ρ_p of the wheat and shelled corn dust from at least three replicates. The measured ρ_p values for wheat and shelled corn dust were 1.48 and 1.51 g·cm^{-3} (standard deviation (SD) = 0.022 and 0.014 g·cm^{-3}), respectively. The percentages of PM-2.5, PM-10 and PM-4 were interpolated from the cumulative volume percentages of the dust PSD based on their aerodynamic diameters.

4.2.5 Data Analysis

The four wheat grain lots were the experimental units in the first part of the study. The class variables were the four grain lots (Lots 1 to 4), two transfers (T1, T2), and two ducts (upper, lower). The null hypothesis was there were no mean differences in GMD, GSD, and mass flow rates among the four grain lots, between the two transfers, and between the two ducts. Analysis of Variance (ANOVA) and Bonferroni Multiple Comparison Test in SAS (version 9.1.3, SAS Institute Inc., Cary, N.C.) were used for analysis at the 5% level of significance. Differences between grain lots were not expected so we used Bonferroni because of its strict requirements prior to rejecting the null hypotheses, which minimizes Type I errors. The differences in results between the lower and upper ducts were compared to determine the necessity of sampling from both ducts.

The shelled corn lot was the experimental unit in the second part of the study. The eight transfers (T1 to T8) and the two ducts (upper, lower) were the class variables. The null hypothesis was there were no mean differences in the parameters among the eight transfers and between the two ducts. Similar to the first part of the study, data were analyzed by using ANOVA and Bonferroni.

Comparisons of results between wheat and shelled corn dust were also performed by using ANOVA and Bonferroni. The differential volume percentages of the PSD of wheat and shelled corn dust were analyzed by using the Kruskal-Wallis test, a non-parametric method for testing equality of sample medians among groups (Hollander and Wolfe, 1973; SAS, 1990). Combinations of variables were also analyzed by using ANOVA and Bonferroni (Table 4.3).

4.3 Results and Discussion

GMS, GSD, and mass flow rate values were analyzed on the basis of the combination of statistical variables in Table 4.3. Results of data analysis for wheat dust were narrowed down to differences among the four grain lots, between the two transfers, and between the two ducts because the results of the variable combinations closely followed general trends. For corn dust, presentation of results followed that indicated in Table 4.3.

Table 4.3 Combination of variables for the wheat and shelled corn dust data analysis for GMD, GSD, and mass flow rate.

Wheat Dust			
Variable	**Grain Lot (Lots 1 to 4)**	**Transfer (T1, T2)**	**Duct (Upper, Lower)**
Grain Lot (Lots 1 to 4)	-	compare ducts	compare transfers
Transfer (T1, T2)	compare ducts	-	compare grain lots
Duct (Upper, Lower)	compare transfers	compare grain lots	-

Shelled Corn Dust		
Variable	**Transfer (T1 to T8)**	**Duct (Upper, Lower)**
Transfer (T1 to T8)	-	compare ducts within each transfer
Duct (Upper, Lower)	compare transfers within each duct	-

4.3.1 Mass Flow Rate

The dust mass flow rates of wheat did not differ significantly ($p > 0.05$) among the four grain lots or between the two transfers ($p > 0.05$). The dust mass flow rate for the upper duct (39.4 $g \cdot t^{-1}$) was significantly greater ($p < 0.05$) than that for the lower duct (25.2 $g \cdot t^{-1}$) (Table 4.4). The total dust mass flow rate for wheat (64.6 g/t) collected upstream of the cyclone separators was within the range of published emission factors for grain receiving (8.30 to 90.0 $g \cdot t^{-1}$; Table 4.1).

Similar to wheat, for shelled corn, the dust mass flow rates were not significantly different ($p > 0.05$) among the eight transfers but differed significantly ($p < 0.05$) between the two ducts. Again, the dust mass flow rate for the upper duct (119.6 $g \cdot t^{-1}$) was significantly greater than that of the lower duct (65.5 $g \cdot t^{-1}$) (Table 4.4). The total dust mass flow rate for shelled corn (185.1 $g \cdot t^{-1}$) collected upstream of the cyclone separators was greater than the published emission factors for grain receiving (8.30 to 90.0 $g \cdot t^{-1}$) but within the emission factors for grain drying (110 to 1500 $g \cdot t^{-1}$; Table 4.1). For both wheat and shelled corn in the elevator in this study, more dust was generated and then collected by the pneumatic dust control system from the upper duct (elevator head and the storage bin headspace) than from the lower duct (elevator boot).

Table 4.4 Mean dust mass flow rates for wheat and shelled corn collected from the upper and lower ducts, upstream of the cyclones.[a]

Source	Mean Dust Mass Flow Rate (SD)			
	($g \cdot s^{-1}$)		($g \cdot t^{-1}$ of grain handled)	
Wheat				
Upper Duct (storage bin and elevator head)	0.571 A a	(0.113)	39.4 A a	(7.78)
Lower Duct (elevator boot)	0.365 B b	(0.159)	25.2 B b	(10.9)
Total	**0.937**	**(0.271)**	**64.6**	**(18.7)**
Shelled Corn				
Upper Duct (storage bin and elevator head)	1.88 A c	(0.270)	119.6 A c	(17.2)
Lower Duct (elevator boot)	1.03 B d	(0.169)	65.5 B d	(10.8)
Total	**2.91**	**(0.440)**	**185.1**	**(28.0)**

[a] For the same type of grain, mean values with the same upper case letters within a column are not significantly different at the 5% level of significance in Bonferroni. For comparison among both location and grain, mean values with the same lower case letters within a column are not significantly different at the 5% level of significance in Bonferroni. Values in parentheses represent standard deviation (SD).

Of the two grain types, shelled corn (185.1 $g \cdot t^{-1}$) had significantly greater dust generated, as given by the mass flow rates, than wheat (64.6 $g \cdot t^{-1}$), likely because of the tendency of corn to generate more dust than wheat during handling (Martin and Sauer, 1976; Martin and Lai, 1978; Parnell et al., 1986). Fiscus et al. (1971) found that corn had the highest breakage during various handling techniques compared with wheat and soybean because of the structurally weak kernel of corn that fragmentized into random particles sizes during the breakage process. Wheat, on the other hand, had the lowest breakage and generated dust (Martin et al., 1985) and small kernel particles mainly by abrasion (Fiscus et al., 1971). The values of dust mass flow rates for both wheat and shelled corn in this study were relatively high compared with other published values because both collection points were upstream of the cyclone separators.

4.3.2 Particle Size Distribution and Size Fractions

4.3.2.1 Wheat – Effect of Grain Lot

In general, the GMD and GSD values were not significantly different ($p > 0.05$) among the four grain lots and between the two transfers (Table 4.5). The GMD values from the upper duct (10.5 to 13.7 μm) were significantly smaller ($p < 0.05$) than those from the lower duct (12.9

to 16.9 μm). However, the GSD values from the upper duct (2.60 to 2.98) were not significantly different ($p > 0.05$) than those from the lower duct (2.74 to 2.99).

The mean GMD from the upper duct (12.3 μm), which had a corresponding mass median diameter (MMD) of 12.2 μm, was smaller than the MMD reported by Parnell et al. (1986) (i.e., 13.4 μm for dust fraction of wheat < 100 μm) and Martin and Lai (1978) (i.e., 13 μm for residual wheat dust). The mean GMD from the lower duct (14.9 μm), which had the same MMD value (14.9 μm), was greater than both of these published MMD values.

The mean GSD values from the upper (2.81) and lower (2.86) ducts were greater than the GSD from Parnell et al. (1986), which was 2.08. This is characteristic of wheat dust PSD from a wider range of particle sizes than the wheat dust of Parnell et al. (1986), which was limited to the dust fraction < 100 μm. These differences in the GMD and GSD could possibly be due to variation in grain properties, grain elevator operation and characteristics, and sampling methods and measurement.

Table 4.5 Geometric mean diameter (GMD) and geometric standard deviation (GSD) of wheat dust collected from the upper and lower ducts, upstream of the cyclones.[a]

Transfer (T) – Grain Lot (W)	GMD, μm (SD, μm)				GSD (SD)			
	Upper Duct		Lower Duct		Upper Duct		Lower Duct	
T1 – W1	12.6 a	(3.63)	12.9 b	(1.69)	2.75 a	(0.283)	2.76 a	(0.264)
T1 – W2	10.5 a	(2.03)	13.6 bc	(1.26)	2.60 a	(0.350)	2.74 a	(0.209)
T1 – W3	12.8 a	(2.65)	14.4 bc	(0.323)	2.94 a	(0.321)	2.84 a	(0.077)
T1 – W4	11.7 a	(1.56)	15.7 cd	(2.03)	2.75 a	(0.243)	2.87 a	(0.132)
T2 – W1	12.8 a	(1.76)	13.9 b	(1.76)	2.98 a	(0.333)	2.79 a	(0.145)
T2 – W2	11.8 a	(1.35)	15.5 b	(1.87)	2.83 a	(0.289)	2.93 ab	(0.122)
T2 – W3	12.5 a	(0.676)	16.0 b	(0.825)	2.80 a	(0.100)	2.99 a	(0.128)
T2 – W4	13.7 a	(0.933)	16.9 bd	(2.70)	2.86 a	(0.138)	2.99 a	(0.300)
Mean (SD)	**12.3**	**(0.975)**	**14.9**	**(1.37)**	**2.81**	**(0.120)**	**2.86**	**(0.097)**

[a] Means with the same letter are not significantly different at the 5% level of significance in Bonferroni. Values in parentheses represent standard deviations (SD).

The dust in this study would also be different from that of Parnell et al. (1986) because of the disparity in the dust generation mechanisms. The dust from this study came mainly from the elevator boot, elevator head, and storage bin headspace, whereas Parnell et al.'s (1986) dust was taken from all the operations in the terminal elevators. Although similar sets of equipment were also probably involved, the drop height, speed of impact, and other mechanisms were likely quite

different. The sampling methods were also different. Dust in the Parnell et al. (1986) study was collected from baghouse filters, whereas the dust in this study was collected by a high volume sampler upstream of the cyclone separators.

The mechanisms of dust generation from the upper duct were different than those from the lower duct. There were two sources for the dust generated and collected in the upper duct, the elevator head and filling of the storage bin. Dust generated for the lower duct was from a single source, the elevator boot. The various sources of generated dust have disparate mechanisms for damaging the grain and thus might be expected to generate dust with diverse characteristics. Apparently, these disparate mechanisms for dust generation led to the differences in dust particle sizes from the upper and lower ducts.

Figure 4.2 shows a representative plot of the cumulative and differential volume percentages of PSD of wheat dust. The Kruskal-Wallis test showed that the PSD among the four grain lots from upper and lower ducts and from the two transfers were not significantly different ($p > 0.05$), which is in agreement with the results of GMD and GSD. It appears that differences in grain lots did not affect the PSD of the wheat dust.

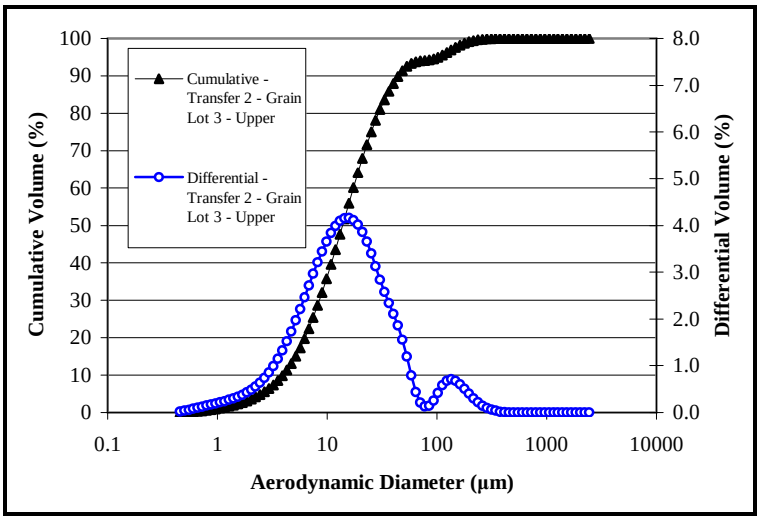

Figure 4.2 Representative plot of mean cumulative and differential volume percentages for the particle size distribution of wheat dust.

With significant difference in GMD (or PSD) between the upper and lower ducts, there were corresponding differences in the three size fractions of interest (i.e., PM-10, PM-2.5, PM-4). The percentage of PM-10 of the dust sample collected upstream of the upper duct (37.3%)

was significantly greater ($p < 0.05$) than that of the sample from the lower duct (27.8%), which was consistent with the findings on mass flow rate. The mean percentage of PM-10 for wheat dust was 33.6% (Table 4.6). This percentage of PM-10 was greater than the values reported by Martin (1981) for dust < 10μm from cyclones (9%) and baghouses (20%) (mean for corn, wheat, sorghum, and soybean dusts) and was smaller than that from the residual wheat dust ≤ 10 μm (45%) obtained by Martin and Lai (1978). This value was also slightly greater than the average percentage of PM-10 emissions (30%) from elevators primarily handling wheat (Midwest Research Institute, 1998). The wheat dust generated, as given by the mass flow rate equivalent of mean PM-10 (21.7 $g \cdot t^{-1}$ of wheat handled), was comparable to the published emission value for grain receiving (0.60 to 29.5 $g \cdot t^{-1}$) (Table 4.1).

The percentage of PM-2.5 for the samples collected from the upper duct (5.42%) was not significantly different ($p > 0.05$) than that from the lower duct (4.73%) (Table 4.6). The mean percentage of PM-2.5 (3.33 $g \cdot t^{-1}$ of wheat handled) was also within the range of published emission values for grain receiving (0.65 to 5.0 $g \cdot t^{-1}$) (Table 4.1).

The percentage of PM-4 for the samples collected from the upper duct (10.7%) was significantly greater ($p < 0.05$) than that from the lower duct (8.0%). The mean of PM-4 was 9.65% (equivalent to 6.24 $g \cdot t^{-1}$ of wheat handled) (Table 4.6). Literature contained no data with which to compare the percentage of PM-4 for wheat dust.

Table 4.6 Percentage of particulate matter of the total dust (% PM) and its mass flow rate equivalent (MFRE). [a]

Aero-dynamic Diameter (μm)	Lower Duct		Upper Duct		Mean for Lower and Upper Ducts	
	% PM (SD)	MFRE (SD), g/t of grain handled	% PM (SD)	MFRE (SD), g/t of grain handled	Mean % PM	Mean MFRE (g/t of grain handled)
Wheat Dust						
2.5	4.73 A a (0.886)	1.19 (0.223)	5.42 A a (0.586)	2.14 (0.231)	5.15 a (0.703)	3.33 (0.454)
4	8.00 A b (0.888)	2.02 (0.224)	10.7 B b (0.897)	4.22 (0.353)	9.65 b (0.893)	6.24 (0.577)
10	27.8 A c (1.61)	7.01 (0.406)	37.3 B c (3.25)	14.7 (1.28)	33.6 c (2.61)	21.7 (1.69)
Corn Dust						
2.5	7.21 A d (0.275)	4.72 (0.180)	7.59 B d (0.240)	9.08 (0.287)	7.46 d (0.252)	13.8 (0.467)
4	9.57 A b (0.257)	6.27 (0.168)	10.2 B e (0.287)	12.2 (0.343)	9.99 b (0.277)	18.5 (0.512)
10	25.5 A e (1.60)	16.7 (1.05)	30.8 B f (1.93)	36.8 (2.30)	28.9 e (1.81)	53.5 (3.35)

[a] For the same type of grain and aerodynamic diameter, mean values for upper and lower ducts with the same upper case letters within a row are not significantly different at the 5% level of significance in Bonferroni. For comparison among both location and grain, mean values with the same lower case letters within a column are not significantly different at the 5% level of significance in Bonferroni. Values in parentheses represent standard deviation (SD).

4.3.2.2 Shelled Corn – Effect of Repeated Transfers

The eight transfers did not significantly differ ($p > 0.05$) in GMD and GSD values (Table 4.7). The GMD values from the upper duct (10.0 to 11.1 μm) were significantly less ($p < 0.05$) than the values from the lower duct (11.2 to 14.4 μm) because of the smaller particles generated and collected by the pneumatic dust collection system from the elevator head and storage bin headspace. The GSD values from the upper duct (2.27 to 2.36) were also significantly different ($p < 0.05$) from those of the lower duct (2.31 to 2.77).

The mean GMD from the upper duct (10.5 μm), with a corresponding MMD of 12.2 μm, was smaller than the MMD obtained by Parnell et al. (1986) (i.e., 13.2 μm for dust fraction of corn < 100 μm). The mean GMD from the lower duct (12.1 μm), with an MMD of 13.5 μm, was greater than the MMD of Parnell et al. (1986) (i.e., 13.2 μm for dust fraction of corn < 100 μm). The mean GSD values from the upper (2.32) and lower (2.44) ducts were also greater than the GSD from Parnell et al. (1986), which was 1.80. The differences in the GMD and GSD between the upper and lower ducts and the differences in MMD of the shelled corn dust in this study and that of Parnell et al. (1986) are likely due to the same factors as explained previously for wheat—differences in grain properties, grain elevator operation and characteristics, and sampling methods and measurement.

Table 4.7 Geometric mean diameter (GMD) and geometric standard deviation (GSD) of shelled corn dust collected from the upper and lower ducts, upstream of the cyclones. [a]

Transfer (T)	GMD, μm (SD, μm)				GSD (SD)			
	Upper Duct		Lower Duct		Upper Duct		Lower Duct	
T1	10.3 a	(0.157)	14.4 b	(4.70)	2.35 a	(0.084)	2.77 b	(0.774)
T2	10.7 a	(0.412)	12.1 b	(0.883)	2.34 a	(0.047)	2.52 b	(0.275)
T3	10.7 a	(0.404)	11.9 b	(0.496)	2.36 a	(0.055)	2.37 b	(0.010)
T4	10.4 a	(0.311)	11.2 b	(0.743)	2.31 a	(0.054)	2.31 b	(0.036)
T5	11.1 a	(0.580)	11.9 b	(0.606)	2.31 a	(0.024)	2.36 b	(0.036)
T6	11.0 a	(0.178)	11.7 b	(0.232)	2.33 a	(0.048)	2.35 b	(0.010)
T7	10.1 a	(0.491)	12.3 b	(1.59)	2.32 a	(0.038)	2.48 b	(0.201)
T8	10.0 a	(0.484)	11.2 b	(0.720)	2.27 a	(0.024)	2.33 b	(0.103)
Mean (SD)	**10.5**	**(0.393)**	**12.1**	**(1.01)**	**2.32**	**(0.028)**	**2.44**	**(0.153)**

[a] Means with the same letter are not significantly different at the 5% level of significance in Bonferroni. Values in parentheses represent standard deviations (SD).

Figure 4.3 shows a representative plot of the cumulative and differential volume percentage of PSD of shelled corn dust. The Kruskal-Wallis test showed that the PSD among the eight transfers from the upper and lower ducts were not significantly different ($p > 0.05$), which is in agreement with the results of GMD and GSD. Apparently, repeated transfers of corn did not affect the PSD of the generated dust.

Similar to wheat, difference in GMD or PSD between the upper and the lower ducts resulted in a significant difference in PM-10, PM-2.5, and PM-4 in terms of percentages or flow rates. The percentage of PM-10 from the upper duct (30.8%) was significantly greater ($p < 0.05$) than that from the lower duct (25.5%) (Table 4.6). The resulting mean percentage of PM-10 was 28.9%, slightly greater than that reported for elevators primarily handling corn and soybean (< 20%) (Midwest Research Institute, 1998). This percentage of PM-10 was greater than the values reported by Martin (1981) from cyclones (9%) and from baghouses (20%) (mean for corn, wheat, sorghum, and soybean dusts), Lai et al. (1984) and Baker et al. (1986) (5% to 12% for corn, wheat, sorghum, and corn starch) and smaller than those from the residual corn dust ≤ 10 μm (33%) obtained by Martin and Lai (1978). The corn dust generated, as given by the mass flow rate equivalent of mean PM-10 (53.5 $g \cdot t^{-1}$ of shelled corn handled), was greater than the published PM-10 for grain receiving (0.60 to 29.5 $g \cdot t^{-1}$) and within the range of published PM-10 for grain drying (27.5 to 375 $g \cdot t^{-1}$) (Table 4.1).

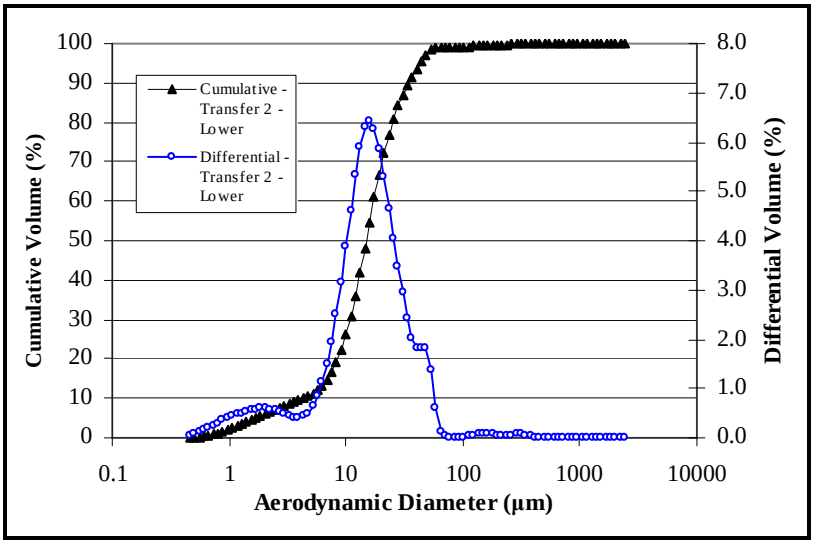

Figure 4.3 Representative plot of mean cumulative and differential volume percentages for the particle size distribution of shelled corn dust.

The percentage of PM-2.5 from the upper duct (7.59%) was significantly greater ($p < 0.05$) than that from the lower duct (7.21%). The weighted mean PM-2.5 in this study (7.46%) (Table 4.6) was greater than the value reported by Baker et al. (1986) (0.2% to 1.0%) for pneumatic conveying of corn (Table 4.2). The difference in values may be explained by the use of velocity compensators to minimize grain damage and dust generation in a pneumatic handling system where grain flow rates and conveying distances were drastically reduced (Baker et al., 1986). The corn dust generated, as given by mass flow rate equivalent (13.8 $g \cdot t^{-1}$ of shelled corn handled), was greater than the published PM-2.5 for grain receiving (0.65 to 5.0 $g \cdot t^{-1}$) and within the range of published PM-2.5 for grain drying (4.7 to 65.0 $g \cdot t^{-1}$) (Table 4.1). This implies that without the pneumatic dust collection system, the PM-2.5 of the elevator handling corn would be similar to that of grain drying.

The percentage of PM-4 from the lower duct (9.57%) was significantly smaller ($p < 0.05$) than that from the upper duct (10.2%) (Table 4.6). The weighted mean PM-4 was 9.99% (equivalent to 18.5 $g \cdot t^{-1}$ of shelled corn handled). Literature contained no data with which to compare the percentage of PM-4 from corn dust.

4.3.2.3 Comparison of Wheat and Shelled Corn – Effect of Grain Type

The GMD values of wheat dust (10.5 to 16.9 μm) were significantly greater ($p < 0.05$) than those of shelled corn dust (10.0 to 14.4 μm). The same was true when comparing the GSD values of wheat dust (2.60 to 2.99) with those of corn (2.27 to 2.77). This implies that handling shelled corn generated dust particles that were generally smaller in diameter than those from wheat.

Comparisons of GMD and GSD values within each duct (upper vs. lower) showed that wheat and corn dust were significantly different ($p < 0.05$). However, GMD and GSD values of wheat dust were not significantly different ($p > 0.05$) from that of shelled corn dust within Transfer 1 but significantly differ ($p < 0.05$) within Transfer 2. This may be due to inherent variability between the transfers and the test materials.

It must be emphasized that the dust collected from the ducts in this study was upstream of the cyclone collectors; thus, most of it was not emitted to the atmosphere. The relationship of this dust (from upstream the cyclone) and the dust that would be emitted without a pneumatic dust collection system is not known. However, it could be speculated that the measurement results for dust taken upstream of the cyclone (or any similar control devices) would likely be greater than

those taken from sources with no pneumatic dust control system. The relative difference would depend on the air velocities and design of the pneumatic dust control system among others. Establishing the relationship between the two measurements could be considered for future work. Another issue for future work includes the effect of air velocities or volumetric flow rate on the measurements.

4.4 Summary

Grain dust generated during handling can pose a safety and health hazard and is an air pollutant. This study was conducted to characterize the particle size distribution (PSD) of grain dusts generated during handling in the research elevator of the USDA Center for Grain and Animal Health Research. The percentages of PM-2.5 and PM-10 (which are regulatory concerns), PM-4 (a health concern), and the mass of generated dust (mass flow rate equivalent) were measured. The effects of different grain lots and repeated transfers on the dust size distribution were studied by using wheat and shelled corn dusts, respectively. The effect of grain types on particle size distribution was also studied. The dust samples were collected on glass fiber filters with high volume samplers from the lower and upper ducts upstream of the cyclone dust collectors. A laser diffraction analyzer was used to measure the PSD of the collected dust.

Shelled corn produced significantly smaller dust particles, and a greater proportion of small particles, than wheat. GMD of shelled corn dust ranged from 10.0 to 14.4 μm; GSD ranged from 2.27 to 2.77. For wheat, GMD ranged from 10.5 to 16.9 μm, and GSD ranged from 2.60 to 2.99. The percentage of PM-2.5, PM-4, and PM-10 generated during the transfer operation were 7.46%, 9.99%, and 28.9%, respectively, of total shelled corn dust and 5.15%, 9.65%, and 33.6%, respectively, of total wheat dust.

Handling shelled corn generated more than twice as much total dust than handling wheat (185 $g \cdot t^{-1}$ of corn handled vs. 64.6 $g \cdot t^{-1}$ of wheat handled). For both wheat and shelled corn, at an average grain flow rate of 54.4 $t \cdot h^{-1}$, the size distribution of dust from the upper and lower ducts showed similar trends among grain lots and repeated transfers but differed between the two grain types and also between the two ducts. Overall, the corn and wheat differed significantly in the dust size distribution and the rate of total dust generated and there were significant differences between the lower and upper ducts, confirming the necessity of sampling from both ducts.

4.5 References

ACGIH. 1997. *1997 Threshold Limit Values and Biological Exposure Indices*. Cincinnati, Ohio: American Conference of Governmental Industrial Hygienists.

Aldis, D. F., and F. S. Lai. 1979. Review of literature related to engineering aspects of grain dust explosions. USDA Miscellaneous Publication No. 1375. Washington, D.C.: U.S. Department of Agriculture. 42p.

ASTM Standards. 2000. D4536-96. Standard test method for high-volume sampling for solid particulate matter and determination of particulate emissions (replaced by D6331). West Conshohocken, Pa.: American Society for Testing and Materials.

Baker, K. D., R. L. Stroshine, K. J. Magee, G. H. Foster, and R. B. Jacko. 1986. Grain damage and dust generation in a pressure pneumatic conveying system. *Transactions of ASAE* 29(2): 840-847.

Beckman-Coulter, Inc. 2006. Laser Diffraction. Fullerton, Calif. Available at: www.beckmancoulter.com. Accessed 09 November 2007.

Billate, R. D., R. G. Maghirang, and M. E. Casada. 2004. Measurement of particulate matter emissions from corn-receiving operations with simulated hopper-bottom trucks. *Transactions of ASAE* 47(2): 521-529.

Fiscus, D. E., G. H. Foster, and H. H. Kaufman. 1971. Physical damage of grain caused by various handling techniques. *Transactions of ASAE* 14(3): 480-485, 491.

Garrett, D. W., F. S. Lai, and L. T. Fan. 1982. Minimum explosible concentration as affected by particle size and composition. ASAE Paper No. 823580. St. Joseph, Mich.: ASAE.

Hollander, M., and D. A. Wolfe. 1973. *Nonparametric Statistical Methods*. New York: John Wiley & Sons.

Jacobsen, M., J. Nagy, A. R. Cooper, and F. J. Ball. 1961. Explosibility of agricultural dusts. U.S. Bureau of Mines - Report of Investigations No. 5753. Washington, D.C.: U.S. Department of the Interior Bureau of Mines.

Kenkel, P., and R. Noyes. 1995. Summary of OSU grain elevator dust-emission study and proposed grain elevator emission factors. Report to the Oklahoma Air Quality Council. Stillwater, Okla.: Oklahoma State University.

Lai, F. S., D. W. Garrett, and L. T. Fan. 1984. Study of mechanisms of grain dust explosion as affected by particle size and composition: part 2. characterization of particle size and composition of grain dust. *Powder Technology* 39(2): 263-278.

Martin, C. R. 1981. Characterization of grain dust properties. *Transactions of ASAE* 24(3): 738-742.

Martin, C. R., and F. S. Lai. 1978. Measurement of grain dustiness. *Cereal Chemistry* 55(5): 779-792.

Martin, C. R., and D. B. Sauer. 1976. Physical and biological characteristics of grain dust. *Transactions of ASAE* 19(4): 720-723.

Martin, C. R., and L. E. Stephens. 1977. Broken corn and dust generated during repeated handling. *Transactions of ASAE* 20(1): 168-170.

Martin, C. R., D. F. Aldis, and R. S. Lee. 1985. In situ measurement of grain dust particle size distribution and concentration. *Transactions of ASAE* 28(4):1319-1327.

Midwest Research Institute. 1998. Emission factor documentation for AP-42 Section 9.9.1. Grain Elevators and Grain Processing Plants: Final Report. U.S. EPA contract 68-D2-0159. Research Triangle Park, N.C.: U.S. Environmental Protection Agency.

NIOSH. 1983. Occupational Safety in Grain Elevators and Feed Mills. Washington, D.C.: National Institute for Occupational Safety and Health. Available at: www.cdc.gov /niosh/pubs/criteria_date_asc_nopubnumbers.html. Accessed 30 January 2008.

Noyes, R. T. 1998. Preventing grain dust explosions. Current Report-1737. Stillwater, Okla.: Oklahoma Cooperative Extension Service. Available at: www.osuextra.okstate.edu/pdfs/CR-1737web.pdf. Accessed 01 April 2008.

Palmer, K. N. 1973. *Dust Explosions and Fires*. London, England: Chapman and Hall.

Parnell, Jr. C. B., D. D. Jones, R. D. Rutherford, and K. J. Goforth. 1986. Physical properties of five grain dust types. *Environmental Health Perspectives* 66: 183-188.

Pearson, T., J. D. Wilson, J. Gwirtz, E. Maghirang, F. Dowell, P. McCluskey, and S. Bean. 2007. Relationship between single wheat kernel particle-size distribution and Perten SKCS 4100 hardness index. *Cereal Chemistry* 84(6): 567-575.

Piacitelli, C. A., and W. G. Jones. 1992. Health Hazard Evaluation (HHE) Report no. 92-0122-2570. Available at: www.cdc.gov/niosh/hhe/reports. Accessed 31 March 2008.

SAS. 1990. *SAS/STAT User's Guide*. Ver. 6. 4th ed. Cary, N.C.: SAS Institute Inc.

Shaw, B. W., P. P. Buharivala, C. B. Parnell, Jr., and M. A. Demny. 1998. Emission factors for grain-receiving and feed-loading operations at feed mills. *Transactions of ASAE* 41(3): 757-765.

US EPA. 1989. Conditional Test Method (CTM)-003. Determination of particulate matter (modified high-volume sampling procedure). Research Triangle Park, N.C.: U.S. Environmental Protection Agency.

US EPA. 1990. The Clean Air Act. Research Triangle Park, N.C.: U.S. Environmental Protection Agency. Available at: www.epa.gov/air/caa/. Accessed 29 May 2008.

US EPA. 2000. Method 1 − Sample and velocity traverses for stationary sources. Code of Federal Regulations (CFR), Title 40, Part 60, App. A. Final Rule: Amendments. *Fed. Reg.* 65(201): 61779-61787. Research Triangle Park, N.C.: U.S. Environmental Protection Agency.

US EPA. 2003. Section 9.9.1: Grain Elevator and Processes. Chapter 9: Food and Agricultural Industries. In *Emission Factors/ AP-42.* 5th ed. Vol. I. Research Triangle Park, N.C.: U.S. Environmental Protection Agency. Available at: www.epa.gov/ttn/chief/ap42/ch09/index.html. Accessed 29 May 2008.

US EPA. 2007. Particulate Matter (PM) Standards. Research Triangle Park, N.C.: U.S. Environmental Protection Agency. Available at: www.epa.gov/pm/standards.html. Accessed 31 March 2008.

Wallace, D. 2000. Grain handling and processing. In *Air Pollution Engineering Manual*, 463-473. W. T. Davis, ed. New York: John Wiley and Sons.

CHAPTER 5 - Material and Interaction Properties of Selected Grains and Oilseeds for Modeling Discrete Particles

5.1 Introduction

Physical characteristics are important in analyzing the behavior of grains in handling operations (Mohsenin, 1986). Bulk handling behavior of the grains can be studied experimentally, but large-scale investigations of grain flow can be expensive and time consuming. On the other hand, computer simulations can reduce the large effort required to evaluate the flow of grain in handling operations.

Recently, grain segregation and identity preservation operations have become important as grain handlers respond to an increased use of specialty grain (Berruto and Maier, 2001; Herrman et al., 2001, 2002). However, limited studies have been conducted to quantify the commingling that may occur during grain handling in grain elevators (Hurburgh, 1999; Ingles et al., 2003, 2006) and with farm equipment (Greenlees and Shouse, 2000; Hirai et al., 2006; Hanna et al., 2006). Limited data on grain commingling during handling in grain elevators (Ingles et al., 2003, 2006) make it difficult to accurately predict levels of impurities that would propagate through grain handling systems. Thus, a validated mechanistic model for predicting grain commingling in various types of elevator equipment will be valuable for extending the knowledge of grain commingling beyond current experimental studies.

Different modeling techniques such as continuum models and discrete element models (Wightman et al., 1998) have potential to simulate grain commingling in elevator equipment. The discrete element method (DEM) is considered one of the most promising techniques to simulate motion of individual grain kernels (Wightman et al., 1998) in bucket-elevator equipment. The discrete element method is an explicit numerical scheme in which particle interaction is monitored contact by contact and the motion of individual particles is modeled (LoCurto et al., 1997). This explicit scheme requires small time steps, resulting in potential problems with developing realistic models that can run in a reasonable time on current computers. The model must use a critical time increment that achieves stability and simulates the

true physics with a manageable number of iterations or calculations (O'Sullivan and Bray, 2004; Li et al., 2005).

Relevant grain physical properties must be known to accurately simulate grain handling operations. The objectives of this study were (1) to review the published physical properties of grains and oilseeds needed to model grain commingling in DEM, and (2) to develop and evaluate an appropriate particle model for one test seed based on these physical properties. Soybeans were chosen as the test seed due to their almost spherical shape for simplicity of modeling. Additionally, other major seeds with non-spherical shapes (e.g., corn, wheat) were also reviewed in this study. Their physical properties can be used for future DEM modeling.

5.2 Physical Properties of Grains and Oilseeds

Different DEM models have used varying parameters for simulation modeling. The most widely used parameters can be divided into two categories: material properties and interaction properties (Mohsenin, 1986; Vu-Quoc et al., 2000; Raji and Favier, 2004a, b). Material properties may be defined as intrinsic characteristics of the particle (i.e., grain kernels) that is being modeled. Among material properties critical as inputs in DEM modeling are shape, size distribution, density, Poisson's ratio, and shear modulus. Interaction properties are characteristics exhibited by the particle in relation to its contact with boundaries, surfaces, and other (or same) particles. Interaction properties, vital in DEM modeling, are coefficients of restitution, and static and rolling friction (LoCurto et al., 1997; Chung et al., 2004). Grain material and interaction properties available in the literature are summarized in Table 5.1.

5.2.1 Particle Shape and Particle Size

Shape and size are inseparable physical properties in a grain kernel. In defining shape, some dimensional parameters of the grain must be measured. Mohsenin (1986) and Nelson (2002) reported measuring three orthogonally oriented dimensions of 50 kernels randomly selected from a grain lot to determine kernel shape and size. The volume was taken as one of the parameters defining kernel shape and the three mutually perpendicular axes were taken as a measure of kernel size.

Table 5.1 Range of published physical properties of grains and oilseeds.

Grain/ Oilseed Kernels		Soybean		Corn		Wheat	
Parameters							
Moisture Content (%) wb		6.9 - 16.7	b, j, k, p, s, t, y, z	6.7 - 25.0	e, f, h, k, s, y, z, aa	6.2 - 20.0	e, f, g, k, s, y, z, aa
Particle Length (mm), *l*		7.0 - 8.2	q, s, t, y	9.4 - 20.3	k, s, u, y, ac	5.5 - 7.3	k, s, y
Particle Width (mm), w		6.1 - 6.7	q, s, t, y	8.0 - 16.4	k, s, u, y, ac	2.6 - 3.8	k, s, y
Particle Thickness (mm), *h*		5.5 - 5.9	q, s, t, y	4.0 - 12.8	k, s, u, y, ac	2.4 - 3.5	k, s, y
Equivalent Particle Diameter (mm), d_e		6.0	k, w	8.0	k	3.6 - 4.1	k
Equivalent Particle Radius (mm), r_e		3.0	k, w	4.0	k	1.8 - 2.1	k
Particle Mass (mg), *m*		100 - 200	q, r, s, t, y	250 - 349.7	e, k, *l* , s, u, y,	26 - 51	k, *l* , r, s, y
Particle Volume (mm^3), *V*		134.1 - 152.8	s	274	s	18.5 - 28.6	s
Particle Density (kg/m^3), ρ_p		1130 - 1325.2	s, w, y, z	1270 - 1396.5	k, s, y, z, ac	1290 - 1430	k, s, y, z
Bulk Density (kg/m^3), ρ_b		705 - 876	i, p, s, y, z	661 - 810	ı, κ, *l* , s, y, z	690 - 823.2	ı, κ, *l* , s, y, z
Particle Poisson Ratio, *v*		0.08 - 0.4134	j, q, t, w, y	0.17 - 0.4	h, k, v, y, aa, ac	0.16 - 0.42	g, y, aa
Particle Elastic Modulus (MPa), *E*		31.2 - 176.9	j, t, w, y	10.9 - 2320	h, v, y, aa, ac	10 - 2834	g, y
Particle Shear Modulus (MPa), *G*		13.3 - 63.2	j, t, w, y	4.5 - 828.6	h, v, y, aa, ac	4.2 - 997.9	g, y
Particle Restitution Coefficient, *e*	generic	0.5, 0.7	w, q	-		-	
	with aluminum	0.6, 0.7	p	-		-	
	with acrylic	-		0.59	aa	-	
Particle Static Friction Coefficient, μ_s	with self (grain)	0.267, 0.55	q, d, k	0.52, 0.51	a, d, k	0.47, 0.53	a, b, d, k
	with galvanized sheet (or sheet metal)	0.18 - 0.27	f, k, y	0.20 - 0.34	f, k, y,	0.10 - 0.44	f, k, y
	with steel (or stainless steel)	0.223 - 0.247, 0.37	y, d, k	0.235 - 0.76	a, d, e, k, v, y	0.248 - 0.55	a, b, d, e, k, y
	with transparent perspex	0.30	w	-		-	
	with aluminum	-		0.226 - 0.276	v	-	
	with acrylic	-		0.34	t	-	
	with glass	0.328	q				
Bulk Static Angle of Repose (degree)	for filling or piling	16	d, k	16	d, k	16	d, k
	for emptying or funneling	29 - 33	d, k, y	23.1 - 34.7	d, k, y	23.8 - 38.1	d, k, y
Bulk Angle of Internal Friction (degree)		29.2 - 31	y	26.1 - 35.1	y	25.4 - 36.0	y

* Unhulled seed or paddy
** Dehulled kernel
\+ Oil type
\+\+ Non-oil type

[a] Airy (1898)
[b] Jamieson (1903)
[c] Kramer (1944)
[d] Stahl (1950)
[e] Lorenzen (1957)
[f] Brubaker and Pos (1965)
[g] Arnold and Roberts (1969)
[h] Shelef and Mohsenin (1969)
[i] Henderson and Perry (1976)
[j] Misra and Young (1981)
[k] Mohsenin (1986)
[l] Hoseney and Faubion (1992)
[m] Bilanski et al. (1994)
[n] Shroyer et al. (1996)
[o] Gupta and Das (1997)
[p] LoCurto et al. (1997)
[q] Vu-Quoc et al. (2000)
[r] McLelland and Miller (2001)
[s] Nelson (2002)
[t] Zhang and Vu-Quoc (2002)
[u] Watson (2003)
[v] Chung et al. (2004)
[w] Raji and Favier (2004a, b)
[x] Calisir et al. (2005)
[y] Molenda and Horabik (2005)
[z] *ASABE Standards* (2006a) - D241.4
[aa] *ASAE Standards* (2006b) - S368.4
[ab] Boyles et al. (2006)
[ac] Chung and Ooi (2008)

Table 5.1 Range of published physical properties of grains and oilseeds. (cont.)

Grain/ Oilseed Kernels		Grain Sorghum		Rice		Barley	
Parameters							
Moisture Content (%) wb		9.2 - 11.2	k, s, z	8.6 - 15.7	c, d, k, s, z	7.5 - 20.0	e, f, k, s, y, z
Particle Length (mm), *l*		4.3, 4.5	k, s	5.3 - 8.9**, 7.6 - 9.8	k, s	7.9 - 10.9	k, s, y
Particle Width (mm), w		4.1	k, s	2.1 - 2.9**, 2.5 - 3.6	k, s	2.9 - 3.8	k, s, y
Particle Thickness (mm), *h*		2.8, 3.4	k, s	1.7 - 2.0**, 2.1 - 2.5	k, s	2.2 - 3.0	k, s, y
Equivalent Particle Diameter (mm), d_e		3.5	k	3.3 - 3.5	k	3.7 - 4.2	k
Equivalent Particle Radius (mm), r_e		1.8	k	1.7 - 1.8	k	1.9 - 2.1	k
Particle Mass (mg), *m*		28 - 33.2	k, *l* , s	17.5 - 24.9**, 25 - 29.1	k, *l* , s	25.1 - 53.9	k, s, y, z
Particle Volume (mm^3), *V*		24.7	s	12 - 18**	s	19.7 - 25.9	s
Particle Density (kg/m^3), ρ_p		1220 - 1344	k, s, z	1382-1462 , 1110-1120 , 1360-1390	k, s, z	1130 - 1420	k, s, y, z
Bulk Density (kg/m^3), ρ_b		643.5 - 775	[illegible]	641-851 , 579 , 573.2-579	[illegible]	566 - 691	[illegible]
Particle Poisson Ratio, *v*		-		-		0.14 - 0.20	y
Particle Elastic Modulus (MPa), *E*		-		-		8.0 - 15.8	y
Particle Shear Modulus (MPa), *G*		-		-		3.3 - 6.87	y
Particle Restitution Coefficient, *e*	generic	-		-		-	
	with aluminum	-		-		-	
	with acrylic	-		-		-	
Particle Static Friction Coefficient, μ_s	with self (grain)	0.65	d, k	0.68*, 0.73*	c, d, k	0.51, 0.53	a, d, k
	with galvanized sheet (or sheet metal)	-		0.40 - 0.45*	c, k	0.17 - 0.352	f, k, y
	with steel (or stainless steel)	0.37	d, k	0.48*	d, k	0.226 - 0.40	a, d, e, k, y
	with transparent perspex	-		-		-	
	with aluminum	-		-		-	
	with acrylic	-		-		-	
	with glass						
Bulk Static Angle of Repose (degree)	for filling or piling	20	d, k	20*	d, k	16	d, k
	for emptying or funneling	33	d, k	36*	d, k	26.1 - 32.9	d, k, y
Bulk Angle of Internal Friction (degree)		-		-		27.4 - 33.7	y

* Unhulled seed or paddy
** Dehulled kernel
+ Oil type
++ Non-oil type

[a] Airy (1898)
[b] Jamieson (1903)
[c] Kramer (1944)
[d] Stahl (1950)
[e] Lorenzen (1957)
[f] Brubaker and Pos (1965)
[g] Arnold and Roberts (1969)
[h] Shelef and Mohsenin (1969)
[i] Henderson and Perry (1976)
[j] Misra and Young (1981)
[k] Mohsenin (1986)
[l] Hoseney and Faubion (1992)
[m] Bilanski et al. (1994)
[n] Shroyer et al. (1996)
[o] Gupta and Das (1997)
[p] LoCurto et al. (1997)
[q] Vu-Quoc et al. (2000)
[r] McLelland and Miller (2001)
[s] Nelson (2002)
[t] Zhang and Vu-Quoc (2002)
[u] Watson (2003)
[v] Chung et al. (2004)
[w] Raji and Favier (2004a, b)
[x] Calisir et al. (2005)
[y] Molenda and Horabik (2005)
[z] *ASABE Standards* (2006a) - D241.4
[aa] *ASAE Standards* (2006b) - S368.4
[ab] Boyles et al. (2006)
[ac] Chung and Ooi (2008)

Table 5.1 Range of published physical properties of grains and oilseeds. (cont.)

Grain/ Oilseed Kernels		Oats		Sunflower		Canola	
Parameters							
Moisture Content (%) wb		8.5 -20.0	f, k, s, y, z	3.9 - 16.7	o, s	4.5 - 19.3	m, s, x, y, z
Particle Length (mm), *l*		10.2 - 14.9	k, s, y	9.5*, 8.3**, 10.7+, 14.4++	o, s	1.6 - 2.305	s, x, y
Particle Width (mm), w		2.7 - 3.1	k, s, y	5.1*, 4.1**, 5.2+, 8.1++	o, s	1.4, 1.7	s, y
Particle Thickness (mm), *h*		2.1 - 2.6	k, s, y	3.3*, 2.4**, 3.1+, 4.6++	o, s	1.7	y
Equivalent Particle Diameter (mm), d_e		3.5 - 3.8	k	5.4 , 4.3	o	1.824 - 2.0	m, w, x
Equivalent Particle Radius (mm), r_e		1.8 - 1.9	k	2.7 , 2.15	o	0.9 - 1.0	m, w, x
Particle Mass (mg), *m*		28.1 - 39.5	k, *l* , s, y	49*, 34**, 59.5-126+, 115.8++	o, r, s	2.9 - 6.6	r, s, x, y
Particle Volume (mm^3), *V*		21.4, 26.8	s	58.2+, 105.4++	s	2.7 - 5.225	s, x
Particle Density (kg/m^3), ρ_p		950 - 1397	k, s, y, z	706-765 , 1050-1250 , 1023 , 1099	o, s	1053 - 1150	w, s, y, z
Bulk Density (kg/m^3), ρ_b		412 - 576	k, *l* , s, y, z	434-462 , 574-628 , 386-412 , 309-339 , 361.2	n, o, s, z	640 - 671	s, y, z
Particle Poisson Ratio, *v*		0.14 - 0.21	y	-		0.09 - 0.4	m, w, y
Particle Elastic Modulus (MPa), *E*		8.3 - 20.6	y	-		5.7 - 50.1	m, w, y
Particle Shear Modulus (MPa), *G*		3.52 - 8.80	y	-		2.57 - 17.9	m, w, y
Particle Restitution Coefficient, *e*	generic	-		-		0.6	w
	with aluminum	-		-		-	
	with acrylic	-		-		-	
Particle Static Friction Coefficient, μ_s	with self (grain)	0.53, 0.62	a, d, k	-		0.5	w
	with galvanized sheet (or sheet metal)	0.18 - 0.41	f, k, y	0.40 - 0.58*, 0.43 - 0.81**	o	0.211 - 0.322	x, y
	with steel (or stainless steel)	0.233 - 0.45	a, d, k, y	-		0.234 - 0.301	y
	with transparent perspex	-		-		0.30	w
	with aluminum	-		-		-	
	with acrylic	-		-		-	
	with glass						
Bulk Static Angle of Repose (degree)	for filling or piling	18	d, k	-		-	
	for emptying or funneling	27.7 - 35.1	d, k, y	34 - 41*, 27 - 38**	o	22 - 29.8	y, ab
Bulk Angle of Internal Friction (degree)		21.0 - 28.1	y	-		24.2 - 35.5	y

* Unhulled seed or paddy
** Dehulled kernel
\+ Oil type
\++ Non-oil type

[a] Airy (1898)
[b] Jamieson (1903)
[c] Kramer (1944)
[d] Stahl (1950)
[e] Lorenzen (1957)
[f] Brubaker and Pos (1965)
[g] Arnold and Roberts (1969)
[h] Shelef and Mohsenin (1969)
[i] Henderson and Perry (1976)
[j] Misra and Young (1981)
[k] Mohsenin (1986)
[l] Hoseney and Faubion (1992)
[m] Bilanski et al. (1994)
[n] Shroyer et al. (1996)
[o] Gupta and Das (1997)
[p] LoCurto et al. (1997)
[q] Vu-Quoc et al. (2000)
[r] McLelland and Miller (2001)
[s] Nelson (2002)
[t] Zhang and Vu-Quoc (2002)
[u] Watson (2003)
[v] Chung et al. (2004)
[w] Raji and Favier (2004a, b)
[x] Calisir et al. (2005)
[y] Molenda and Horabik (2005)
[z] *ASABE Standards* (2006a) - D241.4
[aa] *ASAE Standards* (2006b) - S368.4
[ab] Boyles et al. (2006)
[ac] Chung and Ooi (2008)

5.2.2 Particle Density

Particle density (ρ_p) of the grain is determined by measuring the volume occupied by the kernels in a known sample weight, randomly taken from each grain lot. Nelson (2002) measured the volume of an approximately 20- to 25-g sample with a Beckman model 930 air-comparison pycnometer. Kernel density was calculated by dividing the weighed mass by the measured volume.

5.2.3 Particle Poisson's Ratio and Particle Shear Modulus

Poisson's ratio (ν) is the absolute value of the ratio of transverse strain (perpendicular to the axis) to the corresponding axial strain (parallel to the longitudinal axis) resulting from uniformly distributed axial stress below the proportional limit of the material (Mohsenin, 1986). Based on Hooke's law and together with Poisson's ratio, shear modulus or modulus of rigidity (G) for an elastic, homogenous, and isotropic material is the ratio of the stress component tangential to the plane on which the forces acts (i.e., shear stress) over its strain. Shear modulus defined in terms of Poisson's ratio and Young's modulus or modulus of elasticity (E) is given by (Mohsenin, 1986):

$$G = \frac{E}{2 + 2\nu} \tag{5.1}$$

Several values of Poisson's ratio and elastic or Young's modulus for different grains and oilseeds were cited in the literature (Table 5.1).

5.2.4 Particle Coefficient of Restitution

Different methods have been used to determine the coefficient of restitution, e (Sharma and Bilanski, 1971; Smith and Liu, 1992; Yang and Schrock, 1994; LoCurto et al., 1997). LoCurto et al. (1997) described the e as the square root of the total kinetic energy before (KE_i) and after (KE_r) collisions that did not involve tangential frictional losses. They measured e values of soybeans impacting different surfaces at varying drop heights and moisture contents. The e values decreased with increased moisture content and drop height, and contact with aluminum gave the highest value. Drop and rebound heights were measured only from those soybeans that fell with minimal rotation and whose rebound trajectories were almost vertical (90 ± 1.6% to the plate). This was different from the results of Yang and Schrock (1994) which involved cases of

grain kernels with and without rotation. Assuming no loss of energy except during contact, the *e* value was computed as the ratio of the square root of the initial height of drop (H_i) and the height of rebound (H_r) (LoCurto et al., 1997; Zhang and Vu-Quoc, 2002):

$$e \equiv \left(\frac{H_r}{H_i} \right)^{\frac{1}{2}} \tag{5.2}$$

5.2.5 Particle Coefficient of Static Friction

The coefficient of friction (μ) is the ratio of the force of friction (F) to the force normal to the surface of contact (W) (Mohsenin, 1986):

$$\mu = \frac{F}{W} \tag{5.3}$$

Frictional forces acting between surfaces at rest with respect to each other and those existing between the surfaces in relative motion are, respectively, called forces of static and kinetic friction and denoted by μ_s and μ_k, respectively (Mohsenin, 1986).

Published coefficients of static friction of grain-on-grain and grain-on-surfaces such as sheet metal, stainless steel, acrylic, aluminum, and glass are listed in Table 5.1. Static friction of soybean-steel contact is 67% of that of soybean on itself (Stahl, 1950).

5.2.6 Particle Coefficient of Rolling Friction

The coefficient of rolling friction (μ_r) is defined as the ratio of the force of friction to the force normal to the surface of contact that prevents a particle from rolling. Rolling friction or resistance can be a couple (or pure moment) that may be transferred between the grains via the contacts, and this couple resists particle rotations (Jiang et al., 2005) without affecting translation. It may exist even at contacts between cylindrical grains (Bardet and Huang, 1993). In Jiang et al.'s (2005) micro-mechanical model, only the normal basic element, composed of a spring and dashpot in parallel with a divider series, contributes to rolling resistance at grain contact. Rolling resistance directly affects only the angular motion and not the translational motion of grains.

Zhou et al. (2002) investigated the effect of rolling friction on the angle of repose of coarse glass beads. They included coefficients of rolling friction with a base value of 0.05 (range: 0 - 0.1) on particle-to-particle contact and twice that value for particle-wall contact in

their simulations. The authors found that increasing both rolling frictions increased the angle of repose. This is due to a large resistance force to the rotational motion of spheres providing an effective mechanism to consume the kinetic energy, stop the rotational motion, and lead to the formation of a "sand pile" with high potential energy (Zhou et al., 1999).

5.2.7 Bulk Density

Bulk density (ρ_b) is the ratio of the mass to a given volume of a grain sample including the interstitial voids between the particles (Hoseney and Faubion, 1992; Gupta and Das, 1997). In the U. S., bulk density or test weight per bushel is the weight (in lb) per Winchester bushel (2,150.42 in.^{3}) as determined using an approved device (USDA GIPSA, 2004). The USDA GIPSA (2004) method involves allowing a sufficient amount of grain from a hopper, suspended two inches above, to overflow the test weight kettle, leveling the kettle by three full-length, zigzag motions with a stroker, and weighing the grain from the kettle with an appropriate scale. Several ρ_b values for grains and oilseeds were found in the literature (Table 5.1).

5.2.8 Angle of Repose

Angle of repose (θ) is defined as the angle with the horizontal at which the granular material will stand when piled (Mohsenin, 1986; Hoseney and Faubion, 1992). The angle of repose of grains is determined by numerous factors which include frictional forces generated by the grain flowing against itself, distribution of weight throughout the grain mass, and moisture content of the grain (Hoseney and Faubion, 1992). At least two angles of repose are commonly defined, namely the static angle of repose and the dynamic angle of repose. The dynamic angle of repose is generally smaller than the static angle of repose by at least 3 - 10º (Fowler and Wyatt, 1960).

It is generally believed that the angle of repose and the angle of internal friction are approximately the same (Mohsenin, 1986; Walton, 1994). Fowler and Chodziesner (1959) noted that when the "relative roughness factor" is equal to unity (i.e., materials are sliding over themselves) and is zero (i.e., smooth surface), the angle of repose is equal to the angle of friction and is independent of the diameter of the granular material. Stewart (1968), however, showed that for at least one seed (i.e., grain sorghum), the angle of repose and internal friction are different.

There are several methods for measuring the angle of repose. The method to measure static angle includes (1) the fixed funnel and the free-standing cone, (2) the fixed-diameter cone and the funnel, and (3) the tilting box (Kramer, 1944; Train, 1958; Burmistrova et al., 1963; Fraczek et al., 2007). For dynamic angle, the methods include (1) the revolving cylinder (Train, 1958) and (2) that of Brown and Richards (1959) (Fowler and Wyatt, 1960; Fraczek et al., 2007).

Fraczek et al. (2007) recommended using digital-image analysis for a more precise measurement of angle of repose. Deviations from the cone shape increased with increasing moisture content of the material as was also noted by other authors (Horabik and Lukaszuk, 2000). However, the more spherical-like the materials, the more regular the cone that forms.

Zhou et al. (2002) found that the angle of repose of mono-sized coarse glass spheres is significantly affected by sliding and rolling frictions, particle size, and container thickness, but not density, Poisson's ratio, damping coefficient, or Young's modulus. The authors observed that the angle of repose increases with increasing rolling or sliding friction coefficients and with decreasing particle size or container thickness. However, container thickness larger than a critical value (about a 20-particle diameter) gives a constant angle of repose corresponding to a situation without any wall effects.

Published angles of repose of grains and oilseeds for filling or piling and for emptying or funneling are summarized in Table 5.1.

5.3 Modeling with DEM

Table 5.1 lists published values on the physical properties for soybeans, corn, wheat, grain sorghum, rice, barley, oats, sunflower, and canola seeds. Table 5.2 lists the moisture-dependent characteristics of soybean and Table 5.3 is a summary of published and representative values of material and interaction properties of soybeans. Selected representative values of material properties (i.e., particle density, particle Poisson's ratio, and particle shear modulus) and interaction properties (i.e., particle coefficient of restitution and particle coefficient of static friction) were used as base values in DEM modeling. DEM modeling software package was EDEM 2.1.2 (DEM Solutions, Lebanon, N.H.). A range of each of these five physical properties was investigated in DEM simulations of basic physical property tests, using four particle shapes.

Table 5.2 Moisture-dependent properties of soybean kernel.

Parameters	Moisture Content (% wb)													
	6.9	**7.0**	**7.1**	**8.0**	**8.1**	**9.7**	**9.8**	**10.0**	**10.7**	**12.2**	**13.0**	**13.4**	**15.5**	**16.7**
Particle Length (mm), *l*				8.2 [F]		7.3 [E]		7.0 [D]				7.1 [D]		7.3 [D]
Particle Width (mm), w				6.6 [F]		6.1 [E]		6.6 [D]				6.6 [D]		6.7 [D]
Particle Thickness (mm), *h*				5.6 [F]		5.5 [E]		5.7 [D]				5.7 [D]		5.9 [D]
Particle Mass (mg), m				185.0 [F]		149.0 [E]		167.6 [D]				173.9 [D]		189.5 [D]
Particle Volume (mm^3), V								134.1 [D]				139.1 [D]		152.8 [D]
Particle Density (kg/m^3), ρ_p	1180 [G]	1130 [G]		1325.2 [F]				1250 [D]				1250 [D]		1243 [D]
Bulk Density (kg/m^3), ρ_b				739 ± 3 [F]				723 [D]	876 [C]			712 [D]	850 [C]	705 [D]
Particle Poisson Ratio, *v*				0.15 ± 0.02 [F]		0.4134 [E]		0.4 [A]			0.4 [A]			
Particle Elastic Modulus (MPa), *E*				32.6 ± 1.4 [F]		128.8 [E]		176.9 [A]			112.7 [A]			
Particle Shear Modulus (MPa), *G = E / (2 + 2v)*				13.33 - 15.04 [F]		45.56 [E]		63.18 [A]			40.25 [A]			
Particle Restitution Coefficient	with aluminum								0.7 [C]				0.6 [C]	
Particle Static Friction Coefficient	with galvanized sheet metal		0.21 [B]	0.23 - 0.27 [F]	0.21 [B]		0.18 [B]			0.20 [B]				
	with stainless steel			0.223 - 0.247 [F]										
Bulk Static Angle of Repose (deg)	for emptying or funneling			32.5 ± 0.5 [F]										
Bulk Angle of Internal Friction (deg)				30.1 ± 0.9 [F]										

[A] Misra and Young (1981)
[B] Mohsenin (1986, p. 801); Brubaker and Pos (1965)
[C] LoCurto et al. (1997)
[D] Nelson (2002)
[E] Zhang and Vu-Quoc (2002)
[F] Molenda and Horabik (2005)
[G] *ASABE Standards* (2006a) - D241.4

Table 5.3 Published properties of soybeans and their representative values.[a]

Soybean					
Parameters		**Range**		**Representative Value**	
Moisture Content (%) wb		6.9 - 16.7	B, D, E, F, I, J, L, M		
Particle Length (mm), *l*		7.0 - 8.2	G, I, J, L	7.6	G, I, J, L
Particle Width (mm), w		6.1 - 6.7	G, I, J, L	6.4	G, I, J, L
Particle Thickness (mm), *h*		5.5 - 5.9	G, I, J, L	5.7	G, I, J, L
Equivalent Particle Diameter (mm), de		6	E, K	6	E, K
Equivalent Particle Radius (mm), re		3	E, K	3	E, K
Particle Mass (mg), *m*		100 - 200	G, H, I, J, L	150	G, H, I, J, L
Particle Volume (mm^3), *V*		134.1 - 152.8	I	143.5	I
Particle Density ($kg \cdot m^{-3}$), ρ_p		1130.0 - 1325.2	I, K, L, M	**1228**	I, K, L, M
Bulk Density ($kg \cdot m^{-3}$), ρ_b		705.0 - 876.0	C, F, I, L, M	790.5	C, F, I, L, M
Particle Poisson Ratio, *v*		0.08 - 0.4134	D, G, J, K, L	**0.25**	D, G, J, K, L
Particle Elastic Modulus (MPa), *E*		31.2 - 176.9	D, J, K, L	104.1	D, J, K, L
Particle Shear Modulus (MPa), *G = E / (2 + 2v)*		13.8 - 63.2	D, J, K, L	**41.7**	D, J, K, L
Particle Restitution Coefficient, *e*	with self (grain)	-		**0.60**	F, G, K
	generic	0.5, 0.7	K, G		
	with aluminum	0.6, 0.7	F		
	with steel	-		**0.60**	F, G, K
Particle Static Friction Coefficient, μ_s	with self (grain)	0.267, 0.55	A, E, G	**0.55**	A, E
	with galvanized sheet metal	0.18 - 0.27	B, E, L		
	with steel	0.223 - 0.247, 0.37	A, E, L	**0.37**	A, E
	with transparent perspex	0.30	K		
	with glass	0.328	G		
Particle Rolling Friction Coefficient	with self (grain)	-		**0.10**	assume
	with steel	-		**0.10**	assume
Bulk Static Angle of Repose (degree)	for filling or piling	16	A, E	16	A, E
	for emptying or funneling	29 - 33	A, E, L	31	A, E, L
Bulk Angle of Internal Friction (degree)		29.2 - 31	L	30	L

[a] Base values in bold letters were used in simulation.

A Stahl (1950)
B Brubaker and Pos (1965)
C Henderson and Perry (1976)
D Misra and Young (1981)
E Mohsenin (1986)
F LoCurto et al. (1997)
G Vu-Quoc et al. (2000)
H McLelland and Miller (2001)
I Nelson (2002)
J Zhang and Vu-Quoc (2002)
K Raji and Favier (2004a, 2004b)
L Molenda and Horabik (2005)
M *ASAE Standards* (2006a) - D241.4

DEM is a numerical modeling technique that simulates dynamic motion and mechanical interactions of each particle using Newton's Second Law of Motion and the force-displacement law. The calculation cycle involves explicit numerical scheme with very small time step as discussed in detail by Cundall and Strack (1979). In DEM modeling, particle interaction is treated as a dynamic process, which assumes that equilibrium states develop whenever internal forces in the system balance (Theuerkauf et al., 2007). Contact forces and displacements of a stressed particle assembly are found by tracking the motion of individual particles. Newton's Law of Motion gives the relationship between particle motion and the forces acting on each particle. Translational and rotational motions of particle *i* are defined by the following equations (Remy et al., 2009):

$$m_i \frac{dv_i}{dt} = \sum_j \left(F_{n_{ij}} + F_{t_{ij}} \right) + m_i g \tag{5.4}$$

$$I_i \frac{d\omega_i}{dt} = \sum_j \left(R_i \times F_{t_{ij}} \right) + \tau_{ij} \tag{5.5}$$

where m_i, R_i, v_i, ω_i, and I_i are the mass, radius, linear velocity, angular velocity, and moment of inertia of particle *i*; $F_{n_{ij}}$, $F_{t_{ij}}$, and τ_{ij} are, respectively, normal force, tangential force, and torque acting on particles *i* and *j* at contact points; *g* is the acceleration due to gravity; and *t* is the time.

Particles interact only at contact points with their motion independent of other particles. The soft-sphere approach commonly used in DEM models allows particles to overlap each other, giving realistic contact areas. The force-displacement law at the contact point is represented by Hertz-Mindlin no-slip contact model (Mindlin, 1949; Mindlin and Deresiewicz, 1953; Tsuji et al., 1992; Di Renzo and Di Maio, 2004, 2005). Forces on the particles at contact points include contact force and viscous contact damping force (Zhou et al., 2001). These forces have normal and tangential components. The normal force, F_n, is given as follows (Tsuji et al., 1992; Remy et al., 2009):

$$F_n = -K_n \delta_n^{3/2} - \eta_n \dot{\delta}_n \delta_n^{1/4} \tag{5.6}$$

where K_n is the normal stiffness coefficient; δ_n is the normal overlap or displacement; $\dot{\delta}_n$ is the normal velocity; and η_n is the normal damping coefficient. The tangential force, F_t, is governed by the following equation (Tsuji et al., 1992; Remy et al., 2009):

$$F_t = -K_t \delta_t - \eta_t \dot{\delta}_t \delta_n^{1/4} \tag{5.7}$$

where K_t is the tangential stiffness coefficient; δ_t is the tangential overlap; $\dot{\delta}_t$ is the tangential velocity; and η_t is the tangential damping coefficient.

In addition, there is a tangential force limited by Coulomb friction $\mu_s F_n$, where μ_s is the coefficient of static friction. When necessary, rolling friction can be accounted for by applying a torque to contacting surfaces. The rolling friction torque, τ_i, is given by (DEM Solutions, 2009; Remy et al., 2009):

$$\tau_i = -\mu_r F_n R_0 \omega_0 \tag{5.8}$$

where μ_r is the coefficient of rolling friction, R_0 is the distance of the contact point from the center of the mass, and ω_0 is the unit angular velocity vector of the object at the contact point (Tsuji et al., 1992; Di Renzo and Di Maio, 2004; Li et al., 2005; DEM Solutions, 2009; Remy et al., 2009).

In this study, DEM simulations were conducted with varying physical properties of soybean kernels, based on values in the literature, to find property combinations that gave simulation results that correlate well with measured bulk properties of soybeans while maintaining or improving computational speed. Thus, an appropriate particle model was established for DEM simulations of soybean handling operations. The following input parameters were included: (1) coefficient of restitution, (2) particle coefficient of static friction, (3) particle coefficient of rolling friction, (4) particle size distribution (PSD), (5) particle shear modulus, and (6) particle shape (i.e., from one to four overlapping spheres). Table 5.4 lists the variations in input parameters and includes test combination codes for the parameters: (1^{st} digit) particle coefficient of restitution, (2^{nd} digit) particle coefficient of static friction, (3^{rd} digit) particle coefficient of rolling friction, (4^{th} digit) particle size distribution (PSD), and (5^{th} digit) particle shear modulus.

The base value (represented by 1 in the test combination codes) of the particle coefficient of restitution was 0.6, which is the mean of published values. The second (0.3) and third (0.9) values for coefficients of restitution were chosen as extreme values inclusive of the published range (from 0.5 to 0.7). The base value of the particle coefficient of static friction on soybean-soybean contact was 0.55. The coefficient of static friction for soybean-steel interaction was computed to be 67% of the base value for soybean-soybean contact from Stahl (1950) and Mohsenin (1986).

Table 5.4 Variations of each model parameter.

Parameter	Symbol	Base Value (1)	Second Value (2)	Third Value (3)
1. Particle Restitution Coefficient	e	0.60	0.30	0.90
2. Particle Static Friction Coefficient				
(soybean-soybean)	$\mu_{s\,(so\text{-}so)}$	0.55	0.35	0.75
(soybean-steel)	$\mu_{s\,(so\text{-}st)}$	0.37	0.23	0.50
3. Particle Rolling Friction Coefficient (soybean-soybean is assumed same as soybean-steel)	μ_r	0.10	0.05	0.20
4. Particle Size Distribution	PSD	fixed or uniform	normal	normal
Mean factor	MF	1.0	1.0	1.0
Standard deviation factor	SDF	0.0	0.20	0.40
5. Particle Shear Modulus (MPa)	G	41.7	13.8	1.04

For particle rolling friction, the base value assumed in the simulation was 0.1, which was twice that of Zhou et al.'s (2002) for coarse glass beads, since grain surface is rougher than that of glass beads. For PSD, fixed or uniform size distribution was used as the base value; normal PSD with a standard deviation factor (SDF) of 0.2 was second; and normal PSD with SDF of 0.4 was third. SDF was obtained from the coefficient of variation of single-kernel mass from 10 soybean lots (Table 5.5).

For particle shear modulus, the base value was the mean of the published values (41.7 MPa). Typically, shear modulus values do not greatly affect results, but smaller values of shear modulus are known to reduce computational time (Chung and Ooi, 2008; Remy et al., 2009); thus, the variation of shear modulus was towards lower values. The second value chosen was the lowest limit of the range of published shear modulus for soybeans (13.8 MPa). The very low third value (1.04 MPa), computed from Remy et al.'s (2009) particle Young's modulus (2.6 MPa) and the base value of the particle Poisson's ratio for soybeans (0.25), was selected for the potential to significantly reduce computation times. Table 5.6 shows the test combinations of the five parameters used with the 1-sphere particle shape. Simulations using test combination 11111 were performed with the 2-, 3-, and 4-sphere particle shapes.

Four particle shapes were evaluated to represent soybean kernels (Figure 5.1). Particle shape was defined using one to four overlapping spheres. Overlapping spheres allow the creation of complex particle shapes but require increased computation times because each sphere in the shape requires individual calculation at each time step (LoCurto et al., 1997; Raji and Favier, 2004b). Thus, a 1-sphere geometry is desirable based on computation time if particle physics can be adequately addressed without a more complex shape. Geometry and dimension (length, width, and thickness) of the 4-sphere model were based on the soybean model of LoCurto et al. (1997) and Vu-Quoc et al. (2000), with slight differences in dimension to fit soybeans' published base values for particle density and particle volume (Table 5.3). Table 5.7 shows basic physical properties of the four particle shapes and positions of their spheres employed in the simulation. The position of each sphere in the x-, y-, and z-direction composing a particle shape is needed to define the particle shape in the simulation. Positions of the 1-, 2-, and 3-sphere particle shapes were modified to match the volume and particle density of the 4-sphere particle shape.

Table 5.5 Experimental data for standard deviation factor (SDF) for particle size distribution.[a]

						Single Kernel Mass, mg		
No.	Variety	Source	Location Planted	Crop Year	No. of Kernels Weighed	Mean	Standard Deviation (SD)	Coefficient of Variation (CV), %
1	9A411NRR	Kaufman Seeds	Reno County, Kansas	2008	55	144.24	25.41	17.62
2	9A385NRS	Kaufman Seeds	Reno County, Kansas	2007	50	112.85	20.14	17.85
3	KS-5005sp	KSU Agronomy Farm	Riley County, Kansas	2007	51	221.40	40.00	18.06
4	KS-3406RR	KSU Agronomy Farm	Riley County, Kansas	2007	55	132.97	26.14	19.66
5	KS-4607	KSU Agronomy Farm	Riley County, Kansas	2007	51	157.34	31.16	19.80
6	KS-4702sp	KSU Agronomy Farm	Riley County, Kansas	2007	56	122.64	26.12	21.29
7	Mixed (100-lb)	Manhattan Farmers COOP	Northeastern Kansas	2007	53	149.48	32.07	21.46
8	Mixed (7080-lb)	Manhattan Farmers COOP	Northeastern Kansas	2007	53	149.91	32.35	21.58
9	KS-5002N (4RL9542)	KSU Agronomy Farm	Riley County, Kansas	2004	55	157.42	34.39	21.84
10	KS-4103sp (4RL4976)	KSU Agronomy Farm	Riley County, Kansas	2004	56	124.19	28.46	22.91
				Mean	**53.50**	**147.24**	**29.62**	**20.21**
				SD	**2.22**	**30.27**	**5.57**	**1.88**

[a] SDF value of 0.2 was taken from the mean CV of individually weighing soybean kernels.

Table 5.6 Combinations of model parameters. [a]

Test No.	Test Combinations				
	Coefficient of Restitution	Coefficient of Static Friction	Coefficient of Rolling Friction	Size Distribution	Shear Modulus (MPa)
1-sphere					
11111	0.6	0.55	0.1	uniform, SDF=0	41.7
21111	0.3	0.55	0.1	uniform, SDF=0	41.7
31111	0.9	0.55	0.1	uniform, SDF=0	41.7
12111	0.6	0.35	0.1	uniform, SDF=0	41.7
13111	0.6	0.75	0.1	uniform, SDF=0	41.7
11211	0.6	0.55	0.05	uniform, SDF=0	41.7
11311	0.6	0.55	0.2	uniform, SDF=0	41.7
11121	0.6	0.55	0.1	normal, SDF=0.2	41.7
11131	0.6	0.55	0.1	normal, SDF=0.4	41.7
11112	0.6	0.55	0.1	uniform, SDF=0	13.8
11113	0.6	0.55	0.1	uniform, SDF=0	1.04
2-sphere					
11111	0.6	0.55	0.1	uniform, SDF=0	41.7
3-sphere					
11111	0.6	0.55	0.1	uniform, SDF=0	41.7
4-sphere					
11111	0.6	0.55	0.1	uniform, SDF=0	41.7

[a] Refer to Table 5.4 for complete interpretation.
Coefficient of restitution (1 stands for e = 0.6, 2 for e = 0.3, 3 for e = 0.9).
Coefficient of static friction (1 for $\mu_{s(so\text{-}so)}$ = 0.55, $\mu_{s(so\text{-}st)}$ = 0.37; 2 for $\mu_{s(so\text{-}so)}$ = 0.35, $\mu_{s(so\text{-}st)}$ = 0.23; 3 for $\mu_{s(so\text{-}so)}$ = 0.75, $\mu_{s(so\text{-}st)}$ = 0.50).
Coefficient of rolling friction (1 for μ_r = 0.1, 2 for μ_r = 0.05, 3 for μ_r = 0.2).
Particle size distribution (PSD) (1 for uniform particle size, 2 for normal PSD with standard deviation factor (SDF) = 0.2, 3 for normal PSD with SDF = 0.4).
Shear modulus (1 stands for G = 41.7 MPa, 2 for G = 13.8 MPa, 3 for G = 1.04 MPa).
For bulk density and bulk angle of repose tests, three and seven replications, respectively, were performed for each test combination.

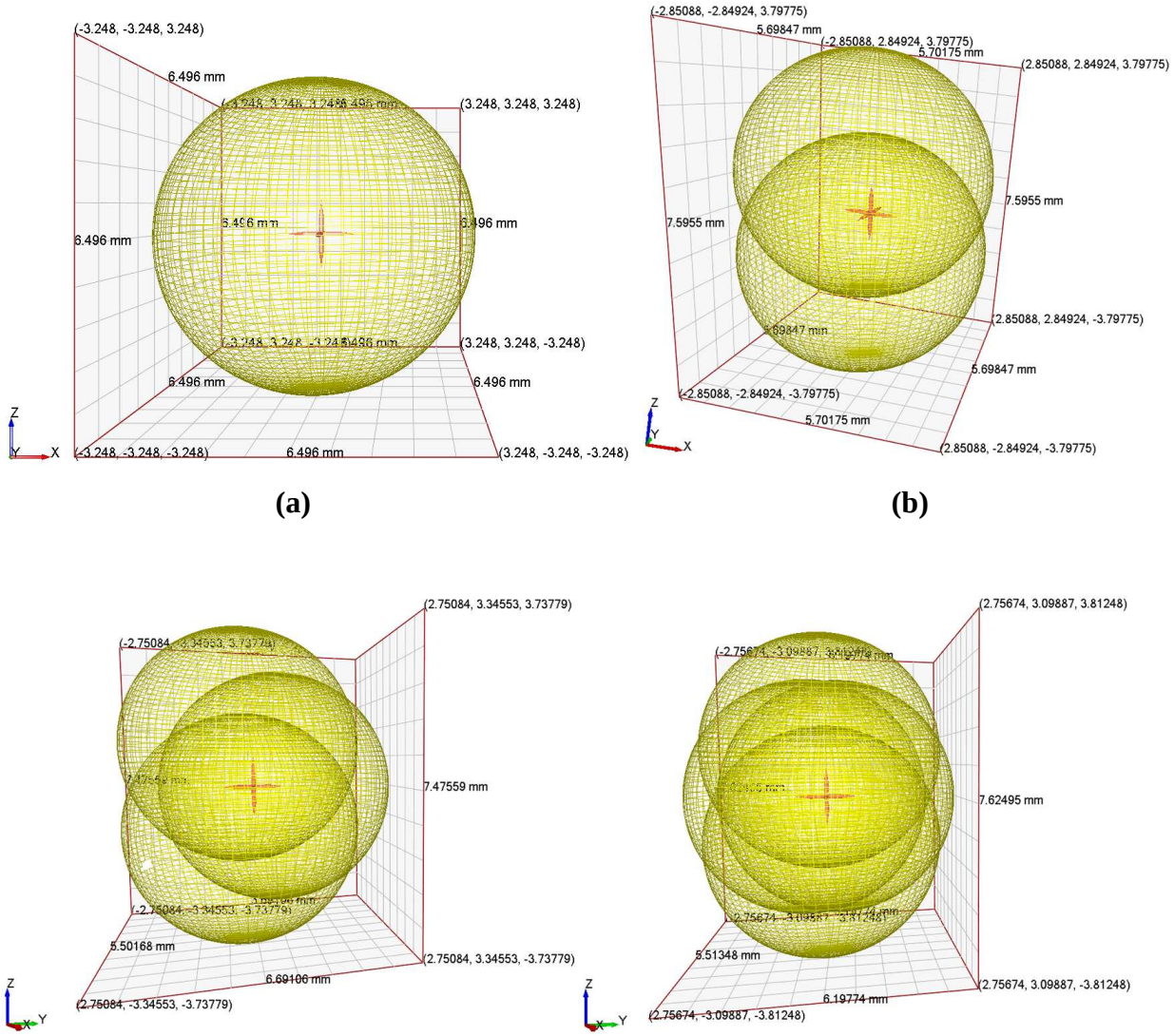

Figure 5.1 Particle shapes of soybean in the simulation: (a) 1-sphere model; (b) 2-sphere model; (c) 3-sphere model; and (d) 4-sphere model (drawn in EDEM software).

Table 5.7 Properties of the four particle models and positions (x, y, z) of each sphere in EDEM.

Parameter		Particle Model			
		1-Sphere	2-Sphere	3-Sphere	4-Sphere
Length of soybean (mm)	l_b	6.496	7.59550	7.47559	7.62495
Width of soybean (mm)	w_b	6.496	5.70175	6.69106	6.19774
Height of soybean (mm)	h_b	6.496	5.69847	5.50168	5.51348
Radius of sphere (mm)	R	3.248	2.85	2.75	2.75
Particle Volume (m^3)	V	1.4350E-07	1.4350E-07	1.4350E-07	1.4350E-07
Particle Mass (kg)	m	0.0001763	0.0001762	0.0001762	0.0001762
Particle Density ($kg \cdot m^{-3}$)	ρ_b	1228.0	1228.0	1228.0	1228.0
Position		**Particle Model**			
		1-Sphere	**2-Sphere**	**3-Sphere**	**4-Sphere**
Surface 1 (X, Y, Z)		(0, 0, 0)	(0, 0, 0)	(0, 0, 0)	(0, -0.35, 0)
Surface 2 (X, Y, Z)		-	(0, 0, 1.89)	(0, 0, 1.975)	(0, 0.35, 0)
Surface 3 (X, Y, Z)		-	-	(0, 0.8, 0.9875)	(0, 0, 1.062)
Surface 4 (X, Y, Z)		-	-	-	(0, 0, -1.062)

Accuracy tests for the particle coefficient of restitution was performed for all test combinations by simulating the dropping of 50 soybean particles from a height of 151 mm on a flat steel surface. The height was based on the drop tests of LoCurto et al. (1997) for soybeans. Drop and rebound heights were extracted from the simulation only from those particles with rebound trajectories that were vertical (LoCurto et al., 1997). The simulated rebound heights were used to calculate particle restitution coefficients using equation 5.2. The calculated restitution coefficients were compared with the input restitution coefficients, which gave an indication of the simulation accuracy.

5.3.1 Bulk Density Test

The bulk density test was based on the USDA GIPSA's (2004) procedure for test-weight-per-bushel apparatus (Figure 5.2). Dimensions of the inside diameter and height of the kettle were 117.475 mm (4.625 in.) and 101.60 mm (4.0 in.), respectively. The test weight kettle was drawn in a computer-aided design (CAD) software package (DS SolidWorks Corp., Concord, Mass.) and imported to establish model geometries in EDEM. The hopper above the kettle was

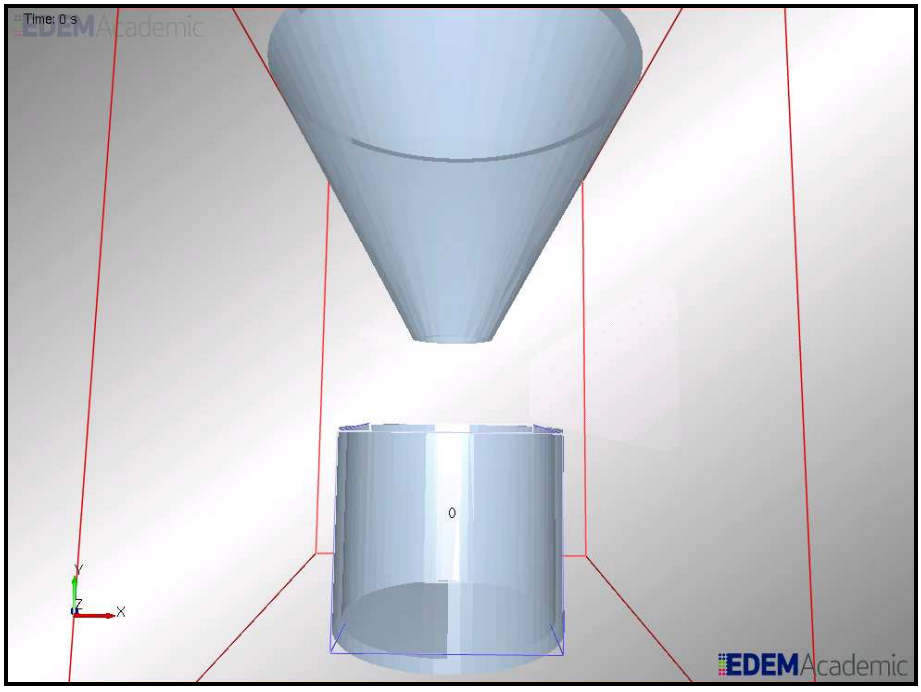

(a)

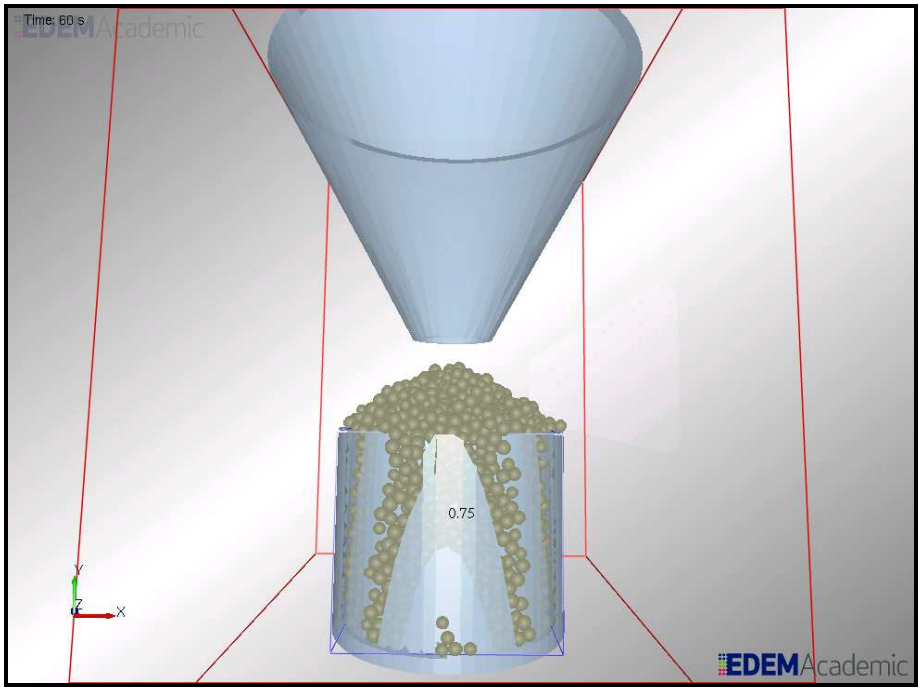

(b)

Figure 5.2 Bulk density test in simulation: (a) empty test weight (TW) kettle and (b) full TW kettle.

also drawn with the standard 31.75-mm (1.25 in.) opening and standard distance from the kettle of 50.8 mm (2.0 in.) (USDA-GIPSA, 1996).

Particles coming from the hopper dropped to fill the kettle. Excess particles were allowed to overflow. Simulation time for each test combination was between 20 to 120 s, depending on the time the kettle was filled and the particles stopped flowing. Simulation time was determined by the particles stabilizing on top of the kettle and the kinetic energy of the whole system approaching zero. To get the bulk density (ρ_b) in kg·m^{-3}, only the total mass of particles filling the kettle (m_p) in kg was computed from the simulation. The mass of piled particles on top and outside of the kettle was excluded in the calculation. The computed mass of particles inside the kettle was divided by the volume of the kettle (V_k) in m^3 in the following equation. The mean bulk density for three replications for each test combination was computed.

$$\rho_b = \frac{m_p}{V_k} \tag{5.9}$$

5.3.2 Bulk Angle of Repose Test

The tilting box method was employed to simulate the angle of repose test of soybean particles in DEM (Figure 5.3). A box measuring 240 x 120 x 40 mm was drawn and filled with soybean particles in the simulation. Train (1958) recommended that the width of the box be at least one-third of its length to reduce wall effects. In this simulation, the width was one-half of the length, which satisfied Train's (1958) recommendation.

Moreover, periodic boundaries were used on opposite sides of the simulation box (in the direction of the width = 120 mm). Periodic boundary conditions enable any particle leaving the domain in that direction to instantly re-enter on the opposite side, simulating infinite length in that direction and, thereby eliminating wall friction. Base friction was also removed by ensuring the base of the box had the same frictional coefficients as that of the particles.

After 0.15 s of filling the box up to the rim, the box was then tilted at a constant angular velocity, ω_b, of 90 deg·s^{-1} until particles begin to move, and then the simulation was stopped after 0.65 to 0.85 s depending on the test combinations being evaluated. The time when the particles began to move was recorded, t_θ, which allowed calculation of the angle of repose, θ, of the soybeans based on the angular velocity of the tilting box. The equation is given by:

$$\theta = t_\theta \times \omega_b \tag{5.10}$$

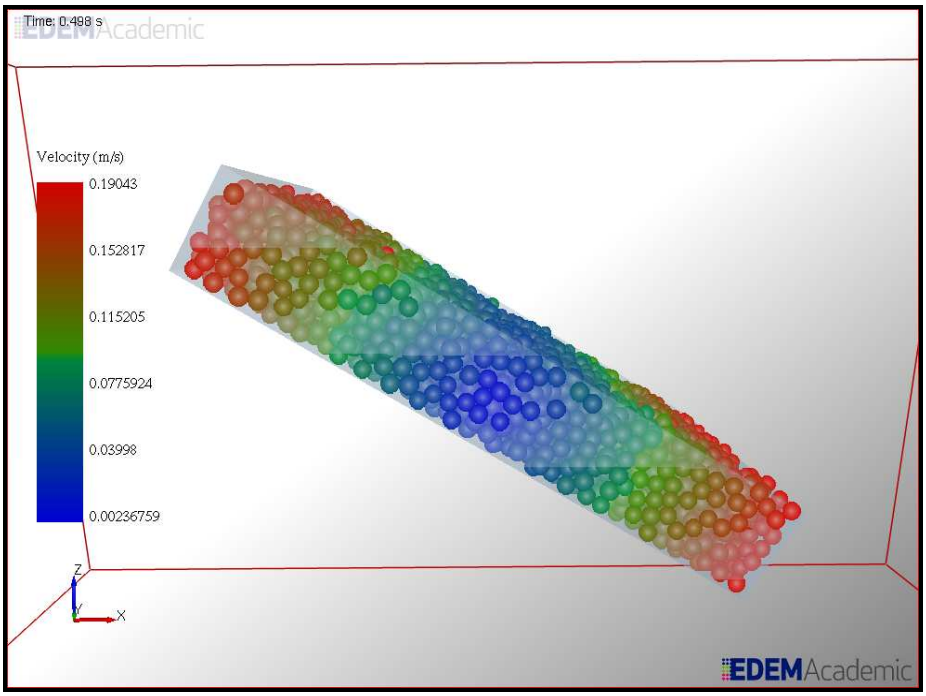

(a)

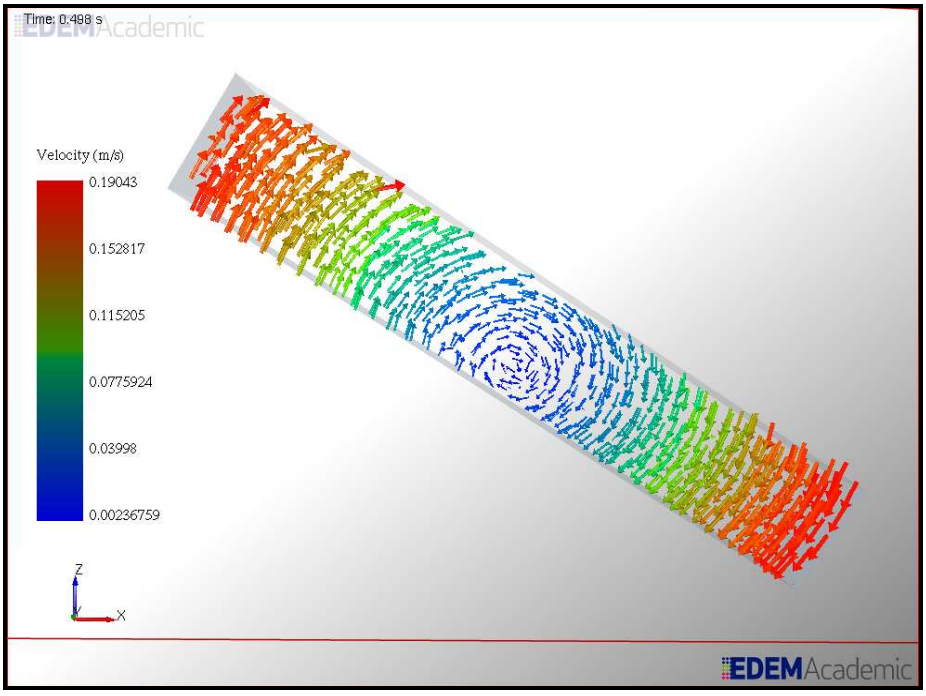

(b)

Figure 5.3 Angle of repose test in simulation at t_θ = 0.498 s: (a) particle mode and (b) vector mode.

Both the actual particle motions and the vectors of the particle motions were evaluated to determine the start of particle movement. The mean angle of repose for seven replications for each test combination was calculated.

5.3.3 Data Analysis

Results were analyzed using the generalized linear model (GLM) procedure of SAS statistical software (version 9.2, SAS Institute, Inc., Cary, NC). Mean, standard deviation, and percentage difference from expected input and published values were determined for the coefficient of restitution, angle of repose, and bulk density tests. The simulation results were compared with the literature values based on their percentage differences. Differences among test combinations within the coefficient of restitution, angle of repose, and bulk density tests were compared using the Bonferroni Multiple Comparison Test in SAS at the 5% level of significance. Bonferroni uses strict requirements prior to rejecting the null hypotheses, which minimizes Type I errors. Test combinations having simulation results best correlating with the literature values were chosen to simulate soybeans in succeeding simulation of grain commingling.

5.4 Results and Discussion

In choosing the best particle model for soybeans, tradeoffs between the three criteria (i.e., bulk density, angle of repose, and computation time) were required. The particle model was also revised by combining and refining input parameters that performed well in the initial tests.

In the accuracy tests, the input parameter was the particle coefficient of restitution and the output calculated from the rebound height had the same particle restitution values (Table 5.8). All test combinations with the base particle restitution value of 0.6 had percent deviations ranging from 0.68% to 1.77% and were not significantly different ($p > 0.05$) from each other. When the restitution coefficient was varied (cases 21111 and 31111), the percent deviation from the input value ranged from 0.25% to 7.56%. The 0.25% deviation was obtained from the test combination with the highest particle restitution value (0.9) and the 7.56% deviation was from that with the lowest particle restitution (0.3). Thus, only the artificially low value of the restitution coefficient caused excessive accuracy issues, and this low value was not pursued further for the particle models.

Table 5.8 Accuracy test using particle coefficient of restitution. [a]

	Coefficient of Restitution				
Combination No.	**Simulation Value**			**Expected Value**	**% Diff**
Restitution					
1s_11111 (e =0.6)	0.61	a	(0.0064)	0.6	1.73
1s_21111 (e =0.3)	0.32	b	(0.0058)	0.3	7.56
1s_31111 (e =0.9)	0.90	c	(0.0009)	0.9	0.25
Static Friction					
1s_11111 (μ_s =0.55)	0.61	a	(0.0064)	0.6	1.73
1s_12111 (μ_s =0.35)	0.61	a d	(0.0041)	0.6	1.27
1s_13111 (μ_s =0.75)	0.61	a	(0.0060)	0.6	1.54
Rolling Friction					
1s_11111 (μ_r =0.1)	0.61	a	(0.0064)	0.6	1.73
1s_11211 (μ_r =0.05)	0.61	a d	(0.0057)	0.6	1.40
1s_11311 (μ_r =0.2)	0.61	a d	(0.0038)	0.6	1.03
Size Distribution					
1s_11111 (SDF=0)	0.61	a	(0.0064)	0.6	1.73
1s_11121 (SDF=0.2)	0.61	a d	(0.0046)	0.6	1.12
1s_11131 (SDF=0.4)	0.61	a	(0.0061)	0.6	1.53
Shear Modulus					
1s_11111 (G =41.7MPa)	0.61	a	(0.0064)	0.6	1.73
1s_11112 (G =13.8 MPa)	0.60	d	(0.0119)	0.6	0.68
1s_11113 (G =1.04 MPa)	0.61	a d	(0.0093)	0.6	1.04
Particle Model					
1s_11111	0.61	a	(0.0064)	0.6	1.73
2s_11111	0.61	a	(0.0057)	0.6	1.50
3s_11111	0.61	a d	(0.0070)	0.6	1.08
4s_11111	0.61	a	(0.0060)	0.6	1.77

[a] Mean values with the same lower case letters within a column are not significantly different at the 5% level of significance in Bonferroni. Values in parentheses represent standard deviation (SD).
Particle shape (1s = 1-sphere; 2s = 2-sphere; 3s = 3-sphere; 4s = 4-sphere).
Coefficient of restitution (1 stands for e = 0.6; 2 for e = 0.3; 3 for e = 0.9).
Coefficient of static friction (1 for $\mu_{s(so\text{-}so)}$ = 0.55, $\mu_{s(so\text{-}st)}$ = 0.37; 2 for $\mu_{s(so\text{-}so)}$ = 0.35, $\mu_{s(so\text{-}st)}$ = 0.23; 3 for $\mu_{s(so\text{-}so)}$ = 0.75, $\mu_{s(so\text{-}st)}$ = 0.50).
Coefficient of rolling friction (1 for μ_r = 0.1; 2 for μ_r = 0.05; 3 for μ_r = 0.2).
Particle size distribution (PSD) (1 for uniform particle size; 2 for normal PSD with standard deviation factor (SDF) = 0.2; 3 for normal PSD with SDF = 0.4).
Shear modulus (1 stands for G = 41.7 MPa, 2 for G = 13.8 MPa, 3 for G = 1.04 MPa).

5.4.1 Bulk Density Test

Bulk density increased with the coefficient of restitution but decreased with coefficients of static and rolling friction (Table 5.9). Wider size distributions increased bulk density as observed from test combinations 11121 to 11131. This may be explained by the increasing standard deviation factor (from 0.2 to 0.4) in the particle size distribution, which increases the smaller particles in the normal size distribution. These small particles were filling the void in between large particles, thereby increasing the bulk density.

Simulations involved fixed particle size within each particle shape. Particle density and mass were constant among particle shapes. Results showed that bulk density decreased as the number of spheres in a particle shape increased, except for the case of 1-sphere particle shape. This can be explained by a 4-sphere particle shape occupying a slightly higher volume than a 2-sphere particle shape, thus, slightly decreasing the bulk density. Bulk densities from 2- to 4-sphere particle shapes, however, were not significantly different ($p > 0.05$) from each other. Bulk densities of the 1- and 4-sphere particle shapes were also not significantly different ($p > 0.05$).

In general, the simulations resulted in lower bulk densities than the published values. Test combinations 31111, 12111, 11211, 11131, and 11113 for 1-sphere particle shape and 11111 for 2-sphere particle shape gave bulk densities closer to the literature value of 720.72 $kg \cdot m^{-3}$. Test combination 31111 was significantly different ($p < 0.05$) from all other test combinations. Test combinations 12111, 11211, and 11113 were significantly different ($p < 0.05$) from 11131 for the 1-sphere particle shape, but did not differ ($p > 0.05$) from test combination 11111 for the 2-sphere particle shape.

5.4.2 Bulk Angle of Repose Test

Static and rolling friction coefficients affect the angle of repose. In general, as the static and rolling friction coefficients increased so did the angle of repose in the simulation (Table 5.9). This observation was similar to those of Zhou et al. (2002) and Walton (1994).

The greater the number of spheres in a particle model, the higher the angle of repose. Walton and Braun (1993) and Walton (1994) found increasing values of dynamic angle of repose as spheres increased from mono to cubic (8-sphere). Simulation results of static angle of repose, however, did not exactly agree with those authors' findings. This was likely due to the volume of the particle models always being the same during simulation so particles did not increase in size

Table 5.9 Results of bulk density and bulk angle of repose tests for each test combination.[a]

Combination No.	Bulk Density, kg·m^{-3} Simulation Value		Published Value	% Diff	Bulk Angle of Repose, deg. Simulation Value		Published Value	% Diff
1st Iteration								
Restitution								
1s_11111 (e=0.6)	669.00 a h	(1.60)	720.72	-7.18	31.50 a e	(0.35)	31.0	1.61
1s_21111 (e=0.3)	660.39 b	(0.77)	720.72	-8.37	32.31 a	(0.82)	31.0	4.23
1s_31111 (e=0.9)	687.12 c	(0.93)	720.72	-4.66	37.17 b	(0.47)	31.0	19.91
Static Friction								
1s_11111 (μ_s=0.55)	669.00 a h	(1.60)	720.72	-7.18	31.50 a e	(0.35)	31.0	1.61
1s_12111 (μ_s=0.35)	678.30 d g	(2.00)	720.72	-5.89	31.50 a e	(1.25)	31.0	1.62
1s_13111 (μ_s=0.75)	665.67 a	(3.03)	720.72	-7.64	37.35 b	(1.47)	31.0	20.49
Rolling Friction								
1s_11111 (μ_r=0.1)	669.00 a h	(1.60)	720.72	-7.18	31.50 a e	(0.35)	31.0	1.61
1s_11211 (μ_r=0.05)	680.08 d	(0.33)	720.72	-5.64	30.52 c e	(0.50)	31.0	-1.54
1s_11311 (μ_r=0.2)	656.61 b	(0.72)	720.72	-8.89	35.28 d	(0.98)	31.0	13.81
Size Distribution								
1s_11111 (SDF=0)	669.00 a h	(1.60)	720.72	-7.18	31.50 a e	(0.35)	31.0	1.61
1s_11121 (SDF=0.2)	668.51 a h	(0.28)	720.72	-7.24	29.30 c	(0.48)	31.0	-5.48
1s_11131 (SDF=0.4)	670.60 e h	(2.89)	720.72	-6.95	32.64 a	(1.10)	31.0	5.31
Shear Modulus								
1s_11111 (G=41.7MPa)	669.00 a h	(1.60)	720.72	-7.18	31.50 a e	(0.35)	31.0	1.61
1s_11112 (G=13.8 MPa)	671.44 e f h	(2.25)	720.72	-6.84	31.45 a e	(0.50)	31.0	1.45
1s_11113 (G=1.04 MPa)	679.93 d	(0.28)	720.72	-5.66	32.75 a	(0.66)	31.0	5.65
Particle Model								
1s_11111	669.00 a h	(1.60)	720.72	-7.18	31.50 a e	(0.35)	31.0	1.61
2s_11111	675.55 d g f	(0.95)	720.72	-6.27	29.28 c	(0.29)	31.0	-5.56
3s_11111	673.89 e f g	(1.05)	720.72	-6.50	29.12 c	(0.55)	31.0	-6.06
4s_11111	672.53 e f h	(0.59)	720.72	-6.69	29.42 c	(1.18)	31.0	-5.10

[a] Mean values with the same lower case letters within a column are not significantly different at the 5% level of significance in Bonferroni. Values in parentheses represent standard deviation (SD).
Particle shape (1s = 1-sphere; 2s = 2-sphere; 3s = 3-sphere; 4s = 4-sphere).
Coefficient of restitution (1 stands for e = 0.6, 2 for e = 0.3, 3 for e = 0.9).
Coefficient of static friction (1 for $\mu_{s(so\text{-}so)}$ = 0.55, $\mu_{s(so\text{-}st)}$ = 0.37; 2 for $\mu_{s(so\text{-}so)}$ = 0.35, $\mu_{s(so\text{-}st)}$ = 0.23; 3 for $\mu_{s(so\text{-}so)}$ = 0.75, $\mu_{s(so\text{-}st)}$ = 0.50).
Coefficient of rolling friction (1 for μ_r = 0.1, 2 for μ_r = 0.05, 3 for μ_r = 0.2).
Particle size distribution (PSD) (1 for uniform particle size, 2 for normal PSD with standard deviation factor (SDF) = 0.2, 3 for normal PSD with SDF = 0.4).
Shear modulus (1 stands for G = 41.7 MPa, 2 for G = 13.8 MPa, 3 for G = 1.04 MPa).

as the number of spheres in a particle model increased, unlike the previous authors observed. The 1-sphere particle shape showed the highest angle of repose, whereas the 3-sphere particle shape gave the lowest angle. The 4-sphere particle shape had a higher angle of repose than the 2-sphere shape, which agreed with the published trend of Walton's group.

Angle of repose increased for wider size distribution (i.e., from PSD with SDF = 0.2 to that with SDF = 0.4). This result for static angle agreed with Zenz's (1957) experimental findings for dynamic angle of repose.

For 1-sphere particle models, test combinations 11111, 12111, 11211, 11131, and 11112 gave closer values to the published angle of repose (31°) and were not significantly different ($p > 0.05$) from each other.

For multi-sphere particle models, results of test combination 11111 for the 4-sphere shape were closest to the published angles of repose. This test combination, however, did not significantly differ ($p > 0.05$) from test combination 11111 for 2- and 3-sphere shapes.

5.4.3 Best-Correlated Particle Models

In general, multi-sphere particle shapes did not give promising results in the bulk property tests. During initial testing (Table 5.9), combination 31111 with the highest particle coefficient of restitution (0.9) resulted in the closest bulk density (687.12 $kg \cdot m^{-3}$) to published values (720.72 $kg \cdot m^{-3}$). The angle of repose of the bulk materials from this test combination (37.17°), however, was considerably higher than the literature value (31°). The high bulk density and angle of repose may be explained by the high coefficient of restitution of the particle in the parameter mix of that test combination. In a second iteration, modified testing was performed to determine whether lowering the particle restitution (to 0.7 or 0.8) would result in a more desirable bulk angle of repose, yet still maintain bulk density close to the literature value. Bulk density tests, including coefficients of restitution of 0.7 (test combination 4111) and 0.8 (test combination 5111), resulted in values of 671.77 and 679.45 $kg \cdot m^{-3}$, respectively (Table 5.10). These values, however, were lower than the bulk density values of test combinations 11211 (680.08 $kg \cdot m^{-3}$) and 11113 (679.93 $kg \cdot m^{-3}$) from the initial testing (Table 5.9); thus, they were not tested for angle of repose. For bulk angle of repose, test combinations 11112 (31.45°) and 11211 (30.52°) yielded values closest to the published one with percent deviations of 1.45% and -1.54%, respectively.

Table 5.10 Results of bulk density and bulk angle of repose tests for possible best test combination.

Combination No.		Bulk Density, kg·m^{-3} Simulation Value		Expected Value	% Diff	Bulk Angle of Repose, deg. Simulation Value		Expected Value	% Diff
2nd Iteration									
1s_12233	(μ_s=0.35)	697.90 a	(1.76)	720.7	-3.17	28.54 a	(0.58)	31.0	-7.94
1s_11231	(μ_s=0.55, G=41.7MPa)	682.37 b	(1.50)	720.7	-5.32	31.54 b	(0.53)	31.0	1.74
1s_11232	(μ_s=0.55, G=13.8MPa)	682.47 b	(1.58)	720.7	-5.31	32.15 b c	(0.72)	31.0	3.70
1s_11233	(μ_s=0.55, G=1.04MPa)	685.09 b c	(5.65)	720.7	-4.94	31.90 b	(0.68)	31.0	2.90
1s_14231	(μ_s=0.58, G=41.7MPa)	680.74 b	(1.64)	720.7	-5.55	33.14 c d	(0.40)	31.0	6.90
1s_14232	(μ_s=0.58, G=13.8MPa)	681.77 b	(1.27)	720.7	-5.40	31.03 b	(0.48)	31.0	0.11
1s_14233	(μ_s=0.58, G=1.04MPa)	690.47 c	(0.60)	720.7	-4.20	33.45 d	(1.01)	31.0	7.90
1s_41111	(e=0.7)	671.77 d	(1.36)	720.7	-6.79				
1s_51111	(e=0.8)	679.45 b	(0.68)	720.7	-5.73				
3rd Iteration									
1s_12233	(μ_s=0.35)	697.90 a	(1.76)	720.7	-3.17	28.54 a	(0.58)	31.0	-7.94
1s_17233	(μ_s=0.40)	695.39 a	(0.83)	720.7	-3.51	29.01 a	(0.36)	31.0	-6.42
1s_16233	(μ_s=0.45)	693.73 a	(1.15)	720.7	-3.74	30.89 b	(0.53)	31.0	-0.36
1s_15233	(μ_s=0.50)	693.58 a	(1.82)	720.7	-3.77	31.20 b	(0.45)	31.0	0.66
1s_11233	(μ_s=0.55)	685.09 b	(5.65)	720.7	-4.94	31.90 b	(0.68)	31.0	2.90
1s_14233	(μ_s=0.58)	690.47 a b	(0.60)	720.7	-4.20	33.45 c	(1.01)	31.0	7.90

[a] Mean values with the same lower case letters within a column are not significantly different at the 5% level of significance in Bonferroni.

Values in parentheses represent standard deviation (SD).

Particle shape (1s = 1-sphere).

Coefficient of restitution (1 stands for e = 0.6; 4 for e = 0.7; 5 for e = 0.8).

Coefficient of static friction (1 for $\mu_{s(so\text{-}so)}$ = 0.55, $\mu_{s(so\text{-}st)}$ = 0.37; 2 for $\mu_{s(so\text{-}so)}$ = 0.35, $\mu_{s(so\text{-}st)}$ = 0.23; 4 for $\mu_{s(so\text{-}so)}$ = 0.58, $\mu_{s(so\text{-}st)}$ = 0.39; 5 for $\mu_{s(so\text{-}so)}$ = 0.50, $\mu_{s(so\text{-}st)}$ = 0.34; 6 for $\mu_{s(so\text{-}so)}$ = 0.45, $\mu_{s(so\text{-}st)}$ = 0.30; 7 for $\mu_{s(so\text{-}so)}$ = 0.40, $\mu_{s(so\text{-}st)}$ = 0.27).

Coefficient of rolling friction (1 for μ_r = 0.1; 2 for μ_r = 0.05).

Particle size distribution (PSD) (1 for uniform particle size; 3 for normal PSD with SDF = 0.4).

Shear modulus (1 stands for G = 41.7 MPa, 2 for G = 13.8 MPa, 3 for G = 1.04 MPa).

With tradeoffs between bulk density and bulk angle of repose, test combination 11211 gave the best correlated coefficients of restitution, static friction, and rolling friction, which were 0.6, 0.55 (for soybean-soybean; 0.37 for soybean-steel), and 0.05, respectively (Table 5.9). However, test combination 11211 did not include size distribution of the particles because it only represented uniform or fixed particle sizes. Thus, the normal PSD with SDF of 0.4 was chosen because test combination 11131 performed better in the bulk density and bulk angle of repose tests than 11121. For particle shear modulus, test combination 11113 (G = 1.04 MPa) did better in the bulk density test while test combination 11112 (G = 13.8 MPa), did best in the angle of repose test (Table 5.9). Both particle shear moduli were included in the second iteration, together with the highest shear modulus (G = 41.7 MPa), to determine how these shear moduli performed when combined with the other parameters (i.e., coefficients of restitution, rolling and static friction, and PSD). The second iteration also included the second particle coefficient of static friction of 0.35 (for soybean-soybean; 0.23 for soybean-steel), which was in 12111 due to the test combination's bulk density being higher than that of 11112.

In the second iteration, test combinations 12233 and 14233, with particle static friction of 0.35 and 0.58, respectively, produced the best values for bulk density. The bulk angles of repose results, however, were poor for those combinations (Table 5.10). A third iteration was performed using test combinations with particle static friction between 0.35 and 0.58. This iteration determined which particle static friction would give the highest bulk density while maintaining the best possible value for bulk angle of repose.

The third iteration revealed that the best parameter mix was test combination 16233, which included particle coefficients of restitution static friction for soybean-soybean (soybean-steel) and rolling friction of 0.6, 0.45 (0.30), and 0.05, respectively; PSD with SDF of 0.4; and particle shear modulus of 1.04 MPa (Table 5.10). In addition, test combination 16233 made the computational time faster (Chung and Ooi, 2008; Remy et al., 2009) due to the low particle shear modulus (G=1.04MPa).

5.5 Summary

Material and interaction properties of various grains and oilseeds relevant to discrete element modeling (DEM) were reviewed. Material properties were particle shape and size, Poisson's ratio, shear modulus, and density. Interaction properties included coefficients of restitution, static friction, and rolling friction. Published values were used to establish base values for simulation modeling. Single- and multi-sphere soybean particle models, comprised of one to four overlapping spheres, were compared based on DEM simulations of the bulk properties: bulk density and angle of repose.

A single-sphere particle model best simulated soybean kernels in the bulk property tests. The best particle model included a particle coefficient of restitution of 0.6, particle static friction of 0.45 for soybean-soybean contact (0.30 for soybean-steel interaction), particle rolling friction of 0.05, normal particle size distribution with a standard deviation factor of 0.4, and particle shear modulus of 1.04 MPa. To optimize the simulated bulk properties, most parameters in this particle model varied only a small amount from the base values obtained from the literature. However, the particle shear modulus was set artificially low since that helped speed up the simulations without negatively impacting the simulation of bulk properties. This particle model will be used to simulate soybeans in grain handling and enhance the prediction of grain commingling in bucket-elevator equipment.

5.6 References

Airy, W. 1898. The pressure of grain. In *Minutes of Proceedings of the Institution of Civil Engineers*, vol. 131, 347-358. J. H. T. Tudsbery, ed. London: Institution of Civil Engineers.

Arnold, P. C., and A. W. Roberts. 1969. Fundamental aspects of load-deformation behavior of wheat grains. *Transactions of the ASAE* 12(1): 104-108.

ASAE Standards. 2006a. D241.4. Density, specific gravity, and mass-moisture relationships of grain for storage. St. Joseph, Mich.: ASAE.

ASAE Standards. 2006b. S368.4. Compression test of food materials of convex shape. St. Joseph, Mich.: ASAE.

Bardet, J. P., and Q. Huang. 1993. Rotational stiffness of cylindrical particle contacts. In *Powders and Grains 93*, 39-43. C. Thornton, ed. Rotterdam: Balkema.

Berruto, R., and D. E. Maier. 2001. Analyzing the receiving operation of different grain types in a single–pit country elevator. *Transactions of the ASAE* 44(3): 631–638.

Bilanski, W. K., B. Szot, I. Kushwaha, and A. Stepneiwski. 1994. Comparison of strength features of rape pods and seeds for varieties cultivated in various countries. *International Agrophysics* 8(4): 177-184.

Boyles, M., T. Peeper, and M. Stamm. 2006. Great plains canola production handbook (MF-2734). Manhattan, Kansas: Kansas State University Cooperative Extension Service.

Brown, R. L., and J. C. Richards. 1959. Exploratory study of the flow of granules through apertures. *Chemical Engineering Research and Design (Transactions of the Institution of Chemical Engineers)* 37a: 108-119.

Brubaker, J. E., and J. Pos. 1965. Determining static coefficient of friction of grains on structural surfaces. *Transactions of the ASAE* 8(1): 53-55.

Burmistrova, M. F., I. K. Komol'kova, N. V. Klemm, M. T. Panina, I. M. Polunochev, A. I. P'yankov, A. F. Sokolov, N. G. Tetyanko, V. M. Chaus, and E. G. Eglit. 1963. *Physicomechanical Properties of Agricultural Crops.* Translated from Russian and published for the National Science Foundation. Jerusalem: Israel Program for Scientific Translations, Ltd.

Calisir, S., T. Marakoglu, H. Ogut, and O. Ozturk. 2005. Physical properties of rapeseed (*Brassica napus oleifera* L.). *Journal of Food Engineering* 69(1): 61-66.

Chung, Y. C., and J. Y. Ooi. 2008. Influence of discrete element model parameters on bulk behavior of a granular solid under confined compression. *Particulate Science and Technology* 26(1):83-96.

Chung, Y. C., J. Y. Ooi, and J. F. Favier. 2004. Measurement of mechanical properties of agricultural grains for DE models. In *17th ASCE Engineering Mechanics Conference*. Newark, Del.: American Society of Civil Engineers.

Cundall, P. A., and O. D. L. Strack. 1979. A discrete numerical model for granular assemblies. *Geotechnique* 29(1): 47-65.

DEM Solutions. 2009. *EDEM 2.1.2 User Guide*. Lebanon, N.H.: DEM Solutions (USA), Inc. 138p.

Di Renzo, A., and F. P. Di Maio. 2004. Comparison of contact-force models for the simulation of collisions in DEM-based granular flow codes. *Chemical Engineering Science* 59(3): 525-541.

Di Renzo, A., and F. P. Di Maio. 2005. An improved integral non-linear model for the contact of particles in distinct element simulations. *Chemical Engineering Science* 60(5): 1303-1312.

Fowler, R. T., and W. B. Chodziesner. 1959. The influence of variables upon the angle of friction of granular materials. *Chemical Engineering Science* 10: 157-162.

Fowler, R. T., and F. A. Wyatt. 1960. The effect of moisture content on the angle of repose of granular solids. *Australian Journal for Chemical Engineers* 1: 5-8.

Fraczek, J., A. Zlobecki, and J. Zemanek. 2007. Assessment of angle of repose of granular plant material using computer image analysis. *Journal of Food Engineering* 83(1): 17-22.

Greenlees, W. J., and S. C. Shouse. 2000. Estimating grain contamination from a combine. ASAE Paper No. MC00103. St. Joseph, Mich.: ASAE.

Gupta, R. K., and S. K. Das. 1997. Physical properties of sunflower seeds. *Journal of Agricultural Engineering Research* 66(1): 1-8.

Hanna, H. M., D. H. Jarboe, and G. R. Quick. 2006. Grain residuals and time requirements for combine cleaning. ASAE Paper No. 066082. St. Joseph, Mich.: ASAE.

Henderson, S. M., and R. L. Perry. 1976. *Agricultural Process Engineering*. 3rd ed. Westport, Conn.: The AVI Publishing Company. 430p.

Herrman, T. J., S. Baker, and F. J. Fairchild. 2001. Characterization of receiving systems and operating performance of Kansas grain elevators during wheat harvest. *Applied Engineering in Agriculture* 17(1): 77–82.

Herrman, T. J., M. A. Boland, K. Agrawal, and S. R. Baker. 2002. Use of a simulation model to evaluate wheat segregation strategies for country elevators. *Applied Engineering in Agriculture* 18(1): 105–112.

Hirai, Y., M. D. Schrock, D. L. Oard, and T. J. Herrman. 2006. Delivery system of tracing caplets for wheat grain traceability. *Applied Engineering in Agriculture* 22(5): 747-750.

Horabik, J., and J. Lukaszuk. 2000. Measurement of internal friction angle of wheat grain using triaxial compression test. *Acta Agrophysica* 37: 39-49 (in Polish).

Hoseney, R. C., and J. M. Faubion. 1992. Chapter 1: Physical properties of cereal grains. In *Storage of Cereal Grains and Their Products*. 4th ed. D. B. Sauer, ed. St. Paul, Minn.: American Association of Cereal Chemists, Inc.

Hurburgh, C. R., Jr. 1999. The GMO controversy and grain handling for 2000. Paper presented at the Iowa State University Integrated Crop Management Conference. Available at: http://www.exnet.iastate.edu/Pages/grain/gmo/99gmoy2k.pdf. Accessed 21 June 2006.

Ingles, M. E. A., M. E. Casada, and R. G. Maghirang. 2003. Handling effects on commingling and residual grain in an elevator. *Transactions of the ASAE* 46(6): 1625-1631.

Ingles, M. E. A., M. E. Casada, R. G. Maghirang, T. J. Herrman, and J. P. Harner, III. 2006. Effects of grain-receiving system on commingling in a country elevator. *Applied Engineering in Agriculture* 22(5): 713-721.

Jamieson, J. A. 1903. Grain pressures in deep bins. *Transactions of the Canadian Society of Civil Engineers* 17(2): 554-607.

Jiang, M. J., H. S. Yu, and D. Harris. 2005. A novel discrete model for granular material incorporating rolling resistance. *Computers and Geotechnics* 32(5): 340-357.

Kramer, H. A. 1944. Factors influencing the design of bulk storage bins for rough rice. *Agricultural Engineering* 25(12): 463-466.

Li, Y., Y. Xu, and C. Thornton. 2005. A comparison of discrete element simulations and experiments for ‘sandpiles’ composed of spherical particles. *Powder Technology* 160(3): 219-228.

LoCurto, G. J., X. Zhang, V. Zarikov, R. A. Bucklin, L. Vu-Quoc, D. M. Hanes, and O. R. Walton. 1997. Soybean impacts: experiments and dynamic simulations. *Transactions of the ASAE* 40(3):789-794.

Lorenzen, R. T. 1957. Effect of moisture content on mechanical properties of small grains. M.S. thesis. Davis, Cal.: University of California-Davis.

McLelland, M., and N. Miller. 2001. Using 1,000 kernel weight for calculating seeding rates and harvest losses. Agdex 100/22-1. Available on http://www1.agric.gov.ab.ca/ $department/ deptdocs.nsf/ all/ agdex81? opendocument Accessed 13 April 2007.

Mindlin, R. 1949. Compliance of elastic bodies in contact. *Journal of Applied Mechanics* 16: 259-268.

Mindlin, R. D., and H. Deresiewicz. 1953. Elastic spheres in contact under varying oblique forces. *Transactions of ASME, Series E. Journal of Applied Mechanics* 20: 327-344.

Misra, R. N., and J. H. Young. 1981. A model for predicting the effect of moisture content on the modulus of elasticity of soybeans. *Transactions of the ASAE* 24(5): 1338-1341, 1347.

Mohsenin, N. N. 1986. *Physical Properties of Plant and Animal Materials*. 2nd ed. New York: Gordon and Breach Science Publishers.

Molenda, M., and J. Horabik. 2005. Characterization of mechanical properties of particulate solids for storage and handling. Part 1. In *Mechanical Properties of Granular Agro-Materials and Food Powders for Industrial Practice*. J. Horabik and J. Laskowski. eds. Lublin: Institute of Agrophysics Polish Academy of Sciences.

Nelson, S. O. 2002. Dimensional and density data for seeds of cereal grain and other crops. *Transactions of the ASAE* 45(1):165-170.

O'Sullivan, C., and J. D. Bray. 2004. Selecting a suitable time step for discrete element simulations that use the central-difference time integration scheme. *Engineering Computations* 21(2-4): 278-303.

Raji, A. O., and J. F. Favier. 2004a. Model for the deformation in agricultural and food particulate materials under bulk compressive loading using discrete element method, part

I: theory, model development and validation. *Journal of Food Engineering* 64(3): 359-371.

Raji, A. O., and J. F. Favier. 2004b. Model for the deformation in agricultural and food particulate materials under bulk compressive loading using discrete element method, part II: compression of oilseeds. *Journal of Food Engineering* 64(3): 373-380.

Remy, B., J. G. Khinast, and B. J. Glasser. 2009. Discrete element simulation of free-flowing grains in a four-bladed mixer. *AIChE Journal* 55(8): 2035-2048.

Sharma, R. K., and W. K. Bilanski. 1971. Coefficient of restitution of grains. *Transactions of the ASAE* 14(2): 216-218.

Shelef, L., and N. N. Mohsenin. 1969. Effect of moisture content on mechanical properties of shelled corn. *Cereal Chemistry* 46(3): 242-253.

Shroyer, J. P., P. D. Ohlenbusch, S. Duncan, C. Thompson, D. L. Fjell, G.L. Kilgore, R. Brown, and S. Staggenborg. 1996. Kansas Crop Planting Guide. L-818. Manhattan, Kansas: Kansas State University Cooperative Extension Service.

Smith, C. E., and P. Liu. 1992. Coefficient of restitution. *Journal of Applied Mechanics* 59(4): 963-969

Stahl, B. M. 1950. Grain Bin Requirements. USDA Circular 835. Washington, D. C.: U.S. Department of Agriculture.

Stewart, B. R. 1968. Effect of moisture content and specific weight on internal-friction properties of sorghum grain. *Transactions of the ASAE* 11(2): 260-266.

Theuerkauf, J., S. Dhodapkar, and K. Jacob. 2007. Modeling granular flow using discrete element method – from theory to practice. *Chemical Engineering* 114(4): 39-46.

Train, D. J. 1958. Some aspects of the property of angle of repose of powders. *Journal of Pharmacy and Pharmacology (Supplement)* 10: 127-135.

Tsuji, Y., T. Tanaka, and T. Ishida. 1992. Lagrangian numerical simulation of plug flow of cohesionless particles in a horizontal pipe. *Powder Technology* 71(3): 239-250.

Ullidtz, P. 1997. Modelling of granular materials using the discrete element method. In *Proceedings of the 8th International Conference on Asphalt Pavements*, Vol. 1, 757-769. August 10-14. Seattle, Wash.: University of Washington.

USDA GIPSA. 1996. Chapter 5: Test weight per bushel apparatuses. In *Equipment Handbook.* Washington, D.C.: USDA Grain Inspection, Packers, and Stockyards Administration, Federal Grain Inspection Service.

USDA GIPSA. 2004. *Grain Inspection Handbook, Book II, Grain Grading Procedures.* Washington, D.C.: USDA Grain Inspection, Packers, and Stockyards Administration, Federal Grain Inspection Service.

Vu-Quoc, L., X. Zhang, and O. R. Walton. 2000. A 3-D, discrete element method for dry granular flows of ellipsoidal particles. *Computer Methods in Applied Mechanics and Engineering* 187(3-4): 483-528.

Walton, O. R. 1994. Effects of interparticle friction and particle shape on dynamic angles of repose via particle-dynamic simulation. Presented at the Workshop on Mechanics and Statistical Physics of Particulate Materials, June 8-10, La Jolla, Cal.

Walton, O. R., and R. L. Braun. 1993. Simulation of rotary-drum and repose tests for frictional spheres and rigid sphere clusters. In *Proceedings of DOE/NSF Workshop on Flow of Particulates and Fluids*, Sept. 29-Oct. 1, Ithaca, N.Y.

Watson, S. A. 2003. Chapter 3: Description, development, structure and composition of the corn kernel. In *Corn: Chemistry and Technology*. P. J. White and L. A. Johnson, eds. St. Paul, Minn.: American Association of Cereal Chemists, Inc.

Wightman, C., M. Moakher, F. J. Muzzio, and O. R. Walton. 1998. Simulation of flow and mixing of particles in a rotating and rocking cylinder. *AIChE Journal* 44(6): 1266-1276.

Yang, Y., and M. D. Schrock. 1994. Analysis of grain kernel rebound motion. *Transactions of the ASAE* 37(1): 27-31.

Zenz, F. A. 1957. How solid catalysts behave. *Petroleum Refiner* 36(4): 173-178.

Zhang, X., and L. Vu-Quoc. 2002. A method to extract the mechanical properties of particles in collision based on a new elasto-plastic, normal force-displacement model. *Mechanics of Materials* 34(12): 779-794.

Zhou, Y. C., B. D. Wright, R. Y. Yang, B. H. Xu, and A. B. Yu. 1999. Rolling friction in the dynamic simulation of sandpile formation. *Physica A* 269(2-4): 536-553.

Zhou, Y. C., B. H. Xu, A. B. Yu, and P. Zulli. 2001. Numerical investigation of the angle of repose of monosized spheres. *Physical Review E: Statistical Physics, Plasmas, Fluids, and Related Interdisciplinary Topics* 64(2): 0213011-0213018.

Zhou, Y. C., B. H. Xu, A. B. Yu, and P. Zulli. 2002. An experimental and numerical study of the angle of repose of coarse spheres. *Powder Technology* 125(1): 45-54.

CHAPTER 6 - 3D and Quasi-2D DEM Modeling of Grain Commingling in a Bucket Elevator Boot System

6.1 Introduction

Identity preservation programs are aimed at maintaining the genetic and physical purity of the grain. Segregation of grain with specific attributes has been increasing in the grain industry in recent years and is anticipated to continue growing. The introduction of genetically modified (also called transgenic or biotech) crops for feed, pharmaceutical, and industrial uses into the U.S. grain handling system has shown that the infrastructure is often unable to identity-preserve the grains to the desired level of purity (Ingles et al., 2006). This was exemplified by the incidents of Starlink corn (Bucchini and Goldman, 2002) and GT200-containing canola seed (Kilman and Carroll, 2002).

Grain commingling involves unintentional introduction of other grains or impurities that directly reduces the level of purity in grain entering an elevator facility. There are three approaches for addressing commingling during grain handling: (1) ignore it; (2) containerize the identity-preserved grain or handle it only in dedicated facilities and transportation equipment; or (3) segregate in non-dedicated facilities. The first two are the most common and the latter method has limited scientific data for evaluating its effectiveness. The latter method is the subject of this study.

In addition to unintentional and natural threats to grain purity, intentional introduction of contaminants is also possible. The Strategic Partnership Program Agroterrorism (SPPA) Initiative listed grain elevator and storage facilities as sites that are critical nodes for assessment because of vulnerability to terrorist attack with biological weapons (US FDA, 2006).

For both intentional and unintentional commingling, previous research in commercial elevator equipment (Ingles, et al., 2003; 2006; Ingles, 2005) showed large variations between and within facilities for commingling of grain. These large variations can greatly increase the number of experiments necessary to make widely-applicable inferences. However, the inference space can also be greatly increased by using theoretical modeling, generally known as mechanistic modeling, to add extensive additional information from established laws of motion

from physics. A mechanistic model of the particle movement in the bucket elevator leg could enhance prediction capabilities on grain commingling.

Both continuum models and the discrete element method (DEM) (Wightman et al., 1998) have been used to model the motion of particles such as grain in bucket elevator legs. Because of its ability to track individual particles, the DEM is a proven way to simulate discrete objects like grain kernels and to predict their movement and commingling in a bucket elevator equipment. Simulations with DEM could involve two-dimensional (2D) (Fillot et al., 2004; Fazekas et al., 2005; Sykut et al., 2008); three-dimensional (3D) (Hart et al., 1988; Sudah et al., 2005; Goda and Ebert, 2005; Takeuchi et al., 2008); or quasi-2D (Kawaguchi et al., 2000; Samadani and Kudrolli, 2001; Li et al., 2005; Kamrin et al., 2007; Ketterhagen et al., 2008) modeling depending on the object of interest. Quasi-2D modeling uses 2D system but with added depth or width usually equivalent to a given number of particle diameters. It can also be referred to as quasi-3D with reference to 3D system but with reduced depth or width.

The objectives of this study were to: (1) simulate grain commingling in a pilot-scale boot using DEM models and evaluate the tradeoffs of computational speed versus accuracy for 3D and quasi-2D boot models, and (2) validate the models using soybeans as the test grain.

6.2 Simulation of Grain Commingling

6.2.1 Discrete Element Method

DEM is a numerical modeling technique that simulates the dynamic motion and mechanical interaction of each particle using Newton's Second Law of Motion and the force-displacement law. It was first introduced by Cundall (1971) and Cundall and Strack (1979) to model soil and rock mechanics. The calculation cycle involves explicit numerical scheme with very small time step as discussed in detail by Cundall and Strack (1979). This method has been successfully applied to processes such as particle mixing in a rotating cylinder (Wightman et al., 1998), 3D, horizontal- and vertical-type screw conveyors (Shimizu and Cundall, 2001), filling and discharge of a plane rectangular silo (Masson and Martinez, 2000), and deformation in agricultural and food particulate materials under bulk compressive loading (Raji and Favier, 2004a, b).

In DEM modeling, particle interaction is treated as a dynamic process, which assumes that equilibrium states develop whenever internal forces in the system balance (Theuerkauf et al., 2007). Contact forces and displacement of a stressed particle assembly are found by tracking the motion of individual particles. Motion results from disturbances that propagate through the assembly. Mechanical behavior of the system is described by the motion of each particle and force and moment acting at each contact. Newton's Law of Motion gives the relationship between the particle motion and forces acting on each particle. Translational and rotational motions of particle *i* are defined as (Remy et al., 2009):

$$m_i \frac{dv_i}{dt} = \sum_j \left(F_{n_{ij}} + F_{t_{ij}} \right) + m_i g \qquad (6.1)$$

$$I_i \frac{d\omega_i}{dt} = \sum_j \left(R_i \times F_{t_{ij}} \right) + \tau_{ij} \qquad (6.2)$$

where m_i, R_i, v_i, ω_i, and I_i are the mass, radius, linear velocity, angular velocity, and moment of inertia of particle *i*; $F_{n_{ij}}$, $F_{t_{ij}}$, and τ_{ij} are, respectively, normal force, tangential force, and torque acting on particles *i* and *j* at contact points; *g* is the acceleration due to gravity; and *t* is the time.

Particles interact only at contact points with their motion independent of other particles. Forces on the particles at contact points include contact force and viscous contact damping force (Zhou et al., 2001). These forces have normal and tangential components. The soft-sphere approach commonly used in DEM models allows particles to overlap each other, giving realistic contact areas.

The force-displacement law at the contact point is represented by Hertz-Mindlin no-slip contact model (Mindlin, 1949; Mindlin and Deresiewicz, 1953; Tsuji et al., 1992; Di Renzo and Di Maio, 2004, 2005). This non-linear model features both the accuracy and simplicity derived from combining Hertz's theory in the normal direction and Mindlin no-slip model in the tangential direction (Tsuji et al., 1992; Remy et al. 2009).

The normal force, F_n, is given as follows (Tsuji et al., 1992; Remy et al., 2009):

$$F_n = -K_n \delta_n^{3/2} - \eta_n \dot{\delta}_n \delta_n^{1/4} \qquad (6.3)$$

where K_n is the normal stiffness coefficient; δ_n is the normal overlap or displacement; $\dot{\delta}_n$ is the normal velocity; and η_n is the normal damping coefficient. Normal stiffness and normal damping

coefficients are given, respectively, by (Tsuji et al., 1992; DEM Solutions, 2009; Remy et al., 2009):

$$K_n = \frac{4}{3} E^* \sqrt{R^*} \tag{6.4}$$

$$\eta_n = \frac{\ln e}{\sqrt{\ln^2 e + \pi^2}} \sqrt{m^* K_n} \tag{6.5}$$

where E^* is the equivalent Young's modulus, R^* is the equivalent radius, m^* is the equivalent mass, and e as the coefficient of restitution. Equivalent properties (R^*, m^*, and E^*) during collision of particles with different materials such as particles i and j are defined as (Di Renzo and Di Maio, 2004; DEM Solutions, 2009):

$$R^* = \left(\frac{1}{R_i} + \frac{1}{R_j} \right)^{-1} \tag{6.6}$$

$$E^* = \left(\frac{1-\nu_i^2}{E_i} + \frac{1-\nu_j^2}{E_j} \right)^{-1} \tag{6.7}$$

$$m^* = \left(\frac{1}{m_i} + \frac{1}{m_j} \right)^{-1} \tag{6.8}$$

where ν is the Poisson's ratio (Di Renzo and Di Maio, 2004; DEM Solutions, 2009). Similarly, for a collision of a sphere i with a wall j, the same relations apply for Young's modulus E^*, whereas $R^* = R_i$ and $m^* = m_i$.

The tangential force, F_t, is governed by the following equation (Tsuji et al., 1992; Remy et al., 2009):

$$F_t = -K_t \delta_t - \eta_t \dot{\delta}_t \delta_n^{1/4} \tag{6.9}$$

where K_t is the tangential stiffness coefficient; δ_t is the tangential overlap; $\dot{\delta}_t$ is the tangential velocity; and η_t is the tangential damping coefficient. Tangential stiffness and tangential damping coefficients, are defined, respectively, as follows (Tsuji et al., 1992; DEM Solutions, 2009; Remy et al., 2009):

$$K_t = 8G^* \sqrt{R^* \delta_n} \tag{6.10}$$

$$\eta_t = \frac{\ln e}{\sqrt{\ln^2 e + \pi^2}} \sqrt{m^* K_t} \tag{6.11}$$

where G^* is the equivalent shear modulus defined by (Li et al, 2005):

$$G^* = \left(\frac{2-\nu_i}{G_i} + \frac{2-\nu_j}{G_j} \right)^{-1} \tag{6.12}$$

G_i and G_j are shear moduli of particles *i* and *j*, respectively. The tangential overlap is calculated by (Remy et al, 2009):

$$\delta_t = \int v_{rel}^t dt \tag{6.13}$$

where v_{rel}^t is the relative tangential velocity of colliding particles and is defined by (Remy et al., 2009):

$$v_{rel}^t = \left(v_i - v_j\right) \cdot s + \omega_i R_i + \omega_j R_j \tag{6.14}$$

where *s* is the tangential decomposition of the unit vector connecting the center of the particle.

Additionally there is a tangential force limited by Coulomb friction $\mu_s F_n$, where μ_s is the coefficient of static friction. When necessary, rolling friction can be accounted for by applying a torque to contacting surfaces. The rolling friction torque, τ_i, is given by (DEM Solutions, 2009; Remy et al., 2009):

$$\tau_i = -\mu_r F_n R_0 \omega_0 \tag{6.15}$$

where μ_r is the coefficient of rolling friction, R_0 is the distance of the contact point from the center of the mass, and ω_0 is the unit angular velocity vector of the object at the contact point (Tsuji et al., 1992; Di Renzo and Di Maio, 2004; Li et al., 2005; DEM Solutions, 2009; Remy et al., 2009).

For dynamic processes, important factors to consider are the propagation of elastic waves across the particles, the time for load transfer from one particle to adjacent contacting particles, and the need not to transmit energy across a system that is faster than nature (Li et al., 2005). In the non-linear contact model (e.g., Hertzian), the critical time increment or critical time step cannot be calculated beforehand, unlike with the linear contact model in which the critical time step is related to the ratio of contact stiffness to particle density. Miller and Pursey (1955), however, showed that Rayleigh waves or surface waves account for 67% of the radiated energy, whereas dilational or pressure waves and distortional or shear waves, respectively, are 7% and

26% of the radiated energy. Thus, it is assumed that all of the energy is transferred by the Rayleigh waves since the difference between the speeds of the Rayleigh wave and the distortional wave is small and the energy transferred by the dilational wave is negligible (Li et al., 2005). Moreover, the average time of arrival of the Rayleigh wave at any contact is the same irrespective of the location of the contact point. For simplicity, the critical time step is based on the average particle size and a fraction of this is used in the simulations (Li et al., 2005; DEM Solutions, 2009). The critical time step is given by the following equation (Li et al., 2005; DEM Solutions, 2009):

$$t_c = \frac{\pi \overline{R}}{\beta} \sqrt{\frac{\rho}{G}} \tag{6.16}$$

where $\overline{R}$ is the average particle radius, ρ is the particle density, and β can be approximated by (Li et al., 2005):

$$\beta = 0.8766 + 0.163\nu \tag{6.17}$$

Simulations were performed at 20% Rayleigh time steps as listed in Table 6.1.

6.2.2 Particle Model

The DEM modeling software used was EDEM 2.2 (DEM Solutions, Lebanon, N.H.). A single-sphere particle model that best simulated soybean kernels was chosen (see Chapter 5), which conform to known geometric properties of kernels as well as published experimental values of particle and bulk densities, coefficients of restitution and friction, and angle of repose. From Chapter 5, the best particle model found for predicting angle of repose and bulk density of soybeans has a particle coefficient of restitution of 0.6, particle static friction of 0.45 for soybean-soybean contact (0.30 for soybean-steel interaction), particle rolling friction of 0.05, normal particle size distribution with standard deviation factor of 0.4, and particle shear modulus of 1.04 MPa. Table 6.1 lists the physical properties of the soybeans and the surfaces used in the simulation.

Table 6.1 Input parameters for DEM modeling.

Variable	Symbol	Red Soybean	Clear Soybean	Steel	Rubber
Particle coefficient of restitution	e	0.60 [a]	0.60 [a]	0.60 [a]	0.60 [a]
Particle coefficient of static friction (soybean on)	μ_s	0.45 [a]	0.45 [a]	0.30 [a]	0.50 [a]
Particle coefficient of rolling friction	μ_r	0.05 [a]	0.05 [a]	0.05 [a]	0.05 [a]
Particle size distribution	*PSD*	normal [a]	normal [a]		
Mean factor	*MF*	1.0 [a]	1.0 [a]		
Standard deviation factor	*SDF*	0.4 [a]	0.4 [a]		
Particle shear modulus, MPa	G	1.04 [a]	1.04 [a]	70,000 [b, c, e]	1.00 [b, d]
Particle Poisson's ratio	v	0.25 [a]	0.25 [a]	0.30 [b, c, e]	0.45 [b, d]
Particle Young's modulus, MPa	E	2.60 [a]	2.60 [a]	182,000 [b, c, e]	2.90 [b, d]
Particle density, kg·m^{-3}	ρ	1243 [f]	1247 [f]	7800 [b, c, e]	9100 [b, d]
Particle mass, g	m	0.1597 [f]	0.1389 [f]		
Particle radius, mm	R	3.13 [g]	2.985 [g]		
Number of particles	N	5,000-35,000	800,000-1,365,000		
Calculated Rayleigh time step, s	t_R	3.71E-01	3.54E-01		
Simulation time step, s	t_S	7.08E-02	7.08E-02		

[a] Boac et al., 2009
[b] DEM Solutions, 2009
[c] Boresi and Schmidt, 2003
[d] Ciesielski, 1999
[e] Baumeister et al., 1978
[f] Measured values
[g] Calculated values

6.2.3 Three-Dimensional (3D) Modeling in Pilot-Scale Bucket Elevator Boot

A 3D model of a pilot-scale B3 bucket elevator leg (Universal Industries, Inc., Cedar Falls, Iowa) was simulated to determine grain commingling. The pilot-scale B3 leg is a back-feeding bucket elevator with one hopper and a discharge spout at the end of the elevator head. The elevator boot is the enclosed base of an elevator leg casing, where static grain, called residual grain, accumulates after material loading.

Geometries of the pilot-scale B3 bucket elevator boot were drawn in a computer-aided design (CAD) software package (DS SolidWorks Corp., Concord, Mass.) and imported to establish model geometries in EDEM. The material for bucket cups and enclosure of the B3 leg was specified as steel and the belt was rubber (Table 6.1). The input parameters for a single-sphere particle model for the soybean kernel (Boac et al., 2009) are listed in Table 6.1.

In the simulation, red soybean particles were handled first in the 3D pilot-scale B3 leg geometries (Figure 6.1a). The leg was allowed to run until the residual grain stabilized after a run time of 11 s. After handling red soybeans, the mass of residual grain was determined by extracting the particle mass remaining in the boot geometry. With red soybean particles as the residual grain in the 3D leg geometry, clear soybean particles were run next for 287 s or approximately 5 min (Figure 6.1b). The total particle mass of red and clear soybeans were determined from each bucket cup leaving the control volume. The instantaneous commingling (C_i) from each cup was computed based on the following equation:

$$C_i = \frac{m_r}{m_r + m_c} \tag{6.18}$$

where m_r is mass of red soybeans (kg) and m_c is mass of clear soybeans (kg). Average commingling per given load mass (C_a) was computed as given by:

$$C_a = \frac{\sum \left(\dot{m}_s \times t_i \times C_i \right)}{\sum \left(\dot{m}_s \times t_i \right)} \tag{6.19}$$

where $\dot{m}_s$ is mass flow rate of soybeans (kg·s^{-1}) and t_i is sampling time interval (s). The simulation data with one replication were calculated from three bucket cups, representing a sample from the experiments. The mean sample mass from the experiments was divided by the computed mass of soybeans in a bucket cup (i.e., mean bucket cup filling (m_{cf})) to determine the three bucket cups.

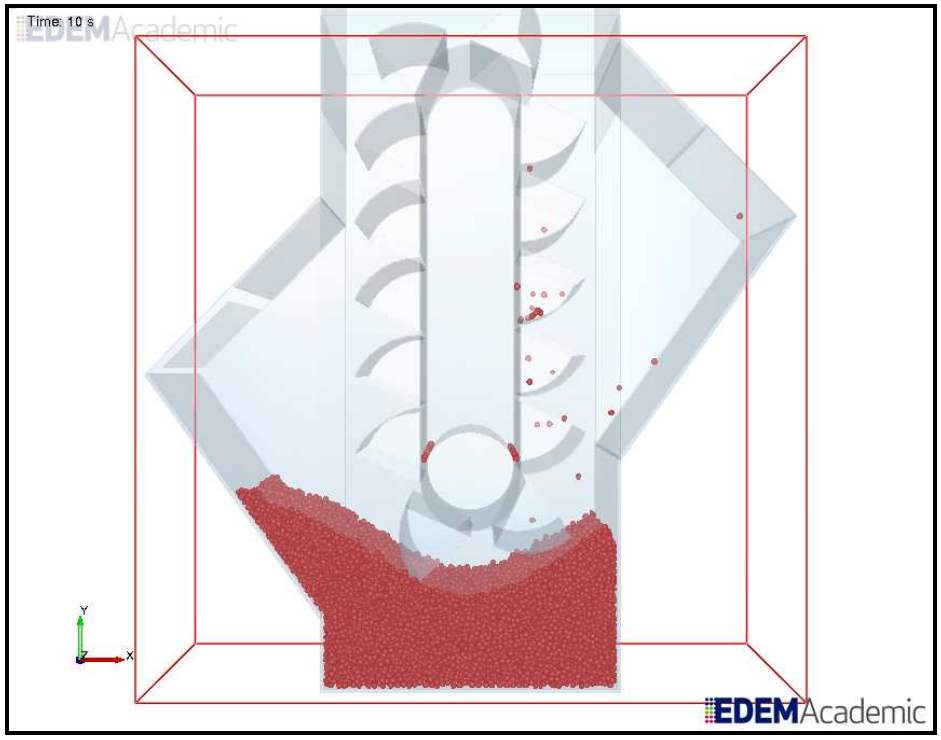
Time: 10 s
EDEMAcademic
Y
Z
X
EDEMAcademic

(a)

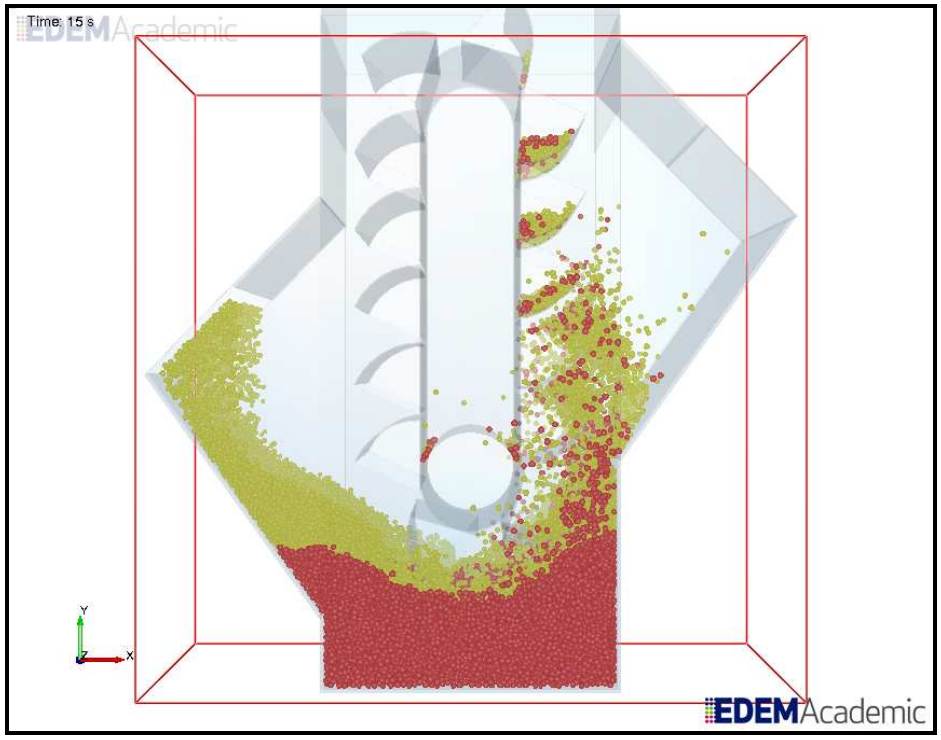
Time: 15 s
EDEMAcademic
Y
Z
X
EDEMAcademic

(b)

Figure 6.1 Initial 3D simulation during handling of (a) red and (b) clear soybeans.

The start time was also calculated based on the best estimated initial time simulating the experiments. The time it took for the soybeans to be scooped by bucket cups to the time they were collected in the Gamet DT sampler was measured to be 5.0 s. Simulation data time were adjusted accordingly. The trends of instantaneous and average commingling from simulation were compared with experimental data.

6.2.4 Quasi-Two-Dimensional (Quasi-2D) Modeling in Pilot-scale Bucket Elevator Boot

To further reduce computational time and implementation complexities, a quasi-2D model for the pilot-scale B3 bucket elevator boot was implemented. This made the boot modeling simpler than its 3D counterpart by reducing most geometry consideration to essentially 2D. The same geometries of the pilot-scale B3 bucket elevator boot drawn in a CAD software (DS SolidWorks Corp., Concord, Mass.) were imported to establish model geometries in simulation.

To model a quasi-2D pilot-scale boot, dimension in the z-direction (i.e., width) of the boot was reduced by using periodic boundaries on both front and back walls. Periodic boundary conditions enable any particle leaving the domain in that direction to instantly re-enter on the opposite side (DEM Solutions, 2009), simulating infinite length in that direction, thereby eliminating wall friction and reducing the total number of particles inside the control volume.

Four quasi-2D models were tested to determine which best simulates the initial 3D boot model and the experimental data. The quasi-2D models had widths of four to seven times the diameter of red soybean particle (4d, 5d, 6d, 7d) (Table 6.2). The reduction factor, ζ_n, for each quasi-2D model is defined as

$$\zeta_n = \frac{w_{bc}}{w_{Q2D}} \qquad (n = 4, 5, 6, 7) \qquad (6.20)$$

where w_{bc} is the original width of the bucket cup and w_{Q2D} is the width of the quasi-2D model (i.e., 4d, 5d, 6d, or 7d). A single-sphere particle model with the same material and interaction properties of soybean used in the initial 3D model was employed in the quasi-2D pilot-scale boot simulations. The total number of particles created was also reduced based on the reduction factor.

Red soybean particles were handled first in the quasi-2D pilot-scale leg until the residual grain stabilized after a run time of 10 s (Figure 6.2a). Red soybeans were left as residual grain in the quasi-2D pilot-scale boot geometry and clear soybean particles were introduced next for 35 s in the initial trials (Figure 6.2b). Instantaneous and average commingling for one replication were computed based on equations 6.18 and 6.19, respectively, and at start time where clear soybeans was introduced in the model. The trends of the instantaneous and average commingling results from the four quasi-2D boot models were compared with those of the initial 3D boot model. The quasi-2D model that best simulated the initial 3D model was chosen.

Table 6.2 Input parameters for the quasi-2D boot models with reduced control volume.

		Quasi-2D Boot Model			
Variable	**Symbol**	**4d**	**5d**	**6d**	**7d**
Particle diameter, mm	d	6.26	6.26	6.26	6.26
Width of bucket cup of B3 leg, mm	w_{bc}	95.25	95.25	95.25	95.25
Width of the quasi-2D model, mm	w_{Q2D}	25.04	31.30	37.56	43.82
Reduction factor, dimensionless	ζ_n	3.80	3.04	2.54	2.17
Original mass flowrate, kg·s^{-1}	$\dot{m}_0$	0.95	0.95	0.95	0.95
Reduced mass flowrate, kg·s^{-1}	$\dot{m}_n$	0.25	0.31	0.37	0.44
Original particle rate, particles·s^{-1}	$\dot{n}_0$				
red soybeans		5,931	5,931	5,931	5,931
clear soybeans		6,819	6,819	6,819	6,819
Reduced particle rate, particles·s^{-1}	$\dot{n}_n$				
red soybeans		1,559	1,949	2,339	2,729
clear soybeans		1,793	2,241	2,689	3,137

6.3 Pilot-Scale Boot Experiment

6.3.1 Grain Materials

Two types of soybeans were used for the grain commingling tests in the pilot-scale B3 leg. Test material 1 was red colored soybeans with clear-hilum from a 2008 crop variety KS4702. Five bags of these red soybeans were purchased from Kansas State University (KSU) Agronomy Farm on January 30, 2009. Each bag had a mean mass of 25.7 kg (standard deviation (SD) = 0.14 kg). Test material 2 was clear or uncolored soybeans with brown- and black-hilum from 2008 crop. The clear soybeans were purchased from a local elevator on December 4, 2008,

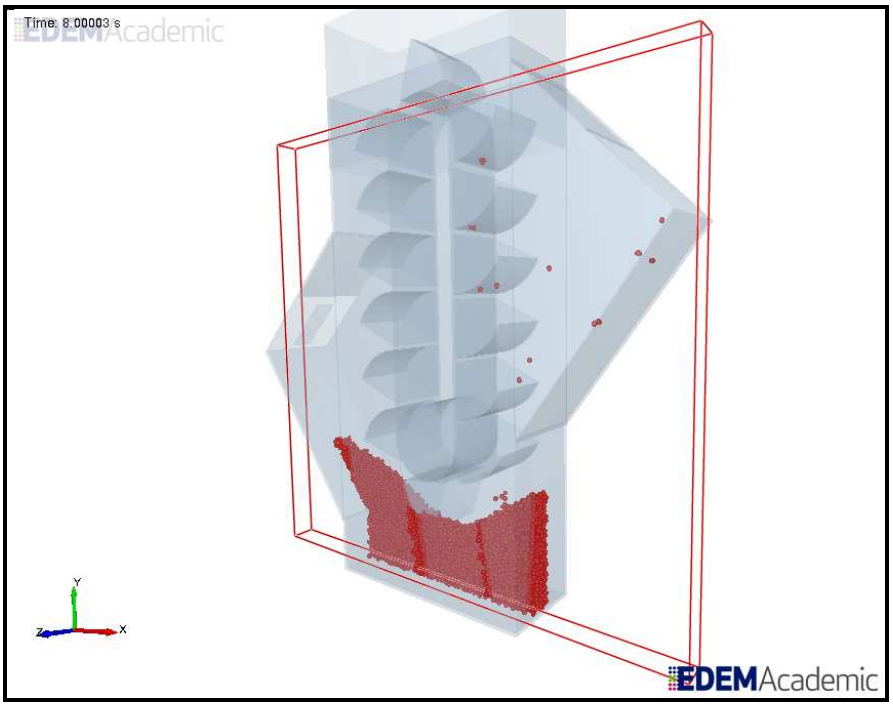

(a)

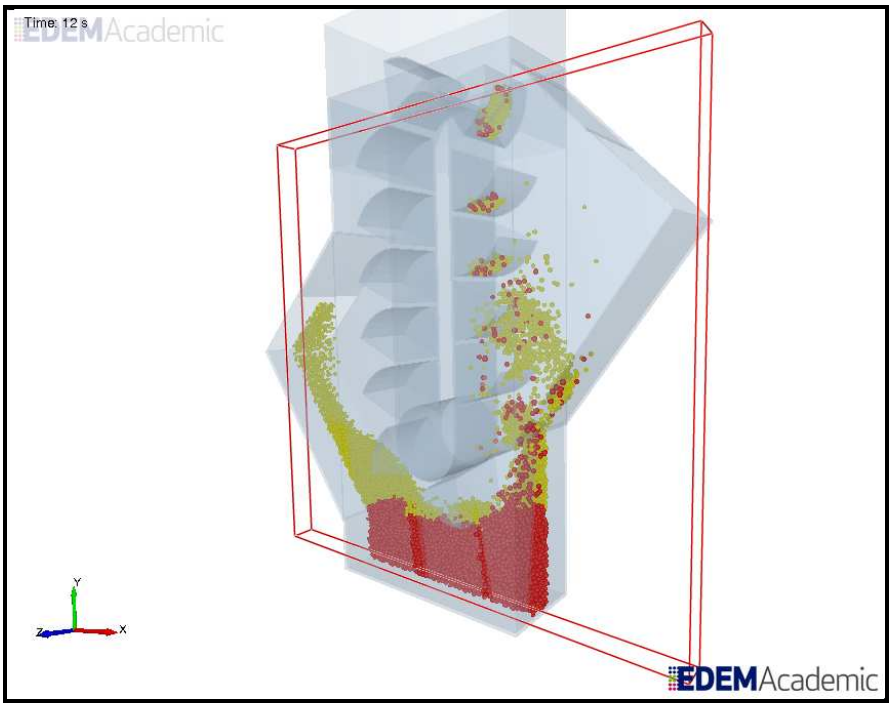

(b)

Figure 6.2 Quasi-2D simulation during handling of (a) red and (b) clear soybeans.

and were cleaned through a fanning mill at KSU Agronomy Farm on December 5, 2008. After cleaning, the clear soybeans were then transferred in five grain tote bags with a mean mass of 563.9 kg (SD = 84.07 kg) for each bag.

Representative samples from both test materials were collected using a grain probe (USDA GIPSA, 1995) and graded (USDA GIPSA, 2004). Initial moisture content, test weight, foreign materials, splits, damaged kernels, 1000-kernel weight, particle density, and purity based on the amount of soybean of different color mixed in the whole lot were measured. The initial quality and characteristics of red and clear soybeans are shown in Table 6.3.

Table 6.3 Initial quality and characteristics of soybeans before transfers.[a]

Soybeans	Grade	Impurity [b] (%)	Damaged Kernels (%)	Foreign Material (%)	Splits (%)
Red	U.S. No. 1	0	0.337 a (0.131)	0.030 a (0.013)	1.114 a (0.167)
Clear	U.S. No. 1	0	1.207 b (0.486)	0.013 b (0.008)	0.329 b (0.103)

Soybeans	Test Weight ($kg \cdot m^{-3}$)	Moisture Content (% wet basis)	Mass of 1000 Kernels (g)	Particle Density ($g \cdot cm^{-3}$)
Red	700.72 a (3.21)	9.75 a (0.23)	138.90 a (4.46)	1.244 a (0.003)
Clear	728.75 b (1.48)	10.09 b (0.34)	159.73 b (5.15)	1.247 b (0.004)

[a] Mean values with the same lower case letters within a column are not significantly different at the 5% level of significance in Bonferroni. Values in parenthesis represent standard deviation (SD).
[b] Impurity = red soybeans in clear, or clear soybeans in red

6.3.2 Test Facility

Five tests were performed in the pilot-scale B3 bucket elevator leg (Universal Industries, Inc., Cedar Falls, Iowa) at the USDA-ARS, CGAHR, Manhattan, Kansas. The B3 leg is a back-feeding bucket elevator with one hopper and a discharge spout at the end of the elevator head (Figure 6.3). The metal covers of the right hand side (RHS) and boot openings were replaced by plexi-glass to allow visual observation of the behavior of the grain inside the boot. The B3 leg has a handling capacity of 6 $t \cdot h^{-1}$ at 75% bucket filling (manufacturer's data). In this research, the B3 leg was operated at a mean soybean mass flow rate of 3.41 $t \cdot h^{-1}$ (range: 3.20 to 3.65 $t \cdot h^{-1}$), which is 41.2% of the leg's full-cup capacity and corresponding to the same percent of capacity

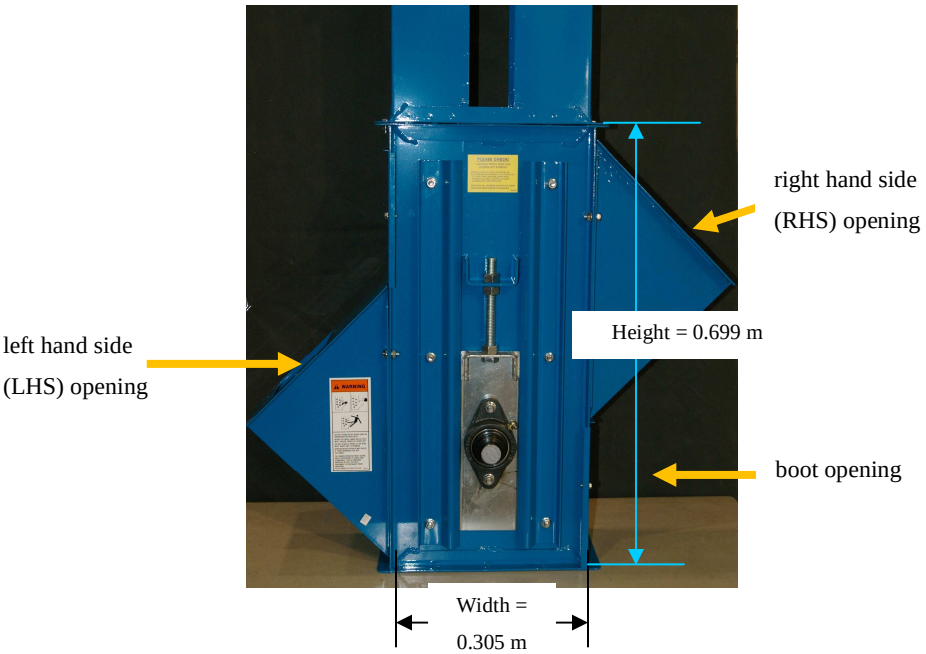

Figure 6.3 Pilot-scale B3 bucket elevator leg.

for the full-scale CGAHR research elevator at an average grain mass flow rate of 47 $t \cdot h^{-1}$ (Ingles et al., 2003).

6.3.3 Test Procedure

Figure 6.4 shows a schematic diagram of the grain flow during each grain transfer. The grain transfers simulated the receiving operation of two consecutive grain types without additional (separate) cleaning of equipment between operations. Two types of soybeans of different color and hilum were used to easily identify grain commingling between grain loads.

6.3.3.1 Before the Transfers

Prior to each test, the B3 leg was allowed to self-clean by letting the leg to run on empty for 10 min to self-clean. Compressed air was used through the RHS opening of the leg (Figure 6.3) to clean the bucket cups while it is running. Grain residuals and impurities were vacuumed from the boot and other parts of the B3 leg. Before each transfer operation, the ambient and grain temperatures and ambient relative humidity were measured using a mercury thermometer and psychrometer (model 3312-40, Cole-Parmer Instrument Co., Vernon Hills, Ill.), respectively. The stop of the hopper's slide gate was checked and tightened for proper position giving a specific opening (width = 32.54 mm).

6.3.3.2 Transfer of First Grain — Red Soybeans

The first soybean lot handled in the B3 leg was the red soybeans. One bag of red soybeans was poured into the hopper of the leg. A 125-L plastic container was placed at the end of the spout connected to the head of the B3 leg to catch the red soybeans after being handled.

The B3 leg was switched on and the slide gate was opened to run the red soybeans. After the transfer of red soybeans, the B3 leg was allowed to continuously run for 5 min for self-cleaning. Then, the B3 leg was switched off.

After the red soybean handling, the residual grain heights were measured in the left hand side (LHS) (i.e., from the top of the LHS opening to the grain) and in the RHS (i.e., from the boot floor to the height of the grain) of the B3 leg. The mean residual grain heights of red soybeans in the LHS and RHS from five tests were 123.19 (standard deviation, SD = 2.78) mm and 95.66 (SD = 0.91) mm, respectively.

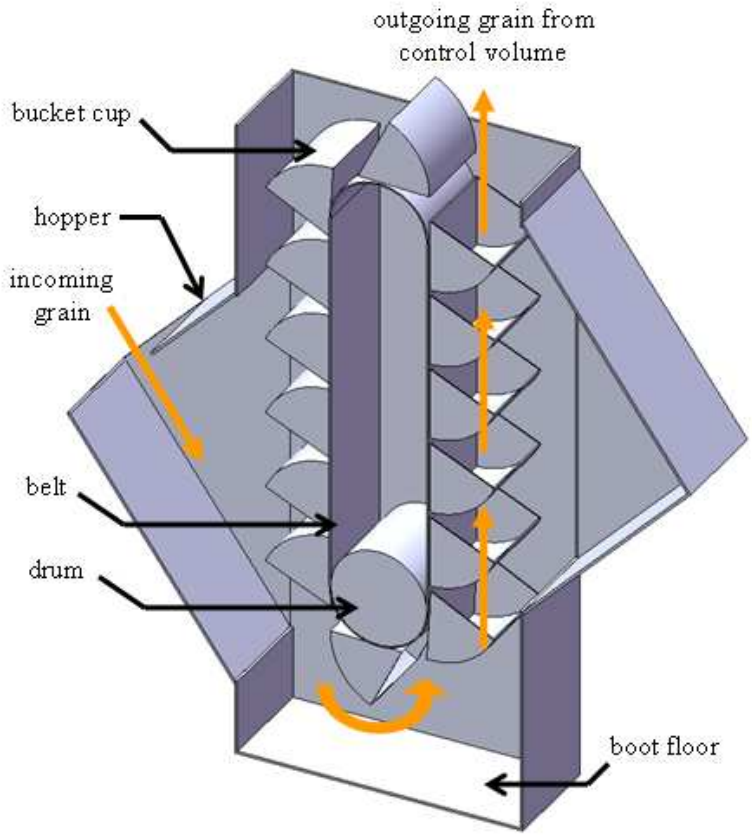

Figure 6.4 Schematic diagram of the grain flow as represented by arrows.

The end of the spout connected to the head was transferred from the plastic container to the Gamet diverter-type (DT) sampler (Seedburo Equipment Co., Chicago, Ill.) to collect grain samples from the next soybean flow. The Gamet DT sampler was placed on top of a plastic hopper (1.07 x 1.37 x 1.59 m) that collected that rest of the flow.

Split-core AC current sensors (0-20 Amp model CTV-A, Onset HOBO, Bourne, Mass.) plugged directly into a 4-channel external input data logger (model HOBO H8) was attached to the control panel of the Gamet DT sampler. The clock on a laptop computer (model Sony Vaio PCG-Z505R, Sony Electronics, Inc., New York, N.Y.) was synchronized with the HOBO time.

6.3.3.3 Transfer of Second Grain — Clear Soybeans

The second soybean lot handled on the B3 leg was the clear soybeans. The clear soybean lot in a tote bag was weighed on a platform scale with digital weight indicator (IQ Plus 310A, Rice Lake Weighing System, Inc., Rice Lake, Wisc.). After weighing, the tote bag was placed directly over the hopper of the B3 leg. The protective guard of the tote bag was put in place. The tote bag was opened by reaching under the protective guard and letting the soybeans fill the hopper of the B3 leg. The tube at the bottom of the tote bag was choked preventing overflow. The height of the tote bag was then adjusted to maintain the flow of clear soybeans at a consistent level.

The B3 leg was switched on. The slide gate of the hopper was opened to the same opening width each time using the stop on the slide gate. The control panel of the Gamet DT sampler was turned on. The stopwatch was started when the clear soybeans entered the boot. The real time for this start as displayed by the laptop clock (in seconds) was recorded. The RPM of the boot pulley shaft was measured with a digital tachometer (model 1726, AMETEK, Largo, Fla.).

6.3.4 Grain Sampling, Sorting, and Analysis

The grain samples were diverted from the flow by the Gamet DT sampler every 15 s for the first 2 min, every 30 s for the next 3 min, and every 60 s for the rest of the handling time. The stopwatch was stopped when the last normal bucket cup scooping was seen through the plexi-glass cover. The real time for this stop was recorded as displayed by the laptop clock. The total handling time from the stopwatch was also recorded.

After the clear soybean handling, the B3 leg was allowed to self-clean for another 5 min. The residual grain heights were measured in the LHS and RHS. The mean residual grain heights of clear soybeans in the LHS and RHS from five tests were 127.0 (SD = 0) mm and 96.09 (SD = 1.38) mm, respectively. The mean residual grain that was vacuumed from the boot and weighed from the five tests was 2.48 (SD = 0.02) kg.

The test simulating the receiving operation of two consecutive grain types (red and clear soybeans) with only self-cleaning between operations was replicated five times. The grain samples collected by the Gamet DT sampler were weighed. The red soybeans were manually sorted from the clear soybeans.

The mass of grain in a bucket cup or mean bucket cup filling (m_{cf}) in g·cup^{-1} was computed based on the following equation:

$$m_{cf} = \frac{\dot{m}_s}{f_c} \tag{6.21}$$

where $\dot{m}_s$ is the mean mass flow rate of soybeans in t·h^{-1} and f_c is the measured bucket cup rate in cup·s^{-1} defined by:

$$f_c = \frac{v_b}{s_c} \tag{6.22}$$

where v_b is the boot belt speed in m·s^{-1} and s_c is the bucket cup spacing in m·cup^{-1}. The boot belt speed was computed as:

$$v_b = 2\pi r_b N_b \tag{6.23}$$

where r_b is the radius of the boot pulley (and the belt thickness) in m and N_b is the boot pulley rpm.

From the experiments, the mean mass flow rate for soybeans ($\dot{m}_s$) was measured as 3.41 t·h^{-1} (0.95 kg·s^{-1}). The mean boot pulley rpm (N_b) and radius of the boot pulley including belt thickness (r_b) were 203.7 rpm and 0.0535 m, respectively. These values gave a boot belt speed (v_b) of 1.141 m·s^{-1}. The bucket cup spacing (s_c) and frequency (f_c) were 0.08255 m·cup^{-1} and 13.82 cups·s^{-1}, respectively, resulting in mean bucket cup filling (m_{cf}) of 68.54 g·cup^{-1}. These data were verified in the initial 3D pilot-scale boot model simulations.

6.3.5 Data Analysis

Grain commingling of red and clear soybeans was simulated in 3D and quasi-2D pilot-scale B3 boot models. Experiments on grain commingling involving red and clear soybeans were conducted with five replications. Instantaneous commingling was defined as the amount of red soybeans in the collected samples and computed based on equation 6.18. Average commingling was the amount of red soybeans mixed with the soybean lot that accumulated at a given time and computed based on equation 6.19. Since the clear soybeans used were sieved and cleaned before the experiments, the calculated values of average commingling do not need to be adjusted based on initial purity of the clear soybean load. Statistical analysis was performed using the General Linear Model (GLM) procedure of SAS statistical software (ver. 9.2, SAS Institute, Inc., Cary, N.C.). Basic descriptive statistics (i.e., mean and standard deviation) were determined for the parameters evaluated. Predicted results were compared with the mean, and lower and upper limits of the 95% confidence interval of the experimental data.

6.5 Results and Discussion

6.5.1 Grain Commingling in 3D Boot Model

6.5.1.1 Instantaneous Commingling

Experimental instantaneous commingling started at 4.25% during the first 5 s, decreased to 0.85% after 21 s, went to 0.02% after 3.2 min, and reached 0% after 6.7 min (Figure 6.5). Instantaneous commingling from the 3D simulation agreed well with experimental data after the first 7 s (Figure 6.6). During the first 7 s, simulation data from this initial 3D simulation were higher than experimental data.

Instantaneous commingling data from the 3D simulation were computed from three bucket cups, representing the mass of soybeans in one sampling in the experiments. One advantage of the simulation was that it can predict commingling from individual bucket cups, which may be difficult to obtain through experiments. Figure 6.7 shows the instantaneous commingling computed from individual bucket cups, which was compared with the smoothing effect from the data based on three bucket cups.

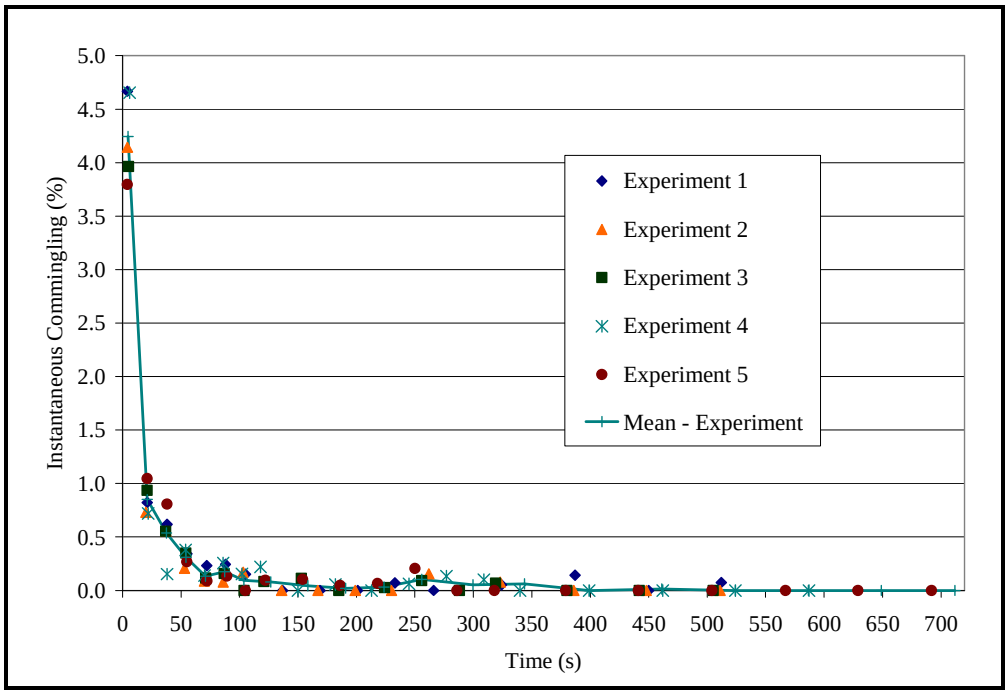

Figure 6.5 Instantaneous commingling from five experiments.

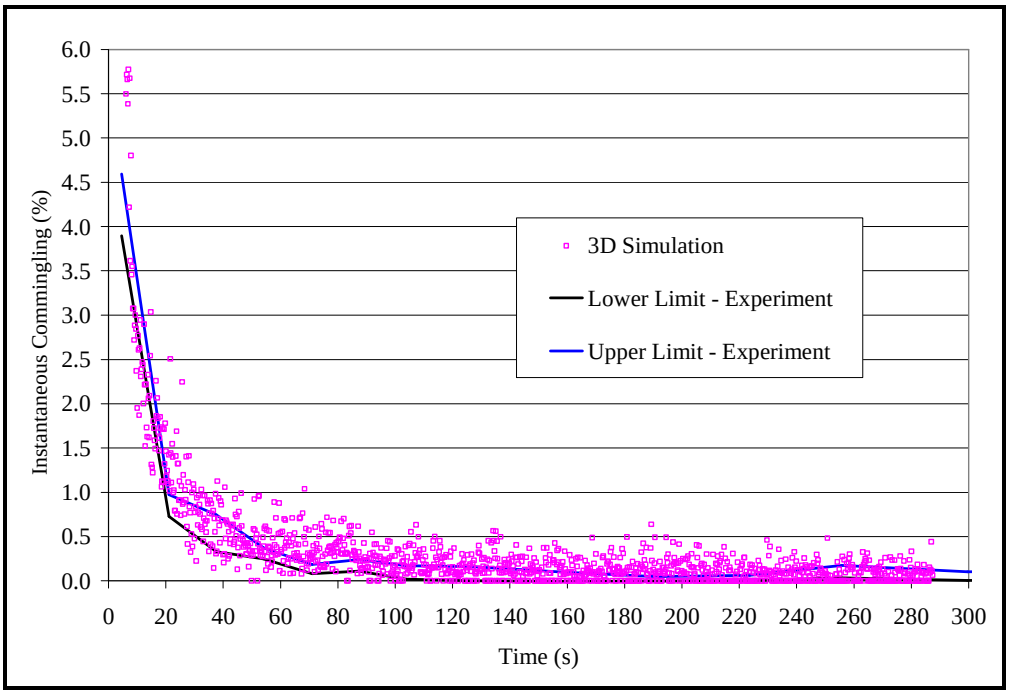

Figure 6.6 Instantaneous commingling from the initial 3D simulation and experiments showing 95% confidence limits.

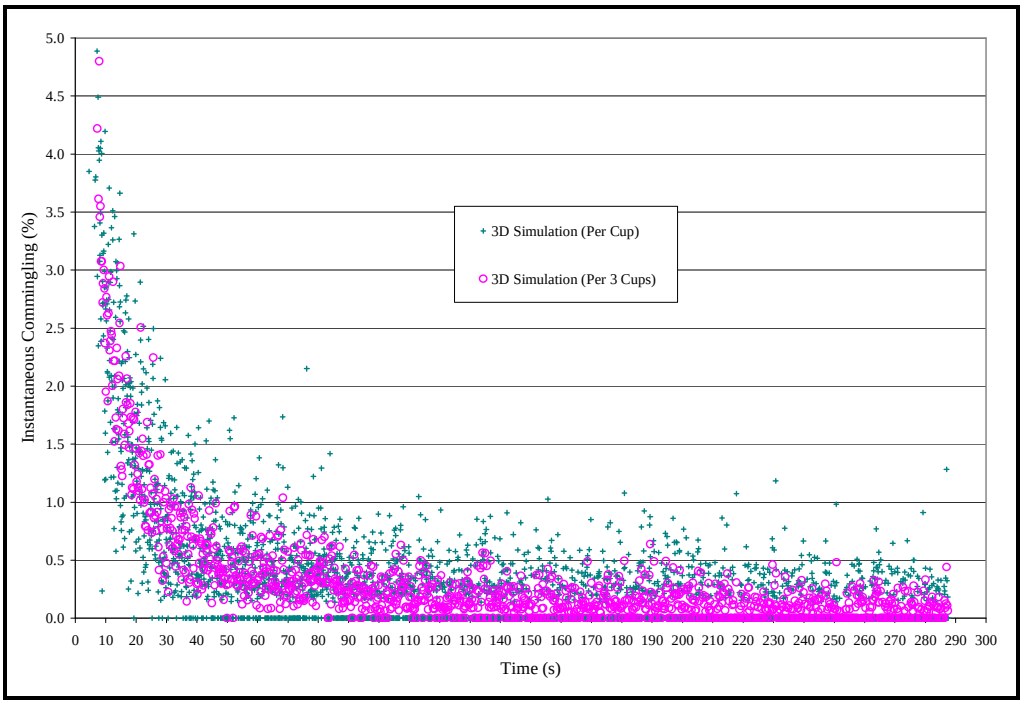

Figure 6.7 Instantaneous commingling from one- and three-bucket cup initial 3D simulation.

6.5.1.2 Average Commingling

Figure 6.8 also shows an over prediction of commingling for this initial 3D model as in the instantaneous commingling data. The values of average commingling (in discrete time) in this graph was computed based on the same discrete time periods as in the experiments, neglecting the simulation values in between those discrete times even if those values can be computed from the simulation. The average commingling accentuated the high predicted values further as the over predictions accumulated.

Mean experimental data from five tests showed that average commingling started at 4.25% during the first 5 s, decreased to 2.52% after 21 s, went to 0.89% after 1.7 min, and reached 0.41% after 4.3 min. Simulation data started at 7.37% during the first 5 s, decreased to 4.61% after 21 s, went to 1.66% after 1.7 min and reached 1.02% after 4.3 min. Experimental data decreased at a rate of 41%, 79%, and 90% from the initial value at times 21 s, 1.7 min, and 4.3 min, respectively. Simulation data had slower decreasing rate of 38%, 78%, and 86% from the initial value at the same given times, respectively, which caused the average commingling to lag behind.

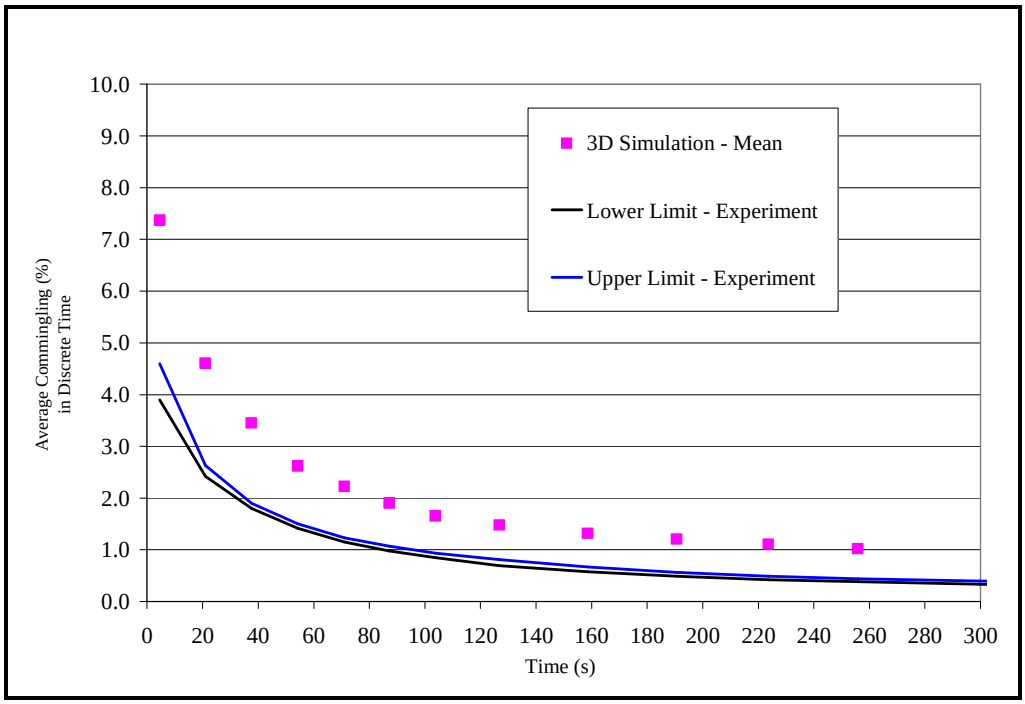

Figure 6.8 Average commingling from the initial 3D simulation compared at the same discrete time with experiments.

6.5.2 Quasi-2D Boot Model

The best quasi-2D model was chosen based on average plots that best represented the 3D model. Quasi-2D model with 4d reduced control volume did not perform well in the simulation due to instability of the system in the reduced domain. Figure 6.9 shows that quasi-2D with 6d reduced control volume closely mimicked the initial 3D model. The average commingling in this plot was computed based on complete simulation time period as opposed to discrete time periods similar to the experiment. The quasi-2D (6d) boot model was chosen as a faster alternative to the initial 3D boot model in predicting grain commingling.

In the initial 3D model, it was evident that the predicted average grain commingling was high. Further simulation tests were conducted to improve the quasi-2D (6d) boot model to more closely simulate the experimental data.

Vibration of the boot geometry with frequency of 37 Hz and amplitude of 0.4 mm was introduced into the quasi-2d (6d) model during the onset of the clear soybeans. Preliminary 3D simulations using published vibration frequency and amplitude values (Jones and Block, 1996; Ge et al., 2000) showed that this combination gave best results in terms of residual grain layout.

Figure 6.10 shows the instantaneous commingling from the quasi-2D (6d_vib0) and initial 3D simulations. The two models was compared with experimental data using average commingling computed based on discrete time periods similar to that in the experiments (Figure 6.11). Introduction of vibration during the onset of clear soybeans enabled the quasi-2D (6d_vib0) model to do a slightly better job of predicting commingling than the initial 3D boot model. Vibration increased the bucket cup uptake. However, as higher amount of red soybeans was picked up in the quasi-2D (6d_vib0) model than in the initial 3D model, the amount of clear soybeans picked up was also higher, leading to slightly lower average commingling in discrete time than in the initial 3D simulation. Vibration should have the same effect on 3D models as it was in the quasi-2D, but it was not attempted.

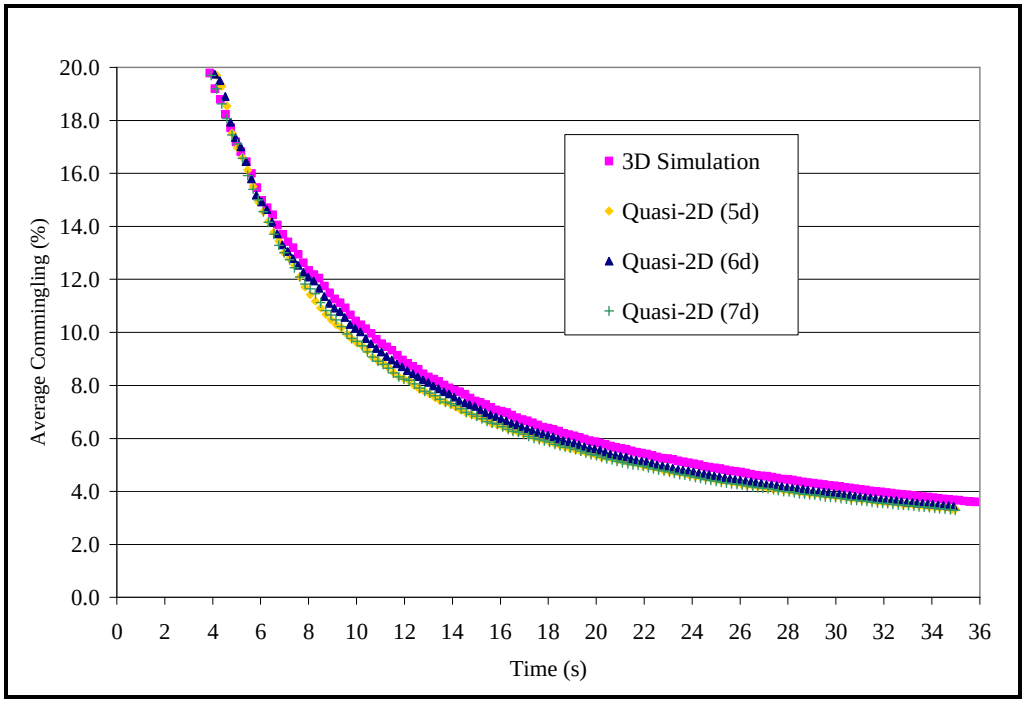

Figure 6.9 Average commingling from four quasi-2D models with reduced control volume.

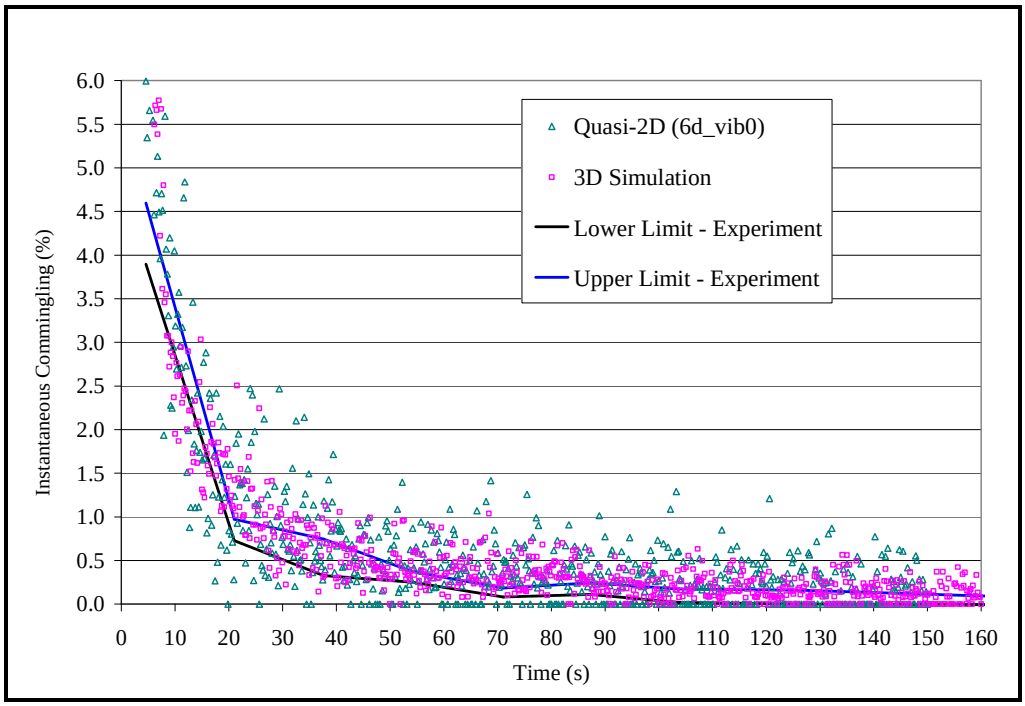

Figure 6.10 Instantaneous commingling from Quasi-2D (6d_vib0) and the initial 3D simulations compared at the same discrete time with experiments.

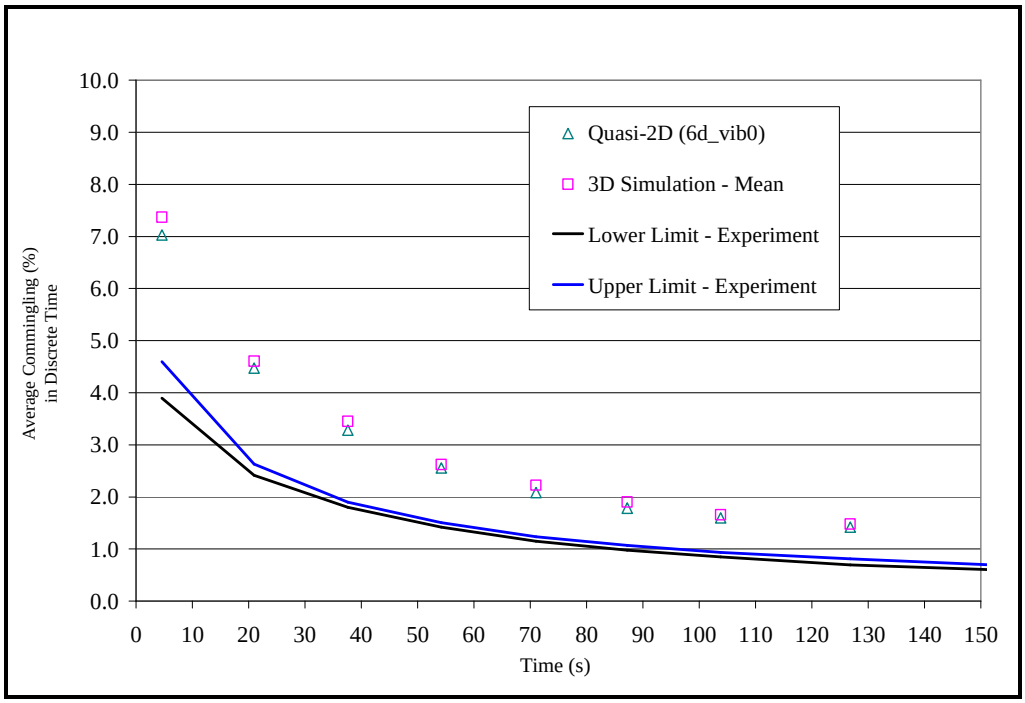

Figure 6.11 Average commingling from Quasi-2D (6d_vib0) and the initial 3D simulations compared at the same discrete time with experiments.

The difficulty of matching the initial time in the experiments to that in the simulations was an important issue for the accuracy in time of predicted commingling. The time of initial particle uptake in the experiments was carefully timed with a stopwatch and then carefully matched to the initial uptake of particles in the simulations.

Refining of the physics of the quasi-2D (6d_vib0) model was performed. One possible improvement in the model was the accounting for the sudden surge of particles from the hopper when the slide gate was opened in the actual experiment that stirs up more particles initially than is being simulated in the model.

The sudden surge of particles during the opening of the slide gate was investigated using the quasi-2D (6d_vib0_gate) model with one replication. Instead of simulating the open slide gate as were in previous simulations, a closed slide gate was modeled and the hopper was filled first with clear soybeans before opening the slide gate (Figure 6.12a). When the gate was opened, a sudden surge of particles was observed (Figure 6.12b).

Accounting for the particle surge (i.e., quasi-2D (6d_vib0_gate) model) better predicted grain commingling than did the quasi-2D (6d_vib0) model (Figure 6.13). The average commingling in discrete times from this model was closer to that in the experiments than the previous ones (Figure 6.14).

The sudden surge of clear soybean particles pushed the red soybeans from the LHS towards the RHS. The action increased the bucket cup uptake of the red soybeans (Figure 6.15). This led to two processes eventually resulting in less grain commingling: (1) a high amount of red soybeans was picked up early in the simulation and less was left for commingling later; and (2) as high amounts of red soybeans was picked up, higher amounts of clear soybeans went with them in the same cup due to the repositioning of the particles from the surge. It is assumed that the effect of particle surge flow on the grain commingling that occurred in the quasi-2D model would also be demonstrated in the 3D model.

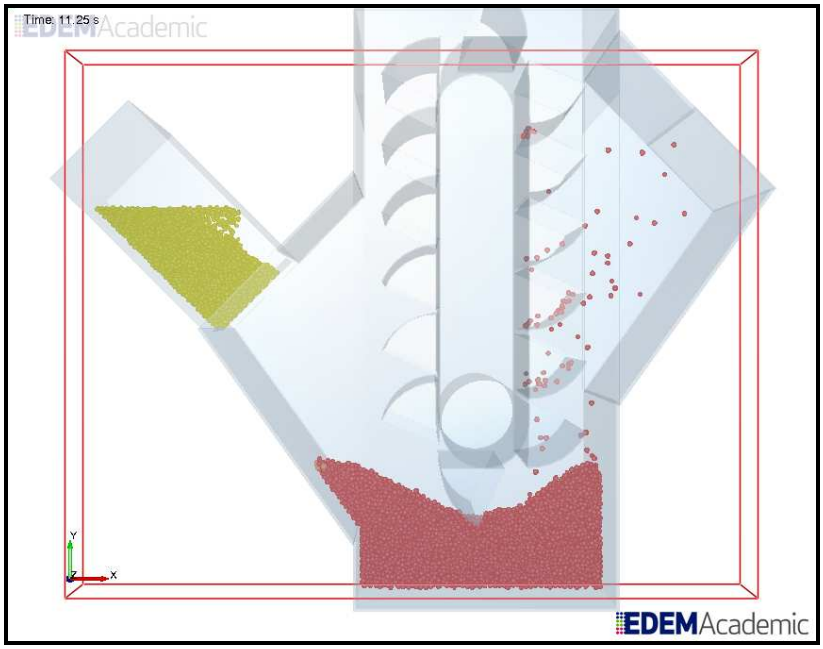

(a)

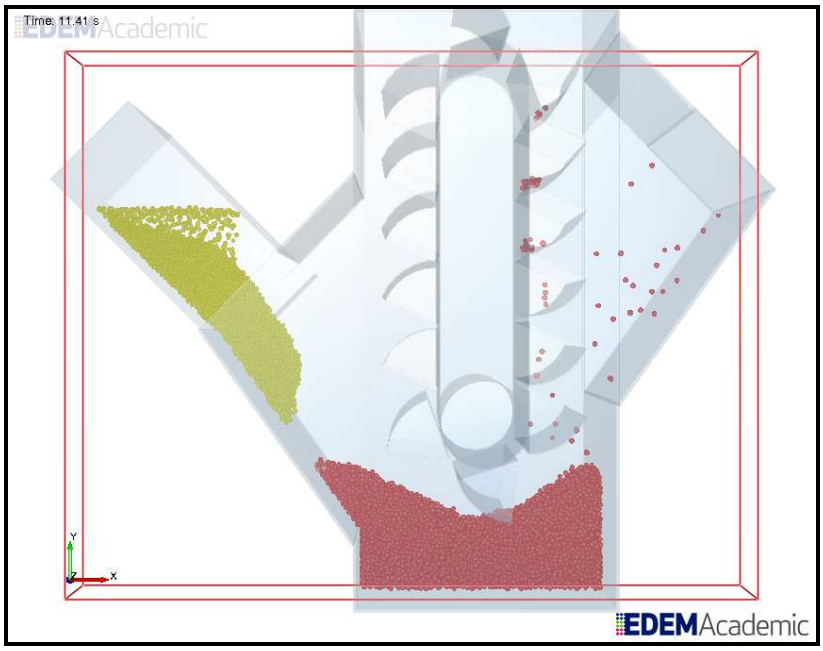

(b)

Figure 6.12 Quasi-2D (6d_vib0_gate) model with particles: (a) accumulating at the gate and (b) with surge flow.

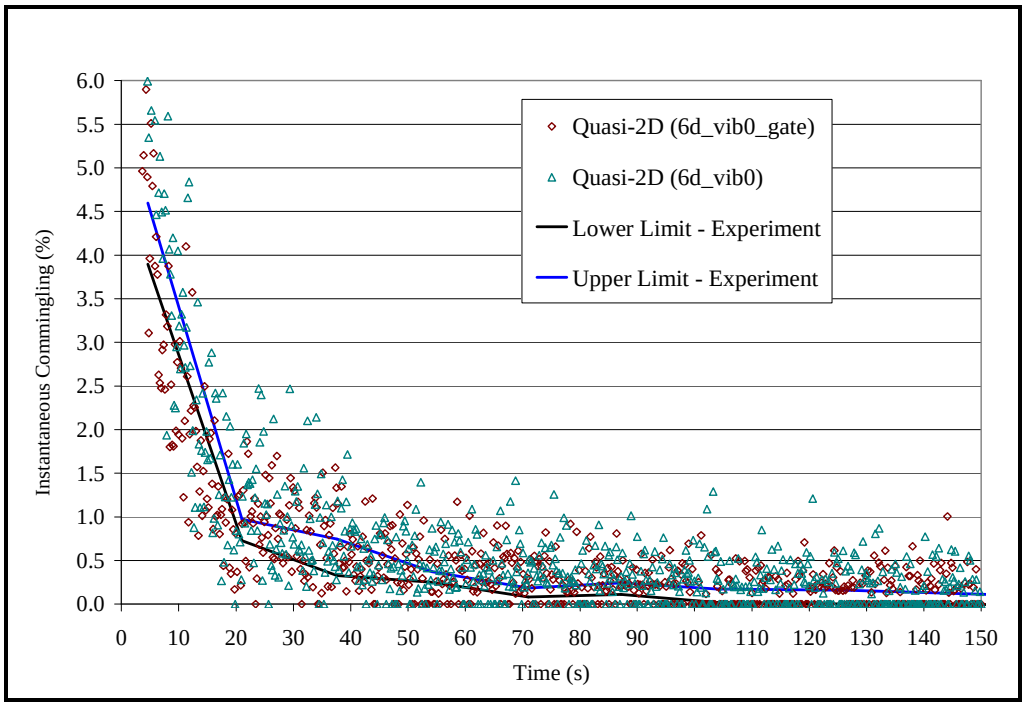

Figure 6.13 Instantaneous commingling from Quasi-2D (6d_vib0_gate) model accounting for particle surge.

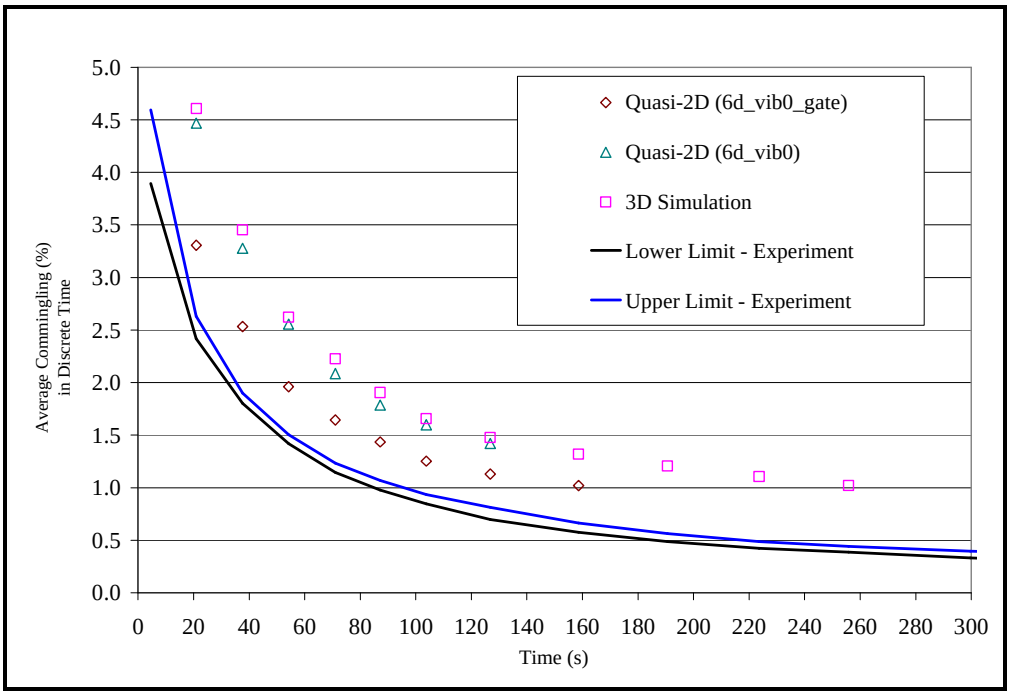

Figure 6.14 Average commingling from Quasi-2D (6d_vib0_gate), Quasi-2D (6d_vib0) and the initial 3D simulations compared at the same discrete time with experiments.

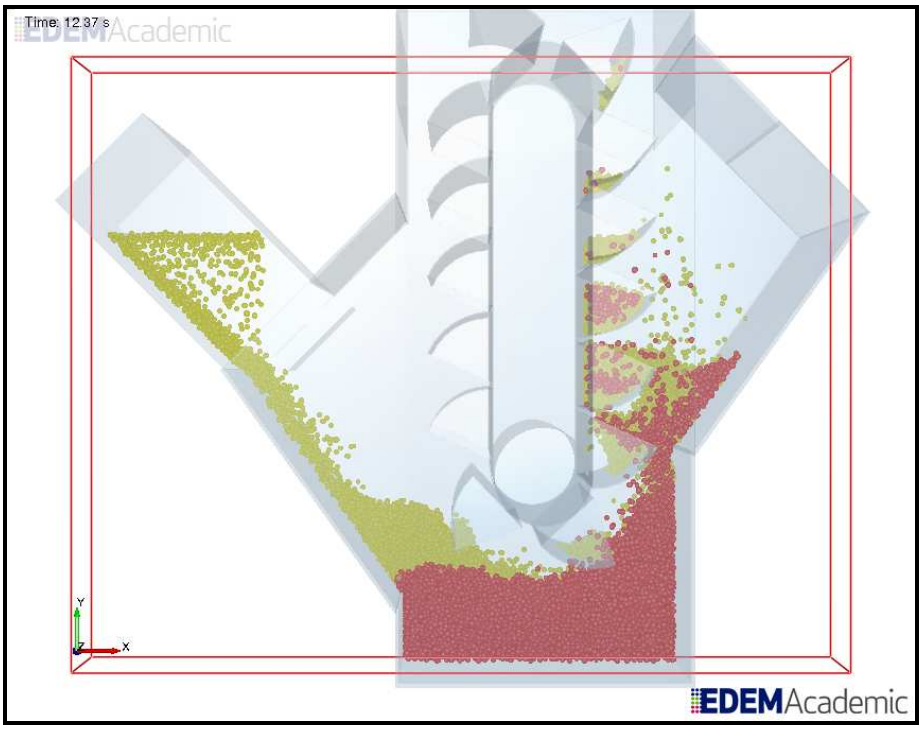

Figure 6.15 Quasi-2D (6d_vib0_gate) model with surge flow increasing the uptake of red and clear soybeans.

Another possible improvement in the model was the reduction of the large gap between the bucket cups and the boot wall. In the actual experiment, the belt of the bucket elevator leg is not rigid and sways away from the boot pulley making the gap between the bucket cups and the boot wall smaller. The smaller gap between bucket cups and boot wall may contribute to a higher bucket cup uptake and grain commingling in the actual experiment.

In the simulation, the belt is rigid thus making this gap wider, enabling some soybeans to slip back to towards the boot bottom without the bucket cup collecting them. This gap, together with the sudden surge of particles after the slide gate was open, was considered in the following simulation (quasi-2D_6d_vib0_gate_gap) with one replication. The original gap in the simulation with rigid belt was reduced to half its size (14.75 mm), which was the measured gap while the bucket cups were moving in the experiment (14.29 – 22.23 mm). Figure 6.16 shows the quasi-2D (6d_vib0_gate) model with reduced gap between bucket cups and boot wall as compared with the original gap.

Accounting for the particle surge and reducing the gap between bucket cups and boot wall better predicted commingling than not including them as in the case of the quasi-2D (6d_vib0) model (Figure 6.17). Including both surge flow and reduced gap (i.e., the quasi-2D (6d_vib0_gate_gap) model) was better in predicting high values of initial commingling than just accounting for surge flow alone (i.e., the quasi-2D (6d_vib0_gate) model) as shown by the average commingling based on the complete simulation time (Figure 6.18). The inclusion of particle surge flow and reduced gap predicted the closest value of average commingling in discrete time with experimental data (Figure 6.19).

Further improvements in the model might be achieved by predicting the effect of different vibration motions in the residual grain mass and height and investigating different particle properties (i.e., soybean material and interaction properties as well as its particle size distribution) in the system. It is expected that the same improvements seen in the quasi-2D model by accounting for the initial particle surge and reducing the gap between the buckets and wall would also occur in the 3D model with these changes, but that has not been attempted.

In general, the quasi-2D (6d) models reduced simulation run time by 29% compared to the 3D model of the pilot-scale boot. It is postulated that a higher reduction in time will be achieved in the full-scale boot using a quasi-2D (6d) model.

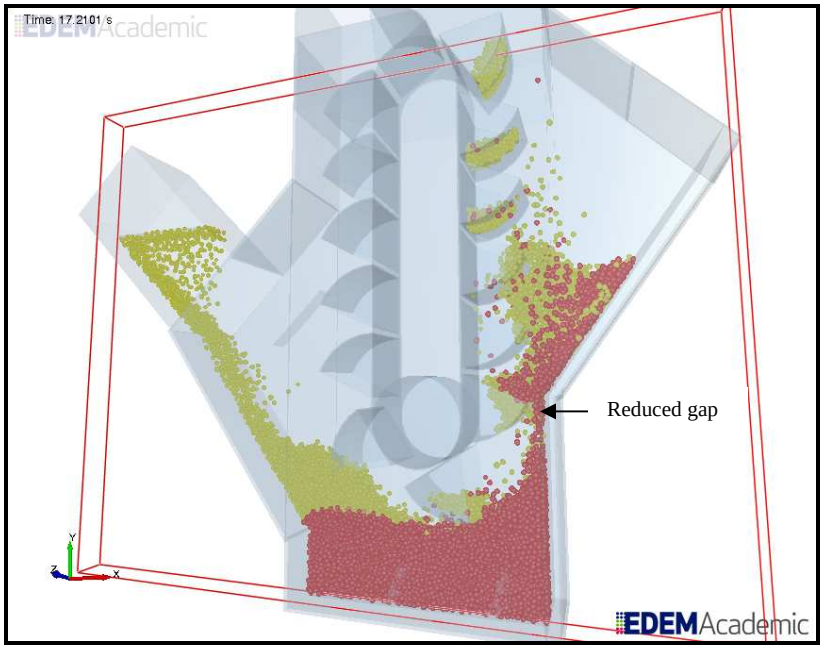

(a)

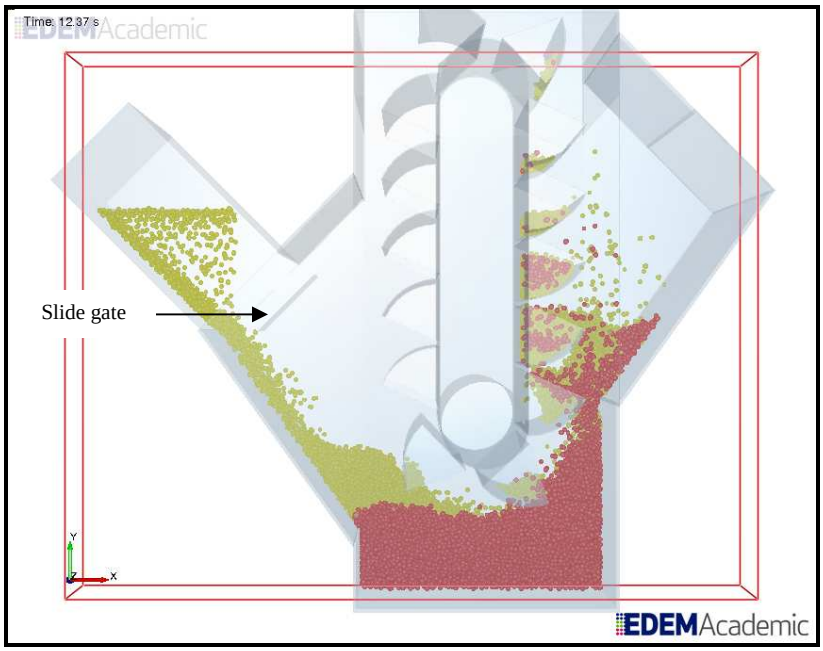

(b)

Figure 6.16 Quasi-2D (6d_vib0_gate_gap) model with (a) reduced gap and (b) original gap between bucket cups and boot wall.

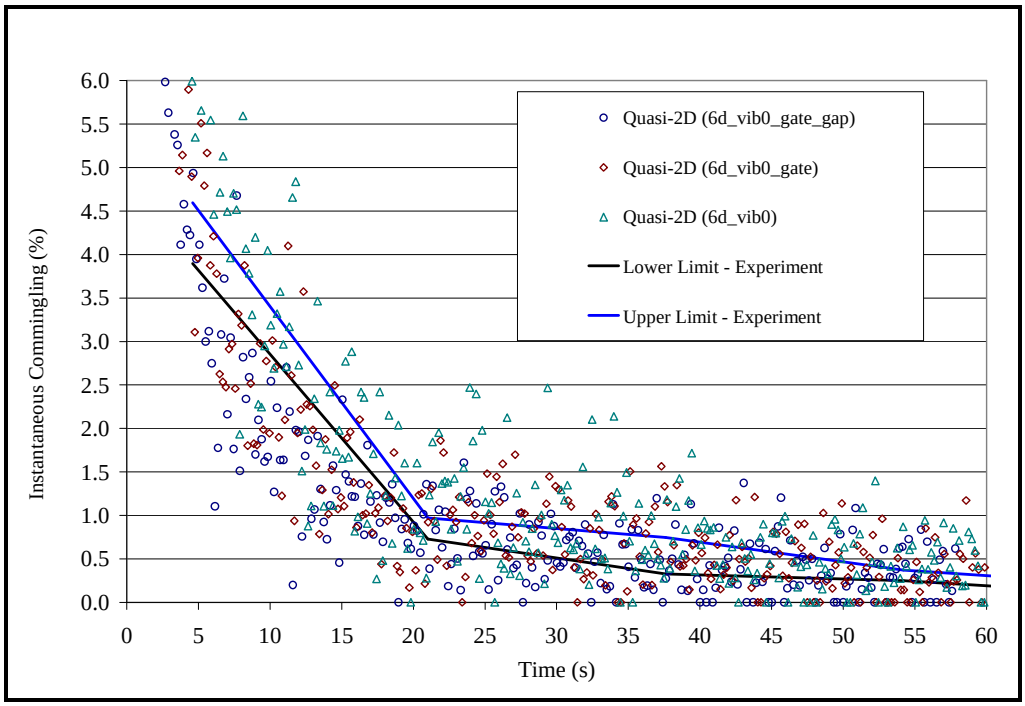

Figure 6.17 Instantaneous commingling from Quasi-2D (6d_vib0_gate) model accounting for particle surge and gap reduction.

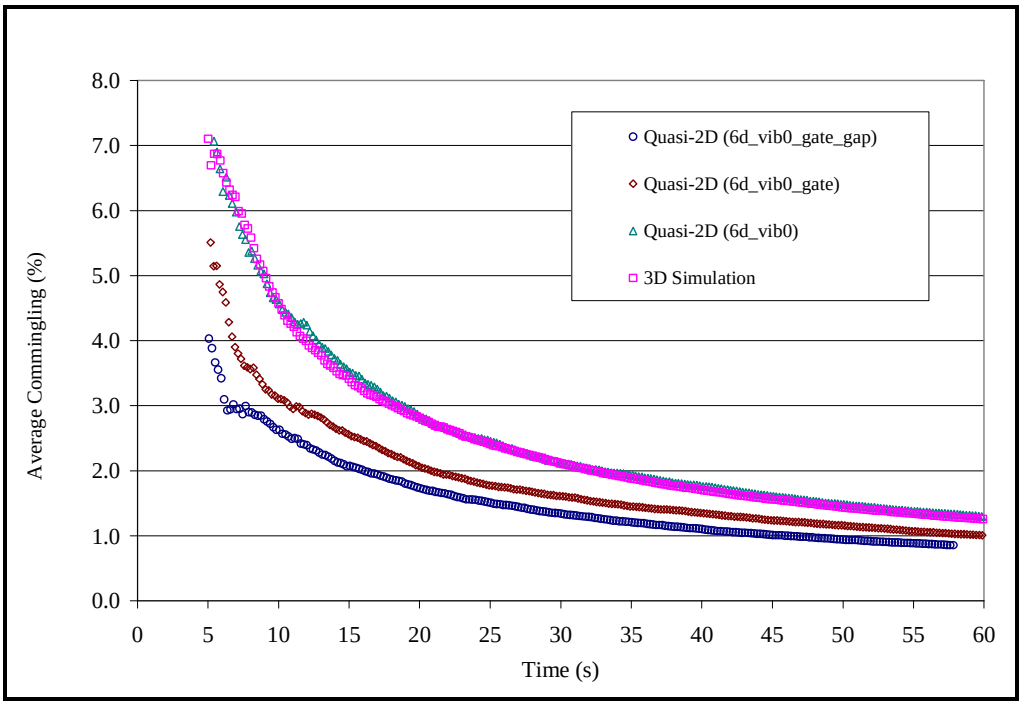

Figure 6.18 Average commingling from Quasi-2D (6d_vib0), Quasi-2D (6d_vib0_gate) with and without reduced gap, and the initial 3D models.

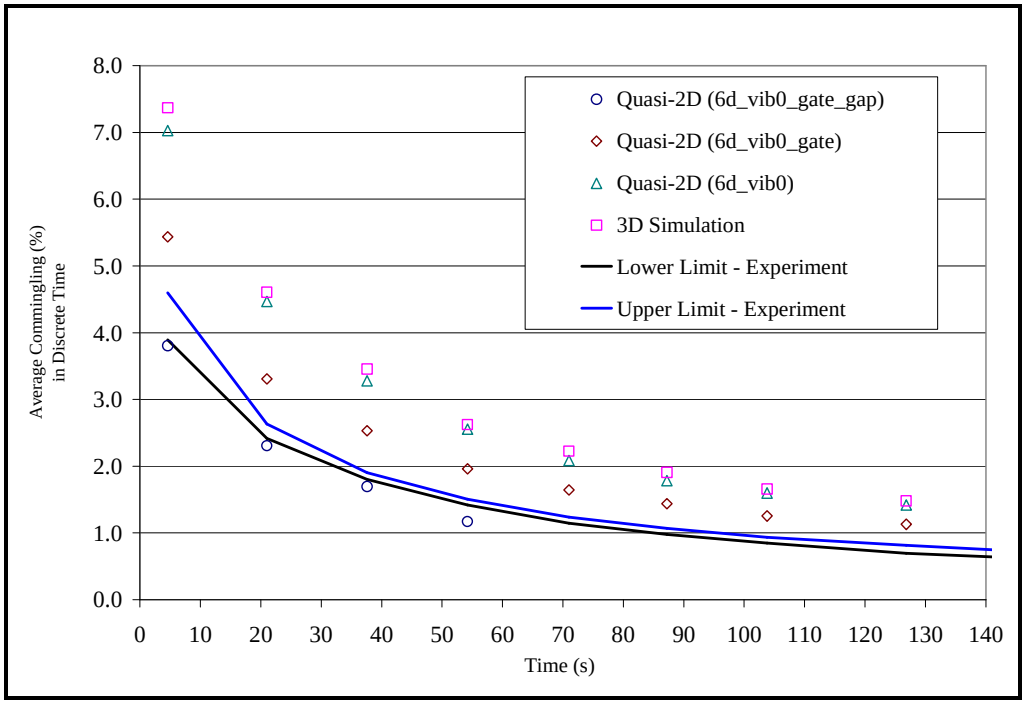

Figure 6.19 Average commingling from Quasi-2D (6d_vib0_gate) with and without reduced gap, and the initial 3D simulations compared at the same discrete time with experiment.

6.6 Summary

Unwanted grain commingling impedes new quality-based grain handling systems and has proven to be an expensive and time consuming issue to study experimentally. To provide a more economical method to study the problem, grain commingling in a pilot-scale bucket elevator boot was modeled in three-dimensional (3D) and quasi-two-dimensional (quasi-2D) discrete element method (DEM) simulations. Experiments on grain commingling were performed to validate the 3D DEM model on a pilot-scale boot.

Experimental data showed that mean instantaneous commingling started at 4.25% during the first 5 s, decreased to 0.85% after 21 s, went to 0.02% after 3.2 min, and reached 0% after 6.7 min. Results from DEM modeling with the initial 3D pilot-scale boot model generally agreed with experimental data after the first 7 s. In the simulation, instantaneous commingling reached 4% later than in the experiments and gradually decreased later than in the experiment.

Comparison of predicted average commingling of four quasi-2D boot models with reduced control volumes (i.e., 4d, 5d, 6d, and 7d) showed the quasi-2D (6d) model provided the best match to the 3D model. Introduction of vibration during the onset of clear soybeans improved the prediction capability of the quasi-2D (6d) model.

The physics of the quasi-2D (6d) model was refined by accounting for the sudden surge of particles during the entrance and reducing the gap between the bucket cups and the boot wall. Inclusion of the particle surge flow and reduced gap better predicted commingling than did the models without those refinements included. Further improvements in the model might be achieved by predicting the effect of different vibration motions in the residual grain mass and height and investigating different particle properties. However, the average commingling in discrete time of the quasi-2D (6d_vib0_gate_gap) model shows that there is little room for additional improvement. This study showed that grain commingling in a bucket elevator boot system can be simulated in 3D and quasi-2D DEM models and gave results that generally agreed with experimental data. The quasi-2D (6d) models reduced simulation run time by 29% compared to the 3D model of the pilot-scale boot. It is postulated that a higher reduction in time will be achieved in the full-scale boot using a quasi-2D (6d) model. Results of this study will be used to accurately predict impurity levels and improve grain handling, which can help farmers

and grain handlers reduce costs during transport and export of grains and make the U.S. grain more competitive in the world market.

6.7 References

Baumeister, T., E. A. Avallone, and T. Baumeister III. 1978. *Marks' Standard Handbook for Mechanical Engineers*. 8th ed. New York: McGraw-Hill Book Co.

Boac, J. M., M. E. Casada, R. G. Maghirang, and J. P. Harner, III. 2009. Material and interaction properties of selected grains and oilseeds for modeling discrete particles. ASABE Paper No. 097166. St. Joseph, Mich.: ASABE.

Boresi, A. P. and R. J. Schmidt. 2003. *Advanced Mechanics of Materials*. 6th ed. New York: Wiley and Sons.

Bucchini, L. and L. R. Goldman. 2002. Starlink corn: a risk analysis. *Environmental Health Perspectives* 110(1): 5-12.

Ciesielski, A. 1999. *An Introduction to Rubber Technology*. United Kingdon: Rapra Technology, Ltd.

Cundall, P. A. 1971. A computer model for simulating progressive large-scale movements in blocky rock systems. In *Proceedings of the Symposium of the International Society of Rock Mechanics*, Vol. 1, Paper No. II-8: 132-150. Nancy, France: International Society of Rock Mechanics.

Cundall, P. A., and O. D. L. Strack. 1979. A discrete numerical model for granular assemblies. *Geotechnique* 29(1):47-65.

DEM Solutions. 2009. *EDEM 2.1.2 User Guide*. Lebanon, N.H.: DEM Solutions (USA), Inc. 138p.

Di Renzo, A., and F. P. Di Maio. 2004. Comparison of contact-force models for the simulation of collisions in DEM-based granular flow codes. *Chemical Engineering Science* 59(3): 525-541.

Di Renzo, A., and F. P. Di Maio. 2005. An improved integral non-linear model for the contact of particles in distinct element simulations. *Chemical Engineering Science* 60(5): 1303-1312.

Fazekas, S., J. Kertesz, and D. E. Wolf. 2005. Piling and avalanches of magnetized particles. *Physical Review E* 71(6): 0613031-0613039.

Fillot, N., I. Iordanoff, and Y. Berthier. 2004. A granular dynamic model for the degradation of material. *Transactions of the ASME, Journal of Tribology* 126(3): 606-614.

Ge, T., Q. Zhang, and M. G. Britton. 2000. Predicting grain consolidation caused by vertical vibration. *Transactions of the ASAE* 43(6): 1747-1753.

Goda, T. J., and F. Ebert. 2005. Three-dimensional discrete element simulations in hoppers and silos. *Powder Technology* 158(1-3): 58-68.

Hart, R., P. A. Cundall, and J. Lemos. 1988. Formulation of a three-dimensional distinct element method, part II: mechanical calculations for motion and interaction of a system composed of many polyhedral blocks. *International Journal of Rock Mechanics and Mining Sciences and Geomechanics Abstracts* 25(3):117-125.

Ingles, M. E. A. 2005. Identity preservation of grain in elevators. Unpublished PhD dissertation. Manhattan, Kansas: Kansas State University Department of Biological and Agricultural Engineering.

Ingles, M. E. A., M. E. Casada, and R. G. Maghirang. 2003. Handling effects on commingling and residual grain in an elevator. *Transactions of the ASAE* 46(6): 1625-1631.

Ingles, M. E. A., M. E. Casada, R. G. Maghirang, T. J. Herrman, and J. P. Harner, III. 2006. Effects of grain-receiving system on commingling in a country elevator. *Applied Engineering in Agriculture* 22(5): 713-721.

Jones, C. J. C., and J. R. Block. 1996. Prediction of ground vibration from freight trains. *Journal of Sound and Vibration* 193(1): 205-213.

Kamrin, K., C. H. Rycroft, and M. Z. Bazant. 2007. The stochastic flow rule: a multi-scale model for granular plasticity. *Modelling and Simulation in Materials Science and Engineering* 15(4): 449-464.

Kawaguchi, T., M. Sakamoto, T. Tanaka, and Y. Tsuji. 2000. Quasi-three-dimensional numerical simulation of spouted beds in cylinder. *Powder Technology* 109(1-3): 3-12.

Ketterhagen, W. R., J. S. Curtis, C. R. Wassgren, and B. C. Hancock. 2008. Modeling granular segregation in flow from quasi-three-dimensional, wedge-shaped hoppers. *Powder Technology* 179(3): 126-143.

Kilman, S., and J. Carroll. 2002. Monsanto says crops may contain genetically-modified canola seed. *The Wall Street Journal*. Available at: http://www.connectotel.com/gmfood/monsanto.html. Accessed 15 May 2008.

Li, Y., Y. Xu, and C. Thornton. 2005. A comparison of discrete element simulations and experiments for 'sandpiles' composed of spherical particles. *Powder Technology* 160(3): 219-228.

Masson, S., and J. Martinez. 2000. Effect of particle mechanical properties on silo flow and stresses from distinct element simulations. *Powder Technology* 109:164-178.

Miller, G. F., and H. Pursey. 1955. On the partition of energy between elastic waves in a semi-infinite solid. *Proceedings of the Royal Society of London Series A: Mathematical and Physical Sciences* 233(1192): 55-69.

Mindlin, R. 1949. Compliance of elastic bodies in contact. *Journal of Applied Mechanics* 16: 259-268.

Mindlin, R. D., and H. Deresiewicz. 1953. Elastic spheres in contact under varying oblique forces. *Transactions of ASME, Series E. Journal of Applied Mechanics* 20: 327-344.

Raji, A. O., and J. F. Favier. 2004a. Model for the deformation in agricultural and food particulate materials under bulk compressive loading using discrete element method, part I: theory, model development and validation. *Journal of Food Engineering* 64:359-371.

Raji, A. O., and J. F. Favier. 2004b. Model for the deformation in agricultural and food particulate materials under bulk compressive loading using discrete element method, part II: compression of oilseeds. *Journal of Food Engineering* 64:373-380.

Remy, B., J. G. Khinast, and B. J. Glasser. 2009. Discrete element simulation of free-flowing grains in a four-bladed mixer. *AIChE Journal* 55(8): 2035-2048.

Samadani, A., and A. Kudrolli. 2001. Angle of repose and segregation in cohesive granular matter. *Physical Review E* 64(5): 513011-513019.

Shimizu, Y., and P. A. Cundall. 2001. Three-dimensional DEM simulations of bulk handling by screw conveyors. *Journal of Engineering Mechanics* 127(9):864-872.

Sudah, O. S., P. E. Arratia, A. Alexander, and F. J. Muzzio. 2005. Simulation and experiments of mixing and segregation in a tote blender. *Journal of American Institute of Chemical Engineers* 51(3): 836-844.

Sykut, J., M. Molenda, and J. Horabik. 2008. DEM simulation of the packing structure and wall load in a 2-dimensional silo. *Granular Matter* 10(4): 273-278.

Takeuchi, S., S. Wang, and M. Rhodes. 2008. Discrete element method simulation of three-dimensional conical-based spouted beds. *Powder Technology* 184(2): 141-150.

Theuerkauf, J., S. Dhodapkar, and K. Jacob. 2007. Modeling granular flow using discrete element method – from theory to practice. *Chemical Engineering* 114(4): 39-46.

Tsuji, Y., T. Tanaka, and T. Ishida. 1992. Lagrangian numerical simulation of plug flow of cohesionless particles in a horizontal pipe. *Powder Technology* 71(3): 239-250.

US FDA. 2006. Strategic Partnership Program Agroterrorism (SPPA) Initiative. First Year Status Report. September 2005 - June 2006. Silver Spring, Md.: U.S. Food and Drug Administration. Available at: http://www.cfsan.fda.gov/~dms/agroter5.html. Accessed 15 May 2007.

USDA GIPSA. 1995. *Grain Inspection Handbook, Book I, Grain Sampling*. Washington, D.C.: USDA Grain Inspection, Packers, and Stockyards Administration, Federal Grain Inspection Service.

USDA GIPSA. 2004. *Grain Inspection Handbook, Book II, Grain Grading Procedures*. Washington, D.C.: USDA Grain Inspection, Packers, and Stockyards Administration, Federal Grain Inspection Service.

Wightman, C., M. Moakher, F. J. Muzzio, and O. R. Walton. 1998. Simulation of flow and mixing of particles in a rotating and rocking cylinder. *Journal of American Institute of Chemical Engineers* 44(6): 1266-1276.

Zhou, Y. C., B. H. Xu, A. B. Yu, and P. Zulli. 2001. Numerical investigation of the angle of repose of monosized spheres. *Physical Review E: Statistical Physics, Plasmas, Fluids, and Related Interdisciplinary Topics* 64(2): 0213011-0213018.

CHAPTER 7 - CONCLUSIONS AND RECOMMENDATIONS

7.1 Conclusions

Experiments were conducted at the research elevator of the USDA-ARS Center for Grain and Animal Health Research to characterize the quality of grain and feed during bucket elevator handling to meet customer demand for high quality and safe products. The following conclusions were drawn from the research:

- Repeated handling did not significantly affect the durability index of the feed pellets, which ranged from 92.0% to 93.4%, nor that of shelled corn, which ranged from 99.6% to 99.8%.
- The feed pellets had significantly greater breakage (3.83% per transfer) than the shelled corn (0.382% per transfer).
- The average mass of dust removed per transfer was 0.069% of the mass of pellets, which was not significantly different from that of shelled corn (0.061%).
- The mass of particulate matter <125 μm was less for feed pellets (50% of pellet dust) than for shelled corn (66% of corn dust).
- The mean mass of dust <125 μm of the pellets (0.337 $kg \cdot t^{-1}$ of pellet mass) was significantly less ($p < 0.05$) than that of shelled corn (0.403 $kg \cdot t^{-1}$ of corn mass), indicating that these pellets produced less dust in the range of 10 to 125 μm during handling than did shelled corn.
- Shelled corn produced significantly smaller dust particles, and a greater proportion of small particles, than wheat. The geometric mean diameter (GMD) of shelled corn dust ranged from 10.0 to 14.4 μm; the geometric standard deviation (GSD) ranged from 2.27 to 2.77. For wheat, GMD ranged from 10.5 to 16.9 μm, and GSD ranged from 2.60 to 2.99. The percentage of PM-2.5, PM-4, and PM-10 generated during the transfer operation were 7.46%, 9.99%, and 28.9%, respectively, of total shelled corn dust and 5.15%, 9.65%, and 33.6%, respectively, of total wheat dust.
- Handling shelled corn produced more than twice as much total generated dust than handling wheat (185 $g \cdot t^{-1}$ of corn handled vs. 64.6 $g \cdot t^{-1}$ of wheat handled).

- For both wheat and shelled corn, at an average grain flow rate of 54.4 $t \cdot h^{-1}$, the size distribution of dust from the upper and lower ducts showed similar trends among grain lots and repeated transfers but differed between the two grain types and also between the two ducts.
- The corn and wheat differed significantly in the dust size distribution and the rate of total dust generated and there were significant differences between the lower and upper ducts, confirming the necessity of sampling from both ducts.
- With discrete element method, a single-sphere particle model best simulated soybean kernels in the bulk property tests. The best particle model included a particle coefficient of restitution of 0.6, particle static friction of 0.45 for soybean-soybean contact (0.30 for soybean-steel interaction), particle rolling friction of 0.05, normal particle size distribution with a standard deviation factor of 0.4, and particle shear modulus of 1.04 MPa.
- Experimental data on soybeans in a pilot-scale boot showed that mean instantaneous commingling started at 4.25% during the first 5 s, decreased to 0.85% after 21 s, went to 0.02% after 3.2 min, and reached 0% after 6.7 min.
- Predicted results from the 3D boot model generally agreed with experimental data after the first 7 s. Instantaneous commingling reached 4% later than in the experiments and also gradually decreased later than in the experiment.
- Comparison of predicted average commingling of four quasi-2D boot models with reduced control volumes (i.e., 4d, 5d, 6d, and 7d) showed the quasi-2D (6d) model provided the best match to the 3D model.
- Introduction of vibration motion during the onset of clear soybeans improved the prediction capability of the quasi-2D (6d) model. Further refinements of the physics of the quasi-2D (6d) model by accounting for the sudden surge of particles during the entrance and reducing the gap between the bucket cups and the boot wall better predicted commingling than did the models without those refinements.
- This study showed that grain commingling in a bucket elevator boot system can be simulated in 3D and quasi-2D DEM models and gave results that generally agreed with experimental data. The quasi-2D (6d) models reduced simulation run time by 29% compared to the 3D model of the pilot-scale boot. Results of this study can be used to

predict impurity levels in grain handling, which can help farmers and grain handlers reduce costs during transport and export of grains and make the U.S. grain more competitive in the world market.

7.2 Recommendations for Further Study

The following are recommended for future studies:

1. Measure and compare dust emitted in grain elevators with and without pneumatic dust control system;
2. Predict the effect of different vibration motions in the residual grain mass and height;
3. Investigate different particle properties (i.e., soybean material and interaction properties as well as its particle size distribution);
4. Develop particle models for other major grains and oilseeds as well as infested grains and insects in stored grains;
5. Model grain commingling in various bucket elevator boot geometries and other bucket elevator equipment; and
6. Apply simulation results to design better elevator boot systems

Appendix A - Supporting Data

Data for Chapter 3

Table A.1 Material flow rate of feed pellets from repeated handling.

Transfer	Bins	Time, min	Initial Mass on Bin Before Transfer, kg	Mass of Samples, kg	Mass of Dust, kg	Material Flow Rate, $t \cdot h^{-1}$
0	truck hopper to bin 8		22579.8	10.8	11.3	
1	bin 8 to bin 2	23.7	22557.7	5.1	14.2	57.2
2	bin 2 to bin 8	19.7	22538.4	4.8	16.2	68.6
3	bin 8 to bin 2	20.9	22517.4	5.1	15.3	64.7
4	bin 2 to bin 8	21.1	22496.9	5.7	15.9	64.0
5	bin 8 to bin 2	20.0	22475.3	5.6	15.1	67.4
6	bin 2 to bin 8	22.7	22454.6	5.7	18.8	59.5
7	bin 8 to bin 2	21.2	22430.0	6.2	11.6	63.4
8	bin 2 to bin 8	25.5	22412.2	5.8	17.8	52.7
Mean		**21.8**	**22495.8**	**6.1**	**15.1**	**62.2**
SD		**2.0**	**57.7**	**1.8**	**2.5**	**5.4**

Table A.2 Initial mass of feed pellet samples from repeated handling.

	Initial Mass, g								
Sample No.	Transfer 0	Transfer 1	Transfer 2	Transfer 3	Transfer 4	Transfer 5	Transfer 6	Transfer 7	Transfer 8
1	795.0	479.6	655.6	596.5	229.4	645.6	768.2	619.5	502.8
2	590.2	571.7	655.1	605.7	549.3	670.1	568.6	666.1	519.0
3	607.5	565.6	488.9	660.1	775.9	702.4	776.8	717.9	599.7
4	612.7	586.1	764.3	660.6	776.8	704.8	816.5	693.3	589.7
5	591.5	589.1	701.1	677.9	777.7	761.3	556.0	732.0	607.9
6	575.6	542.9	726.1	609.3	770.8	742.6	532.1	739.9	646.3
7		575.6	837.6	697.7	528.9	727.9	552.4	691.1	576.4
8		588.6		637.9	604.4	680.4	542.9	640.9	550.8
9		533.6			680.4		611.6	691.5	595.2
10									630.0
11									
12									
Mean	**628.8**	**559.2**	**689.8**	**643.2**	**632.6**	**704.4**	**636.1**	**688.0**	**581.8**
SD	**82.5**	**35.7**	**109.2**	**36.9**	**181.9**	**38.7**	**116.1**	**40.3**	**45.8**

Table A.3 Feed pellet length before durability test.

Transfer	No. of Pellets per 20-g Sample	No. of Pellets per gram	Mean Pellet Length, mm
1-1	56	2.8	11.8
1-2	62	3.1	11.2
1-3	85	4.3	9.0
2-1	74	3.7	9.0
2-2	62	3.1	11.0
2-3	65	3.3	10.7
Mean	**67.3**	**3.4**	**10.5**
SD	**10.5**	**0.5**	**1.2**

Table A.4 Test weight of feed pellets from selected transfers.

	Test Weight, kg·m^{-3}		
Sample No.	**Transfer 0**	**Transfer 4**	**Transfer 8**
1	653.8	661.0	658.9
2	633.2	670.5	664.1
3	638.4	663.4	684.7
4	658.9	669.6	684.7
5	674.4	658.6	710.4
6	633.2	662.3	695.0
7	638.4		684.7
8	628.1		669.2
9	628.1		689.8
10			700.1
Mean	**642.9**	**664.2**	**684.2**
SD	**16.0**	**4.8**	**16.2**

Table A.5 Moisture content (%) of feed pellet samples from repeated handling.

	Moisture Content, %								
Sample No.	**Transfer 0**	**Transfer 1**	**Transfer 2**	**Transfer 3**	**Transfer 4**	**Transfer 5**	**Transfer 6**	**Transfer 7**	**Transfer 8**
1	10.4	10.4	10.0	10.0	10.0	10.4	10.4	10.4	9.6
2	10.4	10.4	10.0	10.0	10.8	10.4	10.4	10.4	9.7
3	10.0	10.0	10.4	10.0	10.4	10.4	10.8	10.4	9.7
4	10.4	10.4	10.4	10.0	10.4	10.8	10.8	10.4	9.8
5	10.8	10.0	10.0	13.6	10.8	10.4	10.4	10.4	9.5
6	10.8	10.0	10.0	7.6	9.6	10.4	10.4	10.4	9.6
7		10.4	10.4	10.4	10.4	10.8	10.8	10.4	9.4
8		10.4		10.8	10.8	10.4	10.4	10.8	9.5
9		10.4			10.4		10.8	10.8	9.4
10									
11									
12									
Mean	**10.5**	**10.3**	**10.2**	**10.3**	**10.4**	**10.5**	**10.6**	**10.5**	**9.6**
SD	**0.3**	**0.2**	**0.2**	**1.6**	**0.4**	**0.2**	**0.2**	**0.2**	**0.2**

Table A.6 Percentage of whole and broken feed pellets from sieving through 5.60-mm sieve.

Transfers	**Whole Pellet (> 5.60 mm), %**	**Broken Pellet (< 5.60 mm), %**	**Change in % Breakage**
0	82.47	17.53	
1	75.05	24.95	7.42
2	67.76	32.24	7.29
3	67.22	32.78	0.543
4	54.32	45.68	12.90
5	55.32	44.68	-0.992
6	55.36	44.64	-0.048
7	49.78	50.22	5.58
8	51.80	48.20	-2.02
Mean	**62.12**	**37.88**	**3.83**
SD	**11.46**	**11.46**	**5.26**

Table A.7 Pellet durability index (PDI) of feed pellet samples from selected transfers.

	Durability Index, %			
Sample No.	Transfer 0	Transfer 1	Transfer 4	Transfer 7
1	92.42	92.09	93.28	96.24
2	92.46	92.22	93.20	91.82
3	94.92	90.09	93.16	92.39
4	93.24	93.78	93.60	93.28
5	91.41			
6	92.08			
Mean	**92.8**	**92.0**	**93.3**	**93.4**
SD	**1.22**	**1.51**	**0.20**	**1.97**

Table A.8 Apparent geometric mean diameter (GMD), geometric standard deviation (GSD), and apparent geometric standard deviation of the particle diameter by mass (GSDw) of feed pellets from repeated handling.

Transfer	Apparent GMD, mm	GSD	Apparent GSDw, mm
0	5.621	1.691	3.092
1	5.011	1.880	3.376
2	4.547	2.004	3.420
3	4.542	1.990	3.380
4	3.709	2.191	3.217
5	3.904	2.098	3.164
6	3.871	2.119	3.188
7	3.603	2.145	3.024
8	3.807	2.087	3.061
Mean	**4.291**	**2.023**	**3.213**
SD	**0.688**	**0.156**	**0.147**

Table A.9 Total collected dust from repeated handling of feed pellets.

Transfer	Total Tailing Dust, kg	Pellets Handled, t	Total Collected Dust, kg/t of pellets
1	14.2	22.6	0.629
2	16.2	22.5	0.718
3	15.3	22.5	0.681
4	15.9	22.5	0.706
5	15.1	22.5	0.674
6	18.8	22.5	0.838
7	11.6	22.4	0.516
8	17.8	22.4	0.793
Mean	**15.6**	**22.5**	**0.694**
SD	**2.2**	**0.1**	**0.099**

Table A.10 Percentage of feed pellet dust <125µm from repeated handling.

	Percentage of Feed Pellet Dust <125µm, %							
Sample No.	**Transfer 1**	**Transfer 2**	**Transfer 3**	**Transfer 4**	**Transfer 5**	**Transfer 6**	**Transfer 7**	**Transfer 8**
1	43.225	48.103	49.083	47.703	48.264	47.625	45.833	48.495
2	45.981	47.951	49.048	48.043	48.411	51.571	45.562	51.765
3	46.076	47.395	48.969	46.526	48.099	51.055	46.104	51.419
4	51.815	47.826	49.573	46.093	48.633	48.172	46.958	49.638
5	51.855	47.348	48.744	46.348	47.702	45.743	45.928	51.843
6	51.051	48.017	47.770	46.932	48.559	48.380	45.185	51.436
7	51.867	47.045	48.751	45.912	47.892	49.436	45.638	53.341
8	52.385	47.463	48.341	45.562	48.366	51.701	45.518	53.447
9	51.686	46.409	48.556	46.484	48.559	50.224	46.071	49.585
Mean	**49.549**	**47.506**	**48.759**	**46.623**	**48.276**	**49.323**	**45.866**	**51.219**
SD	**3.455**	**0.545**	**0.511**	**0.814**	**0.321**	**2.014**	**0.503**	**1.689**

Table A.11 Mass of feed pellet dust <125µm from repeated handling.

	Mass of Feed Pellet Dust <125µm, kg							
Sample No.	**Transfer 1**	**Transfer 2**	**Transfer 3**	**Transfer 4**	**Transfer 5**	**Transfer 6**	**Transfer 7**	**Transfer 8**
1	6.137	7.789	7.525	7.573	7.312	8.965	5.301	8.623
2	6.528	7.765	7.520	7.627	7.334	9.708	5.270	9.204
3	6.542	7.675	7.508	7.386	7.287	9.611	5.333	9.143
4	7.356	7.745	7.600	7.318	7.368	9.068	5.431	8.826
5	7.362	7.667	7.473	7.358	7.227	8.611	5.312	9.218
6	7.248	7.776	7.324	7.451	7.357	9.107	5.226	9.146
7	7.364	7.618	7.474	7.289	7.256	9.306	5.279	9.485
8	7.437	7.686	7.411	7.233	7.327	9.732	5.265	9.503
9	7.338	7.515	7.444	7.380	7.357	9.454	5.329	8.817
Mean	**7.035**	**7.693**	**7.476**	**7.402**	**7.314**	**9.285**	**5.305**	**9.107**
SD	**0.490**	**0.088**	**0.078**	**0.129**	**0.049**	**0.379**	**0.058**	**0.300**

Table A.12 Collected feed pellet dust <125µm from repeated handling.

	Collected Dust <125µm, kg·t^{-1} of pellets handled							
Sample No.	**Transfer 1**	**Transfer 2**	**Transfer 3**	**Transfer 4**	**Transfer 5**	**Transfer 6**	**Transfer 7**	**Transfer 8**
1	0.272	0.346	0.334	0.337	0.325	0.399	0.236	0.385
2	0.289	0.345	0.334	0.339	0.326	0.432	0.235	0.411
3	0.290	0.341	0.333	0.328	0.324	0.428	0.238	0.408
4	0.326	0.344	0.338	0.325	0.328	0.404	0.242	0.394
5	0.326	0.340	0.332	0.327	0.322	0.383	0.237	0.411
6	0.321	0.345	0.325	0.331	0.327	0.406	0.233	0.408
7	0.326	0.338	0.332	0.324	0.323	0.414	0.235	0.423
8	0.330	0.341	0.329	0.322	0.326	0.433	0.235	0.424
9	0.325	0.333	0.331	0.328	0.327	0.421	0.238	0.393
Mean	**0.312**	**0.341**	**0.332**	**0.329**	**0.325**	**0.413**	**0.237**	**0.406**
SD	**0.022**	**0.004**	**0.003**	**0.006**	**0.002**	**0.017**	**0.003**	**0.013**

Table A.13 Material flow rate of corn from repeated handling.

Transfer	**Bins**	**Time, min**	**Initial Mass on Bin Before Transfer, kg**	**Mass of Samples, kg**	**Mass of Dust, kg**	**Material Flow Rate, t·h^{-1}**
0	to bin 9		25306.7	8.0		
1	bin 9 to bin 2	29.2	25298.7	7.7	13.4	52.0
2	bin 2 to bin 9	25.1	25277.7	6.6	20.6	60.5
3	bin 9 to bin 2	28.8	25250.4	7.1	15.0	52.7
4	bin 2 to bin 9	24.2	25228.4	6.6	17.9	62.5
5	bin 9 to bin 2	28.0	25203.9	7.4	13.2	54.1
6	bin 2 to bin 9	23.2	25183.3	6.6	16.8	65.1
7	bin 9 to bin 2	27.8	25159.9	7.2	13.6	54.2
8	bin 2 to bin 9	29.4	25139.2	7.1	13.4	51.4
Mean		**26.9**	**25227.6**	**7.1**	**15.5**	**56.6**
SD		**2.4**	**60.5**	**0.5**	**2.7**	**5.3**

Table A.14 Initial mass of corn samples from repeated handling.

	Initial Mass, g								
Sample No.	**Transfer 0**	**Transfer 1**	**Transfer 2**	**Transfer 3**	**Transfer 4**	**Transfer 5**	**Transfer 6**	**Transfer 7**	**Transfer 8**
1	731.4	553.0	738.0	641.6	730.7	679.6	757.4	662.7	630.6
2	633.3	638.8	722.5	666.5	741.9	691.4	794.4	633.9	690.7
3	741.1	640.3	737.1	642.4	749.6	593.9	776.5	696.8	660.2
4	633.3	602.9	684.9	627.3	784.8	652.3	798.6	706.4	711.1
5	671.0	653.8	705.8	624.6	692.9	700.8	651.0	703.0	610.6
6	630.8	666.4	703.8	644.3	755.6	647.4	668.1	628.6	660.1
7	617.0	635.3	748.0	632.1	707.1	643.9	726.8	647.2	600.6
8	615.9	584.9	677.2	680.1	712.3	685.6	711.1	653.1	638.2
9	623.2	691.8	740.8	665.4	720.2	670.2	732.9	614.5	652.7
10	714.1	695.7		626.5		693.9		602.4	620.6
11	656.6	680.9		618.5		704.9		614.6	599.6
12	707.9	614.3							
Mean	**664.6**	**638.2**	**717.6**	**642.7**	**732.8**	**669.4**	**735.2**	**651.2**	**643.2**
SD	**46.90**	**43.66**	**25.77**	**20.02**	**28.34**	**32.90**	**52.41**	**37.20**	**36.06**

Table A.15 Test weight of corn samples from repeated handling.

	Test Weight, $kg \cdot m^{-3}$								
Sample No.	**Transfer 0**	**Transfer 1**	**Transfer 2**	**Transfer 3**	**Transfer 4**	**Transfer 5**	**Transfer 6**	**Transfer 7**	**Transfer 8**
1	752.12	746.97	735.65	746.97	754.70	759.33	744.40	762.93	741.31
2	759.33	744.40	742.86	756.24	750.58	745.43	752.12	748.52	752.64
3	760.36	751.09	746.46	751.09	745.43	748.52	758.82	750.58	743.89
4	750.58	750.58	748.52	751.09	748.52	745.43	742.86	749.55	741.31
5	751.09	761.90	749.55	746.46	750.58	743.89	740.28	744.40	750.58
6	744.40	757.79	734.62	749.55	742.34	752.64	742.34	742.86	748.00
7	749.55	758.82	748.00	745.43	743.89	748.52	741.31	742.34	741.31
8	751.09	736.16	748.52	745.43	748.52	742.86	754.70	744.40	750.58
9	750.58	742.86	751.09	745.43	748.52	744.40	760.87	750.58	742.34
10	751.09	742.86		742.86		751.09		748.52	751.09
11	746.97	742.86		749.55		743.89		744.40	752.64
12	752.12	729.99							
Mean	**751.61**	**747.19**	**745.03**	**748.19**	**748.12**	**747.82**	**748.63**	**748.10**	**746.88**
SD	**4.44**	**9.40**	**6.06**	**3.76**	**3.78**	**4.96**	**8.04**	**5.80**	**4.85**

Table A.16 Broken corn and foreign material (BCFM) of corn samples from repeated handling.

	Broken Corn and Foreign Material (BCFM), %								
Sample No.	**Transfer 0**	**Transfer 1**	**Transfer 2**	**Transfer 3**	**Transfer 4**	**Transfer 5**	**Transfer 6**	**Transfer 7**	**Transfer 8**
1	2.72	2.80	4.18	2.88	5.44	4.18	4.20	6.82	3.87
2	2.61	3.33	4.04	5.37	3.78	5.08	4.61	6.20	4.73
3	2.99	4.02	5.50	5.71	4.52	5.14	3.88	7.43	4.08
4	2.83	3.07	6.69	4.13	4.06	5.64	7.28	5.84	4.28
5	3.46	3.86	4.60	5.97	4.22	4.95	4.68	5.89	5.57
6	2.79	4.69	3.95	5.39	3.03	4.43	4.02	5.89	6.14
7	3.08	11.74	6.45	5.76	5.38	5.33	4.48	6.40	6.22
8	3.78	5.39	4.97	4.92	5.64	5.12	6.77	5.94	4.98
9	3.14	4.65	6.09	5.64	7.05	4.74	7.25	4.81	7.91
10	3.55	5.28		5.40		7.91		6.52	9.42
11	3.37	4.38		4.91		4.57		7.14	10.80
12	3.22	4.95							
Mean	**3.13**	**4.85**	**5.16**	**5.10**	**4.79**	**5.19**	**5.24**	**6.26**	**6.18**
SD	**0.36**	**2.33**	**1.06**	**0.90**	**1.21**	**1.00**	**1.43**	**0.72**	**2.28**

Table A.17 Moisture content (%) of corn samples from repeated handling.

	Moisture Content, %								
Sample No.	**Transfer 0**	**Transfer 1**	**Transfer 2**	**Transfer 3**	**Transfer 4**	**Transfer 5**	**Transfer 6**	**Transfer 7**	**Transfer 8**
1	12.7	12.9	12.7	12.8	12.8	12.8	12.3	12.1	12.2
2	12.6	12.6	12.7	12.8	12.8	12.8	12.3	12.1	12.2
3	12.6	12.8	12.6	12.6	12.8	12.8	12.2	12.0	12.4
4	12.7	12.8	12.6	12.7	12.8	13.0	12.0	12.1	12.3
5	12.7	12.5	12.7	12.8	12.8	12.9	12.1	12.0	12.3
6	12.7	12.9	12.7	12.8	12.8	12.8	12.1	12.1	12.3
7	12.7	12.7	12.7	12.8	12.9	12.9	12.2	12.2	12.2
8	12.6	12.9	12.7	12.8	12.9	12.8	12.2	12.2	12.3
9	12.6	12.8	12.7	12.8	12.8	12.8	12.1	12.3	12.4
10	12.7	12.7		12.8		12.8		12.3	12.3
11	12.6	12.6		12.8		12.7		12.2	12.2
12	12.7	12.7							
Mean	**12.6**	**12.7**	**12.7**	**12.8**	**12.8**	**12.8**	**12.2**	**12.2**	**12.3**
SD	**0.045**	**0.125**	**0.040**	**0.058**	**0.040**	**0.065**	**0.100**	**0.107**	**0.061**

Table A.18 Percentage of broken corn that passed through 4.76-mm (12/64-in.) round-hole sieve.

	Broken Corn (< 4.76-mm), %								
Sample No.	**Transfer 0**	**Transfer 1**	**Transfer 2**	**Transfer 3**	**Transfer 4**	**Transfer 5**	**Transfer 6**	**Transfer 7**	**Transfer 8**
1	2.72	2.80	4.18	2.88	5.44	4.18	4.20	6.82	3.87
2	2.61	3.33	4.04	5.37	3.78	5.08	4.61	6.20	4.73
3	2.99	4.02	5.50	5.71	4.52	5.14	3.88	7.43	4.08
4	2.83	3.07	6.69	4.13	4.06	5.64	7.28	5.84	4.28
5	3.46	3.86	4.60	5.97	4.22	4.95	4.68	5.89	5.57
6	2.79	4.69	3.95	5.39	3.03	4.43	4.02	5.89	6.14
7	3.08	11.74	6.45	5.76	5.38	5.33	4.48	6.40	6.22
8	3.78	5.39	4.97	4.92	5.64	5.12	6.77	5.94	4.98
9	3.14	4.65	6.09	5.64	7.05	4.74	7.25	4.81	7.91
10	3.55	5.28		5.40		7.91		6.52	9.42
11	3.37	4.38		4.91		4.57		7.14	10.80
12	3.22	4.95							
Mean	**3.13**	**4.85**	**5.16**	**5.10**	**4.79**	**5.19**	**5.24**	**6.26**	**6.18**
SD	**0.36**	**2.33**	**1.06**	**0.90**	**1.21**	**1.00**	**1.43**	**0.72**	**2.28**

Table A.19 Percentage of whole corn on top of the 4.76-mm (12/64-in.) round-hole sieve.

	Whole Corn (> 4.76-mm), %								
Sample No.	**Transfer 0**	**Transfer 1**	**Transfer 2**	**Transfer 3**	**Transfer 4**	**Transfer 5**	**Transfer 6**	**Transfer 7**	**Transfer 8**
1	97.28	97.20	95.82	97.12	94.56	95.82	95.80	93.18	96.13
2	97.39	96.67	95.96	94.63	96.22	94.92	95.39	93.80	95.27
3	97.01	95.98	94.50	94.29	95.48	94.86	96.12	92.57	95.92
4	97.17	96.93	93.31	95.87	95.94	94.36	92.72	94.16	95.72
5	96.54	96.14	95.40	94.03	95.78	95.05	95.32	94.11	94.43
6	97.21	95.31	96.05	94.61	96.97	95.57	95.98	94.11	93.86
7	96.92	88.26	93.55	94.24	94.62	94.67	95.52	93.60	93.78
8	96.22	94.61	95.03	95.08	94.36	94.88	93.23	94.06	95.02
9	96.86	95.35	93.91	94.36	92.95	95.26	92.75	95.19	92.09
10	96.45	94.72		94.60		92.09		93.48	90.58
11	96.63	95.62		95.09		95.43		92.86	89.20
12	96.78	95.05							
Mean	**96.87**	**95.15**	**94.84**	**94.90**	**95.21**	**94.81**	**94.76**	**93.74**	**93.82**
SD	**0.36**	**2.33**	**1.06**	**0.90**	**1.21**	**1.00**	**1.43**	**0.72**	**2.28**

Table A.20 Percentage of whole and broken corn.

Transfers	Whole Corn (> 4.76-mm), %	Broken Corn (< 4.76-mm), %	Change in % Breakage
0	96.87	3.13	
1	95.15	4.85	1.72
2	94.84	5.16	0.315
3	94.90	5.10	-0.066
4	95.21	4.79	-0.308
5	94.81	5.19	0.401
6	94.76	5.24	0.051
7	93.74	6.26	1.02
8	93.82	6.18	-0.079
Mean	**94.90**	**5.10**	**0.382**
SD	**0.91**	**0.91**	**0.676**

Table A.21 Durability index of corn samples from selected transfers.

	Durability Index, %			
Sample No.	Transfer 0	Transfer 1	Transfer 4	Transfer 7
1	99.72	99.62	99.58	99.52
2	99.80	99.68	99.76	99.62
3	99.70	99.64	99.64	99.50
4	99.82	99.80	99.60	99.62
Mean	**99.8**	**99.7**	**99.6**	**99.6**
SD	**0.059**	**0.080**	**0.079**	**0.064**

Table A.22 Apparent geometric mean diameter (GMD) of corn samples from repeated handling.

	Apparent GMD, mm								
Sample No.	Transfer 0	Transfer 1	Transfer 2	Transfer 3	Transfer 4	Transfer 5	Transfer 6	Transfer 7	Transfer 8
1	6.97	6.82	6.59	6.84	6.62	6.99	6.79	6.71	6.67
2	6.95	6.96	6.74	6.64	6.71	6.25	6.76	6.37	6.64
3	6.99	6.83	6.87	6.58	6.75	6.74	6.82	6.35	6.74
4	6.93	6.88	6.68	6.88	6.68	6.68	6.63	6.72	6.73
5	6.80	6.92	6.61	6.86	6.80	6.60	6.52	6.60	6.63
6	6.87	6.86	6.87	6.55	6.65	6.69	6.76	6.74	6.64
7	6.95	6.21	6.88	6.77	6.66	6.73	6.46	6.63	6.64
8	6.81	6.64	6.82	6.54	6.81	6.53	6.75	6.70	6.43
9	6.88	6.69	6.74	6.76	6.58	6.55	6.63	6.61	6.35
10	6.93	6.44		6.44		6.45		6.53	6.43
11	6.90	6.61		6.56		6.59		6.48	6.29
12	6.98	6.48							
Mean	**6.91**	**6.69**	**6.75**	**6.67**	**6.70**	**6.62**	**6.68**	**6.58**	**6.56**
SD	**0.06**	**0.23**	**0.11**	**0.15**	**0.08**	**0.19**	**0.13**	**0.14**	**0.16**

Table A.23 Geometric standard deviation (GSD) of corn samples from repeated handling.

	GSD								
Sample No.	**Transfer 0**	**Transfer 1**	**Transfer 2**	**Transfer 3**	**Transfer 4**	**Transfer 5**	**Transfer 6**	**Transfer 7**	**Transfer 8**
1	1.26	1.31	1.33	1.33	1.32	1.32	1.31	1.37	1.37
2	1.26	1.30	1.30	1.44	1.32	1.57	1.28	1.53	1.32
3	1.24	1.27	1.25	1.45	1.28	1.34	1.30	1.48	1.28
4	1.26	1.34	1.31	1.31	1.30	1.35	1.33	1.33	1.31
5	1.30	1.28	1.35	1.35	1.32	1.41	1.38	1.37	1.33
6	1.30	1.32	1.28	1.41	1.35	1.33	1.29	1.32	1.35
7	1.29	1.58	1.27	1.32	1.34	1.34	1.40	1.32	1.33
8	1.34	1.34	1.31	1.37	1.31	1.36	1.34	1.30	1.41
9	1.31	1.35	1.35	1.31	1.38	1.38	1.42	1.35	1.45
10	1.27	1.38		1.40		1.37		1.34	1.43
11	1.29	1.34		1.33		1.34		1.40	1.48
12	1.29	1.41							
Mean	**1.28**	**1.35**	**1.31**	**1.37**	**1.32**	**1.38**	**1.34**	**1.37**	**1.37**
SD	**0.03**	**0.08**	**0.03**	**0.05**	**0.03**	**0.07**	**0.05**	**0.07**	**0.06**

Table A.24 Apparent geometric standard deviation (GSDw) of corn samples from repeated handling.

	Apparent GSD, mm								
Sample No.	**Transfer 0**	**Transfer 1**	**Transfer 2**	**Transfer 3**	**Transfer 4**	**Transfer 5**	**Transfer 6**	**Transfer 7**	**Transfer 8**
1	1.61	1.84	1.90	1.97	1.85	1.96	1.86	2.15	2.14
2	1.62	1.82	1.80	2.48	1.91	2.94	1.71	2.78	1.88
3	1.51	1.62	1.57	2.50	1.70	2.01	1.81	2.55	1.68
4	1.60	2.02	1.85	1.90	1.78	2.06	1.93	1.96	1.83
5	1.80	1.75	1.99	2.07	1.89	2.31	2.15	2.09	1.89
6	1.83	1.94	1.72	2.28	2.01	1.95	1.73	1.88	2.01
7	1.77	2.96	1.67	1.88	1.98	2.00	2.20	1.89	1.92
8	2.01	1.95	1.87	2.08	1.84	2.06	1.99	1.78	2.23
9	1.88	2.02	2.05	1.87	2.13	2.16	2.37	2.02	2.41
10	1.67	2.11		2.23		2.08		1.94	2.34
11	1.75	1.96		1.91		1.98		2.24	2.54
12	1.78	2.26							
Mean	**1.74**	**2.02**	**1.83**	**2.11**	**1.90**	**2.14**	**1.97**	**2.12**	**2.08**
SD	**0.14**	**0.34**	**0.15**	**0.23**	**0.13**	**0.29**	**0.23**	**0.30**	**0.27**

Table A.25 Total collected dust from repeated handling of corn.

Transfer	**Total Tailing Dust, kg**	**Corn Handled, t**	**Total Collected Dust, kg·t^{-1} of corn handled**
1	13.4	25.3	0.529
2	20.6	25.3	0.816
3	15.0	25.3	0.593
4	17.9	25.2	0.710
5	13.2	25.2	0.522
6	16.8	25.2	0.666
7	13.6	25.2	0.541
8	13.4	25.1	0.532
Mean	**15.5**	**25.2**	**0.614**
SD	**2.7**	**0.1**	**0.108**

Table A.26 Percentage of corn dust <125µm from repeated handling.

	Percent Corn Dust <125µm, %							
Sample No.	**Transfer 1**	**Transfer 2**	**Transfer 3**	**Transfer 4**	**Transfer 5**	**Transfer 6**	**Transfer 7**	**Transfer 8**
1	73.626	59.703	67.994	65.466	78.326	68.024	72.042	56.239
2	77.264	57.860	62.322	65.274	71.177	62.290	67.476	60.210
3	68.939	60.331	68.007	60.993	71.962	71.670	62.477	59.557
4	69.960	60.603	69.932	63.728	74.406	67.904	65.213	57.358
5	66.267	57.414	63.350	65.109	77.045	68.436	71.220	54.716
6	78.093	59.279	68.803	64.693	74.503	66.576	69.130	50.846
7	66.097	53.659	60.436	64.972	76.560	61.905	70.211	59.853
8	68.168	58.941	71.145	61.657	75.304	69.003	64.226	60.952
9	68.391	58.308	70.059	60.627	76.023	75.554	73.699	63.193
Mean	**70.756**	**58.455**	**66.894**	**63.613**	**75.034**	**67.929**	**68.411**	**58.103**
SD	**4.507**	**2.094**	**3.850**	**1.970**	**2.325**	**4.235**	**3.818**	**3.738**

Table A.27 Mass of corn dust <125µm from repeated handling.

	Mass of Corn Dust <125µm, kg							
Sample No.	**Transfer 1**	**Transfer 2**	**Transfer 3**	**Transfer 4**	**Transfer 5**	**Transfer 6**	**Transfer 7**	**Transfer 8**
1	9.852	12.322	10.178	11.729	10.303	11.416	9.803	7.525
2	10.339	11.941	9.329	11.695	9.363	10.454	9.182	8.057
3	9.225	12.451	10.180	10.928	9.466	12.028	8.502	7.969
4	9.361	12.508	10.468	11.418	9.787	11.396	8.874	7.675
5	8.867	11.849	9.483	11.666	10.135	11.486	9.691	7.322
6	10.450	12.234	10.299	11.591	9.800	11.173	9.407	6.804
7	8.844	11.074	9.046	11.641	10.071	10.389	9.554	8.009
8	9.122	12.165	10.649	11.047	9.906	11.581	8.740	8.156
9	9.151	12.034	10.487	10.863	10.000	12.680	10.029	8.456
Mean	**9.468**	**12.064**	**10.013**	**11.398**	**9.870**	**11.400**	**9.309**	**7.775**
SD	**0.603**	**0.432**	**0.576**	**0.353**	**0.306**	**0.711**	**0.520**	**0.500**

Table A.28 Collected corn dust <125µm during repeated handling.

	Collected Dust <125µm, $kg \cdot t^{-1}$ of corn handled							
Sample No.	**Transfer 1**	**Transfer 2**	**Transfer 3**	**Transfer 4**	**Transfer 5**	**Transfer 6**	**Transfer 7**	**Transfer 8**
1	0.389	0.487	0.403	0.465	0.409	0.453	0.390	0.299
2	0.409	0.472	0.369	0.464	0.371	0.415	0.365	0.320
3	0.365	0.493	0.403	0.433	0.376	0.478	0.338	0.317
4	0.370	0.495	0.415	0.453	0.388	0.453	0.353	0.305
5	0.350	0.469	0.376	0.462	0.402	0.456	0.385	0.291
6	0.413	0.484	0.408	0.459	0.389	0.444	0.374	0.271
7	0.350	0.438	0.358	0.461	0.400	0.413	0.380	0.319
8	0.361	0.481	0.422	0.438	0.393	0.460	0.347	0.324
9	0.362	0.476	0.415	0.431	0.397	0.504	0.399	0.336
Mean	**0.374**	**0.477**	**0.397**	**0.452**	**0.392**	**0.453**	**0.370**	**0.309**
SD	**0.024**	**0.017**	**0.023**	**0.014**	**0.012**	**0.028**	**0.021**	**0.020**

Data for Chapter 4

Table A.29 Material flow rate of wheat during handling.[a]

Transfer	Grain Lot	Time, min	Initial Mass on Bin Before Transfer, kg	Mass of Dust, kg	Material Flow Rate, $t \cdot h^{-1}$
1	1	38.2	28217.7	2.5	44.3
1	2	36.0	28217.7	1.5	47.0
1	3	31.5	28638.8	2.5	54.6
1	4	30.2	28638.8	1.1	56.9
2	1	30.0	28217.7	3.6	56.4
2	2	30.3	28217.7	2.2	55.9
2	3	30.3	27796.5	0.6	55.1
2	4	35.7	28217.7	1.9	47.4
Mean		**32.8**	**28270.3**	**2.0**	**52.2**
SD		**3.3**	**269.9**	**0.9**	**5.1**

[a] Material mass was measured using in-line weighing scale.

Table A.30 Mass concentration of wheat dust collected from lower duct (set A).

		Mass Concentration, $mg \cdot m^{-3}$				
Transfer	Grain Lot	Sample 1	Sample 2	Sample 3	Mean	SD
1	1	169.0	44.3	37.5	83.6	74.1
1	2	24.1	32.9	39.8	32.3	7.9
1	3	25.1	61.6	56.7	47.8	19.8
1	4	49.2	70.8	55.3	58.4	11.1
2	1	171.2	79.2	64.3	104.9	57.9
2	2	33.5	68.0	42.2	47.9	18.0
2	3	44.3	47.8	39.2	43.8	4.3
2	4	37.1	31.2	39.4	35.9	4.2

Table A.31 Mass concentration of wheat dust collected from upper duct (set B).

		Mass Concentration, $mg \cdot m^{-3}$				
Transfer	Grain Lot	Sample 1	Sample 2	Sample 3	Mean	SD
1	1	145.6	108.7	92.2	115.5	27.3
1	2	50.2	97.0	67.4	71.5	23.7
1	3	85.9	109.4	115.0	103.5	15.4
1	4	99.4	108.9	100.4	102.9	5.2
2	1	233.5	139.1	152.4	175.0	51.1
2	2	88.9	146.5	129.4	121.6	29.6
2	3	102.2	109.4	137.4	116.4	18.6
2	4	98.0	116.9	108.7	107.8	9.5

Table A.32 Mass flow rate of wheat dust – lower duct (set A).

		Dust Mass Flowrate, g·s^{-1}				
Transfer	Grain Lot	Sample 1	Sample 2	Sample 3	Mean	SD
1	1	1.09	0.28	0.24	0.54	0.48
1	2	0.16	0.21	0.26	0.21	0.05
1	3	0.16	0.40	0.36	0.31	0.13
1	4	0.32	0.46	0.36	0.38	0.07
2	1	1.10	0.51	0.41	0.67	0.37
2	2	0.22	0.44	0.27	0.31	0.12
2	3	0.28	0.31	0.25	0.28	0.03
2	4	0.24	0.20	0.25	0.23	0.03

Table A.33 Mass flow rate of wheat dust – from upper duct (set B).

		Dust Mass Flowrate, g·s^{-1}				
Transfer	Grain Lot	Sample 1	Sample 2	Sample 3	Mean	SD
1	1	0.73	0.54	0.46	0.58	0.14
1	2	0.25	0.49	0.34	0.36	0.12
1	3	0.43	0.55	0.58	0.52	0.08
1	4	0.50	0.54	0.50	0.51	0.03
2	1	1.17	0.70	0.76	0.88	0.26
2	2	0.44	0.73	0.65	0.61	0.15
2	3	0.51	0.55	0.69	0.58	0.09
2	4	0.49	0.58	0.54	0.54	0.05

Table A.34 Geometric mean diameter (GMD) of wheat dust collected from lower duct (set A).

		Geometric Mean Diameter, µm							
Transfer	Grain Lot	Sample 1	Sample 2	Sample 3	Sample 4	Sample 5	Sample 6	Mean	SD
1	1	10.7	10.8	13.6	13.6	14.6	14.0	12.9	1.7
1	2	12.2	12.7	13.3	13.1	15.4	15.0	13.6	1.3
1	3	14.3	15.0	14.2	14.1	14.2	14.4	14.4	0.3
1	4	14.2	14.9	14.1	14.5	18.4	18.3	15.7	2.0
2	1	11.9	12.1	13.8	13.7	15.6	16.2	13.9	1.8
2	2	17.2	17.8	13.4	13.3	15.8	15.6	15.5	1.9
2	3	15.9	15.6	16.7	15.4	15.0	17.3	16.0	0.8
2	4	15.8	15.6	21.9	17.9	15.1	14.8	16.9	2.7

Table A.35 Geometric mean diameter (GMD) of wheat dust collected from upper duct (set B).

		Geometric Mean Diameter, µm								
Transfer	Grain Lot	Sample 1	Sample 2	Sample 3	Sample 4	Sample 5	Sample 6	Sample 7	Mean	SD
1	1	17.1	17.3	11.4	11.2	8.7	10.3		12.7	3.6
1	2	12.3	12.9	11.5	11.5	8.4	8.3	8.3	10.5	2.0
1	3	13.1	13.2	16.4	14.7	10.0	9.6		12.8	2.6
1	4	13.2	13.2	12.2	12.0	10.1	9.6		11.7	1.6
2	1	13.1	13.4	14.3	14.8	10.6	10.8		12.8	1.8
2	2	13.0	14.0	10.7	10.9	11.0	11.4		11.8	1.4
2	3	13.2	13.0	12.7	12.5	11.5	11.9		12.5	0.7
2	4	14.7	15.0	13.0	12.8	13.0	13.6		13.7	0.9

Table A.36 Geometric standard deviation (GSD) of wheat dust collected from lower duct (set A).

		Geometric Standard Deviation							
Transfer	**Grain Lot**	**Sample 1**	**Sample 2**	**Sample 3**	**Sample 4**	**Sample 5**	**Sample 6**	**Mean**	**SD**
1	1	2.43	2.44	2.79	2.93	3.05	2.92	2.76	0.26
1	2	2.45	2.50	2.90	2.86	2.90	2.83	2.74	0.21
1	3	2.85	2.98	2.86	2.84	2.76	2.79	2.84	0.08
1	4	2.73	2.86	2.75	2.82	3.01	3.05	2.87	0.13
2	1	2.61	2.65	2.81	2.81	2.88	3.00	2.79	0.14
2	2	3.03	3.09	2.80	2.79	2.96	2.94	2.93	0.12
2	3	2.99	2.94	3.12	2.90	2.82	3.15	2.99	0.13
2	4	2.91	2.87	3.57	2.99	2.83	2.74	2.99	0.30

Table A.37 Geometric standard deviation (GSD) of wheat dust collected from upper duct (set B).

		Geometric Standard Deviation								
Transfer	**Grain Lot**	**Sample 1**	**Sample 2**	**Sample 3**	**Sample 4**	**Sample 5**	**Sample 6**	**Sample 7**	**Mean**	**SD**
1	1	3.00	3.07	2.67	2.65	2.29	2.83		2.75	0.28
1	2	2.82	2.97	2.85	2.85	2.23	2.22	2.22	2.60	0.35
1	3	3.04	3.07	3.37	3.05	2.62	2.50		2.94	0.32
1	4	2.99	3.00	2.78	2.78	2.54	2.39		2.75	0.24
2	1	3.21	3.25	3.09	3.22	2.56	2.55		2.98	0.33
2	2	3.05	3.31	2.67	2.72	2.58	2.63		2.83	0.29
2	3	2.92	2.84	2.86	2.82	2.64	2.72		2.80	0.10
2	4	3.00	3.07	2.84	2.78	2.71	2.80		2.86	0.14

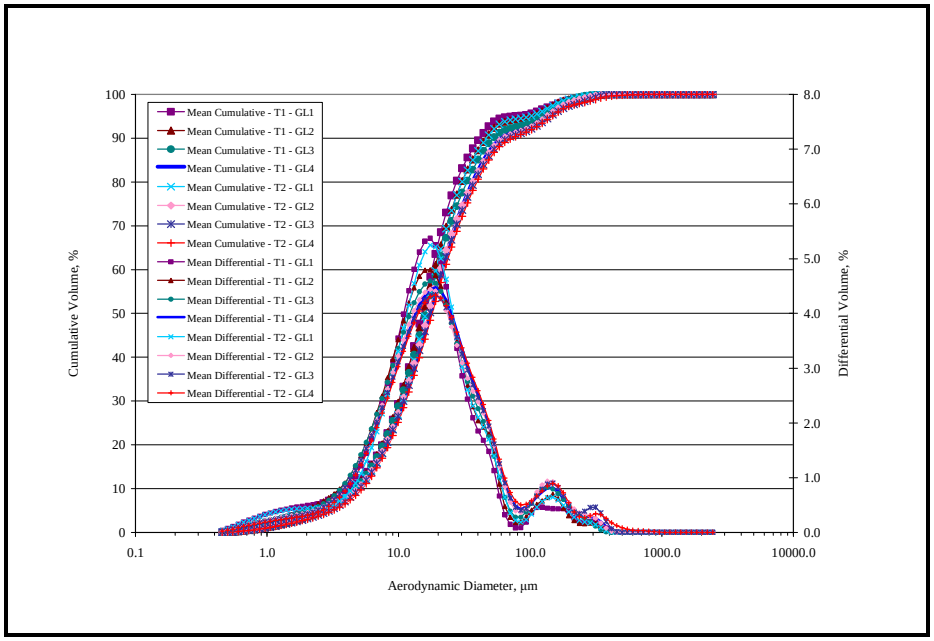

Figure A.1 Mean cumulative and mean differential volume percentages for the particle size distribution of wheat dust collected from the lower duct (set A) during Transfers 1 and 2 (T1, T2) on Grain Lots 1 to 4 (GL1 to GL4).

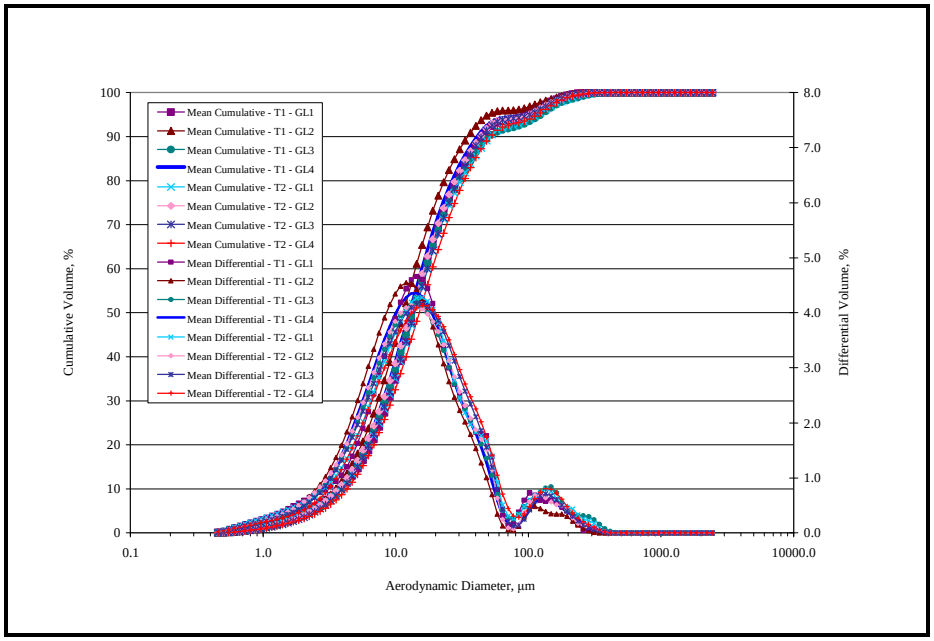

Figure A.2 Mean cumulative and mean differential volume percentages for the particle size distribution of wheat dust collected from the upper duct (set B) during Transfers 1 and 2 (T1, T2) on Grain Lots 1 to 4 (GL1 to GL4).

Table A.38 Percentage of particulate matter of the total wheat dust (% PM) from the lower duct (set A).

Transfer	Grain Lot	% PM 2.5	% PM 4.0	% PM 10
1	1	6.25	9.51	29.7
1	2	4.75	8.51	30.0
1	3	4.54	8.13	29.2
1	4	4.14	7.37	26.6
2	1	5.91	8.71	27.2
2	2	4.38	7.64	27.6
2	3	4.05	7.32	26.9
2	4	3.82	6.79	25.5
	Mean	**4.73**	**8.00**	**27.8**
	SD	**0.89**	**0.89**	**1.6**

Table A.39 Percentage of particulate matter of the total wheat dust (% PM) from the upper duct (set B).

Transfer	Grain Lot	% PM 2.5	% PM 4.0	% PM 10
1	1	6.18	10.7	35.2
1	2	5.84	12.2	43.6
1	3	5.27	10.6	37.3
1	4	5.11	10.7	39.0
2	1	6.02	10.9	35.4
2	2	5.56	11.3	38.8
2	3	4.95	10.2	36.1
2	4	4.46	9.0	32.8
	Mean	**5.42**	**10.7**	**37.3**
	SD	**0.59**	**0.9**	**3.3**

Table A.40 Material flow rate of corn during handling. [a]

Transfer	Bins	Time, min	Initial Mass on Bin Before Transfer, kg	Mass of Samples, kg	Mass of Dust, kg	Material Flow Rate, $t \cdot h^{-1}$
0	to bin 9		25306.7	8.0		
1	bin 9 to bin 2	29.2	25298.7	7.7	13.4	52.0
2	bin 2 to bin 9	25.1	25277.7	6.6	20.6	60.5
3	bin 9 to bin 2	28.8	25250.4	7.1	15.0	52.7
4	bin 2 to bin 9	24.2	25228.4	6.6	17.9	62.5
5	bin 9 to bin 2	28.0	25203.9	7.4	13.2	54.1
6	bin 2 to bin 9	23.2	25183.3	6.6	16.8	65.1
7	bin 9 to bin 2	27.8	25159.9	7.2	13.6	54.2
8	bin 2 to bin 9	29.4	25139.2	7.1	13.4	51.4
Mean		**26.9**	**25227.6**	**7.1**	**15.5**	**56.6**
SD		**2.4**	**60.5**	**0.5**	**2.7**	**5.3**

[a] Material mass was measured while in the truck during receiving operation.

Table A.41 Mass concentration of corn dust collected from lower duct (set A).

	Mass Concentration, $mg \cdot m^{-3}$				
Transfer	**Sample 1**	**Sample 2**	**Sample 3**	**Mean**	**SD**
1	131.0	112.9	226.1	156.7	60.8
2	145.9	147.5	217.3	170.2	40.8
3	143.9	150.6	125.3	139.9	13.1
4	129.6	176.7	149.8	152.0	23.6
5	168.2	172.0	135.5	158.6	20.1
6	140.2	178.2	148.2	155.6	20.0
7	180.6	194.1	177.3	184.0	8.9
8	137.8	170.2	183.3	163.8	23.4

Table A.42 Mass concentration of corn dust collected from upper duct (set B).

	Mass Concentration, $mg \cdot m^{-3}$				
Transfer	**Sample 1**	**Sample 2**	**Sample 3**	**Mean**	**SD**
1	275.7	282.2	445.9	334.6	96.4
2	390.0	380.9	383.5	384.8	4.7
3	260.0	321.3	441.9	341.0	92.5
4	243.1	348.0	354.1	315.1	62.4
5	270.6	309.6	361.9	314.0	45.8
6	318.7	373.7	418.0	370.1	49.7
7	527.8	481.7	482.2	497.2	26.5
8	389.1	491.1	472.8	451.0	54.4

Table A.43 Mass flow rate of corn dust – from lower duct (set A).

	Dust Mass Flowrate, $g \cdot s^{-1}$				
Transfer	**Sample 1**	**Sample 2**	**Sample 3**	**Mean**	**SD**
1	0.84	0.73	1.45	1.01	0.39
2	0.94	0.95	1.40	1.09	0.26
3	0.93	0.97	0.81	0.90	0.08
4	0.83	1.14	0.96	0.98	0.15
5	1.08	1.11	0.87	1.02	0.13
6	0.90	1.15	0.95	1.00	0.13
7	1.16	1.25	1.14	1.18	0.06
8	0.89	1.09	1.18	1.05	0.15

Table A.44 Mass flow rate of corn dust – from upper duct (set B).

	Dust Mass Flowrate, $g \cdot s^{-1}$				
Transfer	**Sample 1**	**Sample 2**	**Sample 3**	**Mean**	**SD**
1	1.38	1.41	2.23	1.67	0.48
2	1.95	1.90	1.92	1.92	0.02
3	1.30	1.61	2.21	1.71	0.46
4	1.22	1.74	1.77	1.58	0.31
5	1.35	1.55	1.81	1.57	0.23
6	1.59	1.87	2.09	1.85	0.25
7	2.64	2.41	2.41	2.49	0.13
8	1.95	2.46	2.36	2.25	0.27

Table A.45 Geometric mean diameter (GMD) of corn dust collected from lower duct (set A).

	Geometric Mean Diameter, μm									
Transfer	**Sample 1**	**Sample 2**	**Sample 3**	**Sample 4**	**Sample 5**	**Sample 6**	**Sample 7**	**Sample 8**	**Mean**	**SD**
1	24.0	15.5	15.6	11.9	11.8	10.8	11.1		14.4	4.7
2	11.5	11.9	11.2	11.5	11.9	11.9	12.8	13.9	12.1	0.9
3	11.4	11.4	11.5	12.3	12.4	12.3			11.9	0.5
4	10.2	10.3	11.6	11.7	11.8	11.6			11.2	0.7
5	11.5	11.8	11.3	11.6	12.8	12.5			11.9	0.6
6	11.5	11.6	11.9	12.0	11.6	11.5			11.7	0.2
7	13.8	14.8	11.6	11.6	11.1	11.1			12.3	1.6
8	10.4	10.3	10.9	10.9	12.1	12.3	11.3	11.4	11.2	0.7

Table A.46 Geometric mean diameter (GMD) of corn dust collected from upper duct (set B).

	Geometric Mean Diameter, µm								
Transfer	Sample 1	Sample 2	Sample 3	Sample 4	Sample 5	Sample 6	Sample 7	Mean	SD
1	10.3	10.1	10.4	10.5	10.4	10.4		10.3	0.2
2	11.0	10.9	10.1	10.2	10.9	10.7		10.6	0.4
3	10.0	10.6	11.0	10.8	11.0	10.7		10.7	0.4
4	10.0	10.0	10.6	10.4	10.4	10.8		10.4	0.3
5	10.3	10.5	11.3	11.4	11.6	11.7		11.1	0.6
6	11.0	11.2	10.7	10.9	10.8	11.1	11.1	11.0	0.2
7	10.7	10.4	10.3	10.2	9.7	9.4		10.1	0.5
8	9.3	9.6	10.1	10.0	10.7	10.4		10.0	0.5

Table A.47 Geometric standard deviation (GSD) of corn dust collected from lower duct (set A).

	Geometric Standard Deviation									
Transfer	Sample 1	Sample 2	Sample 3	Sample 4	Sample 5	Sample 6	Sample 7	Sample 8	Mean	SD
1	4.45	2.78	2.79	2.35	2.34	2.31	2.34		2.77	0.77
2	2.37	2.39	2.35	2.37	2.40	2.41	2.70	3.14	2.52	0.27
3	2.37	2.36	2.36	2.38	2.38	2.38			2.37	0.01
4	2.26	2.27	2.33	2.34	2.33	2.32			2.31	0.04
5	2.35	2.36	2.31	2.33	2.42	2.37			2.36	0.04
6	2.35	2.35	2.34	2.35	2.33	2.33			2.35	0.01
7	2.55	2.87	2.39	2.40	2.35	2.35			2.48	0.20
8	2.26	2.25	2.27	2.26	2.48	2.51	2.33	2.33	2.33	0.10

Table A.48 Geometric standard deviation (GSD) of corn dust collected from upper duct (set B).

	Geometric Standard Deviation								
Transfer	Sample 1	Sample 2	Sample 3	Sample 4	Sample 5	Sample 6	Sample 7	Mean	SD
1	2.23	2.26	2.37	2.38	2.43	2.43		2.35	0.08
2	2.32	2.31	2.39	2.40	2.30	2.30		2.34	0.05
3	2.43	2.33	2.33	2.31	2.33	2.43		2.36	0.05
4	2.28	2.27	2.31	2.28	2.41	2.31		2.31	0.05
5	2.28	2.30	2.32	2.34	2.33	2.33		2.31	0.02
6	2.30	2.32	2.42	2.29	2.28	2.34	2.34	2.33	0.05
7	2.34	2.30	2.29	2.28	2.32	2.38		2.32	0.04
8	2.30	2.24	2.25	2.25	2.29	2.27		2.27	0.02

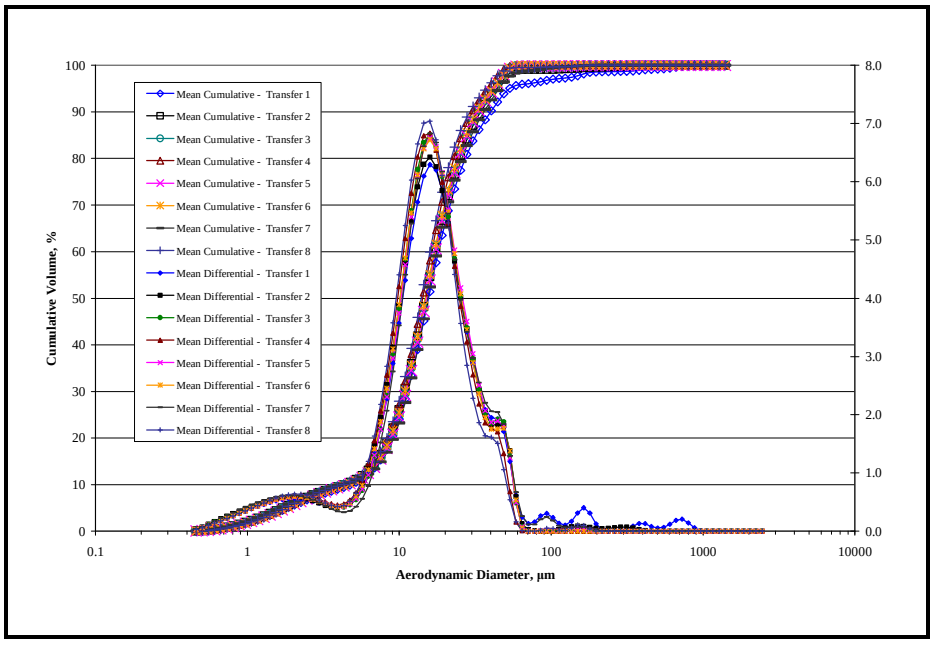

Figure A.3 Mean cumulative and mean differential volume percentages for the particle size distribution of corn dust collected from the lower duct (set A) during Transfers 1 to 8.

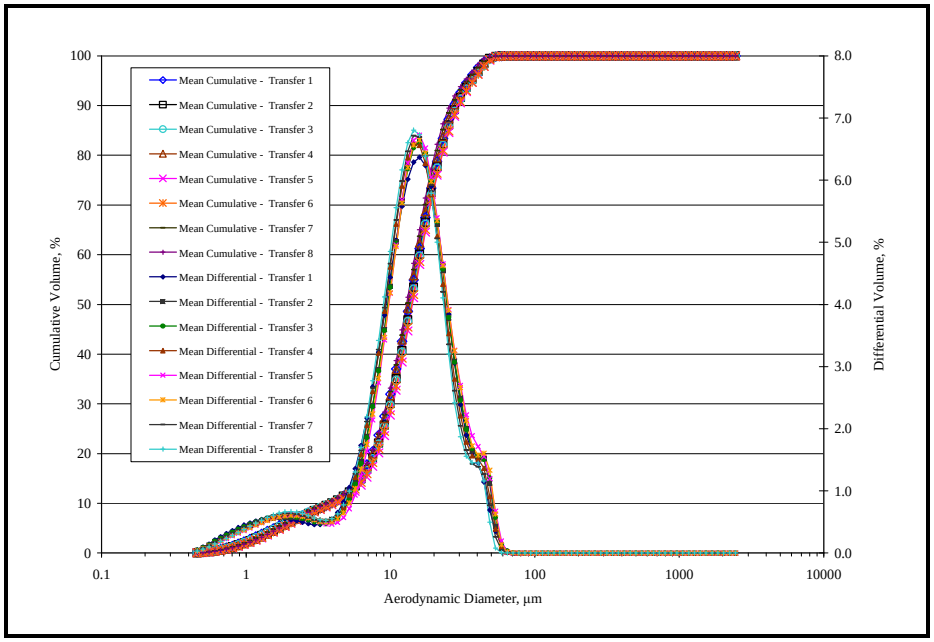

Figure A.4 Mean cumulative and mean differential volume percentages for the particle size distribution of corn dust collected from the upper duct (set B) during Transfers 1 to 8.

Table A.49 Percentage of particulate matter of the total corn dust (% PM) from the lower duct (set A).

Transfer	% PM 2.5	% PM 4.0	% PM 10
1	6.810	9.083	24.164
2	7.376	9.641	26.162
3	7.281	9.670	24.971
4	7.193	9.742	27.334
5	7.025	9.400	24.630
6	7.042	9.415	25.590
7	7.733	9.896	23.320
8	7.252	9.717	28.060
Mean	**7.214**	**9.571**	**25.529**
SD	**0.275**	**0.257**	**1.601**

Table A.50 Percentage of particulate matter of the total corn dust (% PM) from the upper duct (set B).

Transfer	% PM 2.5	% PM 4.0	% PM 10
1	7.68	10.1	32.1
2	7.52	10.2	30.1
3	7.72	10.2	29.9
4	7.56	10.3	31.8
5	7.25	9.8	27.9
6	7.29	9.9	28.8
7	7.98	10.7	32.6
8	7.72	10.5	33.3
Mean	**7.59**	**10.2**	**30.8**
SD	**0.24**	**0.3**	**1.9**

Table A.51 Particle densities of wheat and corn dusts.

	Particle Density, $g \cdot cm^{-3}$	
Sample	**Wheat Dust**	**Corn Dust**
1	1.46	1.52
2	1.47	1.49
3	1.50	1.50
4		1.52
5		1.51
Mean	**1.48**	**1.51**
SD	**0.022**	**0.014**

Data for Chapter 5

Table A.52 Published physical properties of soybeans without moisture content.

Parameters		Published value	
Length (mm), l		7.3 [D]	
Width (mm), w		6.1 [D]	
Thickness (mm), h		5.5 [D]	
Equivalent Diameter (mm), d_e		6.0 [B, F]	
Seed Mass (mg), m		149.0 [D]	100.0 - 200.0 [E]
Seed Volume (mm^3), V			
Seed Density ($kg \cdot m^{-3}$), ρ_p		1180.0 [F]	
Bulk Density ($kg \cdot m^{-3}$), ρ_b		772 [A, G]	
Poisson Ratio, v		0.08 [D]	0.4 [F]
Elastic Modulus (MPa), E			100.0 [F]
Shear Modulus (MPa), $G = E / (2 + 2v)$			35.71 [F]
Restitution Coefficient, e	generic	0.7 [D]	0.5 [F]
Static Friction Coefficient, μ_s	with self (or grain)	0.55 [B, C]	0.267 [D]
	with steel	0.37 [B, C]	
	with transparent perspex	0.3 [F]	
	with glass	0.328 [D]	
Static Angle of Repose (deg)	for filling or piling	16.0 [B, C]	
	for emptying or funneling	29.0 [B, C]	

[A] Henderson and Perry (1976)
[B] Mohsenin (1986)
[C] Stahl (1950)
[D] Vu-Quoc et al. (2000)
[E] McLelland and Miller (2001)
[F] Raji and Favier (2004a, 2004b)
[G] ASABE Standards (2006a) - D241.4

Table A.53 Published physical properties of corn with moisture content.

Parameters	Moisture Content (% wb)																	
	6.7	7.3	7.5	9.9	10.0	10.6	12.2	12.5	13.0	13.9	14.4	15.0	16.2	17.5	19.5	20.0	23.1	25.0
Length (mm), *l*	16.4 [D]				9.4 [F]	12.6 [E]												
Width (mm), w	20.3 [D]				8.2 [F]	8.3 [E]												
Thickness (mm), *h*	12.8 [D]				5.1 [F]	4.5 [E]												
Equivalent Diameter (mm), d_e	8.0 [D]																	
Seed Mass (mg), *m*	349.7 [D]				295.0 [F]	348.8 [E]											349.7 [A, D]	
Seed Volume (mm^3), *V*						274.0 [E]												
Seed Density ($kg \cdot m^{-3}$), ρ_p	1290 [D]				1396.5 [F]	1273 [E]						1300 [G]						1270 [G]
Bulk Density ($kg \cdot m^{-3}$), ρ_b	747.7 [D]				742 ± 3 [F]	810.0 [E]		728 ± 3 [F]				698 ± 3 [F]		672 ± 2 [F]		663 ± 2 [F]		
Poisson Ratio, *v*					0.32, 0.20 ± 0.01 [D, F]			0.20 ± 0.01 [F]			0.4 [C, H]	0.20 ± 0.02 [F]		0.19 ± 0.02 [F]		0.20 ± 0.02 [F]		
Elastic Modulus (MPa), *E*					26.2 ± 3.2 [F]			19.3 ± 2.7 [F]			2030 [C, H]	15.9 ± 0.9 [F]		15.5 ± 2.6 [F]		12.3 ± 1.4 [F]		
Shear Modulus (MPa), *G = E / (2 + 2v)*					9.50 - 12.35 [F]			6.86 - 9.24 [F]			725.0 [C, H]	6.15 - 7.12 [F]		5.33 - 7.74 [F]		4.47 - 5.81 [F]		
Static Friction Coefficient, μ_s with sheet metal			0.2 [B, D]	0.24 [B, D]	0.232 - 0.273 [F]		0.25 [B, D]	0.249 - 0.290 [F]		0.34 [B, D]		0.238 - 0.248 [F]		0.251 - 0.266 [F]		0.254 - 0.284 [F]		
Static Friction Coefficient, μ_s with steel		0.53 [A, D]			0.246 - 0.294 [F]			0.249 - 0.262 [F]	0.47 [A, D]			0.242 - 0.267 [F]	0.48 [A, D]	0.235 - 0.268 [F]	0.59 [A, D]	0.253 - 0.303 [F]	0.76 [A, D]	
Static Angle of Repose (deg) for emptying or funneling					23.5 ± 0.4 [F]			33.8 ± 0.2 [F]				30.6 ± 0.3 [F]		34.2 ± 0.5 [F]		31.9 ± 0.6 [F]		
Angle of Internal Friction (deg)					26.7 ± 0.6 [F]			31.7 ± 0.5 [F]				32.0 ± 1.4 [F]		33.4 ± 0.8 [F]		33.6 ± 1.5 [F]		

[A] Lorenzen (1957)
[B] Brubaker and Pos (1965)
[C] Shelef and Mohsenin (1969)
[D] Mohsenin (1986)
[E] Nelson (2002)
[F] Molenda and Horabik (2005)
[G] ASABE Standards (2006a) - D241.4
[H] ASAE Standards (2006b) - S368.4

Table A.54 Published physical properties of corn without moisture content.

Parameters		Published value		
Length (mm), *l*		12.0 [F]	10.1 [I]	
Width (mm), w		8.0 [F]	9.1 [I]	
Thickness (mm), *h*		4.0 [F]	6.7 [I]	
Equivalent Diameter (mm), d_e				
Seed Mass (mg), *m*		285 [E]		250.0 - 300.1 [F]
Seed Volume (mm^3), *V*				
Seed Density ($kg \cdot m^{-3}$), ρ_p		1280 [I]		
Bulk Density ($kg \cdot m^{-3}$), ρ_b		721 [C, E, H]		
Poisson Ratio, *v*		0.4 [G, I]		
Elastic Modulus (MPa), *E*		1660 [I]		1041 - 2320 [G]
Shear Modulus (MPa), *G = E / (2 + 2v)*		592.86 [I]		371.43 - 828.58 [G]
Restitution Coefficient, *e*	with acrylic	0.59 [I]		
Static Friction Coefficient, μ_s	with self (or grain)	0.52 [A, D]	0.51 [B]	
	with steel	0.37 [A, D]	0.45 [B]	0.476 - 0.597 [G]
	with acrylic	0.34 [I]		
	with aluminum			0.226 - 0.277 [G]
Static Angle of Repose (deg)	for filling or piling	16.0 [B, D]		
	for emptying or funneling	27.0 [B, D]		

[A] Stahl (1950)
[B] Henderson and Perry (1976)
[C] Mohsenin (1986)
[D] Hoseney and Faubion (1992)
[E] Watson (2003)
[F] Chung et al (2004)
[G] ASABE Standards (2006a) - D241.4
[H] Chung and Ooi (2008)

Table A.55 Published physical properties of wheat with moisture content.

Parameters	Moisture Content (% wb)														
	6.2	7.3	7.5	7.8	8.0	8.3	8.6	8.8	9.8	10.0	10.9	11.0	11.2	11.5	11.8
Length (mm), *l*	6.4 [D]		6.9 [D]	6.6, 5.7 [D]	6.7 [D]	6.4 [D]	5.8 [E]	7.3 [D]		6.7 [F]	6.9 [E]				5.6 [E]
Width (mm), w	3.0 [D]		3.8 [D]	3.3, 3.1 [D]	3.2 [D]	3.1 [D]	2.6 [E]	3.0 [D]		3.2 [F]	2.8 [E]				3.2 [E]
Thickness (mm), *h*	3.0 [D]		3.5 [D]	3.0, 3.3 [D]	3.1 [D]	3.0 [D]	2.4 [E]	2.8 [D]		2.9 [F]	2.8 [E]				2.9 [E]
Equivalent Diameter (mm), d_e	4.0 [D]		4.1 [D]	3.8, 3.6 [D]	3.9 [D]	3.6 [D]		4.0 [D]							
Seed Mass (mg), *m*	48.2 [D]		51.0 [D]	41.7, 35.2 [D]	45.0 [D]	33.7 [D]	26.0 [E]	47.3 [D]		40.5 [F]	36.8 [E]				35.7 [E]
Seed Volume (mm^3), *V*							18.5 [E]				26.1 [E]				26.4 [E]
Seed Density ($kg \cdot m^{-3}$), ρ_p	1420 [D]		1430 [D]	1430, 1420 [D]	1420 [D]	1410 [D]	1409 [E]	1410 [D]	1290, 1300, 1320 [G]	1407 [F]	1411 [E]				1345 [E]
Bulk Density ($kg \cdot m^{-3}$), ρ_b	805.5 [D]		813.4 [D]	794.1, 823.2 [D]	799.2 [D]	796.7 [D]	772 [E]	801.8 [D]		773 ± 3 [F]	788 [E]				756 [E]
Poisson Ratio, *v*										0.22 ± 0.01 [F]				0.42 [C, H]	
Elastic Modulus (MPa), *E*										22.4 ± 4.6 [F]				1544 [C]	
Shear Modulus (MPa), *G = E / (2 + 2v)*										7.24 - 11.16 [F]				543.66 [C]	
Static Friction Coefficient, μ_s with sheet metal										0.23 - 0.32 [F]			0.10 [B, D]		
Static Friction Coefficient, μ_s with steel		0.37 [A]								0.249 -0.282 [F]		0.39 [A, D]			
Static Angle of Repose (deg) for emptying or funneling										24.3 ± 0.5 [F]					
Angle of Internal Friction (deg)										25.7 ± 0.3 [F]					

[A] Lorenzen (1957)
[B] Brubaker and Pos (1965)
[C] Arnold and Roberts (1969)
[D] Mohsenin (1986)
[E] Nelson (2002)
[F] Molenda and Horabik (2005)
[G] ASABE Standards (2006a) - D241.4
[H] ASAE Standards (2006b) - S368.4

Table A.55 Published physical properties of wheat with moisture content. (cont.)

Parameters		Moisture Content (% wb)											
		12.1	12.5	13.0	13.8	14.1	15.0	15.7	16.9	17.1	17.5	19.3	20.0
Length (mm), *l*		5.5 [E]			6.4 [E]				5.9 [E]				
Width (mm), w		2.9 [E]			3.4 [E]				2.8 [E]				
Thickness (mm), *h*		2.6 [E]			2.9 [E]				2.6 [E]				
Equivalent Diameter (mm), d_e													
Seed Mass (mg), *m*		29.2 [E]			39.7 [E]				27.7 [E]				
Seed Volume (mm^3), *V*		21.0 [E]			28.6 [E]				20.2 [E]				
Seed Density ($kg \cdot m^{-3}$), ρ_p		1388 [E]			1385 [E]				1373 [E]				
Bulk Density ($kg \cdot m^{-3}$), ρ_b		763 [E]	765 ± 3 [F]				694 ± 4 [F]		722		705 ± 4 [F]		713 ± 5 [F]
Poisson Ratio, *v*			0.42, 0.18 ± 0.02 [C, F, H]	0.42 [C, H]			0.20 ± 0.03 [F]				0.20 ± 0.01 [F]		0.19 ± 0.01 [F]
Elastic Modulus (MPa), *E*			1413 - 2372, 22.2 ± 4.4 [C, F]	2834 [C]			19.3 ± 2.5 [F]				17.2 ± 3.6 [F]		11.1 ± 1.1 [F]
Shear Modulus (MPa), *G = E / (2 + 2v)*			497.54 - 835.21, 7.42 - 11.47 [C, F]	997.89 [C]			6.83 - 9.32 [F]				5.62 - 8.74 [F]		4.17 - 5.17 [F]
Static Friction Coefficient, μ_s	with sheet metal		0.26 - 0.34 [F]	0.14 [B, D]			0.27, 0.26 - 0.34 [B, D, F]	0.33 [B, D]			0.35 - 0.42 [F]		0.34 - 0.44 [F]
	with steel		0.248 - 0.269 [F]			0.43 [A, D]	0.280 - 0.335 [F]			0.44 [A, D]	0.313 - 0.383 [F]	0.55 [A, D]	0.335 - 0.414 [F]
Static Angle of Repose (deg)	for emptying or funneling		29.0 ± 0.7 [F]				33.3 ± 0.6 [F]				37.6 ± 0.5 [F]		35.4 ± 0.4 [F]
Angle of Internal Friction (deg)			26.2 ± 0.4 [F]				27.0 ± 0.5 [F]				33.0 ± 1.0 [F]		35.5 ± 0.5 [F]

[A] Lorenzen (1957)
[B] Brubaker and Pos (1965)
[C] Arnold and Roberts (1969)
[D] Mohsenin (1986)
[E] Nelson (2002)
[F] Molenda and Horabik (2005)
[G] ASABE Standards (2006a) - D241.4
[H] ASAE Standards (2006b) - S368.4

Table A.56 Published physical properties of wheat without moisture content.

Parameters		Published value		
Length (mm), *l*				
Width (mm), w				
Thickness (mm), *h*				
Equivalent Diameter (mm), d_e				
Seed Mass (mg), *m*		37.0 [F]	31.0 - 38.0 [G]	
Seed Volume (mm^3), *V*				
Seed Density ($kg \cdot m^{-3}$), ρ_p				
Bulk Density ($kg \cdot m^{-3}$), ρ_b		772 [D, F, H]		
Static Friction Coefficient, μ_s	with self (or grain)	0.47 [A, E]	0.53 [B, C, E]	
	with steel	0.41 [A, E]	0.37 [C, E]	0.37 - 0.47 [B, E]
Static Angle of Repose (deg)	for filling or piling	16.0 [C, E]		
	for emptying or funneling	27.0 [C, E]		

[A] Airy (1898)
[B] Jamieson (1903)
[C] Stahl (1950)
[D] Henderson and Perry (1976)
[E] Mohsenin (1986)
[F] Hoseney and Faubion (1992)
[G] McLelland and Miller (2001)
[H] ASABE Standards (2006a) - D241.4

Table A.57 Published physical properties of grain sorghum with moisture content.

	Moisture Content (% wb)			
Parameters	**9.2**	**9.5**	**9.9**	**11.2**
Length (mm), *l*	4.3 [A]			4.5 [B]
Width (mm), w	4.1 [A]			4.1 [B]
Thickness (mm), *h*	2.8 [A]			3.4 [B]
Equivalent Diameter (mm), d_e	3.5 [A]			
Seed Mass (mg), *m*	28.8 [A]			33.2 [B]
Seed Volume (mm^3), *V*				24.7 [B]
Seed Density ($kg \cdot m^{-3}$), ρ_p	1320 [A]	1220 [C]	1260 [C]	1344 [B]
Bulk Density ($kg \cdot m^{-3}$), ρ_b	774.3 [A]			775.0 [B]

[A] Mohsenin (1986)
[B] Nelson (2002)
[C] ASABE Standards (2006a) - D241.4

Table A.58 Published physical properties of grain sorghum without moisture content.

Parameters		Published value			
Length (mm), *l*					
Width (mm), w					
Thickness (mm), *h*					
Equivalent Diameter (mm), d_e					
Seed Mass (mg), *m*				28.0 [D]	
Bulk Density (kg·m^{-3}), ρ_b		643.5, 720.72 [B]		733 [D]	721 [E]
Static Friction Coefficient, μ_s	with self (or grain)	0.65 [A, C]			
	with steel	0.37 [A, C]			
Static Angle of Repose (deg)	for filling or piling	20 [A, C]			
	for emptying or funneling	33 [A, C]			

[A] Stahl (1950)
[B] Henderson and Perry (1976)
[C] Mohsenin (1986)
[D] Hoseney and Faubion (1992)
[E] ASABE Standards (2006a) - D241.4

Table A.59 Published physical properties of rice without moisture content.

Parameters		Published value	
Length (mm), *l*			
Width (mm), w			
Thickness (mm), *h*			
Equivalent Diameter (mm), d_e			
Seed Mass (mg), *m*		27.0 [D]	
Seed Volume (mm^3), *V*			
Seed Density (kg·m^{-3}), ρ_p			
Bulk Density (kg·m^{-3}), ρ_b		579 [* B, E]	579 [D]
Static Friction Coefficient, μ_s	with self (or grain)	0.73 [* A, C]	
	with steel	0.48 [* A, C]	
Static Angle of Repose (deg)	for filling or piling	20 [* A, C]	
	for emptying or funneling	36 [* A, C]	

[*] Rough rice or paddy
[A] Stahl (1950)
[B] Henderson and Perry (1976)
[C] Mohsenin (1986)
[D] Hoseney and Faubion (1992)
[E] ASABE Standards (2006a) - D241.4

Table A.60 Published physical properties of rice with moisture content.

Parameters	Moisture Content (% wb)									
	8.6	**8.8**	**9.2**	**11.5**	**11.9**	**12.0**	**12.4**	**14.0**	**15.4**	**15.7**
Length (mm), *l*	7.6 [C]	9.8 [C]	8.0 [C]	7.4, 6.5 [**D]		5.6, 5.3 [***D]			7.8 [***D]	8.9 [***D]
Width (mm), w	3.6 [C]	2.5 [C]	3.2 [C]	2.1 [**D]		2.5 [***D]			2.9 [***D]	2.3 [***D]
Thickness (mm), *h*	2.5 [C]	2.1 [C]	2.3 [C]	1.7 [**D]		1.8, 1.7 [***D]			2.0 [***D]	2.0 [***D]
Equivalent Diameter (mm), d_e	3.5 [C]	3.3 [C]	3.4 [C]							
Seed Mass (mg), *m*	29.1 [C]	25.0 [C]	26.9 [C]	20.9, 18.9 [**D]		21.5, 17.5 [***D]			24.9 [***D]	23.6 [***D]
Seed Volume (mm^3), *V*				14.6, 12.7 [**D]		14.9. 12.0 [***D]			18 [***D]	17 [***D]
Seed Density ($kg \cdot m^{-3}$), ρ_p	1360 [C]	1390 [C]	1360 [C]	1432, 1460 [**D]	1110.0 [*E]	1434, 1462 [***D]	1120 [*E]		1382 [***D]	1388 [***D]
Bulk Density ($kg \cdot m^{-3}$), ρ_b	573.5 [C]	593.8 [C]	573.2 [C]	716, 773 [**D]		802, 851 [***D]			641 [***D]	660 [***D]
Static Friction Coefficient, μ_s with self (or grain)								0.73, 0.68 [*A, C]		
Static Friction Coefficient, μ_s with sheet metal								0.40 - 0.41, 0.45 [*A, C]		

[*] Rough rice or paddy
[**] Long grain
[***] Medium grain
[A] Kramer (1944)
[B] Stahl (1950)
[C] Mohsenin (1986)
[D] Nelson (2002)
[E] ASABE Standards (2006a) - D241.4

Table A.61 Published physical properties of barley with moisture content.

Parameters		Moisture Content (% wb)										
		7.5	7.6	7.9	8.2	9.7	9.8	10.0	10.3	10.4	10.7	10.8
Length (mm), *l*		10.9, 10.6 [C]	10.0 [C]	10.0, 10.6 [C]	10.5 [C]			8.4 [E]				
Width (mm), w		3.8, 3.5 [C]	3.6 [C]	3.2, 3.3 [C]	3.5 [C]			3.6 [E]				
Thickness (mm), *h*		3.0, 2.9 [C]	2.9 [C]	2.5, 2.6 [C]	2.6 [C]			2.8 [E]				
Equivalent Diameter (mm), d_e		4.2, 4.0 [C]	4.0 [C]	3.8, 3.7 [C]	4.0 [C]							
Seed Mass (mg), *m*		53.9, 48.0 [C]	48.9 [C]	38.5, 36.4 [C]	45.5 [C]			45.2 [E]				
Seed Volume (mm^3), *V*												
Seed Density ($kg \cdot m^{-3}$), ρ_p		1400, 1420 [C]	1400 [C]	1380 [C]	1380 [C]	1260.0 [F]	1210 [F]	1346 [E]	1130 [F]	1330 [F]	1240 [F]	
Bulk Density ($kg \cdot m^{-3}$), ρ_b		620.0, 653.6 [C]	628.4 [C]	567.2, 588.8 [C]	589.4 [C]			686 ± 3 [E]				
Poisson Ratio, *v*								0.19 ± 0.01 [E]				
Elastic Modulus (MPa), *E*								14.2 ± 1.6 [E]				
Shear Modulus (MPa), $G = E / (2 + 2v)$								5.25 - 6.69 [E]				
Static Friction Coefficient, μ_s	with sheet metal							0.225 - 0.252 [E]			0.2 [B, C]	
	with steel			0.4 [A, C]				0.226 - 0.257 [E]				0.4 [A, C]
Static Angle of Repose (deg)	for emptying or funneling							26.8 ± 0.7 [E]				
Angle of Internal Friction (deg)								27.8 ± 0.4 [E]				

[A] Lorenzen (1957)
[B] Brubaker and Pos (1965)
[C] Mohsenin (1986)
[D] Nelson (2002)
[E] Molenda and Horabik (2005)
[F] ASABE Standards (2006a) - D241.4

Table A.61 Published physical properties of barley with moisture content. (cont.)

Parameters		Moisture Content (% wb)									
		11.2	12.3	12.5	13.3	14.3	15.0	16.4	16.6	17.5	19.5	20.0
Length (mm), *l*		9.5, 7.9 [D]										
Width (mm), w		3.1, 2.9 [D]										
Thickness (mm), *h*		2.4, 2.2 [D]										
Equivalent Diameter (mm), d_e												
Seed Mass (mg), *m*		25.1, 26.6 [D]										
Seed Volume (mm^3), *V*		25.9, 19.7 [D]										
Seed Density ($kg \cdot m^{-3}$), ρ_p		1356, 1352 [D]										
Bulk Density ($kg \cdot m^{-3}$), ρ_b		566, 615 [D]		689 ± 2 [E]			680 ± 5 [E]			675 ± 4 [E]		667 ± 3 [E]
Poisson Ratio, *v*				0.16 ± 0.01 [E]			0.15 ± 0.01 [E]			0.17 ± 0.01 [E]		0.19 ± 0.01 [E]
Elastic Modulus (MPa), *E*				14.0 ± 1.8 [E]			13.8 ± 1.1 [E]			12.3 ± 0.8 [E]		10.4 ± 2.4 [E]
Shear Modulus (MPa), *G = E / (2 + 2v)*				5.21 - 6.87 [E]			5.47 - 6.54 [E]			4.87 - 5.65 [E]		3.33 - 5.42 [E]
Static Friction Coefficient, μ_s	with sheet metal		0.17 [B, C]	0.233 -0.269 [E]		0.2 [B, C]	0.246 - 0.273 [E]	0.34 [B, C]		0.240 - 0.325 [E]		0.273 - 0.352 [E]
	with steel			0.239 -0.280 [E]	0.4 [A, C]		0.232 - 0.258 [E]		0.38 [A, C]	0.238 - 0.278 [E]	0.39 [A, C]	0.245 - 0.279 [E]
Static Angle of Repose (deg)	for emptying or funneling			28.9 ± 0.7 [E]			29.5 ± 0.7 [E]			30.5 ± 0.8 [E]		32.1 ± 0.8 [E]
Angle of Internal Friction (deg)				28.5 ± 0.5 [E]			31.2 ± 0.3 [E]			30.6 ± 1.0 [E]		33.2 ± 0.5 [E]

[A] Lorenzen (1957)
[B] Brubaker and Pos (1965)
[C] Mohsenin (1986)
[D] Nelson (2002)
[E] Molenda and Horabik (2005)
[F] ASABE Standards (2006a) - D241.4

Table A.62 Published physical properties of barley without moisture content.

Parameters		Published value		
Length (mm), *l*				
Width (mm), w				
Thickness (mm), *h*				
Equivalent Diameter (mm), d_e				
Seed Mass (mg), *m*				37 [F]
Seed Volume (mm^3), *V*				
Seed Density ($kg \cdot m^{-3}$), ρ_p				
Bulk Density ($kg \cdot m^{-3}$), ρ_b		616 [C]	605.0 [E]	618 [F]
Static Friction Coefficient, μ_s	with self (or grain)	0.51 [A, D]	0.53 [B, D]	
	with steel	0.38 [A, D]	0.38 - 0.40 [B, D]	
Static Angle of Repose (deg)	for filling or piling		16 [B, D]	
	for emptying or funneling		28 [B, D]	

[A] Airy (1898)
[B] Stahl (1950)
[C] Henderson and Perry (1976)
[D] Mohsenin (1986)
[E] Hoseney and Faubion (1992)
[F] ASABE Standards (2006a) - D241.4

Table A.63 Published physical properties of oats without moisture content.

Parameters		Published value	
Length (mm), *l*			
Width (mm), w			
Thickness (mm), *h*			
Equivalent Diameter (mm), d_e			
Seed Mass (mg), *m*		32.0 [D]	
Seed Volume (mm^3), *V*			
Seed Density ($kg \cdot m^{-3}$), ρ_p			
Bulk Density ($kg \cdot m^{-3}$), ρ_b		438 [D]	412 [E]
Static Friction Coefficient, μ_s	with self (or grain)	0.53 [A, C]	0.62 [B, C]
	with steel	0.41 [A, C]	0.45 [B, C]
Static Angle of Repose (deg)	for filling or piling		18 [B, C]
	for emptying or funneling		32 [B, C]

[A] Airy (1898)
[B] Stahl (1950)
[C] Mohsenin (1986)
[D] Hoseney and Faubion (1992)
[E] ASABE Standards (2006a) – D241.4

Table A.64 Published physical properties of oats with moisture content.

Parameters	Moisture Content (% wb)									
	8.5	8.6	8.8	9.4	9.7	9.8	10.0	10.3	10.6	10.7
Length (mm), *l*	14.9 [B]	11.4, 13.0 [B]	11.0, 14.2 [B]				11.5 [D]		10.2 [C]	10.9 [C]
Width (mm), w	3.1 [B]	2.7, 2.9 [B]	2.8, 2.9 [B]				3.1 [D]		2.8 [C]	2.8 [C]
Thickness (mm), *h*	2.4 [B]	2.1, 2.2 [B]	2.3, 2.4 [B]				2.6 [D]		2.2 [C]	2.1 [C]
Equivalent Diameter (mm), d_e	3.8 [B]	3.5, 3.6 [B]	3.6 [B]							
Seed Mass (mg), *m*	39.5 [B]	30.5, 33.7 [B]	33.9, 32.9 [B]				35.6 [D]		28.1 [C]	34.8 [C]
Seed Volume (mm^3), *V*									21.4 [C]	26.8 [C]
Seed Density ($kg \cdot m^{-3}$), ρ_p	1380 [B]	1360, 1380 [B]	1370, 1350 [B]	1060 [E]	950 [E]	1050 [E]	1397 [D]	990 [E]	1314 [C]	1295 [C]
Bulk Density ($kg \cdot m^{-3}$), ρ_b	472.01 [B]	513, 485 [B]	502, 360 [B]				557 ± 2 [D]		454 [C]	419 [C]
Poisson Ratio, *v*							0.18 ± 0.01 [D]			
Elastic Modulus (MPa), *E*							17.8 ± 2.8 [D]			
Shear Modulus (MPa), *G = E / (2 + 2v)*							6.30 - 8.80 [D]			
Static Friction Coefficient, μ_s with sheet metal							0.237 - 0.271 [D]		0.22 [A, B]	
Static Friction Coefficient, μ_s with steel							0.237 - 0.268 [D]			
Static Angle of Repose (deg) for emptying or funneling							28.4 ± 0.4 [D]			
Angle of Internal Friction (deg)							22.1 ± 1.1 [D]			

[A] Brubaker and Pos (1965)
[B] Mohsenin (1986)
[C] Nelson (2002)
[D] Molenda and Horabik (2005)
[E] ASABE Standards (2006a) - D241.4

Table A.64 Published physical properties of oats with moisture content. (cont.)

Parameters		Moisture Content (% wb)							
		12.5	13.0	14.0	15.0	16.0	17.3	17.5	20.0
Length (mm), *l*									
Width (mm), w									
Thickness (mm), *h*									
Equivalent Diameter (mm), d_e									
Seed Mass (mg), *m*									
Seed Volume (mm^3), *V*									
Seed Density ($kg \cdot m^{-3}$), ρ_p									
Bulk Density ($kg \cdot m^{-3}$), ρ_b		574 ± 2 [D]			547 ± 2 [D]			528 ± 2 [D]	527 ± 2 [D]
Poisson Ratio, *v*		0.20 ± 0.01 [D]			0.17 ± 0.01 [D]			0.17 ± 0.01 [D]	0.15 ± 0.01 [D]
Elastic Modulus (MPa), *E*		16.0 ± 3.2 [D]			13.2 ± 3.1 [D]			10.7 ± 2.4 [D]	10.4 ± 1.9 [D]
Shear Modulus (MPa), *G = E / (2 + 2v)*		5.29 - 8.07 [D]			4.28 - 7.03 [D]			3.52 - 5.65 [D]	3.66 - 5.39 [D]
Static Friction Coefficient, μ_s	with sheet metal	0.236 - 0.262 [D]	0.24 [A, B]	0.18 [A, B]	0.231 - 0.260 [D]	0.41 [A, B]	0.32 [A, B]	0.230 - 0.265 [D]	0.229 - 0.269 [D]
	with steel	0.245 - 0.257 [D]			0.235 - 0.264 [D]			0.235 - 0.267 [D]	0.233 - 0.276 [D]
Static Angle of Repose (deg)	for emptying or funneling	28.7 ± 1.0 [D]			31.3 ± 0.5 [D]			32.8 ± 0.5 [D]	34.7 ± 0.4 [D]
Angle of Internal Friction (deg)		22.4 ± 0.9 [D]			24.0 ± 0.5 [D]			23.9 ± 1.0 [D]	26.4 ± 1.7 [D]

[A] Brubaker and Pos (1965)
[B] Mohsenin (1986)
[C] Nelson (2002)
[D] Molenda and Horabik (2005)
[E] ASABE Standards (2006a) - D241.4

Table A.65 Published physical properties of sunflower seed and kernel with moisture content.

Parameters	Moisture Content (% wb)			
	5.8	7.6	8.7	3.9 - 16.7
Length (mm), *l*	9.5 [+], 8.3 [++ A]	10.7 [* B]	14.4 [** B]	
Width (mm), w	5.1 [+], 4.1 [++ A]	5.2 [* B]	8.1 [** B]	
Thickness (mm), *h*	3.3 [+], 2.4 [++ A]	3.1 [* B]	4.6 [** B]	
Equivalent Diameter (mm), d_e	5.4 [+], 4.3 [++ A]			
Seed Mass (mg), *m*	49 [+], 34 [++ A]	59.5 [* B]	115.8 [** B]	
Seed Volume (mm^3), *V*		58.2 [* B]	105.4 [** B]	
Seed Density ($kg \cdot m^{-3}$), ρ_p		1023 [* B]	1099 [** B]	706 - 765 [+], 1050 - 1250 [++ A]
Bulk Density ($kg \cdot m^{-3}$), ρ_b		386 [* B]	339 [** B]	434 - 462 [+], 574 - 628 [++ A]
Static Friction Coefficient, μ_s with sheet metal				0.40 - 0.58 [+], 0.43 - 0.81 [++ A]
Static Angle of Repose (deg) for emptying or funneling				34 - 41 [+], 27 - 38 [++ A]

[*] Oil type
[**] Non-oil type
[+] Sunflower seed (unhulled)
[++] Sunflower kernel (dehulled)
[A] Gupta and Das (1997)
[B] Nelson (2002)

Table A.66 Published physical properties of sunflower seed and kernel without moisture content.

Parameters	Published value		
Length (mm), *l*			
Width (mm), w			
Thickness (mm), *h*			
Equivalent Diameter (mm), d_e			
Seed Mass (mg), *m*	126 [* B]		
Seed Volume (mm^3), *V*			
Seed Density ($kg \cdot m^{-3}$), ρ_p			
Bulk Density ($kg \cdot m^{-3}$), ρ_b	361.2 [A]	412.0 [* C]	309 [** C]

[*] Oil type
[**] Non-oil type
[A] Shroyer et al. (1996)
[B] McLelland and Miller (2001)
[C] ASABE Standards (2006a) - D241.4

Table A.67 Published physical properties of canola with moisture content.

Parameters	Moisture Content (% wb)											
	4.5	6.0	6.2	6.5	6.7	7.0	9.0	11.6	12.0	14.0	16.0	19.3
Length (mm), *l*	2.07 ± 0.016 [C]	1.8 [D]	1.6 [B]					2.19 ± 0.014 [C]				2.29 ± 0.015 [C]
Width (mm), w		1.7 [D]	1.4 [B]									
Thickness (mm), *h*		1.7 [D]										
Equivalent Diameter (mm), d_e	1.84 ± 0.016 [C]					2.0 [A]		1.90 ± 0.013 [C]				1.99 ± 0.010 [C]
Seed Mass (mg), *m*	4.0 ± 0.1 [C]	3.5 [D]	2.9 [B]					5.8 ± 0.1 [C]				6.5 ± 0.1 [C]
Seed Volume (mm^3), *V*	3.96 ± 0.085 [C]		2.7 [B]					5.04 ± 0.075 [C]				5.15 ± 0.075 [C]
Seed Density ($kg \cdot m^{-3}$), ρ_p		1131 [D]	1111 [B]	1150 [E]	1100 [E]							
Bulk Density ($kg \cdot m^{-3}$), ρ_b		645 ± 5 [D]	671 [B]				661 ± 2 [D]		655 ± 3 [D]		644 ± 2 [D]	
Poisson Ratio, *v*		0.24 ± 0.03 [D]				0.4 [A]	0.17 ± 0.02 [D]		0.16 ± 0.01 [D]		0.10 ± 0.01 [D]	
Elastic Modulus (MPa), *E*		9.0 ± 0.6 [D]				29.2, 50.1 [A]	8.7 ± 0.8 [D]		7.1 ± 0.6 [D]		6.6 ± 0.9 [D]	
Shear Modulus (MPa), *G = E / (2 + 2v)*		3.31 - 3.97 [D]				10.43, 17.90 [A]	3.32 - 4.13 [D]		2.78 - 3.35 [D]		2.57 - 3.44 [D]	
Static Friction Coefficient, μ_s with sheet metal	0.27 [C]	0.220 - 0.245 [D]					0.211 - 0.245 [D]	0.29 [C]	0.217 - 0.243 [D]		0.215 - 0.240 [D]	0.32 [C]
Static Friction Coefficient, μ_s with steel		0.234 - 0.279 [D]					0.254 - 0.279 [D]		0.287 - 0.301 [D]		0.264 - 0.292 [D]	
Static Angle of Repose (deg) for emptying or funneling		25.3 ± 0.8 [D]					23.2 ± 0.9 [D]		25.5 ± 0.9 [D]	24.5 ± 0.9 [D]	29.1 ± 0.7 [D]	
Angle of Internal Friction (deg)		24.7 ± 0.5 [D]					30.6 ± 0.4 [D]		31.7 ± 0.7 [D]	34.8 ± 0.7 [D]	33.2 ± 0.9 [D]	

[A] Bilanski et al. (1994)
[B] Nelson (2002)
[C] Calisir et al. (2005)
[D] Molenda and Horabik (2005)
[E] ASABE Standards (2006a) - D241.4

Table A.68 Published physical properties of canola without moisture content.

Parameters		Published value
Length (mm), l		
Width (mm), w		
Thickness (mm), h		
Equivalent Diameter (mm), d_e		2.0 [B]
Seed Mass (mg), m		3.0 - 4.0 [A]
Seed Density ($kg \cdot m^{-3}$), ρ_p		1053 [B]
Bulk Density ($kg \cdot m^{-3}$), ρ_b		669 [D]
Poisson Ratio, v		0.4 [B]
Elastic Modulus (MPa), E		30.0 [B]
Shear Modulus (MPa), $G = E / (2 + 2v)$		10.7 [B]
Restitution Coefficient, e	generic	0.6 [B]
Static Friction Coefficient, μ_s	with self (or grain)	0.5 [B]
	with transparent perspex	0.3 [B]
Static Angle of Repose (deg)	for emptying or funneling	22 [C]

[A] McLelland and Miller (2001)
[B] Raji and Favier (2004a, 2004b)
[C] Boyles et al. (2006)
[D] ASABE Standards (2006a) - D241.4

Table A.69 Data of single-kernel mass from 10 soybean lots used for standard deviation factor (SDF) for particle size distribution.

	Single Kernel Mass, mg									
Kernel No.	9A411NRR	9A385NRS	KS-5005sp	KS-3406RR	KS-4607	KS-4702sp	Mixed (100-lb)	Mixed (7080-lb)	KS-5002N (4RL9542)	KS-4103sp (4RL4976)
1	114.793	147.106	214.333	146.56	185.204	163.043	144.944	117.393	87.279	125.523
2	110.892	120.015	277.781	204.984	179.311	147.652	149.107	119.763	141.636	228.693
3	121.208	107.583	201.882	209.601	192.675	175.428	100.361	120.372	128.418	171.566
4	135.559	120.988	262.118	154.869	177.065	155.677	154.166	159.149	164.166	186.928
5	88.924	131.581	219.58	207.796	127.627	127.864	84.899	117.606	125.772	147.688
6	96.088	115.751	228.968	154.479	206.418	109.313	124.754	169.292	146.586	172.652
7	105.021	114.783	199.664	174.381	181.207	189.872	111.467	206.069	151.955	199.252
8	103.863	155.458	212.368	114.126	182.118	159.905	142.335	141.256	171.776	184.242
9	69.085	119.821	273.844	161.121	200.492	161.182	108.978	160.226	140.504	169.584
10	82.966	105.862	240.351	163.219	166.211	194.052	120.803	121.932	113.276	156.975
11	131.86	93.083	274.591	129.845	167.546	136.476	158.821	136.026	146.569	158.421
12	86.636	141.964	236.971	200.771	169.245	180.529	128.747	189.019	117.902	141.065
13	63.203	155.114	198.074	174.328	148.756	151.993	133.988	132.212	130.389	170.814
14	104.507	76.285	188.374	139.56	134.017	123.568	123.256	145.151	152.67	171.899
15	132.351	112.822	176.878	159.957	177.807	206.33	136.73	176.212	105.043	104.116
16	90.77	137.224	267.713	153.297	142.818	145.004	150.573	147.491	143.923	175.889
17	123.314	125.889	241.004	124.65	178.317	188.295	168.022	142.436	162.64	198.681
18	139.952	124.971	222.929	187.329	111.802	126.394	120.242	170.949	168.473	203.825
19	109.783	119.365	209.122	124.729	186.944	146.242	118.363	167.079	136.006	153.413
20	155.207	94.351	206.137	152.387	138.46	146.736	159.791	137.171	102.278	160.516
21	118.521	111.463	260.022	123.605	79.455	189.534	147.418	122.349	138.317	232.946
22	87.69	152.314	237.486	178.91	128.563	161.934	88.532	122.28	132.622	112.779
23	110.83	157.41	209.906	172.951	190.769	185.039	148.113	128.563	75.197	168.512
24	147.419	141.534	193.477	128.635	137.28	152.855	188.814	135.769	138.05	151.645
25	101.503	137.463	244.272	95.708	135.558	136.36	81.795	165.636	189.707	132.006
26	129.602	77.817	287.763	146.749	198.502	177.993	125.782	146.593	141.311	202.837
27	118.61	125.253	241.846	154.998	178.408	185.682	112.077	119.584	149.383	217.599
28	116.444	137.128	238.119	117.47	236.376	229.006	166.882	156.291	147.111	151.657
29	128.245	137.99	257.734	136.888	175.134	156.754	127.667	178.502	113.708	172.114
30	141.564	141.506	195.573	121.678	165.229	147.238	151.285	141.522	144.113	167.634
31	91.15	145.078	237.614	143.201	205.471	140.385	135.778	199.387	96.502	226.115
32	116.128	110.009	188.477	165.132	185.586	172.129	141.949	110.574	68.294	117.639
33	94.964	115.164	199.159	179.872	162.174	146.009	159.244	126.899	116.686	162.531
34	94.336	168.557	172.203	131.877	144.017	146.363	138.99	132.281	120.648	150.882
35	124.903	93.115	150.751	155.451	180.702	180.089	172.405	144.437	106.545	107.772
36	124.289	82.3	129.028	80.38	143.751	116.072	95.226	144.489	75.085	169.182
37	131.558	138.168	185.944	171.521	138.388	142.548	141.397	172.309	143.368	146.339
38	121.468	155.73	250.393	178.856	137.085	148.061	180.261	171.59	115.333	174.241
39	104.815	183.176	196.806	116.527	145.066	175.043	171.788	119.781	125.095	196.714
40	123.314	152.371	138.119	156.528	140.138	190.322	98.315	148.637	106.002	172.912
41	110.364	123.508	258.744	131.075	160.342	139.853	143.148	90.346	141.889	125.366
42	113.481	104.014	225.207	105.051	150.789	145.078	128.269	87.793	103.939	134.145
43	81.201	156.183	245.082	180.761	164.476	166.361	99.453	158.228	59.017	112.646
44	151.59	113.424	231.081	166.807	111.418	101.692	112.789	147.548	123.275	134.025
45	108.182	108.918	270.369	113.189	137.458	137.314	141.036	183.588	108.835	136.412
46	123.294	145.515	257.269	172.426	134.744	103.6	113.677	146.109	73.259	166.255
47	106.622	157.706	232.749	202.219	141.785	115.774	177.609	119.197	89.664	92.881
48	128.668	120.16	274.946	187.516	135.944	118.289	135.702	164.957	126.533	137.127
49	107.67	100.127	202.588	92.058	104.479	120.304	143.571	175.519	61.52	113.882
50	118.225	113.856	225.256	104.675	103.472	99.99	112.144	144.165	105.017	171.512
51		97.928	100.68	170.187	117.823	88.518	91.858	128.154	124.432	96.06
52		77.138		88.231		101.494	154.076	151.816	149.185	161.799
53		129.506		135.986		69.417	114.173	126.593	117.106	93.708
54		75.19					140.534	136.213	125.817	133.216
55		72.824					90.973	108.515	117.589	133.311
56		88.47							147.447	

Table A.70 Coefficient of restitution from test combination 11111 for 1-sphere particle model.

Particle No.	Initial Height, mm	Rebound Height, mm	Restitution Coefficient
1	150.61	55.89	0.61
2	151.13	56.61	0.61
3	151.41	58.64	0.62
4	154.58	59.64	0.62
5	159.28	58.14	0.60
6	151.90	55.90	0.61
7	153.82	59.45	0.62
8	151.62	55.57	0.61
9	157.90	58.60	0.61
10	155.61	56.86	0.60
11	155.87	57.10	0.61
12	151.68	55.59	0.61
13	159.91	61.40	0.62
14	157.18	57.41	0.60
15	154.28	56.78	0.61
16	157.34	57.89	0.61
17	157.11	59.37	0.61
18	159.97	58.84	0.61
19	157.83	57.60	0.60
20	155.91	57.92	0.61
21	157.80	57.82	0.61
22	152.28	58.88	0.62
23	154.43	57.81	0.61
24	156.68	60.34	0.62
25	154.30	56.74	0.61
26	153.45	56.26	0.61
27	154.74	57.90	0.61
28	153.69	56.39	0.61
29	156.48	60.26	0.62
30	154.04	56.48	0.61
31	153.08	56.55	0.61
32	153.01	56.03	0.61
33	150.70	55.35	0.61
34	155.38	58.00	0.61
35	158.29	60.88	0.62
36	154.25	57.04	0.61
37	154.41	56.74	0.61
38	154.66	59.67	0.62
39	151.29	55.48	0.61
40	158.00	58.10	0.61
41	157.01	60.47	0.62
42	155.85	57.66	0.61
43	157.51	57.96	0.61
44	154.96	57.31	0.61
45	156.09	60.12	0.62
46	160.16	58.40	0.60
47	154.36	57.04	0.61
48	159.18	61.16	0.62
49	154.48	56.68	0.61
50	152.45	55.85	0.61

Table A.71 Coefficient of restitution from test combination 21111 for 1-sphere particle model.

Particle No.	Initial Height, mm	Rebound Height, mm	Restitution Coefficient
1	150.61	55.89	0.61
2	151.13	56.61	0.61
3	151.41	58.64	0.62
4	154.58	59.64	0.62
5	159.28	58.14	0.60
6	151.90	55.90	0.61
7	153.82	59.45	0.62
8	151.62	55.57	0.61
9	157.90	58.60	0.61
10	155.61	56.86	0.60
11	155.87	57.10	0.61
12	151.68	55.59	0.61
13	159.91	61.40	0.62
14	157.18	57.41	0.60
15	154.28	56.78	0.61
16	157.34	57.89	0.61
17	157.11	59.37	0.61
18	159.97	58.84	0.61
19	157.83	57.60	0.60
20	155.91	57.92	0.61
21	157.80	57.82	0.61
22	152.28	58.88	0.62
23	154.43	57.81	0.61
24	156.68	60.34	0.62
25	154.30	56.74	0.61
26	153.45	56.26	0.61
27	154.74	57.90	0.61
28	153.69	56.39	0.61
29	156.48	60.26	0.62
30	154.04	56.48	0.61
31	153.08	56.55	0.61
32	153.01	56.03	0.61
33	150.70	55.35	0.61
34	155.38	58.00	0.61
35	158.29	60.88	0.62
36	154.25	57.04	0.61
37	154.41	56.74	0.61
38	154.66	59.67	0.62
39	151.29	55.48	0.61
40	158.00	58.10	0.61
41	157.01	60.47	0.62
42	155.85	57.66	0.61
43	157.51	57.96	0.61
44	154.96	57.31	0.61
45	156.09	60.12	0.62
46	160.16	58.40	0.60
47	154.36	57.04	0.61
48	159.18	61.16	0.62
49	154.48	56.68	0.61
50	152.45	55.85	0.61

Table A.72 Coefficient of restitution from test combination 31111 for 1-sphere particle model.

Particle No.	Initial Height, mm	Rebound Height, mm	Restitution Coefficient
1	158.54	128.91	0.90
2	160.02	130.38	0.90
3	160.72	130.63	0.90
4	159.80	129.97	0.90
5	153.71	125.13	0.90
6	155.62	126.63	0.90
7	155.43	126.46	0.90
8	157.84	128.47	0.90
9	155.21	126.28	0.90
10	159.64	130.00	0.90
11	158.25	129.08	0.90
12	152.98	124.73	0.90
13	152.33	124.07	0.90
14	155.72	126.81	0.90
15	157.96	128.45	0.90
16	152.24	124.17	0.90
17	155.25	126.64	0.90
18	158.68	129.27	0.90
19	154.10	125.40	0.90
20	153.69	125.34	0.90
21	152.71	124.49	0.90
22	156.11	127.08	0.90
23	158.92	129.35	0.90
24	151.69	122.91	0.90
25	160.56	130.57	0.90
26	152.80	124.64	0.90
27	155.08	126.23	0.90
28	156.67	127.43	0.90
29	157.92	127.91	0.90
30	154.11	125.73	0.90
31	159.63	129.93	0.90
32	155.03	126.33	0.90
33	151.26	123.39	0.90
34	160.84	131.21	0.90
35	158.68	129.44	0.90
36	151.48	123.32	0.90
37	153.91	124.63	0.90
38	152.29	124.07	0.90
39	154.61	125.17	0.90
40	157.27	128.24	0.90
41	159.50	130.08	0.90
42	159.38	129.92	0.90
43	157.60	128.39	0.90
44	158.59	129.02	0.90
45	157.75	128.29	0.90
46	156.41	127.54	0.90
47	156.06	126.95	0.90
48	155.20	126.47	0.90
49	156.78	127.75	0.90
50	151.16	123.16	0.90

Table A.73 Coefficient of restitution from test combination 12111 for 1-sphere particle model.

Particle No.	Initial Height, mm	Rebound Height, mm	Restitution Coefficient
1	150.61	55.89	0.61
2	151.13	56.61	0.61
3	151.41	58.64	0.62
4	154.58	59.64	0.62
5	159.28	58.14	0.60
6	151.90	55.90	0.61
7	153.82	59.45	0.62
8	151.62	55.57	0.61
9	157.90	58.60	0.61
10	155.61	56.86	0.60
11	155.87	57.10	0.61
12	151.68	55.59	0.61
13	159.91	61.40	0.62
14	157.18	57.41	0.60
15	154.28	56.78	0.61
16	157.34	57.89	0.61
17	157.11	59.37	0.61
18	159.97	58.84	0.61
19	157.83	57.60	0.60
20	155.91	57.92	0.61
21	157.80	57.82	0.61
22	152.28	58.88	0.62
23	154.43	57.81	0.61
24	156.68	60.34	0.62
25	154.30	56.74	0.61
26	153.45	56.26	0.61
27	154.74	57.90	0.61
28	153.69	56.39	0.61
29	156.48	60.26	0.62
30	154.04	56.48	0.61
31	153.08	56.55	0.61
32	153.01	56.03	0.61
33	150.70	55.35	0.61
34	155.38	58.00	0.61
35	158.29	60.88	0.62
36	154.25	57.04	0.61
37	154.41	56.74	0.61
38	154.66	59.67	0.62
39	151.29	55.48	0.61
40	158.00	58.10	0.61
41	157.01	60.47	0.62
42	155.85	57.66	0.61
43	157.51	57.96	0.61
44	154.96	57.31	0.61
45	156.09	60.12	0.62
46	160.16	58.40	0.60
47	154.36	57.04	0.61
48	159.18	61.16	0.62
49	154.48	56.68	0.61
50	152.45	55.85	0.61

Table A.74 Coefficient of restitution from test combination 13111 for 1-sphere particle model.

Particle No.	Initial Height, mm	Rebound Height, mm	Restitution Coefficient
1	155.69	60.01	0.62
2	153.75	56.29	0.61
3	152.59	56.36	0.61
4	160.05	58.55	0.60
5	159.86	59.72	0.61
6	157.61	60.72	0.62
7	152.72	55.94	0.61
8	160.35	59.01	0.61
9	150.77	55.51	0.61
10	152.91	56.00	0.61
11	156.99	57.87	0.61
12	160.23	58.36	0.60
13	150.55	55.84	0.61
14	159.35	59.85	0.61
15	155.61	59.98	0.62
16	152.89	56.03	0.61
17	154.03	59.53	0.62
18	152.50	56.20	0.61
19	152.77	55.94	0.61
20	158.01	58.92	0.61
21	158.55	57.81	0.60
22	152.65	59.04	0.62
23	156.04	57.48	0.61
24	158.78	58.16	0.61
25	152.86	56.28	0.61
26	152.65	56.54	0.61
27	153.29	56.27	0.61
28	151.29	55.52	0.61
29	155.91	57.50	0.61
30	155.59	57.37	0.61
31	155.02	56.73	0.60
32	157.95	57.84	0.61
33	154.19	57.99	0.61
34	153.26	56.16	0.61
35	155.97	56.97	0.60
36	155.38	59.99	0.62
37	159.38	59.02	0.61
38	158.09	57.66	0.60
39	154.37	56.69	0.61
40	159.94	58.42	0.60
41	158.52	57.80	0.60
42	156.60	60.29	0.62
43	154.37	57.09	0.61
44	151.64	58.71	0.62
45	151.40	55.75	0.61
46	158.77	58.28	0.61
47	158.71	58.40	0.61
48	157.19	60.51	0.62
49	157.76	57.56	0.60
50	151.55	56.17	0.61

Table A.75 Coefficient of restitution from test combination 11211 for 1-sphere particle model.

Particle No.	Initial Height, mm	Rebound Height, mm	Restitution Coefficient
1	153.91	56.48	0.61
2	153.68	59.19	0.62
3	160.61	58.74	0.60
4	153.55	56.61	0.61
5	156.65	58.13	0.61
6	155.43	56.69	0.60
7	159.58	57.98	0.60
8	157.89	58.03	0.61
9	159.16	57.94	0.60
10	158.57	58.79	0.61
11	152.12	55.61	0.60
12	151.82	55.66	0.61
13	154.12	56.34	0.60
14	155.92	56.80	0.60
15	156.07	56.96	0.60
16	154.17	56.86	0.61
17	155.68	59.25	0.62
18	152.28	55.90	0.61
19	153.37	56.04	0.60
20	156.54	57.53	0.61
21	158.78	60.94	0.62
22	154.75	56.47	0.60
23	154.12	56.50	0.61
24	160.28	61.41	0.62
25	152.64	56.30	0.61
26	151.59	55.41	0.60
27	158.87	60.88	0.62
28	151.67	55.46	0.60
29	153.71	57.12	0.61
30	152.67	56.42	0.61
31	157.40	57.57	0.60
32	156.18	60.02	0.62
33	151.80	55.86	0.61
34	151.96	58.67	0.62
35	158.91	59.05	0.61
36	155.71	59.92	0.62
37	157.46	57.30	0.60
38	154.34	56.29	0.60
39	155.92	57.35	0.61
40	157.24	57.40	0.60
41	154.67	56.42	0.60
42	151.15	58.38	0.62
43	151.03	56.13	0.61
44	155.71	57.08	0.61
45	157.77	58.75	0.61
46	159.68	58.77	0.61
47	152.60	55.81	0.60
48	153.33	56.56	0.61
49	154.88	57.04	0.61
50	158.49	58.33	0.61

Table A.76 Coefficient of restitution from test combination 11311 for 1-sphere particle model.

Particle No.	Initial Height, mm	Rebound Height, mm	Restitution Coefficient
1	155.63	58.07	0.61
2	155.76	56.80	0.60
3	154.69	57.22	0.61
4	160.04	58.17	0.60
5	160.20	58.18	0.60
6	160.37	58.29	0.60
7	155.77	57.91	0.61
8	153.83	56.15	0.60
9	152.02	55.59	0.60
10	154.64	57.27	0.61
11	156.46	57.26	0.60
12	157.07	57.40	0.60
13	159.67	58.01	0.60
14	153.22	56.25	0.61
15	156.45	57.66	0.61
16	152.82	55.84	0.60
17	158.26	57.68	0.60
18	155.81	56.91	0.60
19	158.49	57.73	0.60
20	160.37	58.25	0.60
21	155.89	56.87	0.60
22	159.39	59.05	0.61
23	160.65	58.59	0.60
24	154.92	57.29	0.61
25	160.68	59.00	0.61
26	159.29	58.12	0.60
27	154.64	56.83	0.61
28	160.25	58.72	0.61
29	156.18	57.33	0.61
30	155.46	57.17	0.61
31	159.18	58.52	0.61
32	154.14	57.01	0.61
33	158.64	57.85	0.60
34	158.27	59.88	0.62
35	152.24	56.08	0.61
36	151.16	55.55	0.61
37	151.61	55.59	0.61
38	157.66	57.91	0.61
39	160.35	58.24	0.60
40	158.57	58.44	0.61
41	158.41	57.63	0.60
42	157.68	57.49	0.60
43	153.42	56.14	0.60
44	153.47	56.07	0.60
45	156.68	60.18	0.62
46	152.37	55.74	0.60
47	158.38	58.05	0.61
48	159.29	58.04	0.60
49	158.27	58.67	0.61
50	151.90	58.61	0.62

Table A.77 Coefficient of restitution from test combination 11121 for 1-sphere particle model.

Particle No.	Initial Height, mm	Rebound Height, mm	Restitution Coefficient
1	159.73	57.36	0.60
2	151.15	56.19	0.61
3	151.54	55.20	0.60
4	155.72	56.97	0.60
5	156.14	56.41	0.60
6	159.84	58.66	0.61
7	160.59	58.24	0.60
8	152.49	56.35	0.61
9	156.50	57.67	0.61
10	155.18	58.58	0.61
11	160.92	58.38	0.60
12	155.71	57.02	0.61
13	151.09	55.03	0.60
14	157.29	58.56	0.61
15	158.20	57.04	0.60
16	154.87	57.56	0.61
17	158.05	58.27	0.61
18	153.34	56.66	0.61
19	153.99	58.03	0.61
20	153.96	56.90	0.61
21	157.24	56.75	0.60
22	154.30	58.78	0.62
23	157.02	58.18	0.61
24	153.53	56.12	0.60
25	153.52	56.39	0.61
26	153.40	57.72	0.61
27	154.76	58.39	0.61
28	154.65	56.77	0.61
29	152.30	56.32	0.61
30	158.46	57.09	0.60
31	158.14	57.90	0.61
32	152.62	55.79	0.60
33	154.91	57.33	0.61
34	154.96	57.87	0.61
35	157.53	59.20	0.61
36	160.06	57.59	0.60
37	151.31	55.24	0.60
38	157.66	56.72	0.60
39	153.61	56.53	0.61
40	156.23	57.27	0.61
41	152.64	56.33	0.61
42	154.11	56.02	0.60
43	158.87	59.14	0.61
44	155.51	58.83	0.62
45	160.43	59.36	0.61
46	159.26	58.74	0.61
47	156.28	56.66	0.60
48	159.29	60.43	0.62
49	153.77	55.77	0.60
50	159.76	58.20	0.60

Table A.78 Coefficient of restitution from test combination 11131 for 1-sphere particle model.

Particle No.	Initial Height, mm	Rebound Height, mm	Restitution Coefficient
1	159.68	59.43	0.61
2	159.78	61.26	0.62
3	154.44	55.83	0.60
4	153.90	56.32	0.60
5	160.93	58.95	0.61
6	152.53	56.48	0.61
7	160.53	58.35	0.60
8	153.17	56.52	0.61
9	158.13	59.19	0.61
10	152.22	57.70	0.62
11	157.14	58.54	0.61
12	153.60	54.57	0.60
13	153.21	57.59	0.61
14	160.58	59.46	0.61
15	160.23	60.74	0.62
16	157.91	57.80	0.61
17	157.46	59.56	0.61
18	158.22	56.97	0.60
19	155.13	57.74	0.61
20	160.60	57.45	0.60
21	160.89	59.08	0.61
22	151.39	56.93	0.61
23	159.04	59.49	0.61
24	153.80	55.36	0.60
25	160.93	60.76	0.61
26	157.71	56.97	0.60
27	160.11	59.48	0.61
28	156.39	58.54	0.61
29	158.91	57.30	0.60
30	160.07	58.92	0.61
31	155.80	57.37	0.61
32	158.50	60.06	0.62
33	157.73	58.86	0.61
34	153.43	56.40	0.61
35	153.54	58.30	0.62
36	151.36	57.97	0.62
37	158.34	57.46	0.60
38	154.35	58.28	0.61
39	151.98	57.39	0.61
40	157.19	59.47	0.62
41	151.35	57.56	0.62
42	156.63	56.15	0.60
43	159.28	59.35	0.61
44	157.57	59.25	0.61
45	156.63	58.41	0.61
46	158.32	60.20	0.62
47	158.40	57.93	0.60
48	158.34	58.87	0.61
49	158.41	60.75	0.62
50	160.71	58.80	0.60

Table A.79 Coefficient of restitution from test combination 11112 for 1-sphere particle model.

Particle No.	Initial Height, mm	Rebound Height, mm	Restitution Coefficient
1	159.22	60.00	0.61
2	160.47	60.38	0.61
3	158.87	55.22	0.59
4	159.16	55.64	0.59
5	159.61	55.71	0.59
6	152.11	57.80	0.62
7	156.17	59.02	0.61
8	155.88	55.70	0.60
9	155.69	54.09	0.59
10	156.16	59.17	0.62
11	158.13	59.69	0.61
12	154.86	54.84	0.60
13	158.26	59.67	0.61
14	159.58	60.43	0.62
15	151.21	57.46	0.62
16	158.05	56.83	0.60
17	160.65	60.48	0.61
18	151.59	52.62	0.59
19	156.08	58.98	0.61
20	156.40	56.98	0.60
21	155.39	58.76	0.61
22	151.41	52.48	0.59
23	152.49	54.17	0.60
24	157.79	55.31	0.59
25	151.11	57.87	0.62
26	155.40	58.76	0.61
27	152.42	57.84	0.62
28	151.08	57.47	0.62
29	151.61	57.54	0.62
30	153.52	53.23	0.59
31	152.75	53.23	0.59
32	152.48	52.86	0.59
33	157.05	54.67	0.59
34	156.51	55.73	0.60
35	157.22	59.38	0.61
36	155.13	55.60	0.60
37	160.72	55.45	0.59
38	160.65	60.53	0.61
39	151.50	53.44	0.59
40	154.72	58.54	0.62
41	153.17	58.37	0.62
42	158.55	55.94	0.59
43	157.77	59.68	0.62
44	157.83	54.67	0.59
45	154.07	58.99	0.62
46	153.74	53.30	0.59
47	156.58	59.30	0.62
48	155.03	58.64	0.62
49	152.88	55.07	0.60
50	151.04	52.42	0.59

Table A.80 Coefficient of restitution from test combination 11113 for 1-sphere particle model.

Particle No.	Initial Height, mm	Rebound Height, mm	Restitution Coefficient
1	155.44	59.28	0.62
2	160.26	55.09	0.59
3	156.54	58.12	0.61
4	153.96	58.69	0.62
5	157.22	58.93	0.61
6	156.60	55.20	0.59
7	156.37	57.82	0.61
8	156.27	59.53	0.62
9	152.97	52.92	0.59
10	160.78	60.13	0.61
11	158.18	57.95	0.61
12	160.75	54.27	0.58
13	151.09	55.59	0.61
14	156.62	58.21	0.61
15	153.15	57.19	0.61
16	153.80	58.10	0.61
17	151.28	56.17	0.61
18	159.19	58.40	0.61
19	156.56	58.65	0.61
20	160.61	61.14	0.62
21	155.76	52.72	0.58
22	153.70	56.35	0.61
23	151.69	56.45	0.61
24	155.85	57.08	0.61
25	153.24	56.70	0.61
26	152.56	56.12	0.61
27	152.85	56.22	0.61
28	157.48	57.53	0.60
29	155.88	57.96	0.61
30	151.50	51.84	0.58
31	159.10	60.08	0.61
32	160.47	58.93	0.61
33	152.37	55.95	0.61
34	156.60	59.66	0.62
35	151.28	56.20	0.61
36	153.03	56.13	0.61
37	156.75	53.35	0.58
38	157.85	57.92	0.61
39	157.64	57.64	0.60
40	157.78	58.44	0.61
41	156.54	58.05	0.61
42	156.28	58.54	0.61
43	153.20	56.18	0.61
44	151.94	56.56	0.61
45	159.87	58.96	0.61
46	158.95	59.01	0.61
47	159.21	58.93	0.61
48	158.94	59.41	0.61
49	153.15	57.58	0.61
50	157.54	58.44	0.61

Table A.81 Coefficient of restitution from test combination 11111 for 2-sphere particle model.

Particle No.	Initial Height, mm	Rebound Height, mm	Restitution Coefficient
1	154.04	55.96	0.60
2	153.12	57.93	0.62
3	159.14	57.72	0.60
4	158.47	57.76	0.60
5	152.36	55.67	0.60
6	160.51	58.05	0.60
7	151.58	57.47	0.62
8	154.91	58.63	0.62
9	152.11	55.26	0.60
10	154.70	56.36	0.60
11	152.89	56.22	0.61
12	154.16	55.95	0.60
13	154.35	56.09	0.60
14	158.94	59.79	0.61
15	156.50	59.03	0.61
16	157.87	59.44	0.61
17	157.81	59.42	0.61
18	153.63	58.13	0.62
19	154.35	58.33	0.61
20	159.16	59.93	0.61
21	155.14	57.08	0.61
22	155.41	58.65	0.61
23	160.77	60.40	0.61
24	151.04	55.03	0.60
25	158.52	57.94	0.60
26	160.40	60.46	0.61
27	155.42	56.41	0.60
28	160.53	60.61	0.61
29	156.34	56.94	0.60
30	153.25	57.98	0.62
31	159.93	60.14	0.61
32	151.63	57.48	0.62
33	153.74	58.14	0.61
34	151.08	55.23	0.60
35	151.54	55.27	0.60
36	157.82	57.30	0.60
37	156.53	59.01	0.61
38	154.21	55.95	0.60
39	160.69	60.45	0.61
40	155.81	56.51	0.60
41	160.30	58.10	0.60
42	152.11	55.28	0.60
43	157.81	58.98	0.61
44	159.78	57.95	0.60
45	152.07	57.80	0.62
46	152.29	57.63	0.62
47	152.92	55.67	0.60
48	152.62	57.87	0.62
49	159.21	59.87	0.61
50	159.52	60.05	0.61

Table A.82 Coefficient of restitution from test combination 11111 for 3-sphere particle model.

Particle No.	Initial Height, mm	Rebound Height, mm	Restitution Coefficient
1	156.64	56.83	0.60
2	158.59	59.80	0.61
3	159.58	60.12	0.61
4	152.59	55.34	0.60
5	158.08	58.13	0.61
6	156.94	57.82	0.61
7	153.22	55.53	0.60
8	154.35	56.01	0.60
9	152.29	57.87	0.62
10	159.16	57.99	0.60
11	157.74	57.78	0.61
12	155.96	58.96	0.61
13	154.29	55.86	0.60
14	160.76	58.54	0.60
15	152.78	57.97	0.62
16	158.49	59.85	0.61
17	152.32	55.93	0.61
18	156.24	57.77	0.61
19	160.31	58.04	0.60
20	157.19	57.36	0.60
21	152.60	57.89	0.62
22	158.06	55.33	0.59
23	158.62	57.45	0.60
24	158.53	57.49	0.60
25	159.02	60.07	0.61
26	154.53	58.46	0.62
27	157.64	57.22	0.60
28	154.08	52.41	0.58
29	153.28	55.69	0.60
30	160.07	58.22	0.60
31	152.15	57.70	0.62
32	152.95	55.44	0.60
33	151.20	56.03	0.61
34	157.38	59.39	0.61
35	156.25	56.56	0.60
36	158.99	59.96	0.61
37	156.29	56.55	0.60
38	155.91	56.59	0.60
39	158.17	57.43	0.60
40	155.65	58.87	0.61
41	155.69	56.36	0.60
42	156.99	56.86	0.60
43	157.02	59.27	0.61
44	159.15	58.10	0.60
45	157.14	56.79	0.60
46	153.64	56.33	0.61
47	160.53	57.91	0.60
48	158.98	58.20	0.61
49	154.84	58.64	0.62
50	151.99	57.64	0.62

Table A.83 Coefficient of restitution from test combination 11111 for 4-sphere particle model.

Particle No.	Initial Height, mm	Rebound Height, mm	Restitution Coefficient
1	158.48	57.62	0.60
2	157.70	59.82	0.62
3	159.72	58.57	0.61
4	157.35	57.34	0.60
5	158.54	60.12	0.62
6	156.28	59.43	0.62
7	157.35	59.72	0.62
8	159.75	60.51	0.62
9	160.46	60.73	0.62
10	160.26	60.87	0.62
11	159.86	58.10	0.60
12	154.26	56.28	0.60
13	152.95	58.27	0.62
14	153.70	56.00	0.60
15	158.12	60.14	0.62
16	156.54	57.77	0.61
17	156.71	57.88	0.61
18	155.53	56.58	0.60
19	158.29	58.05	0.61
20	153.55	56.40	0.61
21	158.28	60.18	0.62
22	156.34	56.84	0.60
23	159.85	60.54	0.62
24	158.01	60.03	0.62
25	160.86	60.86	0.62
26	159.62	60.45	0.62
27	158.04	57.62	0.60
28	160.43	58.36	0.60
29	159.18	57.79	0.60
30	153.44	57.05	0.61
31	160.05	58.08	0.60
32	152.87	56.60	0.61
33	155.84	57.96	0.61
34	155.18	56.56	0.60
35	160.43	58.29	0.60
36	156.44	59.48	0.62
37	154.20	58.69	0.62
38	151.03	57.81	0.62
39	152.77	56.50	0.61
40	153.74	58.61	0.62
41	160.17	60.62	0.62
42	159.81	60.51	0.62
43	154.11	56.39	0.60
44	151.19	57.71	0.62
45	151.33	55.25	0.60
46	154.44	56.24	0.60
47	158.74	60.16	0.62
48	160.03	60.58	0.62
49	152.06	58.09	0.62
50	160.13	60.74	0.62

Table A.84 Bulk density results from all test combinations.

Test Combination	Run No.	Total Mass, kg	Bulk Density, kg·m^{-3}
1s_11111	1	0.737	668.03
	2	0.740	670.84
	3	0.737	668.12
1s_21111	1	0.729	660.69
	2	0.730	660.96
	3	0.728	659.51
1s_31111	1	0.759	687.51
	2	0.757	686.06
	3	0.759	687.78
1s_12111	1	0.746	676.18
	2	0.749	678.54
	3	0.751	680.17
1s_13111	1	0.732	663.41
	2	0.739	669.12
	3	0.733	664.50
1s_11211	1	0.751	680.44
	2	0.751	679.99
	3	0.750	679.81
1s_11311	1	0.724	655.89
	2	0.725	656.61
	3	0.726	657.34
1s_11121	1	0.738	668.57
	2	0.738	668.21
	3	0.738	668.75
1s_11131	1	0.737	667.30
	2	0.743	672.74
	3	0.741	671.74
1s_11112	1	0.743	673.28
	2	0.738	668.94
	3	0.742	672.11
1s_11113	1	0.751	679.99
	2	0.751	680.17
	3	0.750	679.63
2s_11111	1	0.746	676.00
	2	0.746	676.18
	3	0.744	674.46
3s_11111	1	0.744	673.74
	2	0.745	675.01
	3	0.743	672.92
4s_11111	1	0.742	671.93
	2	0.742	672.56
	3	0.743	673.10

Table A.84 Bulk density results from all test combinations. (cont.)

Test Combination	Run No.	Total Mass, kg	Bulk Density, kg·m^{-3}
	1	0.740	670.38
1s_41111	2	0.743	673.10
	3	0.742	671.83
	1	0.751	680.17
1s_51111	2	0.749	678.81
	3	0.750	679.35
	1	0.755	683.88
1s_11231	2	0.753	682.34
	3	0.752	680.90
	1	0.751	680.71
1s_11232	2	0.755	683.79
	3	0.754	682.89
	1	0.763	691.50
1s_11233	2	0.751	680.80
	3	0.754	682.98
	1	0.773	699.92
1s_12233	2	0.769	696.75
	3	0.769	697.02
	1	0.750	679.54
1s_14231	2	0.753	682.62
	3	0.751	680.08
	1	0.751	680.35
1s_14232	2	0.754	682.80
	3	0.753	682.16
	1	0.763	690.86
1s_14233	2	0.762	690.77
	3	0.761	689.77
	1	0.765	692.76
1s_15233	2	0.768	695.66
	3	0.764	692.31
	1	0.764	692.40
1s_16233	2	0.767	694.49
	3	0.766	694.30
	1	0.767	695.21
1s_17233	2	0.767	694.67
	3	0.769	696.30

Table A.85 Angle of repose results from all test combinations.

Test Combination	Run No.	Start Time of Particle Falling, s	Angle of Repose, deg
1s_11111	1	0.355	31.95
	2	0.347	31.23
	3	0.356	32.04
	4	0.350	31.50
	5	0.347	31.23
	6	0.347	31.23
	7	0.348	31.32
1s_21111	1	0.342	30.78
	2	0.352	31.68
	3	0.368	33.12
	4	0.362	32.58
	5	0.365	32.85
	6	0.365	32.85
	7	0.359	32.31
1s_31111	1	0.404	36.36
	2	0.418	37.62
	3	0.416	37.44
	4	0.415	37.35
	5	0.418	37.62
	6	0.410	36.90
	7	0.410	36.90
1s_12111	1	0.361	32.49
	2	0.359	32.31
	3	0.331	29.79
	4	0.347	31.23
	5	0.368	33.12
	6	0.334	30.06
	7	0.350	31.50
1s_13111	1	0.390	35.10
	2	0.440	39.60
	3	0.405	36.45
	4	0.420	37.80
	5	0.405	36.45
	6	0.425	38.25
	7	0.420	37.80
1s_11211	1	0.343	30.87
	2	0.346	31.14
	3	0.334	30.06
	4	0.335	30.15
	5	0.335	30.15
	6	0.335	30.15
	7	0.346	31.14
1s_11311	1	0.379	34.11
	2	0.389	35.01
	3	0.386	34.74
	4	0.404	36.36
	5	0.397	35.73
	6	0.382	34.38
	7	0.407	36.63

Table A.85 Angle of repose results from all test combinations. (cont.)

Test Combination	Run No.	Start Time of Particle Falling, s	Angle of Repose, deg
1s_11121	1	0.316	28.44
	2	0.328	29.52
	3	0.323	29.07
	4	0.327	29.43
	5	0.330	29.70
	6	0.332	29.88
	7	0.323	29.07
1s_11131	1	0.347	31.23
	2	0.361	32.49
	3	0.361	32.49
	4	0.379	34.11
	5	0.379	34.11
	6	0.353	31.77
	7	0.359	32.31
1s_11112	1	0.354	31.86
	2	0.354	31.82
	3	0.340	30.56
	4	0.346	31.14
	5	0.351	31.59
	6	0.355	31.92
	7	0.347	31.26
1s_11113	1	0.369	33.21
	2	0.356	32.04
	3	0.352	31.68
	4	0.371	33.39
	5	0.369	33.21
	6	0.363	32.66
	7	0.367	33.05
2s_11111	1	0.323	29.07
	2	0.321	28.89
	3	0.328	29.52
	4	0.322	28.98
	5	0.328	29.52
	6	0.326	29.34
	7	0.329	29.61
3s_11111	1	0.313	28.17
	2	0.319	28.71
	3	0.325	29.25
	4	0.322	28.98
	5	0.331	29.79
	6	0.329	29.61
	7	0.326	29.34
4s_11111	1	0.317	28.53
	2	0.316	28.44
	3	0.355	31.95
	4	0.325	29.25
	5	0.325	29.25
	6	0.322	28.98
	7	0.328	29.52

Table A.85 Angle of repose results from all test combinations. (cont.)

Test Combination	Run No.	Start Time of Particle Falling, s	Angle of Repose, deg
1s_11231	1	0.349	31.44
	2	0.345	31.08
	3	0.340	30.63
	4	0.351	31.62
	5	0.355	31.92
	6	0.356	32.01
	7	0.356	32.07
1s_11232	1	0.373	33.54
	2	0.363	32.64
	3	0.351	31.62
	4	0.356	32.04
	5	0.354	31.89
	6	0.354	31.83
	7	0.350	31.47
1s_11233	1	0.362	32.55
	2	0.360	32.40
	3	0.355	31.96
	4	0.341	30.69
	5	0.347	31.26
	6	0.357	32.13
	7	0.359	32.28
1s_12233	1	0.309	27.82
	2	0.312	28.05
	3	0.322	29.01
	4	0.323	29.05
	5	0.326	29.32
	6	0.315	28.35
	7	0.313	28.17
1s_14231	1	0.365	32.85
	2	0.375	33.78
	3	0.370	33.33
	4	0.367	33.00
	5	0.368	33.12
	6	0.371	33.36
	7	0.361	32.52
1s_14232	1	0.343	30.84
	2	0.351	31.56
	3	0.334	30.09
	4	0.344	30.99
	5	0.349	31.38
	6	0.346	31.17
	7	0.347	31.20
1s_14233	1	0.355	31.98
	2	0.363	32.70
	3	0.380	34.23
	4	0.364	32.80
	5	0.378	33.99
	6	0.373	33.54
	7	0.388	34.89

Table A.85 Angle of repose results from all test combinations. (cont.)

Test Combination	Run No.	Start Time of Particle Falling, s	Angle of Repose, deg
1s_15233	1	0.349	31.44
	2	0.352	31.69
	3	0.345	31.09
	4	0.344	30.99
	5	0.337	30.33
	6	0.349	31.44
	7	0.349	31.44
1s_16233	1	0.347	31.27
	2	0.330	29.74
	3	0.345	31.08
	4	0.344	30.96
	5	0.342	30.81
	6	0.347	31.26
	7	0.345	31.09
1s_17233	1	0.323	29.10
	2	0.315	28.38
	3	0.321	28.92
	4	0.319	28.74
	5	0.327	29.43
	6	0.325	29.22
	7	0.325	29.25

Data for Chapter 6

Table A.86 Test weights of red and clear soybean samples used in the experiment.

		Red Soybeans		Clear Soybeans	
Bag No.	**Test No.**	**Test Weight, lb·bu^{-1}**	**Test Weight, kg·m^{-3}**	**Test Weight, lb·bu^{-1}**	**Test Weight, kg·m^{-3}**
1	1	54.53	701.80	56.51	727.28
1	2	54.66	703.47	56.61	728.57
1	3	54.88	706.31	56.77	730.63
2	1	54.18	697.30	56.51	727.28
2	2	54.27	698.45	56.48	726.90
2	3	54.27	698.45	56.48	726.90
3	1	54.21	697.68	56.58	728.18
3	2	54.27	698.45	56.74	730.24
3	3	54.43	700.51	56.58	728.18
4	1	54.78	705.02	56.83	731.40
4	2	54.72	704.25	56.58	728.18
4	3	54.72	704.25	56.80	731.02
5	1	54.05	695.62	56.61	728.57
5	2	54.34	699.36	56.61	728.57
5	3	54.27	698.45	56.67	729.34
5	4	54.56	702.19		

Table A.87 Moisture content of red and clear soybean samples used in the experiment.

		Red Soybeans			Clear Soybeans		
Bag No.	Test No.	Initial Mass, g	Final Mass, g	Moisture Content, % wb	Initial Mass, g	Final Mass, g	Moisture Content, % wb
1	1	16.815	15.183	9.706	16.563	14.951	9.733
1	2	16.633	15.028	9.649	16.556	14.945	9.731
1	3	15.078	13.612	9.723	15.291	13.793	9.797
2	1	15.923	14.331	9.998	15.034	13.435	10.636
2	2	16.298	14.661	10.044	16.298	14.564	10.639
2	3	16.120	14.495	10.081	15.224	13.597	10.687
3	1	16.296	14.753	9.469	16.217	14.573	10.138
3	2	15.507	14.036	9.486	15.170	13.631	10.145
3	3	15.252	13.810	9.454	15.046	13.520	10.142
4	1	15.945	14.418	9.577	15.591	14.001	10.198
4	2	18.389	16.629	9.571	16.321	14.655	10.208
4	3	15.753	14.238	9.617	17.383	15.711	9.619
5	1	14.997	13.500	9.982	16.544	14.904	9.913
5	2	16.340	14.721	9.908	15.266	13.752	9.917
5	3	16.888	15.194	10.031	17.587	15.847	9.894

Table A.88 Percentages of foreign materials, splits, and damaged kernels of red and clear soybean samples used in the experiment.

Material		Red Soybeans					Clear Soybeans				
	Test No.	1	2	3	4	5	1	2	3	4	5
Coarse Foreign Material (FM)	Initial Mass, g	1000.5	1002.0	1006.5	1000.5	1000.5	1000.5	1013.5	1004.0	1001.5	1010.5
	Mass of Coarse FM, g	0.00	0.00	0.00	0.00	0.18	0.00	0.00	0.11	0.00	0.00
	Coarse FM, %	0.00	0.00	0.00	0.00	0.02	0.00	0.00	0.01	0.00	0.00
Fine Foreign Material (FM)	Initial Mass, g	124.85	129.23	128.71	129.07	124.31	123.38	128.23	125.25	129.54	128.12
	Mass of Fine FM, g	0.05	0.05	0.01	0.04	0.02	0.02	0.02	0.01	0	0.02
	Fine FM, %	0.04	0.04	0.01	0.03	0.02	0.02	0.02	0.01	0.00	0.02
Splits	Initial Mass, g	124.8	129.18	128.7	129.03	124.29	123.36	128.21	125.24	129.54	128.1
	Mass of Splits, g	1.45	1.72	1.51	1.16	1.25	0.49	0.35	0.57	0.25	0.42
	Splits, %	1.16	1.33	1.17	0.90	1.01	0.40	0.27	0.46	0.19	0.33
Damaged Kernels	Initial Mass, g	124.8	129.18	128.7	129.03	124.29	123.36	128.21	125.24	129.54	128.1
	Mass of Damaged Kernels, g	0.69	0.48	0.34	0.3	0.33	1.01	1.73	1.41	2.55	0.99
	Damaged Kernels, %	1.16	1.33	1.17	0.90	1.01	0.40	0.27	0.46	0.19	0.33

Table A.89 Thousand-kernel-weight (TKW) of red and clear soybean samples used in the experiment.

	Red Soybeans					Clear Soybeans				
Test No.	Mass of Whole Soybean, g	Seed Count per Sample	Seed Count Per Gram	Seed Count per 1000-Gram	TKW, g per 1000 kernels	Mass of Whole Soybean, g	Seed Count per Sample	Seed Count Per Gram	Seed Count per 1000-Gram	TKW, g per 1000 kernels
1	25.24	156.0	6.2	6181	161.8	25.16	175.0	7.0	6955	143.8
2	25.21	156.0	6.2	6188	161.6	25.96	193.0	7.4	7435	134.5
3	25.58	155.0	6.1	6059	165.0	28.95	210.0	7.3	7254	137.9
4	27.00	170.0	6.3	6296	158.8	25.09	175.0	7.0	6975	143.4
5	25.74	170.0	6.6	6605	151.4	25.24	187.0	7.4	7409	135.0

Table A.90 Summary of soybean grading for red and clear soybean samples used in the experiment.

	Red Soybeans			Clear Soybeans		
Grading Test	Mean	SD	Grade	Mean	SD	Grade
Test Weight, $lb \cdot bu^{-1}$	54.446	0.250	US Grade 1	56.624	0.115	US Grade 1
Test Weight, $kg \cdot m^{-3}$	700.723	3.212	US Grade 1	728.751	1.476	US Grade 1
Damaged Kernels, %	0.337	0.131	US Grade 1	1.207	0.486	US Grade 1
Foreign Material, %	0.030	0.013	US Grade 1	0.013	0.008	US Grade 1
Splits, %	1.114	0.167	US Grade 1	0.329	0.103	US Grade 1
Soybeans of other colors, %	0.000	0.000	US Grade 1	0.000	0.000	US Grade 1

Table A.91 Particle density of red soybean samples used in the experiment.

Bag No.	Test No.	Mass, g	Volume, cm^3	Particle Density, $g \cdot cm^{-3}$
	1	11.40	9.16	1.24
1	2	11.39	9.14	1.25
	3	10.92	8.78	1.24
	1	10.32	8.31	1.24
2	2	11.13	8.94	1.25
	3	11.31	9.09	1.24
	1	11.03	8.90	1.24
3	2	11.02	8.84	1.25
	3	11.24	9.06	1.24
	1	11.45	9.23	1.24
4	2	11.29	9.04	1.25
	3	11.66	9.37	1.24
	1	11.28	9.09	1.24
5	2	11.01	8.85	1.24
	3	10.81	8.68	1.25

Table A.92 Particle density of clear soybean samples used in the experiment.

Bag No.	Test No.	Mass, g	Volume, cm^3	Particle Density, $g \cdot cm^{-3}$
	1	11.40	9.16	1.24
1	2	11.39	9.14	1.25
	3	10.92	8.78	1.24
	1	10.32	8.31	1.24
2	2	11.13	8.94	1.25
	3	11.31	9.09	1.24
	1	11.03	8.90	1.24
3	2	11.02	8.84	1.25
	3	11.24	9.06	1.24
	1	11.45	9.23	1.24
4	2	11.29	9.04	1.25
	3	11.66	9.37	1.24
	1	11.28	9.09	1.24
5	2	11.01	8.85	1.24
	3	10.81	8.68	1.25

Table A.93 Material flow rate of clear soybeans during experiment.[a]

Test No.	Initial Mass, kg	Total Handling Time, min	Material Flow Rate, $t \cdot h^{-1}$
1	539.26	8.86	3.65
2	492.00	9.23	3.20
3	535.40	9.28	3.46
4	543.35	10.16	3.21
5	709.70	12.15	3.51
Mean	**563.94**	**9.93**	**3.41**
SD	**84.07**	**1.33**	**0.20**

[a] Material mass was measured using platform weighing scale.

Table A.94 Residual grain height and mass of clear soybeans after handling tests.

	Residual Grain Height, mm		Residual Grain
Test No.	LHS	RHS	Mass (kg)
Clear Soybeans			
1	127.00	95.25	2.45
2	127.00	95.25	2.45
3	127.00	95.25	2.50
4	127.00	98.43	2.50
5	127.00	96.27	2.50
Mean	**127.00**	**96.09**	**2.48**
SD	**0.00**	**1.38**	**0.02**

Table A.95 Mean, minimum, and maximum mass of red and total soybean samples from five experiments.

Test Run	Total Sample Mass, g			Red Soybean Mass in Total Sample, g		
No.	Mean	Min	Max	Mean	Min	Max
1	192.86	127.38	214.35	0.91	0.00	9.17
2	184.50	167.85	200.40	0.70	0.00	7.49
3	181.33	169.82	195.92	0.28	0.00	1.61
4	174.94	159.59	201.04	0.17	0.00	0.69
5	185.67	170.88	199.07	0.09	0.00	0.38
Mean	**183.86**	**159.10**	**202.16**	**0.43**	**0.00**	**3.87**
SD	**6.53**	**18.28**	**7.10**	**0.36**	**0.00**	**4.14**

Table A.96 Instantaneous commingling during test run no. 1.

Sample No.	Actual Sampling Time Interval, s	Actual Sampling Time, min	Sample Mass, g	Red Soybean Mass, g	Instantaneous Commingling (%)
1	4	0.07	196.45	9.17	4.67
2	17	0.35	190.69	1.57	0.82
3	17	0.63	192.16	1.19	0.62
4	17	0.92	201.70	0.69	0.34
5	17	1.20	206.50	0.48	0.23
6	16	1.47	200.65	0.49	0.24
7	17	1.75	204.96	0.31	0.15
8	32	2.28	187.40	0.00	0.00
9	32	2.82	189.92	0.00	0.00
10	32	3.35	199.61	0.00	0.00
11	32	3.88	214.35	0.15	0.07
12	33	4.43	186.55	0.00	0.00
13	58	5.40	193.52	0.10	0.05
14	63	6.45	127.38	0.18	0.14
15	63	7.50	192.14	0.00	0.00
16	62	8.53	201.79	0.15	0.07

Table A.97 Instantaneous commingling during test run no. 2.

Sample No.	Actual Sampling Time Interval, s	Actual Sampling Time, min	Sample Mass, g	Red Soybean Mass, g	Instantaneous Commingling (%)
1	4	0.07	180.70	7.49	4.14
2	16	0.33	185.04	1.35	0.73
3	17	0.62	167.85	0.93	0.55
4	16	0.88	197.09	0.41	0.21
5	17	1.17	182.44	0.16	0.09
6	16	1.43	200.40	0.16	0.08
7	17	1.72	186.42	0.32	0.17
8	33	2.27	177.86	0.00	0.00
9	31	2.78	188.33	0.00	0.00
10	32	3.32	189.26	0.00	0.00
11	31	3.83	173.45	0.00	0.00
12	32	4.37	190.95	0.30	0.16
13	61	5.38	178.29	0.14	0.08
14	63	6.43	186.40	0.00	0.00
15	62	7.47	178.26	0.00	0.00
16	63	8.52	189.30	0.00	0.00

Table A.98 Instantaneous commingling during test run no. 3.

Sample No.	Actual Sampling Time Interval, s	Actual Sampling Time, min	Sample Mass, g	Red Soybean Mass, g	Instantaneous Commingling (%)
1	5	0.08	177.07	7.02	3.96
2	16	0.35	171.98	1.61	0.94
3	16	0.62	182.65	1.01	0.55
4	17	0.90	173.97	0.61	0.35
5	17	1.18	169.82	0.20	0.12
6	16	1.45	170.76	0.27	0.16
7	17	1.73	188.14	0.00	0.00
8	17	2.02	191.29	0.16	0.08
9	32	2.55	195.18	0.22	0.11
10	32	3.08	175.11	0.00	0.00
11	39	3.73	179.18	0.05	0.03
12	32	4.27	184.18	0.17	0.09
13	32	4.80	174.76	0.00	0.00
14	31	5.32	173.75	0.12	0.07
15	61	6.33	182.96	0.00	0.00
16	62	7.37	195.92	0.00	0.00
17	63	8.42	191.56	0.00	0.00

Table A.99 Instantaneous commingling during test run no. 4.

Sample No.	Actual Sampling Time Interval, s	Actual Sampling Time, min	Sample Mass, g	Red Soybean Mass, g	Instantaneous Commingling (%)
1	6	0.10	187.15	8.71	4.65
2	16	0.37	170.95	1.23	0.72
3	16	0.63	162.85	0.25	0.15
4	16	0.90	182.48	0.69	0.38
5	16	1.17	171.85	0.24	0.14
6	16	1.43	163.66	0.42	0.26
7	16	1.70	168.54	0.26	0.15
8	16	1.97	181.60	0.40	0.22
9	32	2.50	167.41	0.00	0.00
10	32	3.03	174.50	0.10	0.06
11	31	3.55	161.53	0.00	0.00
12	32	4.08	175.89	0.11	0.06
13	32	4.62	179.74	0.24	0.13
14	32	5.15	178.43	0.18	0.10
15	31	5.67	174.44	0.00	0.00
16	59	6.65	201.04	0.00	0.00
17	63	7.70	159.59	0.00	0.00
18	62	8.73	176.46	0.00	0.00
19	63	9.78	181.95	0.00	0.00

Table A.100 Instantaneous commingling during test run no. 5.

Sample No.	Actual Sampling Time Interval, s	Actual Sampling Time, min	Sample Mass, g	Red Soybean Mass, g	Instantaneous Commingling (%)
1	4	0.20	189.70	7.20	3.80
2	17	0.40	187.44	1.96	1.05
3	17	0.60	188.18	1.52	0.81
4	17	0.80	182.18	0.49	0.27
5	17	1.00	170.88	0.15	0.09
6	17	1.20	192.79	0.26	0.13
7	16	1.38	184.45	0.00	0.00
8	17	1.58	199.07	0.19	0.10
9	32	2.03	181.57	0.19	0.10
10	32	2.48	184.63	0.09	0.05
11	32	2.93	186.05	0.12	0.06
12	32	3.38	185.05	0.38	0.21
13	36	3.90	187.03	0.00	0.00
14	32	4.35	192.42	0.00	0.00
15	61	5.28	191.73	0.00	0.00
16	62	6.23	180.96	0.00	0.00
17	63	7.20	175.15	0.00	0.00
18	63	8.17	189.82	0.00	0.00
19	62	9.12	181.56	0.00	0.00
20	63	10.08	187.54	0.00	0.00

Table A.101 Mean instantaneous commingling for five experimental test runs.

Sample No.	Mean Actual Sampling Time Interval, s	Mean Actual Sampling Time, min	Mean Sample Mass, g	Mean Red Soybean Mass, g	Instantaneous Commingling (%)
1	5	0.08	186.21	7.92	4.25
2	16	0.35	181.22	1.54	0.85
3	17	0.63	178.74	0.98	0.54
4	17	0.90	187.48	0.58	0.31
5	17	1.18	180.30	0.25	0.13
6	16	1.45	185.65	0.32	0.17
7	17	1.73	186.50	0.18	0.10
8	23	2.11	187.44	0.15	0.08
9	32	2.64	184.48	0.08	0.04
10	32	3.18	184.62	0.04	0.02
11	33	3.73	182.91	0.06	0.03
12	32	4.26	184.52	0.19	0.10
13	44	4.99	182.67	0.10	0.05
14	44	5.73	171.68	0.10	0.06
15	56	6.66	183.91	0.00	0.00
16	62	7.68	193.80	0.03	0.01
17	63	8.73	175.43	0.00	0.00
18	63	9.78	183.14	0.00	0.00
19	63	10.82	181.76	0.00	0.00
20	63	11.87	187.54	0.00	0.00

Table A.102 Average commingling during test run no. 1.

Sample No.	Actual Sampling Time Interval, s	Actual Sampling Time, min	Instantaneous Commingling, %	Red Soybeans on Load Mass, g	Load Mass[a], g	Running Total of Red Soybeans on Load Mass, g	Running Total of Load Mass, g	Average Commingling, %
1	4	0.07	4.67	710.47	15220.55	710.47	15220.55	4.67
2	17	0.35	0.82	142.02	17249.96	852.50	32470.52	2.63
3	17	0.63	0.62	106.82	17249.96	959.32	49720.48	1.93
4	17	0.92	0.34	59.01	17249.96	1018.33	66970.44	1.52
5	17	1.20	0.23	40.10	17249.96	1058.43	84220.40	1.26
6	16	1.47	0.24	39.65	16235.26	1098.08	100455.66	1.09
7	17	1.75	0.15	26.09	17249.96	1124.17	117705.62	0.96
8	32	2.28	0.00	0.00	32470.52	1124.17	150176.14	0.75
9	32	2.82	0.00	0.00	32470.52	1124.17	182646.66	0.62
10	32	3.35	0.00	0.00	32470.52	1124.17	215117.17	0.52
11	32	3.88	0.07	22.72	32470.52	1146.89	247587.69	0.46
12	33	4.43	0.00	0.00	33485.22	1146.89	281072.91	0.41
13	58	5.40	0.05	30.41	58852.81	1177.30	339925.72	0.35
14	63	6.45	0.14	90.33	63926.33	1267.64	403852.05	0.31
15	63	7.50	0.00	0.00	63926.33	1267.64	467778.38	0.27
16	62	8.53	0.07	46.77	62911.63	1314.40	530690.00	0.25

[a] Mass flow rate of clear soybeans for test 1 is 1.01 $kg \cdot s^{-1}$.

Table A.103 Average commingling during test run no. 2.

Sample No.	Actual Sampling Time Interval, s	Actual Sampling Time, min	Instantaneous Commingling, %	Red Soybeans on Load Mass, g	Load Mass[a], g	Running Total of Red Soybeans on Load Mass, g	Running Total of Load Mass, g	Average Commingling, %
1	4	0.07	4.14	672.95	16235.26	672.95	16235.26	4.14
2	16	0.33	0.73	118.45	16235.26	791.40	32470.52	2.44
3	17	0.62	0.55	95.58	17249.96	886.97	49720.48	1.78
4	16	0.88	0.21	33.77	16235.26	920.75	65955.74	1.40
5	17	1.17	0.09	15.13	17249.96	935.88	83205.70	1.12
6	16	1.43	0.08	12.96	16235.26	948.84	99440.96	0.95
7	17	1.72	0.17	29.61	17249.96	978.45	116690.92	0.84
8	33	2.27	0.00	0.00	33485.22	978.45	150176.14	0.65
9	31	2.78	0.00	0.00	31455.81	978.45	181631.95	0.54
10	32	3.32	0.00	0.00	32470.52	978.45	214102.47	0.46
11	31	3.83	0.00	0.00	31455.81	978.45	245558.28	0.40
12	32	4.37	0.16	51.01	32470.52	1029.46	278028.80	0.37
13	61	5.38	0.08	48.60	61896.92	1078.07	339925.72	0.32
14	63	6.43	0.00	0.00	63926.33	1078.07	403852.05	0.27
15	62	7.47	0.00	0.00	62911.63	1078.07	466763.67	0.23
16	63	8.52	0.00	0.00	63926.33	1078.07	530690.00	0.20

[a] Mass flow rate of clear soybeans for test 2 is 0.89 $kg \cdot s^{-1}$.

Table A.104 Average commingling during test run no. 3.

Sample No.	Actual Sampling Time Interval, s	Actual Sampling Time, min	Instantaneous Commingling, %	Red Soybeans on Load Mass, g	Load Mass[a], g	Running Total of Red Soybeans on Load Mass, g	Running Total of Load Mass, g	Average Commingling, %
1	5	0.08	3.96	643.65	16235.26	643.65	16235.26	3.96
2	16	0.35	0.94	151.99	16235.26	795.64	32470.52	2.45
3	16	0.62	0.55	89.78	16235.26	885.42	48705.77	1.82
4	17	0.90	0.35	60.48	17249.96	945.90	65955.74	1.43
5	17	1.18	0.12	20.32	17249.96	966.22	83205.70	1.16
6	16	1.45	0.16	25.67	16235.26	991.89	99440.96	1.00
7	17	1.73	0.00	0.00	17249.96	991.89	116690.92	0.85
8	17	2.02	0.08	14.43	17249.96	1006.31	133940.88	0.75
9	32	2.55	0.11	36.60	32470.52	1042.91	166411.40	0.63
10	32	3.08	0.00	0.00	32470.52	1042.91	198881.91	0.52
11	39	3.73	0.03	11.04	39573.44	1053.96	238455.36	0.44
12	32	4.27	0.09	29.97	32470.52	1083.93	270925.87	0.40
13	32	4.80	0.00	0.00	32470.52	1083.93	303396.39	0.36
14	31	5.32	0.07	21.72	31455.81	1105.65	334852.20	0.33
15	61	6.33	0.00	0.00	61896.92	1105.65	396749.12	0.28
16	62	7.37	0.00	0.00	62911.63	1105.65	459660.75	0.24
17	63	8.42	0.00	0.00	63926.33	1105.65	523587.08	0.21

[a] Mass flow rate of clear soybeans for test 3 is 0.96 $kg \cdot s^{-1}$.

Table A.105 Average commingling during test run no. 4.

Sample No.	Actual Sampling Time Interval, s	Actual Sampling Time, min	Instantaneous Commingling, %	Red Soybeans on Load Mass, g	Load Mass[a], g	Running Total of Red Soybeans on Load Mass, g	Running Total of Load Mass, g	Average Commingling, %
1	6	0.10	4.65	755.59	16235.26	755.59	16235.26	4.65
2	16	0.37	0.72	116.81	16235.26	872.41	32470.52	2.69
3	16	0.63	0.15	24.92	16235.26	897.33	48705.77	1.84
4	16	0.90	0.38	61.39	16235.26	958.72	64941.03	1.48
5	16	1.17	0.14	22.67	16235.26	981.39	81176.29	1.21
6	16	1.43	0.26	41.66	16235.26	1023.06	97411.55	1.05
7	16	1.70	0.15	25.05	16235.26	1048.10	113646.81	0.92
8	16	1.97	0.22	35.76	16235.26	1083.86	129882.07	0.83
9	32	2.50	0.00	0.00	32470.52	1083.86	162352.58	0.67
10	32	3.03	0.06	18.61	32470.52	1102.47	194823.10	0.57
11	31	3.55	0.00	0.00	31455.81	1102.47	226278.91	0.49
12	32	4.08	0.06	20.31	32470.52	1122.78	258749.43	0.43
13	32	4.62	0.13	43.36	32470.52	1166.13	291219.94	0.40
14	32	5.15	0.10	32.76	32470.52	1198.89	323690.46	0.37
15	31	5.67	0.00	0.00	31455.81	1198.89	355146.27	0.34
16	59	6.65	0.00	0.00	59867.51	1198.89	415013.79	0.29
17	63	7.70	0.00	0.00	63926.33	1198.89	478940.12	0.25
18	62	8.73	0.00	0.00	62911.63	1198.89	541851.74	0.22
19	63	9.78	0.00	0.00	63926.33	1198.89	605778.07	0.20

[a] Mass flow rate of clear soybeans for test 4 is 0.89 $kg \cdot s^{-1}$.

Table A.106 Average commingling during test run no. 5.

Sample No.	Actual Sampling Time Interval, s	Actual Sampling Time, min	Instantaneous Commingling, %	Red Soybeans on Load Mass, g	Load Mass[a], g	Running Total of Red Soybeans on Load Mass, g	Running Total of Load Mass, g	Average Commingling, %
1	4	0.07	3.80	654.72	17249.96	654.72	17249.96	3.80
2	17	0.35	1.05	180.38	17249.96	835.09	34499.92	2.42
3	17	0.63	0.81	139.33	17249.96	974.43	51749.89	1.88
4	17	0.92	0.27	46.40	17249.96	1020.82	68999.85	1.48
5	17	1.20	0.09	15.14	17249.96	1035.97	86249.81	1.20
6	17	1.48	0.13	23.26	17249.96	1059.23	103499.77	1.02
7	16	1.75	0.00	0.00	16235.26	1059.23	119735.03	0.88
8	17	2.03	0.10	16.46	17249.96	1075.69	136984.99	0.79
9	32	2.57	0.10	33.98	32470.52	1109.67	169455.51	0.65
10	32	3.10	0.05	15.83	32470.52	1125.50	201926.02	0.56
11	32	3.63	0.06	20.94	32470.52	1146.44	234396.54	0.49
12	32	4.17	0.21	66.68	32470.52	1213.12	266867.06	0.45
13	36	4.77	0.00	0.00	36529.33	1213.12	303396.39	0.40
14	32	5.30	0.00	0.00	32470.52	1213.12	335866.91	0.36
15	61	6.32	0.00	0.00	61896.92	1213.12	397763.83	0.30
16	62	7.35	0.00	0.00	62911.63	1213.12	460675.45	0.26
17	63	8.40	0.00	0.00	63926.33	1213.12	524601.78	0.23
18	63	9.45	0.00	0.00	63926.33	1213.12	588528.11	0.21
19	62	10.48	0.00	0.00	62911.63	1213.12	651439.74	0.19
20	63	11.53	0.00	0.00	63926.33	1213.12	715366.07	0.17

[a] Mass flow rate of clear soybeans for test 5 is 0.97 $kg \cdot s^{-1}$.

Table A.107 Mean average commingling for five experimental test runs.

Sample No.	Mean Actual Sampling Time Interval, s	Mean Actual Sampling Time, min	Mean Instantaneous Commingling, %	Mean Red Soybeans on Load Mass, g	Mean Load Mass[a], g	Mean Running Total of Red Soybeans on Load Mass, g	Mean Running Total of Load Mass, g	Mean Average Commingling, %
1	5	0.08	4.25	687.48	16235.26	687.48	16235.26	4.25
2	16	0.35	0.85	141.93	16641.14	829.41	32876.40	2.52
3	17	0.63	0.54	91.29	16844.08	920.69	49720.48	1.85
4	17	0.90	0.31	52.21	16844.08	972.90	66564.56	1.46
5	17	1.18	0.13	22.67	17047.02	995.58	83611.58	1.19
6	16	1.45	0.17	28.64	16438.20	1024.22	100049.78	1.02
7	17	1.73	0.10	16.15	16844.08	1040.37	116893.86	0.89
8	23	2.11	0.08	13.33	23338.18	1053.70	140232.04	0.75
9	32	2.64	0.04	14.12	32267.58	1067.81	172499.62	0.62
10	32	3.18	0.02	6.89	32470.52	1074.70	204970.14	0.53
11	33	3.73	0.03	10.94	33485.22	1085.64	238455.36	0.46
12	32	4.26	0.10	33.59	32673.46	1119.24	271128.81	0.41
13	44	4.99	0.05	24.47	44444.02	1143.71	315572.83	0.36
14	44	5.73	0.06	28.96	44849.90	1172.67	360422.73	0.33
15	56	6.66	0.00	0.00	56417.52	1172.67	416840.26	0.28
16	62	7.68	0.01	9.35	62505.74	1182.03	479346.00	0.25
17	63	8.73	0.00	0.00	63926.33	1172.56	509042.99	0.23
18	63	9.78	0.00	0.00	63418.98	1206.01	565189.93	0.21
19	63	10.82	0.00	0.00	63418.98	1206.01	628608.91	0.19
20	63	11.87	0.00	0.00	63926.33	1213.12	715366.07	0.17

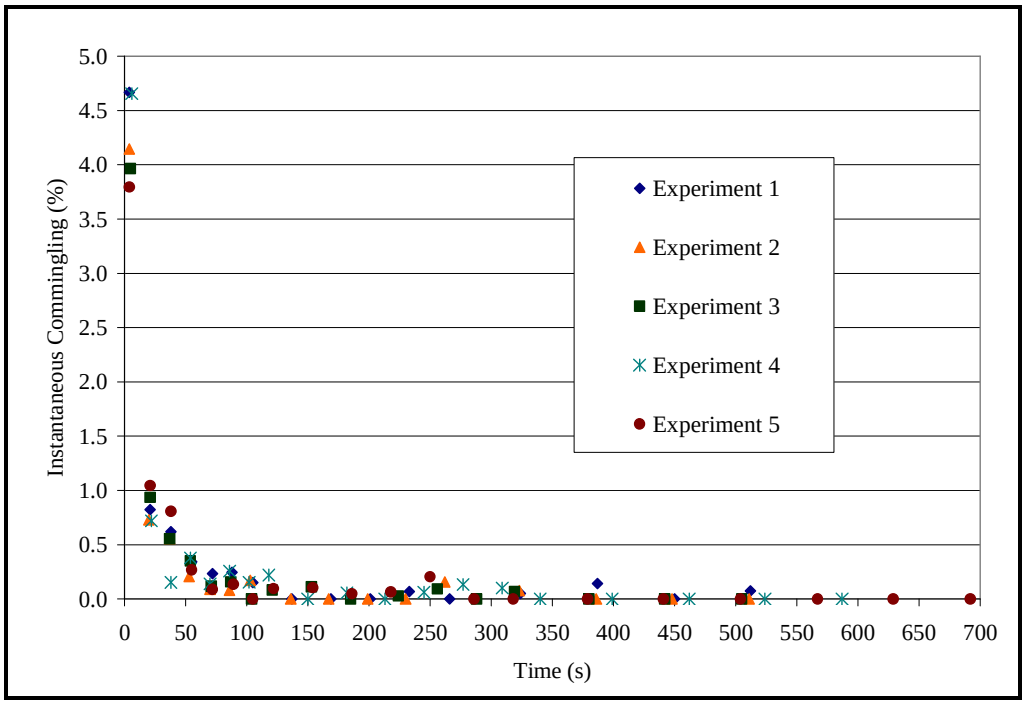

Figure A.5 Instantaneous commingling for five experimental test runs.

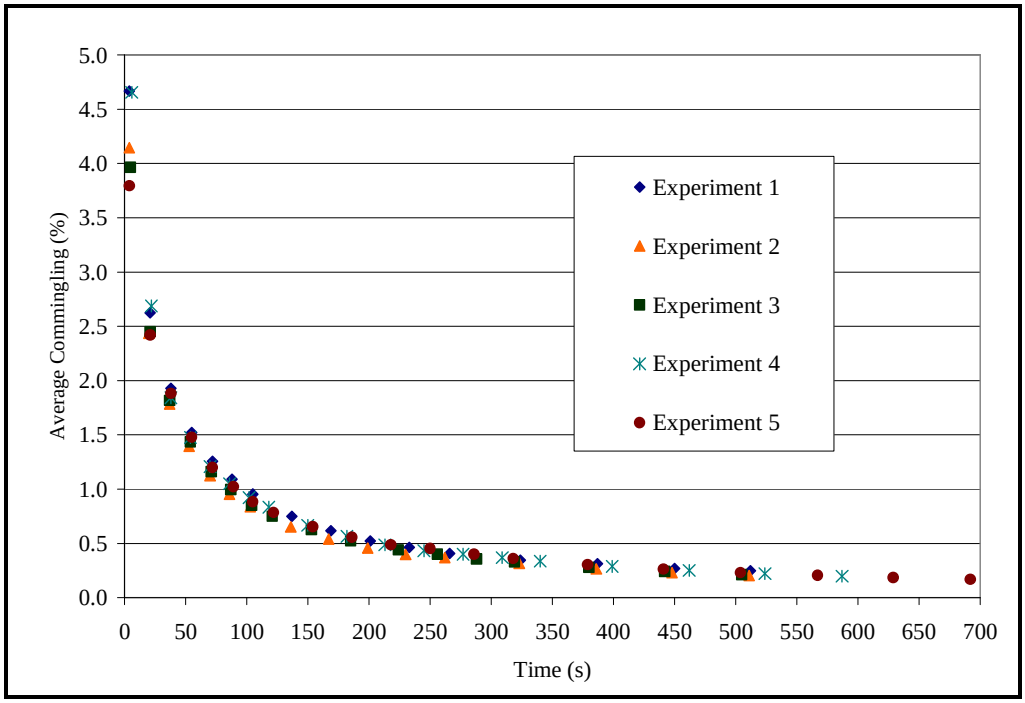

Figure A.6 Average commingling for five experimental test runs.

Appendix B - Summary of Calibration Data

Calibration Data for Chapter 4

Table B.1 Calibration data for isokinetic sampling from velocity traverse.

Parameter	A - Lower Duct	B - Upper Duct	A - Lower Probe	B - Upper Probe
Diameter (d), ft	2.23	1.89	0.115	0.115
Diameter (d), m	0.68	0.58	0.035	0.035
Cross-Sect. Area (A), ft^2	3.89	2.81	0.010	0.010
Cross-Sect. Area (A), m^2	0.36	0.26	0.000958	0.000958
Root Mean Square of Velocity Pressure Readings (VP_{rms}), in.	0.79	0.89	0.79	0.89
Velocity (V), $ft \cdot min^{-1}$	3498.41	3776.91	3498.41	3776.91
Velocity (V), $m \cdot s^{-1}$	17.78	19.19	17.78	19.19
Volumetric Air Flowrate (Q), $ft^3 \cdot min^{-1}$	13624.10	10617.21	36.07	38.95
Volumetric Air Flowrate (Q), $m^3 \cdot s^{-1}$	6.43	5.01	0.017	0.018

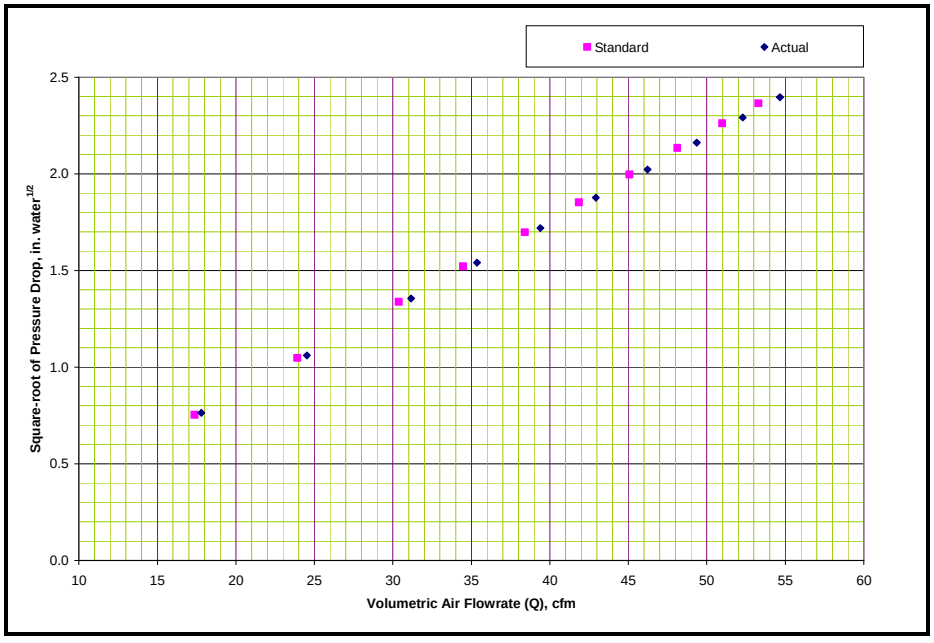

Figure B.1 Calibration graph for Magnehelic pressure gauge for lower duct (set A).

[With a given volumetric flowrate for the sampling probe, calculate the pressure drop (in. water) from the graph to use in maintaining pressure in the Magnehelic gauge.]

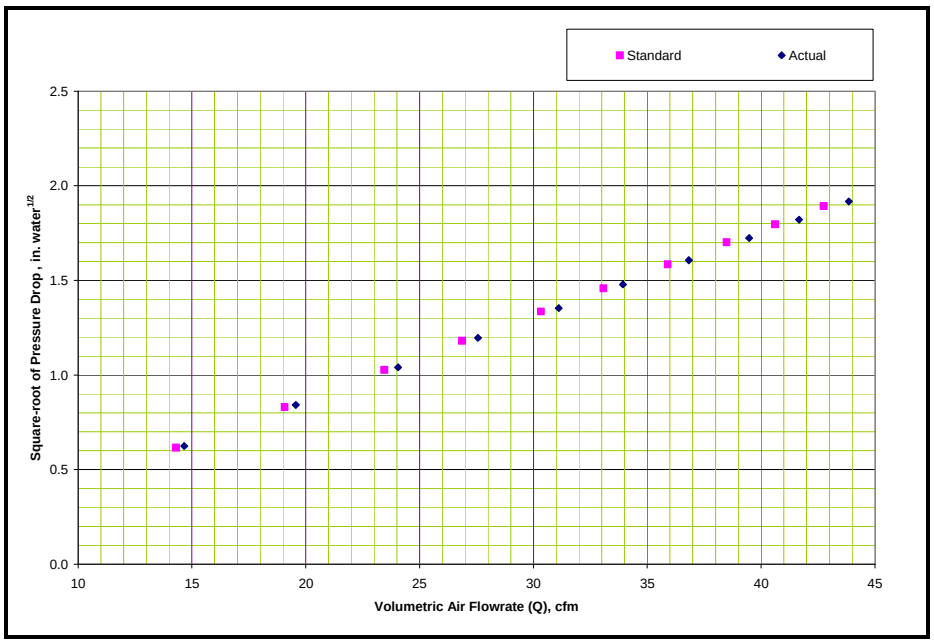

Figure B.2 Calibration graph for Magnehelic pressure gauge for upper duct (set B).

[With a given volumetric flow rate for the sampling probe, calculate the pressure drop (in. water) from the graph to use in maintaining pressure in the Magnehelic gauge.]